รายงานวิจัยฉบับสมบูรณ์

การศึกษาพฤติกรรมวัฏภาคของพอลิเมอร์ผลึกเหลวผสม

STUDY OF PHASE BEHAVIOUR OF LIQUID CRYSTALLINE POLYMER MIXTURES

ศาสตราจารย์ ดร.เสาวรภย์ บัวเล็ก-ลิ้มเจริญ และคณะ

กันยายน 2542

สัญญาเลขที่ RTA3880009

รายงานวิจัยฉบับสมบูรณ์

การศึกษาพฤติกรรมวัฏภาคของพอลิเมอร์ผลึกเหลวผสม

STUDY OF PHASE BEHAVIOUR OF LIQUID CRYSTALLINE POLYMER MIXTURES

คณะผู้วิจัย	สังกัด
ศาสตราจารย์ ดร.เสาวรภย์ บัวเล็ก	ภาควิชาเคมี คณะวิทยาศาสตร์ มหาวิทยาลัยมหิดล
ผู้ช่วยศาสตราจารย์ ดร.ทวีชัย อมรศักดิ์ชัย	ภาควิชาเคมี คณะวิทยาศาสตร์ มหาวิทยาลัยมหิดล
นาวาอากาศเอก ดร.วิริยะ มีศิริ	กรมสรรพวุธ กองทัพอากาศ ดอนเมือง
ดร.อิทธิพล แจ้งชัด	ภาควิชาเคมี สถาบันพระจอมเกล้าเจ้าคุณทหารลาดกระบัง
ผู้ช่วยศาสตราจารย์ ดร.ชาคริต สิริสิงห	ภาควิชาเคมี คณะวิทยาศาสตร์ มหาวิทยาลัยมหิดล
ผู้ช่วยศาสตราจารย์ ดร.ปราณี ภิญโญชีพ	ภาควิชาเคมี คณะวิทยาศาสตร์ มหาวิทยาลัยมหิดล
นายธีรวุฒิ นคินทร์พงษ์	ภาควิชาเคมี คณะวิทยาศาสตร์ มหาวิทยาลัยมหิดล
นายวรพงษ์ ชวลิตอัมพร	ภาควิชาเคมี คณะวิทยาศาสตร์ มหาวิทยาลัยมหิดล
นางสาวจรีรัตน์ สำราญ	คณะวิทยาศาสตร์และเทคโนโลยี มหาวิทยาลัยสงขลานครินทร์
นายสุนันท์ สายกระสุน	ภาควิชาเคมี คณะวิทยาศาสตร์ มหาวิทยาลัยมหาสารคาม
นางสาวอนงค์นุช จันทรัตน์เจริญ	ภาควิชาเคมี คณะวิทยาศาสตร์ มหาวิทยาลัยมหิดล
นายบรรจบ วันโน	ภาควิชาเคมี คณะวิทยาศาสตร์ มหาวิทยาลัยมหิดล
นายธีรนันท์ นคินทร์พงษ์	ภาควิชาเคมี คณะวิทยาศาสตร์ มหาวิทยาลัยมหิดล
นางสาวจันทร์ทิพา วัชรเสถียร	ภาควิชาเคมี คณะวิทยาศาสตร์ มหาวิทยาลัยมหิดล
นางสาวภัควดี สุขอนันท์	ภาควิชาเคมี คณะวิทยาศาสตร์ มหาวิทยาลัยมหิดล
นายสายันต์ แสงสุวรรณ	ภาควิชาเคมี คณะวิทยาศาสตร์ มหาวิทยาลัยมหิดล
นายยอดพันธ์ บุญสนอง	ภาควิชาเคมี คณะวิทยาศาสตร์ มหาวิทยาลัยมหิดล

สนับสนุนโดยสำนักงานกองทุนสนับสนุนการวิจัย

ชุดโครงการพัฒนากลุ่มวิจัย

กิตติกรรมประกาศ

คณะผู้วิจัยขอขอบคุณสำนักงานกองทุนสนับสนุนการวิจัย ที่ให้ทุนอุดหนุนการวิจัยและพัฒนากลุ่มวิจัย ประจำปี 2538-2541

ขอขอบคุณหน่วยงานต่างๆที่อนุเคราะห์ให้ใช้สถานที่และเครื่องมือได้แก่ ภาควิชาเคมี คณะวิทยาศาสตร์ มหาวิทยาลัยมหิดล ศูนย์โลหะและวัสดุแห่งชาติ กระทรวงวิทยาศาสตร์เทคโนโลยีและสิ่งแวดล้อม คณะวิทยาศาสตร์และเทคโนโลยี มหาวิทยาลัยสงขลานครินทร์

ขอขอบคุณบริษัทต่างๆที่ให้พอลิเมอร์ตัวอย่างได้แก่ Shell Chemical Co. Ltd. Chemical Innovation Co. Ltd., Du Pont Ltd., Polyplastics Ltd., Teijin Co. Lid., HMC Polymers Co. Ltd., Mitsubishi Co. Ltd., Uniroyal Chemical Co. Ltd.,

บทคัดย่อ

ระหัสโครงการ RTA/09/2538

หัวข้อโครงการ การศึกษาพฤติกรรมวัฏภาคของพอลิเมอร์ผลึกเหลวผสม

ผู้วิจัย ศาสตราจารย์เสาวรภย์ บัวเล็ก-ลิ้มเจริญ และคณะ
ภาควิชาเคมี คณะวิทยาศาสตร์ มหาวิทยาลัยมหิดล

E-mail address scsbl@mahidol.ac.th

ระยะเวลาที่ทำการวิจัย ตุลาคม 2538 – กันยายน 2542

วัตถุประสงค์ เพื่อศึกษาพฤติกรรมวัฏภาคของพอลิเมอร์ผสมระหว่างพอลิเมอร์ผลึกเหลวกับพอลิเมอร์ทั่วไป โดยการปรับเพิ่มแรงกระทำที่รอยต่อระหว่างวัฏภาคโดยใช้วิธีทางเคมีและการใช้สารช่วยผสมเพื่อเพิ่มสมบัติของพอลิเมอร์ผสมให้ดีขึ้น

ขอบเขตการวิจัย 1) ผสมพอลิเมอร์ผลึกเหลวชนิดไลออทรอปิก (LLCP) หรืออะรามิด ซึ่งอยู่ในรูปของเส้นใยสั้นหรือเยื่อ กับเทอร์โมพลาสติกอีลาสโตเมอร์ (TPE) โดยใช้เครื่องผสมภายในหรือเครื่องรีดเกลียวคู่แล้วขึ้นรูปด้วยวิธีอัดหล่อหรือฉีดหล่อ นำชิ้นงานที่ได้ไปทดสอบสมบัติความทนต่อแรงดึง และพลศาสตร์เชิงกล ใช้วิธีทางเคมีปรับผิวของเส้นใยได้แก่วิธีไฮโดรไลซีสร่วมกับการใช้สารช่วยผสม และการเติมหมู่อัลคิลที่ผิวของเส้นใย รวมทั้งใช้วิธีอาบผิวเส้นใยด้วยออกซิเจนพลาสมา ศึกษาโครงสร้างสัณฐานของพอลิเมอร์ผสมด้วยกล้องจุลทรรศน์อิเล็กตรอนแบบกวาด (SEM)

2) ผสมพอลิเมอร์ผลึกเหลวชนิดเทอร์โมโทรปิก (TLCP) กับเทอร์โมพลาสติก (TP) โดยการหลอมเหลวในเครื่องผสมเกลียวคู่ และขึ้นรูปเป็นฟิล์มบางโดยใช้เครื่องฉีดฟิล์ม TLCP ซึ่งไม่ผสมเป็นเนื้อเดียวกันกับเมทริกซ์ TLCP ถูกยืดออกเป็นเส้นใยเล็กๆ เมื่อฟิล์มถูกทำให้เย็นลงโดยเร็วจะได้คอมพอสิตที่เรียกว่า อิน-ซิทู คอมพอสิต ได้ศึกษาสภาวะที่ใช้ในการผสม อิทธิพลของความหนืดของเมทริกซ์และการเติมสารช่วยผสมที่มีต่อสมบัติการทนต่อแรงดึงและแรงกระแทก ความเป็นระเบียบของโมเลกุล รวมทั้งโครงสร้างสัณฐานของพอลิเมอร์ผสม

ผลการทดลองและวิจารณ์

1) สำหรับคอมพอสิต LLCP/TPE ได้ปรับผิวของเส้นใยพอลิเมอร์ผลึกเหลวเพื่อให้ยึดติดกับเมทริกซ์ที่ไม่มีขั้วดีขึ้น ผลการทดลองพบว่าสามารถปรับการยึดที่รอยต่อระหว่างวัฏภาคได้ดีขึ้นได้ทุกระบบโดยดูจากภาพ SEM และพบว่ามี 5 ระบบที่ได้ค่าการทนต่อแรงดึงที่จุดขาดเพิ่มขึ้นด้วย ได้แก่ระบบ hydrolysed Kevlar/MA-g-PP/Santoprene, hydrolysed Conex/MA-g-SEBS/SEBS, alkylated Conex/SEBS, alkylated Conex/Santoprene, และ Conex/MA-g-PP/Santoprene. ส่วน Conex/TPU จาก SEM พบว่าการยึดติดที่รอยต่อระหว่างวัฏภาคดีอยู่แล้ว การอาบด้วยพลาสมาจึงไม่ช่วยทำให้สมบัติดีขึ้น

2) สำหรับ TLCP/PP in situ composite พบว่าอัตราการดึงฟิล์มมีความสำคัญมากในการเพิ่ม fiber aspect ratio และทำให้ความแข็งแรงของฟิล์มสูงขึ้นมาก นอกจากนี้ยังพบว่าสารช่วยผสมที่เป็นอีลาสโตเมอร์จะให้ผลดีกว่าสารช่วยผสมที่เป็นพลาสติกเพราะนอกจากจะช่วยเพิ่มความแข็งแรงแล้วยังเพิ่มความทนต่อแรงกระแทกด้วย และงานวิจัยนี้ค้นพบเป็นครั้งแรกว่าสารช่วยผสมที่ไม่มีหมู่ฟังก์ชันที่ไวต่อการทำปฏิกิริยา กลับให้ผลดีกว่าสารช่วยผสมที่มีหมู่ที่ไวต่อการทำปฏิกิริยา ทั้งนี้อาจเป็นเพราะไม่มีพันธะเคมีหรือพันธะไฮโดรเจนที่จะขัดขวางการยืดตัวของเส้นใย TLCP

Abstract

Project Code : RTA3880009

Project Title : Study of Phase Behavior of Liquid Crystalline Polymer Mixtures

Investigators : Professor Sauvarop Bualek-Limcharoen et al.

Department of Chemistry, Faculty of Science, Mahidol University

E-mail : scsbl@mahidol.ac.th

Project Period : October 1995 – September 1999

Objective : To investigate the phase behavior of mixtures of liquid crystalline polymers (LCP) and commodity polymers. Chemical modification and compatibilizers are used to improve interfacial adhesion and enhance the properties of the blends.

Methodology : 1) Lyotropic liquid crystalline polymers (LLCP, aramid) in the form of short fiber or pulp were blended with thermoplastic elastomers (TPE) using an internal mixer or twin screw extruder. Specimens were prepared by compression molded or injection molded for measurements of tensile and dynamic mechanical properties. Three methods used to modify the fiber surface were partial hydrolysis in conjunction with addition of a reactive compatibilizer, surface N-alkylation and oxygen plasma treatment. The morphology was observed under SEM.

2) Thermotropic liquid crystalline polymer (TLCP) and thermoplastics (TP) were melt blended in a twin screw extruder. The specimens were extruded as cast film comprising TLCP fibrils, a self-reinforced system called *in-situ* composite. Tensile properties and impact strength were measured. The effects of processing conditions, matrix melt viscosity and compatibilizers on mechanical properties, molecular ordering and morphology of the blends were investigated.

Results and Discussion :

1) For LLCP/TPE composites, the results revealed that both chemical treatments and addition of compatibilizers could improve the interfacial adhesion as seen in the SEM micrographs of fracture surfaces. Improvement of the tensile strength could be observed in five systems, namely, hydrolysed Kevlar/MA-g-PP/Santoprene, hydrolysed Conex/MA-g-SEBS/SEBS, alkylated Conex/SEBS, alkylated Conex/Santoprene, and Conex/MA-g-PP/Santoprene. For Conex/ polyurethane composite, good interfacial adhesion is observed by SEM, therefore plasma treatment could not further improve the blend properties.

2) For TLCP/TP blend, it has been shown that winding speed is a very important factor in obtaining films with improved properties. Elastomeric compatibilizers were found to improve both tensile modulus and impact strength of TLCP/PP blends. This research shows, for the first time, that elastomeric compatibilizer with no reactive group gives better TLCP/PP composite than that contains reactive group. This might be due to the absence of bonding which could inhibit the extension of TLCP domains.

Keywords : Polymer blend, In-situ composite, Compatibilization, short-fiber reinforced Composite

Executive Summary

โครงการวิจัยนี้ ได้ทำการศึกษาระบบพอลิเมอร์ผสมระหว่างเส้นใยพอลิเมอร์ผลึกเหลวและพอลิเมอร์ชนิดธรรมดา (commodity polymers) เพื่อให้ได้ระบบพอลิเมอร์ที่รวมสมบัติเชิงกลและสมบัติทางความร้อนที่ดีของเส้นใยพอลิเมอร์ผลึกเหลว และความง่ายในการขึ้นรูป และราคาถูกของพอลิเมอร์ธรรมดาไว้ด้วยกัน เป็นการวิจัยในแนวใหม่ และกำลังได้รับความสนใจมากในปัจจุบัน

เนื่องจากความหลากหลายของเส้นใยพอลิเมอร์ผลึกเหลว และพอลิเมอร์ชนิดธรรมดา ผู้วิจัยจึงได้แบ่งการศึกษาเป็น 2 ระบบหลัก ที่มีจุดมุ่งหมายในการประยุกต์ใช้ที่แตกต่างกัน คือ 1. ระบบของเส้นใยพอลิเมอร์ผลึกเหลวชนิดไลโอโทรปิก (LLCP) กับเทอร์โมพลาสติกอีลาสโตเมอร์ (TPE) และ 2. ระบบของพอลิเมอร์ผลึกเหลวชนิดเทอร์โมโทรปิก (TLCP) กับเทอร์โมพลาสติก (TP) โดยในระบบหลังนี้ เส้นใยพอลิเมอร์ผลึกเหลวจะเกิดขึ้นในระหว่างกระบวนการผลิต ซึ่งเป็นที่มาของชื่อ in-situ composite

พอลิเมอร์ผสมระหว่างเส้นใยพอลิเมอร์ผลึกเหลวชนิดไลโอโทรปิกกับเทอร์โมพลาสติกอีลาสโตเมอร์ เป็นระบบที่มีเส้นใยพอลิเมอร์ผลึกเหลวที่มีสมบัติเชิงกล และสมบัติทางความร้อนดีมากกระจายตัวอยู่ในตัวกลาง (matrix) ที่เป็นยาง จุดเด่นของระบบนี้ คือ การใช้เส้นใยสั้นแทนเส้นใยต่อเนื่องที่ใช้กันโดยปกติ จึงทำให้การผสม และการขึ้นรูปทำได้ง่ายขึ้น เส้นใยที่ใช้ศึกษาเป็นเส้นใยอะรามิด 3 ชนิด คือ Kevlar Conex และ Technora ส่วนพอลิเมอร์เมทริกซ์ (matrix) เลือกใช้ 3 ชนิด คือ SEBS, Santoprene และ Polyurethane เนื่องจาก SEBS และ Santoprene เป็นพอลิเมอร์ที่ค่อนข้างไม่มีขั้ว ในขณะที่เส้นใยอะรามิดมีขั้วสูงมาก การผสมพอลิเมอร์ที่มีโครงสร้างทางเคมีต่างกันมากเช่นนี้ยากที่จะเกิดการยึดติดกันได้ จึงยังไม่มีผู้ใดศึกษามาก่อน ในงานวิจัยนี้ได้ศึกษาหาวิธีการปรับปรุงผิวของเส้นใยเพื่อเพิ่มการยึดติดระหว่างเส้นใยกับเมทริกซ์ด้วยวิธีการทางเคมี เช่น surface hydrolysis, surface N-alkylation หรือ plasma treatment และมีการใช้ compatibilizer ที่มีหมู่ฟังก์ชันที่สามารถทำปฏิกิริยากับผิวของเส้นใยได้ร่วมด้วย จากผลการวิจัยทำให้ทราบว่าระบบพอลิเมอร์ผสมประเภทนี้มีพฤติกรรมที่ซับซ้อนมาก และขึ้นอยู่กับแต่ละคู่พอลิเมอร์ผสมค่อนข้างมาก การเลือกวิธีปรับปรุงพื้นผิวของเส้นใย หรือ compatibilizer จึงสามารถ generalized ได้เพียงระดับหนึ่งเท่านั้น ระบบที่พบว่าได้ผลดี คือ hydrolysed Kevlar/MA-g-PP/Santoprene, hydrolysed Conex/MA-g-SEBS/SEBS, alkylated Conex/SEBS, alkylated Conex/Santoprene, Conex/MA-g-PP/Santoprene และ Conex/polyurethane โดยระบบหลังนี้เป็นตัวอย่างที่ดีว่า การปรับปรุงพื้นผิวไม่มีความจำเป็น เนื่องจากเส้นใยยึดติดกับ polyurethane ได้ดีอยู่แล้วเพราะทั้งคู่เป็นสารประกอบที่มีขั้ว

พอลิเมอร์ผสมระหว่างพอลิเมอร์ผลึกเหลวชนิดเทอร์โมโทรปิกกับเทอร์โมพลาสติก เป็นระบบที่เส้นใยเกิดขึ้นระหว่างกระบวนการผสม และการผลิต ซึ่งสมบัติของพอลิเมอร์ผสมที่ได้ขึ้นอยู่กับสมบัติของเทอร์โมพลาสติก และสภาวะของการผสม และการผลิตมาก ผู้วิจัยได้เลือกผลิตเป็นฟิล์มบาง ซึ่งสามารถทำให้เกิดเส้นใยที่มีความยาวได้ดี และภายในฟิล์มมีการเรียงตัวของ TLCP

domains สม่ำเสมอ ในการทดลองนี้ได้ใช้เทอร์โมพลาสติกพอลิโพรพิลีน (PP) ที่มีความหนืดต่าง ๆ กัน และใช้ compatibilizer ชนิดต่าง ๆ ทั้งที่เป็นพลาสติก ยาง ที่มีหรือไม่มีหมู่ฟังก์ชันด้วย จากผลการวิจัยทำให้ทราบว่า ปัจจัยสำคัญที่ควบคุมการเกิดเส้นใย ไม่ใช่อัตราส่วนของความหนืดระหว่างพอลิเมอร์ผลึกเหลวกับพอลิเมอร์เมทริกซ์ดังที่มีการกล่าวถึงกันเสมอ แต่เป็นความหนืดของพอลิเมอร์เมทริกซ์เอง และปัจจัยที่มีบทบาทสำคัญมากคือการดึงฟิล์มขณะที่พอลิเมอร์ผสมพ้นหัว die จะสามารถเพิ่มความยาวของเส้นใยได้ นอกจากนี้ยังพบว่า compatibilizer ที่เป็นยาง, SEBS, ให้ผลที่ดีมากในการช่วยเพิ่มความทนต่อแรงดึง และความทนต่อแรงกระแทก โดยไม่จำเป็นต้องมีหมู่ฟังก์ชันที่ไวต่อการเกิดพันธะเคมีหรือพันธะไฮโดรเจน สิ่งที่พบนี้นับว่าเป็นครั้งแรกที่มีผลการรายงานในลักษณะดังกล่าว

ส่วนระบบพอลิเอทธิลีนความหนาแน่นต่ำ (LDPE) ผสมพอลิเมอร์ผลึกเหลว เมื่อใช้สภาวะในการผสมเหมือนกับระบบ TLCP/PP พบว่ามีการกระจายตัวของ TLCP ดีมากอยู่แล้ว คือได้เส้นใยของ TLCP เล็กมาก การเติม compatibilizer ยิ่งทำให้ได้เส้นใยเล็กลงอีกจึงไม่เป็นผลดีต่อสมบัติเชิงกลของพอลิเมอร์ผสม จะเห็นว่าลักษณะเฉพาะของเมทริกซ์ ทั้งโครงสร้างทางเคมี ความสามารถในการจัดเรียงตัวของโมเลกุลรวมทั้งความหนืดมีผลต่อการกระจายและการยืดตัวของวัฏภาค TLCP

งานวิจัยที่น่าจะทำต่อไปคือศึกษาวิทยากระแส (Rheology) ของพอลิเมอร์ผสมในสภาวะต่างๆ ซึ่งมีบทบาทสำคัญในการเกิดโครงสร้างสัณฐานแบบต่างๆ และส่งผลต่อสมบัติสุดท้ายของพอลิเมอร์ผสม รวมทั้งการศึกษาในเชิงปริมาณของการเกิดการยึดติดกันที่รอยต่อระหว่างวัฏภาค

บทนำ

การนำพอลิเมอร์ที่มีสมบัติต่างกันมาผสมกันเพื่อให้ได้ผลิตภัณฑ์ใหม่ที่มีสมบัติการใช้งานที่เหมาะสม เป็นวิธีที่นิยมทำกันเนื่องจากสามารถทำได้สะดวกกว่าและประหยัดกว่าการสังเคราะห์พอลิเมอร์ใหม่ให้ได้สมบัติตามต้องการ ถ้าพอลิเมอร์ที่นำมาผสมกันสามารถหลอมเหลวได้ทั้งคู่เรียกว่าเบรนด์ (blend) แต่ถ้าหากพอลิเมอร์เมทริกซ์หลอมเหลวได้แต่สิ่งที่นำมาผสมซึ่งอาจจะเป็นพอลิเมอร์หรือวัสดุอื่นหลอมเหลวไม่ได้จะเรียกว่า คอมพอสิต (composite) สมบัติของพอลิเมอร์ผสมที่ได้ขึ้นกับวิธีการผสม สภาวะที่ใช้ในการผสม พฤติกรรมวัฏภาคซึ่งทำให้ได้โครงสร้างสัณฐานต่างๆโดยเฉพาะอย่างยิ่งแรงกระทำที่รอยต่อระหว่างวัฏภาคจะเป็นตัวกำหนดสมบัติของผลิตภัณฑ์ที่ได้ (1-2)

คอมพอสิตมักได้จากการนำวัสดุเสริมแรงมาผสมซึ่งได้แก่เส้นใยธรรมชาติ โลหะ แก้ว เซรามิกซ์ รวมทั้งเส้นใยจากพอลิเมอร์สังเคราะห์ การเสริมแรงด้วยเส้นใยทำให้ได้คอมพอสิตที่มีความแข็งแรงสูงขึ้น เพิ่มความเสถียรของการคงรูป และเสถียรต่อความร้อน การเสริมแรงด้วยเส้นใยนี้อาจจะใช้เส้นยาว (continuous fiber) หรือ เส้นสั้นก็ได้ การใช้เส้นสั้นจะสะดวกกว่าในแง่กระบวนการผลิตเพราะสามารถใช้เครื่องผสมทั่วไปได้ และสามารถผลิตผลิตภัณฑ์รูปร่างต่างๆได้คล่องตัวกว่า สามารถเตรียมคอมพอสิตของเส้นใยสั้นโดยใช้เมทริกซ์เป็นพลาสติกหรือยางก็ได้ ในกรณีที่เป็นยางชนิดเทอร์โมพลาสติก (thermoplastic elastomer) คือสามารถขึ้นรูปได้แบบเดียวกับพลาสติกและไม่ต้องผ่านกระบวนการเชื่อมโยงโมเลกุล (crosslink) โดยใช้ปฏิกิริยาเคมีแบบยางเทอร์โมเซ็ท ยางเทอร์โมพลาสติกนี้แม้จะมีข้อดีดังกล่าวก็มีข้อเสียคือที่อุณหภูมิสูงจะมีความเสถียรของรูปร่างต่ำ การเติมเส้นใยลงในยางเทอร์โมพลาสติกจะช่วยเสริมแรงและเพิ่มความคงรูปให้ยางชนิดนี้ได้ดี (3-4)

เป็นที่ทราบกันดีว่าเส้นใยอะรามิด (aramid) ซึ่งเป็นพอลิเมอร์ผลึกเหลวชนิดไลออทรอปิก (lyotropic) เช่นเคฟล่า (Kevlar, poly-p-phenylene terephthalamide) และ โคเน็กซ์ (Conex, poly-m-phenylene isophthalamide) ซึ่งมีความแข็งแรงสูง มีความเสถียรต่อความร้อนดีมากและมีน้ำหนักเบา เมื่อเทียบกับเหล็กเส้นที่มีน้ำหนักเท่ากันเส้นใยอะรามิดจะมีความแข็งแรงสูงกว่าเหล็กมาก จึงมักนิยมนำไปเสริมแรงพอลิเมอร์ชนิดต่างๆ เช่นอิป็อกซี เพื่อทำหมวกทหาร เกราะกันกระสุน ส่วนประกอบของรถถัง และชิ้นส่วนของอากาศยาน เป็นต้น (5) ข้อจำกัดของการเสริมแรงด้วยเส้นใยอะรามิดคือความเฉื่อยของผิวเส้นใย ทำให้การยึดเกาะกับเมทริกซ์ไม่ดีเนื่องจากโครงสร้างโมเลกุลเป็นประเภทมีขั้วและมีพันธะไฮโดรเจนระหว่างโมเลกุลสูงมาก จึงมีงานวิจัยที่ศึกษาหาวิธีปรับผิวของเส้นใยโดยการเติมสารช่วยผสมหรือปรับผิวโดยวิธีทางเคมี (6-10) โดยเฉพาะอย่างยิ่งถ้านำอะรามิดมาผสมกับพอลิเมอร์เมทริกซ์ที่ไม่มีขั้วจะมีปัญหาการยึดเกาะที่รอยต่อระหว่างวัฏภาคมากขึ้นอีก งานวิจัยนี้จึงมุ่งเน้นที่จะแก้ปัญหานี้โดยศึกษาการเตรียมคอมพอสิตระหว่างพอลิเมอร์เมทริกซ์ซึ่งเป็นเทอร์โมพลาสติกอีลาสโตเมอร์ที่ไม่มีขั้วได้แก่ Styrene ethylene butylene styrene (SEBS) และ Santoprene (polypropylene/crosslinked EPDM) กับเส้นใย

อะรามิดโดยการปรับสภาพผิวของเส้นใยโดยวิธีทางเคมีและการเติมสารช่วยผสมเพื่อให้การยึดเกาะระหว่างเส้นใยกับเมทริกซ์ดีขึ้น และน่าจะส่งผลให้สมบัติเชิงกลของพอลิเมอร์ผสมดีขึ้น นอกจากนี้ยังได้ศึกษาคอมพอสิตระหว่างพอลิเมอร์เมทริกซ์ที่มีขั้วเช่นพอลิยูรีเทนเทอร์โมพลาสติกอีลาสโตเมอร์ (Polyurethane thermoplastic elastomer) กับเส้นใยอะรามิด ปรับผิวของเส้นใยโดยการอาบด้วยออกซิเจนพลาสมา

ในการศึกษาระบบที่ใช้พอลิเมอร์เมทริกซ์ประเภทเทอร์โมพลาสติกอีลาสโตเมอร์ที่ไม่มีขั้วนี้เป็นระบบที่ยังไม่มีผู้ศึกษาและรายงานมาก่อน เนื่องจากมีความยุ่งยากมากกว่าการใช้เมทริกซ์ที่มีขั้วซึ่งมีผู้ศึกษามาบ้างแล้ว (4) ทั้งนี้เพื่อให้การใช้งานของเส้นใยอะรามิดและยางเทอร์โมพลาสติกกว้างขวางมากขึ้น และเพื่อให้ได้ความรู้พื้นฐาน และความเข้าใจเกี่ยวกับอิทธิพลของแรงกระทำที่รอยต่อระหว่างวัฏภาคซึ่งมีผลต่อสมบัติของคอมพอสิต ในงานวิจัยนี้ได้ใช้วิธีปรับผิวของเส้นใยอะรามิดเพื่อเพิ่มแรงกระทำระหว่างเส้นใยกับเมทริกซ์โดยวิธีทางเคมี 2 วิธี ได้แก่ การทำ hydrolysis ที่ผิวของเส้นใยเล็กน้อยเพื่อตัดโมเลกุลบางจุดทำให้ได้หมู่ที่ไวต่อการทำปฏิกิริยาคือหมู่ NH_2 ซึ่งจะทำปฏิกิริยากับสารช่วยผสม maleic anhydride grafted SEBS (MA-g-SEBS) ในกรณีที่ใช้เมทริกซ์ SEBS หรือทำปฏิกิริยากับ maleic anhydride grafted polypropylene (MA-g-PP) ในกรณีที่ผสมกับเมทริกซ์ Santoprene อีกวิธีหนึ่งที่ใช้ปรับผิวเส้นใยคือทำให้ความมีขั้วของผิวเส้นใยลดลงโดยการเติมหมู่อัลคิลซึ่งจะทำให้เส้นใยเข้ากันได้กับเมทริกซ์ที่ไม่มีขั้ว ส่วนวิธีปรับผิวโดยใช้ออกซิเจนพลาสมาจะทำให้ผิวของเส้นใยขรุขระและมีหมู่ที่มีขั้วเกิดขึ้นจึงใช้วิธีนี้ปรับผิวเส้นใยในกรณีที่ผสมกับเมทริกซ์ที่มีขั้วคือพอลิยูรีเทนเทอร์โมพลาสติกอีลาสโตเมอร์

คอมพอสิตอีกประเภทหนึ่งที่ศึกษาได้แก่คอมพอสิตระหว่างพลาสติกกับเส้นใยพอลิเมอร์ผลึกเหลวชนิดเทอร์โมโทรบิก (thermotropic liquid crystalline polymer) โดยที่เริ่มต้นเป็นการผสมแบบเบรนด์คือพอลิเมอร์เหลอมเหลวทั้งคู่แต่ไม่ละลายเป็นเนื้อเดียวกัน พอลิเมอร์ผลึกเหลวชนิดนี้กระจายเป็นหยดเล็กๆในเมทริกซ์ เมื่อได้รับแรงเฉือนหรือแรงดึงในเครื่องผสมหรือเครื่องขึ้นรูป พอลิเมอร์ผลึกเหลวชนิดนี้จะยืดตัวออกเป็นเส้น ซึ่งเมื่อทำให้เย็นลงเร็วๆจะได้พอลิเมอร์ผสมรูปแบบเดียวกับคอมพอสิต จึงเรียกว่า อิน-ซิทูคอมพอสิต (in-situ composite) (11-13) คอมพอสิตชนิดใหม่นี้กำลังเป็นที่สนใจมากในปัจจุบันเนื่องจากมีข้อดีหลายประการ เช่น ความหนืดต่ำเมื่อเทียบกับคอมพอสิตปกติทำให้การขึ้นรูปง่าย เสียพลังงานน้อย และเส้นใยที่เสริมแรงนี้ไม่ทำให้เครื่องมือสึกกร่อนเหมือนเส้นใยจากแก้วหรือสารอนินทรีย์ อย่างไรก็ตามพอลิเมอร์ผสมแต่ละคู่จะต้องศึกษาวิธีและสภาวะในการผสมเพื่อปรับขนาดของวัฏภาคของพอลิเมอร์ผลึกเหลวให้เหมาะสมที่จะทำให้ได้คอมพอสิตที่มีสมบัติดีที่สุด(14) รวมทั้งการเลือกใช้สารช่วยผสมเพื่อทำให้การกระจายตัวของ TLCP พอเหมาะที่จะทำให้ได้เส้นใย TLCP ที่มี aspect ratio (ความยาวต่อเส้นผ่าศูนย์กลาง) ของเส้นใยสูงสุด เพื่อให้ได้สมบัติ modulus สูงที่สุด (15-17) ในงานวิจัยนี้ได้เลือกใช้เมทริกซ์ซึ่งเป็นพอลิเมอร์ชนิดไม่มีขั้ว เช่นพอลีพรอพิลีน และ พอลีเอทธิลีน และเลือกใช้พอลิเมอร์ผลึกเหลวเทอร์โมโทรปิกซึ่งเป็นโคพอลิเมอร์ของไฮดรอกซิเบนโซอิกแอซิดและเอทธิลีนเทอเรพธา

เลท การขึ้นรูปคอมพอสิตชนิดนี้ถ้าชิ้นงานหนาจะมีปัญหาจากการเกิด skin-core effect คือบริเวณผิวและภายในชิ้นงานมีการเรียงตัวของโมเลกุลแตกต่างกัน รวมทั้งการเกิด weld-line คือรอยต่อที่เกิดจากการไหลต่างทิศของพอลิเมอร์เหลวมาจรดกัน ซึ่งทำให้สมบัติตกลง (18) เพื่อหลีกเลี่ยงปัญหาเหล่านี้ ในการทดลองนี้จึงขึ้นรูปตัวอย่างเป็นฟิล์มบางเพื่อให้ได้ตัวอย่างที่มีความสม่ำเสมอ ไม่มี skin-core effect และ ไม่มี weld-line นอกจากนี้ยังสามารถวิเคราะห์โครงสร้างสัณฐานได้รวดเร็วโดยการส่องดูด้วยกล้องจุลทรรศน์ธรรมดา ซึ่งสามารถทำได้ระหว่างการแปรสภาวะการขึ้นรูปฟิล์ม การศึกษา in-situ composite ที่เป็นฟิล์มนี้ยังมีผู้ศึกษาไม่มาก เนื่องจากมีปัญหาจาก anisotropy ของสมบัติเชิงกลคือค่าที่วัดในทิศที่ดึงฟิล์ม (machine direction) และค่าที่วัดในทิศตั้งฉาก (transverse direction) ต่างกัน (19-20) ซึ่งมีงานวิจัยที่แก้ปัญหานี้ด้วยการใช้ counter-rotating die (21) เพื่อพัฒนาการทำบอลลูนที่มีความแข็งแรงสูง สำหรับงานวิจัยนี้ได้ศึกษาอิทธิพลของสภาวะที่ใช้ในการผสมและขึ้นรูปชิ้นงาน เช่น อุณหภูมิ อัตราการดึงฟิล์ม ความหนืดของเมทริกซ์ และการเติมสารช่วยผสมที่มีและไม่มีหมู่ที่ไวต่อการทำปฏิกิริยา โดยเฉพาะอย่างยิ่งสารช่วยผสมที่เป็นอีลาสโตเมอร์ซึ่งจะช่วยเพิ่มสมบัติการทนต่อแรงกระแทกด้วย

พอลิเมอร์คอมพอสิตระบบต่างๆที่ศึกษาทั้งหมด แสดงในตารางที่ 1 ซึ่งสรุปประเภทต่างๆ ของเมทริกซ์ พอลิเมอร์ผลึกเหลว วิธีปรับผิว และสารช่วยผสมต่างๆ

ตารางที่ 1 พอลิเมอร์ผสมระบบต่างๆที่ศึกษาประกอบด้วยพอลิเมอร์ผลึกเหลว (LCP) และพอลิเมอร์เมทริกซ์ ต่างๆ โดยใช้วิธีปรับผิว และการใช้สารช่วยผสม

LCP	Polymer matrix	Surface treatment	Compatibilizer
Kevlar pulp	SEBS	hydrolysis	MA-g-SEBS
Conex sf	SEBS	hydrolysis	MA-g-SEBS
Technora sf	SEBS	hydrolysis	MA-g-SEBS
Kevlar pulp	SEBS	N-alkylation	-
Conex sf	SEBS	N-alkylation	-
Kevlar pulp	Santoprene	N-alkylation	-
Conex sf	Santoprene	N-alkylation	-
Conex sf	Polyurethane	plasma	-
Rodrun LC3000	PP (vary MFR)	-	SEBS, MA-g-SEBS, MA-g-PP
Rodrun LC3000	LDPE	-	SEBS, MA-g-SEBS, EPDM, MA-g-EPDM

วิธีการทดลอง

วัสดุพอลิเมอร์และสารเคมีที่ใช้ สมบัติต่างๆ และบริษัทผู้ผลิตแสดงในตารางที่ 2

ตารางที่ 2 วัสดุที่ใช้

Material	Specification	Supplier
KEVLAR pulp and short fiber (poly-p-phenylene terephthalamide)	Decomposition Temp. 427 - 482°C Specific heat at 25 °C 1420 J/kg K Density 1.44 g/cm^3, non-brittle Surface area 7 - 10 m^2/g Moisture regain 6 %, length ~ 2 mm	DuPont
Teijin Conex fiber (poly-m-phenylene isophthalamide)	Decomposition Temp. 400-430°C Specific heat at 25 °C 0.25 kcal/kg °C Density 1.38 g/cm^3, length ~3 mm, diameter ~ 15 μm Moisture regain 5-5.5%, non-brittle	Teijin Co.Ltd.
Teijin Technora fiber (Poly-p-phenylene-3,4'-oxydiphenylene terephthalamide)	Decomposition Temp. >500°C Specific heat at 25 °C 0.4 kcal/kg °C Density 1.39 g/cm^3, length ~3 mm, diameter ~ 12 μm Moisture regain 1.5 – 2%	Teijin Co.Ltd.
Polypropylene (PRO-FAX 6231, 6331, PW583, 6531, 6631))	MFR 22, 12, 8, 4, 2.5 g/10 min, Density 0.903 g/cm^3 Gel < 2 %, Antioxidant 0.07 %	HMC polymer Company Ltd.
Low density polyethylene (1905F)	Density 0.919 g/cm^3, MFI 5 g/10min (190°C, 2.16 kg)	Thai Polyethylene
Rodrun LC 3000	Density 1.4 g/cm^3 Molar ratio of PHB/PET = 60/40 T_m = 220°C, T_c > 300°C	Unitika Ltd.
SEBS (KRATON G1652)	S/EB ratio 29/71, M_w : of S-block 7200, EB-block 37500, S-block: T_g 95°C T_m 165 °C, EB-block: T_g -60°C	Shell Chemical Co.

ตารางที่ 2 (ต่อ)

Material	Specification	Supplier
Santoprene 691-73W175 thermoplastic elastomer	Density 0.98 g/cm^3 brittle point < -60°C, containing 18% PP and 82% cross-linked EPDM (from DSC)	Advanced Elastomer Systems
Polyurethane (Desmopan) 385)	Polyester-urethane type, density 1.2 g/cm^3, M_W = 341,000 (from GPC)	Bayer
EPDM (Royalene 501)	E/P = 59/41, ene = 4 wt%, density 0.86 g/cm^3,	Uniroyal Chemical Co. Inc.
MA-g-SEBS (Kraton FG1901X)	MA content 1.8 wt%, MFI 22 g/10 min	Shell Chemical Co.
MA-g-EPDM (Royaltuf 490)	Density 0.89, MA content 1.0 wt% , E/P ratio 55/45	Uniroyal Chemical Co. Inc.
MA-g-PP (polybond 3150)	MFR 50g/10 min (230°C/2.16kg), density 0.89 g/cm^3, MA content 0.5 wt%	Uniroyal Chemical Co. Inc.
MA-g-PP (Modic P-300M)	MFR 12 g/10 min, density 0.89 g/cm^3 , MA content 0.1 wt%	Mitsubishi Co.
Pentyl bromide	Synthesis grade	Eastman
Heptyl bromide	synthesis grade	Eastman
Dodecyl bromide	synthesis grade	Eastman
Dimethyl sulfoxide	anhydrous	Fluka
Sodium hydride	60% in paraffin oil suspension	Merck
Sodium hydroxide	Analytical grade	BDH
Toluene	Analytical grade	JT Baker
Xylene	Analytical grade	JT Baker

ตารางที่ 3 เครื่องมือต่างๆที่ใช้ผสม ขึ้นรูป ตรวจโครงสร้างและ ทดสอบสมบัติ

Instrument	Model	Company
FT-IR	PE 2000	Perkin-Elmer
Internal Mixer	Haake Rheocord 90	Haake
Two-roll Mill	NS-76	Nishimura
Tensile Tester	Instron 4301	Instron
Impact Tester	ITR-2000	Radmana
Hot Press	A-251400363	Toyoseiki
SEM	S-2500	Hitachi
Sputtering Coater	E102	Hitachi
Twin Screw Extruder	TSE-16-TC	PRISM
Microtruder Cast Film Line	RC-0625	RANDCASTLE
Injection Moulding	BOY 22S	Dr.BOY
Plasma Reactor (bell jar)	BP-1	Samco
Capillary Rheometer	Rosand RH710	Rosand
Melt Indexer	7053	Keyeness
DMTA	Mk II	Polymer Laboratories

วิธีทดลอง

1. การปรับผิวของเส้นใยพอลิเมอร์ผลึกเหลวไลโอโทรปิก (aramid fibers)

1.1 ปรับผิวเส้นใยโดยวิธี Hydrolysis

ล้างเส้นใยให้สะอาดด้วย acetone และน้ำกลั่น อบให้แห้งที่อุณหภูมิ 50°C ในเตาอบสุญญากาศ แล้วนำไปทำปฏิกิริยา hydrolysis โดยใช้ 10% NaOH เป็นเวลานาน 20 นาที ล้างด้วยน้ำกลั่น และ toluene แล้วอบให้แห้งที่ 60°C ในตู้อบสุญญากาศ

1.2 ปรับผิวเส้นใยโดยวิธี N-alkylation

ทำความสะอาดผิวของเส้นใยทำนองเดียวกับวิธีที่ 1.1 แล้วนำไปทำปฏิกริยา alkylation บนผิวของเส้นใย โดยผสม NaH 0.025 mole ใน ตัวทำละลาย dimethylsulfoxide 37.5 ml. ที่อุณหภูมิห้องเป็นเวลา 20 นาที แล้วจึงเพิ่มอุณหภูมิเป็น 70°C คนเป็นเวลานาน 40 นาที แล้วลดอุณหภูมิลงเหลือ 30°C เติม aramid fiber (แห้ง) 3 g ลงในปฏิกิริยา คนต่อไปเป็นเวลา 10 นาที แล้ว จึงเติม 1-bromoalkane 0.025 mole ปล่อยให้ปฏิกิริยาดำเนินไปเป็นเวลา 2 ชั่วโมง

แล้วหยุดปฏิกิริยาโดยเทของผสมทั้งหมดลงในน้ำกลั่น กรองเส้นใยที่ได้ แล้วอบให้แห้งที่อุณหภูมิ 60°C ในตู้อบสุญญากาศ

1.3 ปรับผิวเส้นใยโดยใช้ออกซิเจนพลาสมา

เตรียมเส้นใยโดยล้างสิ่งสกปรกออกด้วย methylene chloride, methanol และ deionized water ตามลำดับ นำเส้นใยไปอบให้แห้งใน vacuum oven ที่อุณหภูมิ 60°C นำเส้นใยไปปั่นด้วยเครื่อง Moulinex เป็นเวลา 30 วินาที เพื่อให้เส้นใยกระจายออกจากกัน ทำ plasma treatment ด้วยเครื่อง SAMCO model BP-1 bell jar plasma reactor (radio frequency 13.56 MHz) โดยดัดแปลง electrode ให้อยู่ตำแหน่งห่างจากภาชนะที่ใส่เส้นใย และใช้ oxygen gas ในการ generate plasma สภาวะที่ใช้คือความดัน 0.1 torr ใช้ power 100 W และ 60 W สำหรับเส้นใย Conex และ Technora ตามลำดับ โดยแปรเวลาที่อาบพลาสมา

2. การผสมพอลิเมอร์

2.1 การผสมโดยใช้เครื่องผสมภายใน (internal mixer)

ปั่น fiber ด้วยเครื่อง moulinex 30 วินาทีเพื่อให้เส้นใยกระจายออกจากกัน แล้วจึงผสม aramid fibers สารช่วยผสม และ thermoplastic elastomer ลงใน internal mixer ที่อุณหภูมิ 165°C ในกรณีของ SEBS matrix และ ที่อุณหภูมิ 175°C ในกรณีของ Santoprene matrix ใช้ rotor speed 90 rpm เป็นเวลานาน 10 นาที

2.2 ผสมโดยใช้เครื่อง twin screw extruder

ใช้เครื่อง twin screw extruder ในกรณีของการผสมพลาสติกพอลิพรอปิลีน หรือพอลิเอทธิลีน กับพอลิเมอร์ผลึกเหลวชนิดเทอร์โมโทรปิก Rodrun LC3000 โดยใช้ rotor speed 150 rpm อุณหภูมิจาก hopper ถึงหัว die 180/220/220/225/225°C ตามลำดับ และใช้ในกรณีผสม polyurethane กับ aramid short fiber โดยใช้ rotor speed 50 rpm อุณหภูมิจาก hopper ถึงหัว die 175/195/200/195/185°C ตามลำดับ พอลิเมอร์ผสมที่ได้รีดออกมาเป็น strand ทำให้เย็นโดยเร็วในอ่างน้ำ ตัดด้วย pelletizer แล้วนำไปอบให้แห้งที่ 60°C ในตู้อบสุญญากาศ

3. การขึ้นรูปพอลิเมอร์ผสม

3.1 การอัดด้วยแท่นร้อน (compression molding)

สำหรับ aramid fiber ผสมกับ SEBS และ Santoprene หลังจากผสมใน internal mixer เสร็จแล้วนำออกมารีดให้เป็นแผ่นโดยการผ่าน two-roll mill 1-2 ครั้ง แล้วนำไปขึ้นรูปโดยใช้วิธีอัดเป็นแผ่นด้วยแท่นร้อนที่ 195°C นาน 10 นาที โดยใช้ความดัน 15 Mpa

3.2 การฉีด (injection molding)

ขึ้นรูปโดยวิธี injection molding ในกรณีของพอลิเมอร์ผสมระหว่าง polyurethane กับ aramid fiber โดยการฉีดเป็นรูป dumbbell shape ตามขนาดมาตราฐาน ISO/DIS 527 type B โดยมีสภาวะที่ใช้คือ temperature profile จาก hopper ถึง nozzel 180/195/35%°C, Screw speed 150 rpm

3.3 การขึ้นรูปเป็นฟิล์มโดยใช้ microtruder cast film line

นำพอลิเมอร์ผสมที่เตรียมได้ไปขึ้นรูปเป็นฟิล์มโดยใช้ Cast film mini-extruder (Randcastle RCP-0625) สภาวะที่ใช้ในการเตรียมคือ screw speed 70 rpm ในกรณี PP matrix และ 40 rpm ในกรณี PE matrix แรงดันที่หัว die 300-450 psi อุณหภูมิจาก hopper zone ถึง die คือ 190/220/230/240°C และ 220/240/255/255°C ฟิล์มที่ฉีดออกมาพันหัว die ทำให้เย็นโดยเร็วด้วย water-cooled roll ปรับ take-off speed เพื่อให้ได้ฟิล์มที่มีค่า draw ratio (slit width - to - film thickness ratio) อยู่ในช่วง 5 - 33 หรือมีความหนาของฟิล์มอยู่ในช่วง 20 - 100 μm

4. การพิสูจน์โครงสร้างผิวเส้นใย

4.1 โดยใช้ FTIR-DRIFT technique

ผิวของเส้นใยก่อนและหลังการปรับผิว รวมทั้งเส้นใยที่สะกัดออกมาจากคอมพอสิตโดยใช้ตัวทำละลาย สามารถวิเคราะห์โครงสร้างทางเคมีได้โดยใช้ FTIR diffuse reflectance technique (Perkin-Elmer PE2000) ในช่วง 4000 – 600 cm^{-1} โดยวัด 200 scan, resolution 4 cm^{-1}

5. การตรวจสอบโครงสร้างสัณฐาน

5.1 โดยใช้กล้องจุลทรรศน์อิเล็กตรอนแบบกวาด (scanning electron microscope, SEM, Hitachi S-2500) และเคลือบผิวด้วย palladium ได้ใช้ SEM ตรวจสอบโครงสร้างสัณฐานทั้งของ fiber ก่อนและหลังการปรับสภาพผิว และใช้ SEM ตรวจดู fracture surface ของ composite (โดยการแช่ตัวอย่างในไนโตรเจนเหลวประมาณครึ่งชั่วโมง แล้วหักเร็วๆ) เพื่อดูการยึดเกาะระหว่าง fiber และ matrix รวมทั้งดูผิวของ fiber หลัง extract จาก composite เพื่อดูยางที่เกาะติดอยู่ด้วยพันธะเคมี (bound rubber) โดยใช้กำลังขยายจาก 200 – 5000 เท่า accelerating voltage 15 kV

5.2 โดยการใช้กล้องจุลทรรศน์โพลาไรซ์ (polarized optical microscope)

ในกรณีที่ผลิตพอลิเมอร์ผสมเป็นฟิล์มบาง สามารถส่องดูโครงสร้างสัณฐานโดยตรง โดยใช้กล้องจุลทรรศน์ที่มีโพลาไรเซอร์ จะเห็นการกระจายของเส้นใย TLCP รวมทั้งลวดลายของ texture ซึ่งจะบอกให้รู้ถึงความเป็นระเบียบในการเรียงตัวของโมเลกุลด้วย โดยใช้กำลังขยาย 100 – 400 เท่า

6. การวัดสมบัติเชิงกลของพอลิเมอร์ผสม

6.1 การวัดสมบัติ tensile

สมบัติ tensile ได้แก่ค่า modulus, yield strength, tensile strength, elongation at yield, elongation at break สำหรับ aramid fiber ผสม thermoplastic elastomer ใช้วิธีมาตรฐาน ASTM D638 โดยตัดตัวอย่างเป็นรูป dumbbell ขนาด 115 mm x 6 mm, ใช้ cross head speed 500 mm/min, full scale load cell 100 kg ค่าที่ได้เฉลี่ยจากอย่างน้อย 5 ตัวอย่าง ส่วนตัวอย่างที่เป็นฟิล์มใช้วิธีมาตรฐาน ASTM D412 โดยตัดตัวอย่างเป็นรูป dumbbell ขนาด 70 mm x 4 mm, ใช้ cross head speed 50 mm/min, grip length 25 mm, full scale load cell 10 หรือ 100N สำหรับฟิล์มค่าที่ได้เฉลี่ยจากอย่างน้อยจาก 10 ตัวอย่าง

6.2 การวัด Dynamic properties

โดยใช้เครื่อง DMTA Mk II (Polymer Laboratories) โดยใช้ bending mode, frequency 3 - 10 Hz ตัวอย่างยาว 5 mm, displacement 64 μm ที่ อุณหภูมิ -120 – 120°C, scan rate 5°C/min

6.3 การวัด impact strength

วัด impact strength ของฟิล์ม PP/LC3000 โดยใช้เครื่อง pneumatic driving impact tester Radmana ITR-2000 (ASTM D3763) ตัวอย่างหนา 70 μm เฉลี่ยจากอย่างน้อย 10 ตัวอย่าง

7. การวัดความหนืด

7.1 วัดค่า Melt flow rate โดยใช้ melt flow rate tester (Kayeness 7053) ของระบบพอลิเมอร์ผสม TLCP/thermoplastic เช่น TLCP/PP ที่ 230°C โดยใช้น้ำหนัก 2.16 kg เป็นเวลา 10 นาที (ASTM D1328)

7.2 วัด melt viscosity ของ thermoplastics และ พอลิเมอร์ผสม TLCP/thermoplastic โดยใช้เตรื่อง capillary rheometer (Rosand RH710) ที่อุณหภูมิ 240 และ 250 °C ใช้ capillary ที่มีเส้นผ่าศูนย์กลาง 1 mm ยาว 16 mm (L/D = 16) แปร shear rate

ระหว่าง 60 -10^4 s^{-1} ปรับข้อมูลที่ได้ให้ถูกต้องโดยวิธี Bagley corrections และ Rabinowitsch corrections ตามวิธีของระบบ Rosand

8. การวัด order parameter

สำหรับตัวอย่างที่เป็นฟิล์ม PP/LC3000 ได้วัดดัชนีแสดงความเป็นระเบียบของโมเลกุล (order parameter) โดยใช้ FTIR วัด absorbance โดยวาง polarizer ในแนวขนาน ($A_{\parallel}$) และตั้งฉาก ($A_{\perp}$) กับทิศที่ฉีดฟิล์ม คำนวณค่า dichroic ratio, $R = A_{\parallel}/A_{\perp}$, และคำนวณค่า order parameter จากสูตร $S = (R - 1)/(R + 2)$ ในกรณีที่ $R > 1$ คือเป็น absorption band ที่ได้จาก parallel transition moment หรือ $S = 2(1 - R)/(R + 2)$ กรณีที่ $R < 1$ คือเป็น absorption band ที่ได้จาก perpendicular transition moment

ตัวอย่างของ IR spectra ของฟิล์ม TLCP/PP แสดงในรูปข้างล่าง peak ที่นำมาคำนวณ order parameter คือที่ตำแหน่ง 1601 cm^{-1} และ 726 cm^{-1} ซึ่งเป็น parallel และ perperducular band ตามลำดับ

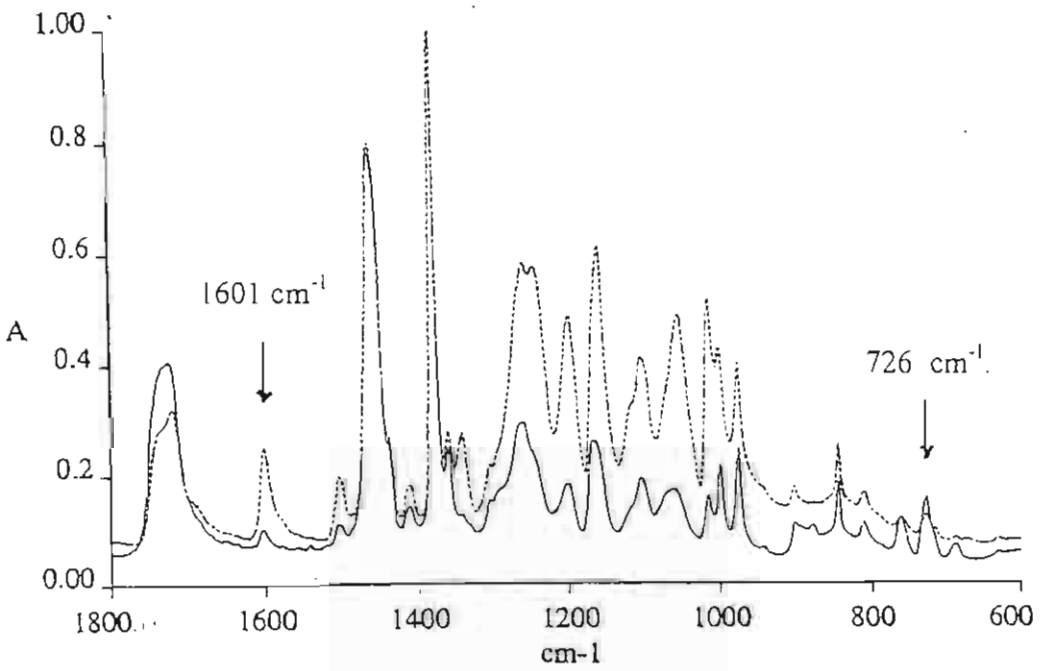

IR spectra ของฟิล์ม TLCP/PP วัดโดยวาง polarizer ขนาน (----------) และตั้งฉาก (——) กับทิศการฉีดฟิล์ม

ผลการทดลองและวิจารณ์

1. ผลของการปรับผิวเส้นใยอะรามิด

1.1 ผลของการปรับผิวด้วยวิธี hydrolysis

ปฏิกิริยาที่เกิดขึ้นจากการทำ hydrolysis บนผิวของเส้นใยอะรามิด ทำให้โมเลกุลถูกตัดบางจุด ได้หมู่ที่ไวต่อการทำปฏิกิริยาเพิ่มขึ้นได้แก่หมู่ NH_2 และ COOH ตัวอย่างปฏิกิริยา hydrolysis ของ Conex แสดงในรูปที่ 1.1

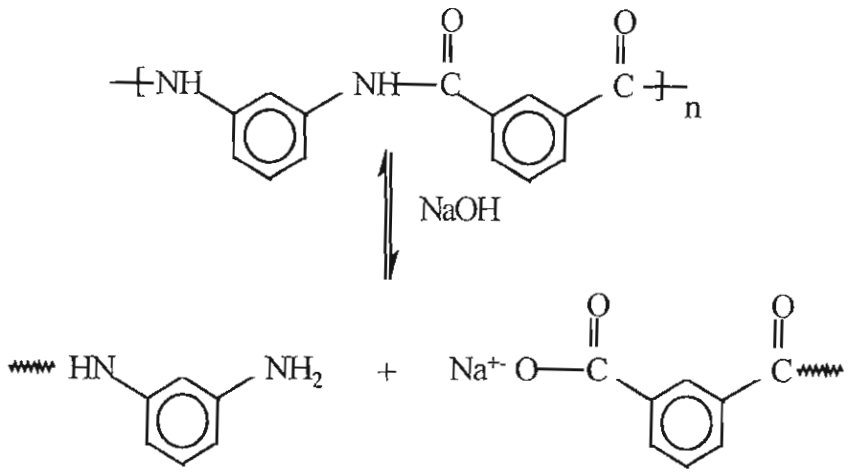

รูปที่ 1.1 ปฏิกิริยา hydrolysis ของ Conex

หลังจากทำปฏิกิริยา นำเส้นใยที่ได้ไปตรวจสอบโครงสร้างโมเลกุลโดยใช้ FTIR DRIFT technique ได้ spectra ดังแสดงในรูปที่ 1.2 ของ Conex, Kevlar และ Technora ก่อนและหลังการปรับผิวด้วยวิธี hydrolysis พบว่ามี peak ใหม่เกิดขึ้นที่ตำแหน่ง 880, 884 และ 881 cm-1 ตามลำดับ ซึ่งเกิดจากหมู่ C-H out-of-plane bending ของ benzene ring ที่อยู่ติดกับ หมู่ $COONa^+$ แสดงว่าการทำ hydrolysis ประสบความสำเร็จ

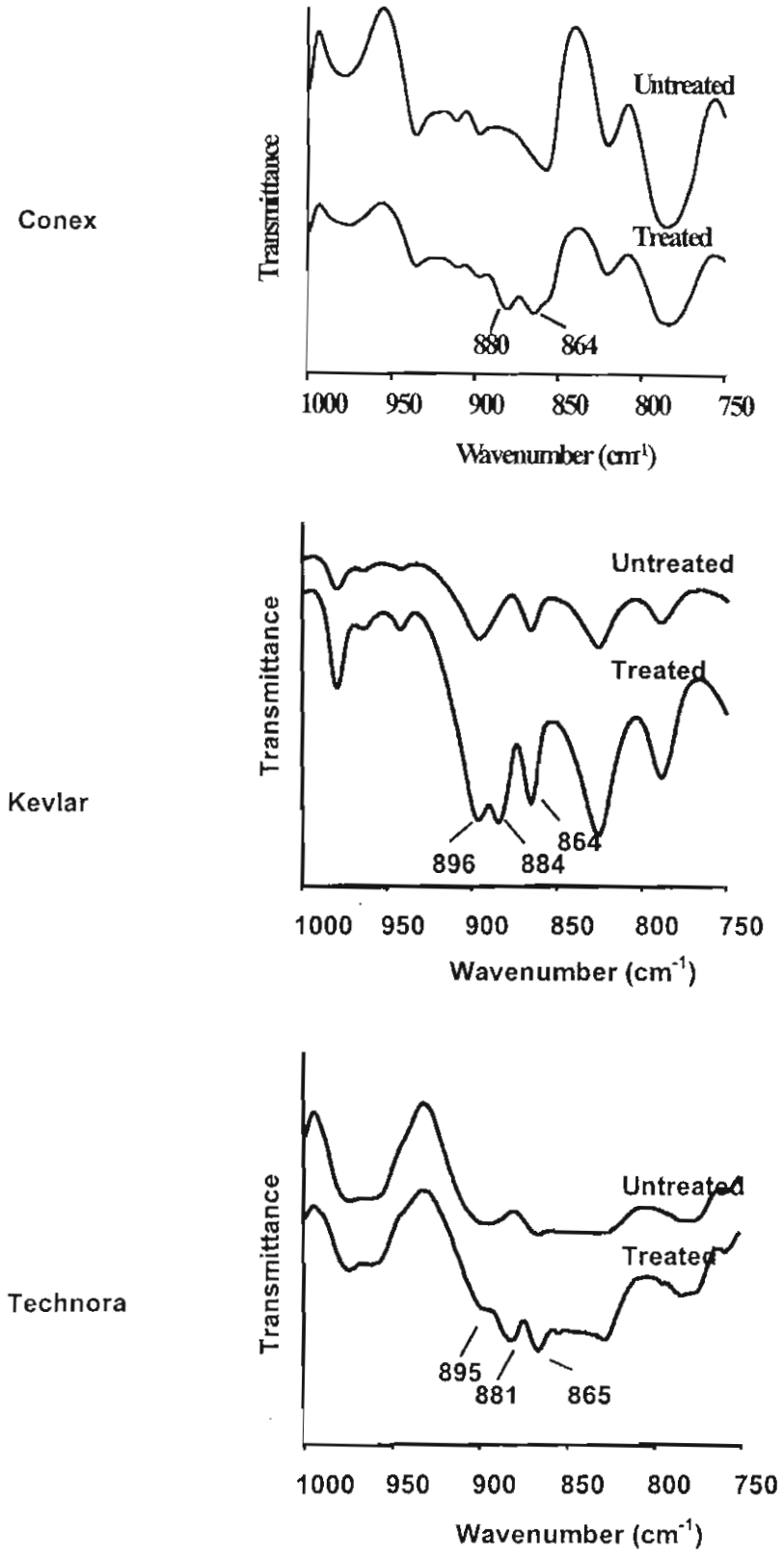

รูปที่ 1.2 FTIR DRIFT spectra ของเส้นใย Conex, Kevlar และ Technora ก่อนและหลังการทำ hydrolysis

1.2 ผลของการปรับผิวโดยวิธี N-alkylation

ปฏิกิริยา N-alkylation บนผิวของเส้นใยอะรามิด แสดงตัวอย่างปฏิกิริยาในสมการข้างล่างในกรณีของ Conex

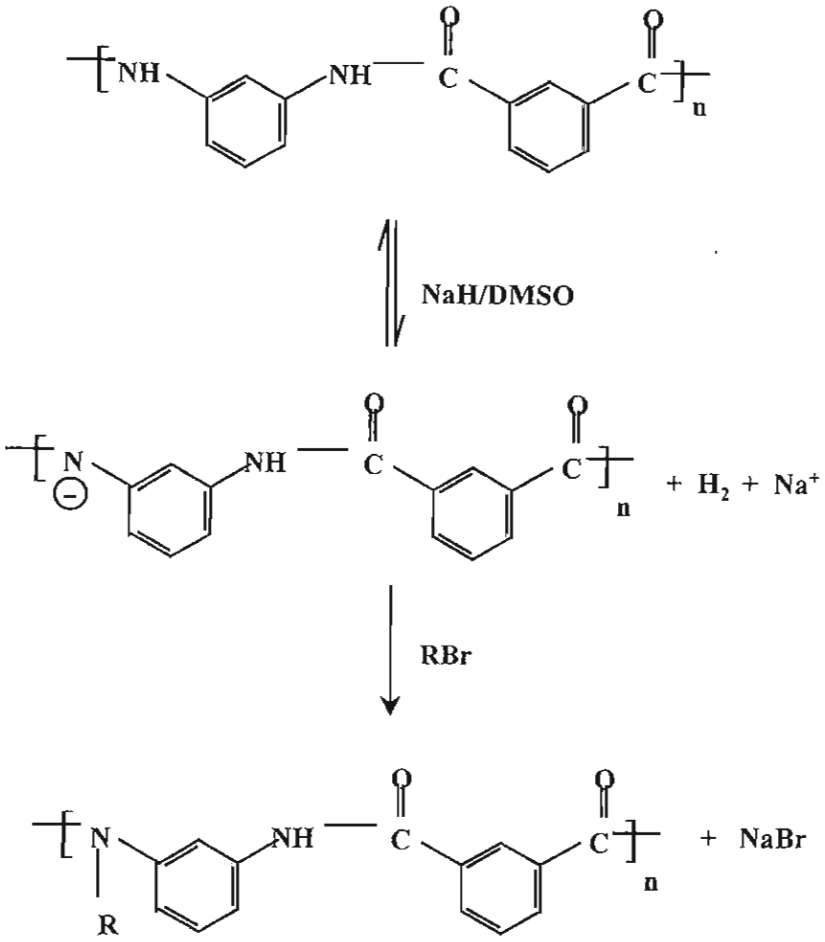

รูปที่ 1.3 แสดงปฏิกิริยา N-alkylation ของ Conex

เมื่อนำเส้นใยที่ได้หลังจากทำ N-alkylation ไปวัด FTIR DRIFT spectra ได้ผลดังแสดงในรูปที่ 1.4 ของ Conex จะเห็น stretching vibration ของ heptyl group ที่ ตำแหน่ง 2932 และ 2858 cm^{-1} และของ dodecyl group ที่ตำแหน่ง 2925 และ 2854 cm^{-1} ตามลำดับ ซึ่งเดิมไม่ปรากฏใน aramid fiber เนื่องจากไม่มี alkyl group ในโมเลกุล แสดงว่าบนผิวของ fiber มีหมู่ alkyl ไปเกาะดังที่ต้องการ

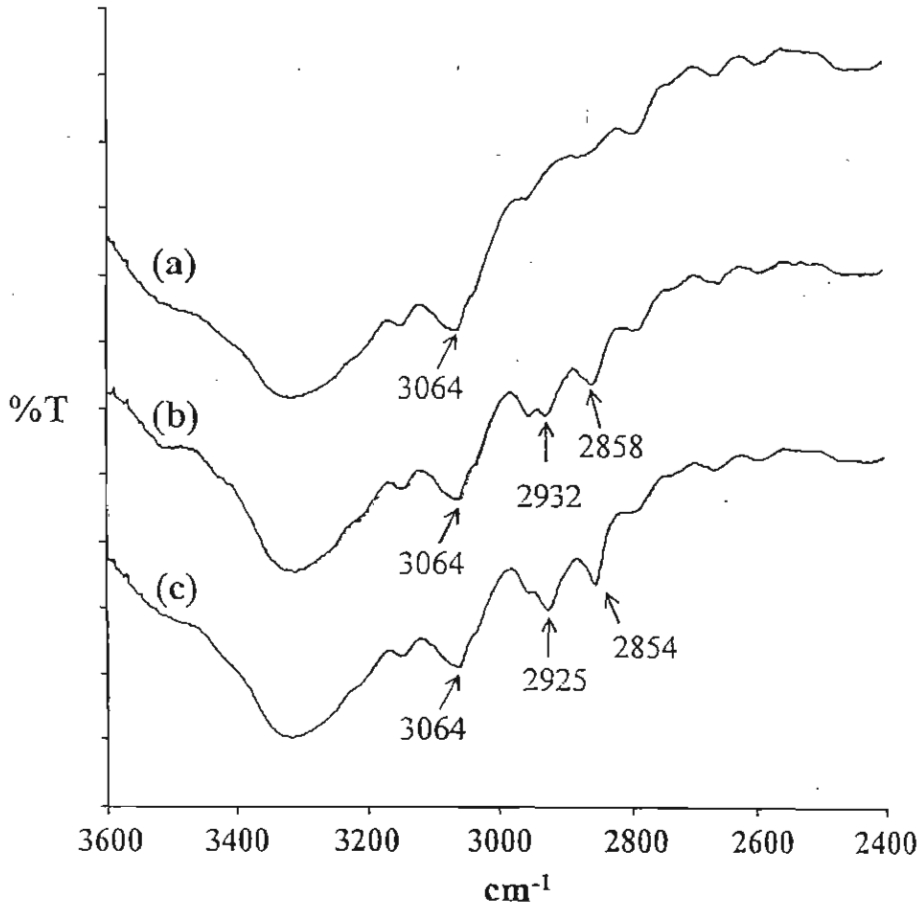

รูปที่ 1.4 FTIR spectra ของ (a) untreated Conex (b) heptylated Conex
(c) dodecylated Conex

1.3 โครงสร้างสัณฐานของเส้นใย

จาก SEM micrographs จะเห็นลักษณะของเส้นใย Kevlar Conex และ Technora ก่อนการปรับผิวดังแสดงในรูปที่ 1.5 จะเห็นว่า short fiber มีผิวเรียบ ส่วน pulp มี fibrillation มาก และหลังการปรับผิวของเส้นใย Kevlar และ Conex โดยวิธี hydrolysis และ N-alkylation แสดงในรูปที่ 1.6 และ รูปที่ 1.7 ตามลำดับ แสดงให้เห็นถึงลักษณะผิวที่เปลี่ยนไป มีความขรุขระของผิวเกิดขึ้นมากหลังการทำปฏิกิริยา

รูปที่ 1.8 และ 1.9 แสดง SEM micrographs ของเส้นใย Conex และ Technora ที่ผ่านการทำ oxygen plasme treatment โดยใช้ความดัน 0.1 torr, กำลังงาน 100W และ 60W ที่เวลาต่างๆ จะเห็นว่า เส้นใย Conex มีลักษณะถูกเซาะเป็นร่องลึกขึ้น ส่วนเส้นใย Technora ผิวจะมีลักษณะพองล่อนออกเป็นแผ่น เมื่อใช้เวลาในการอาบพลาสมานานขึ้น

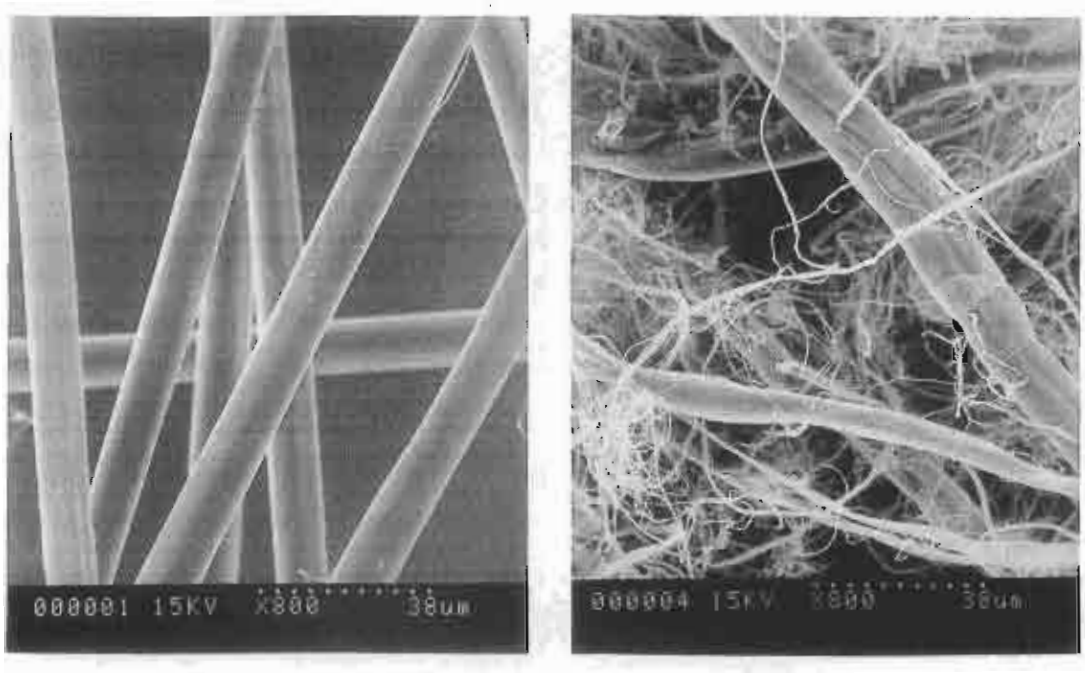

(a) (b)

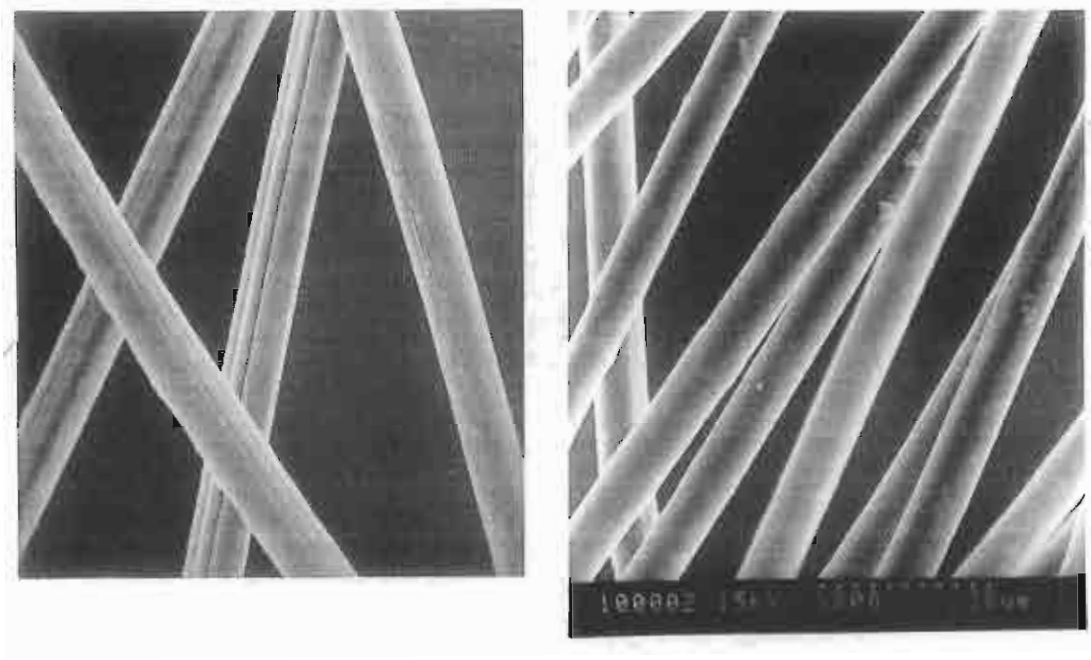

(c) (d)

รูปที่ 1.5 SEM micrographs ของ (a) Kevlar short fiber, (b) Kevlar pulp, (c) Conex short fiber และ (d) Technora short fiber ก่อนปรับผิว

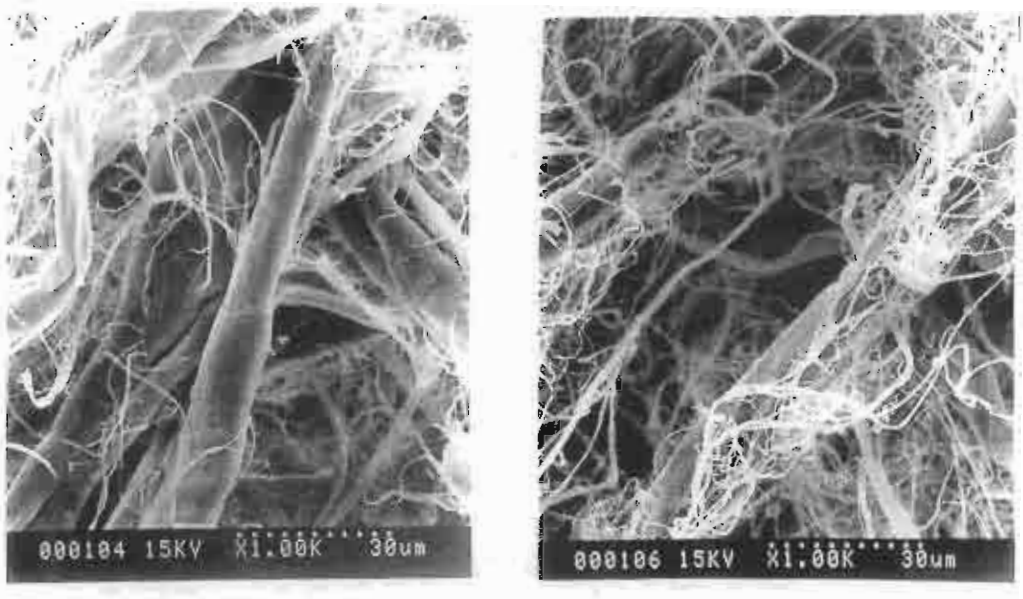

(a) (b)

(c)

รูปที่ 1.6 SEM micrographs Kevlar pulp (a) ก่อนปรับผิว (b) หลังปรับผิวด้วยวิธี hydrolysis (c) หลังปรับผิวด้วยวิธี dodecylation

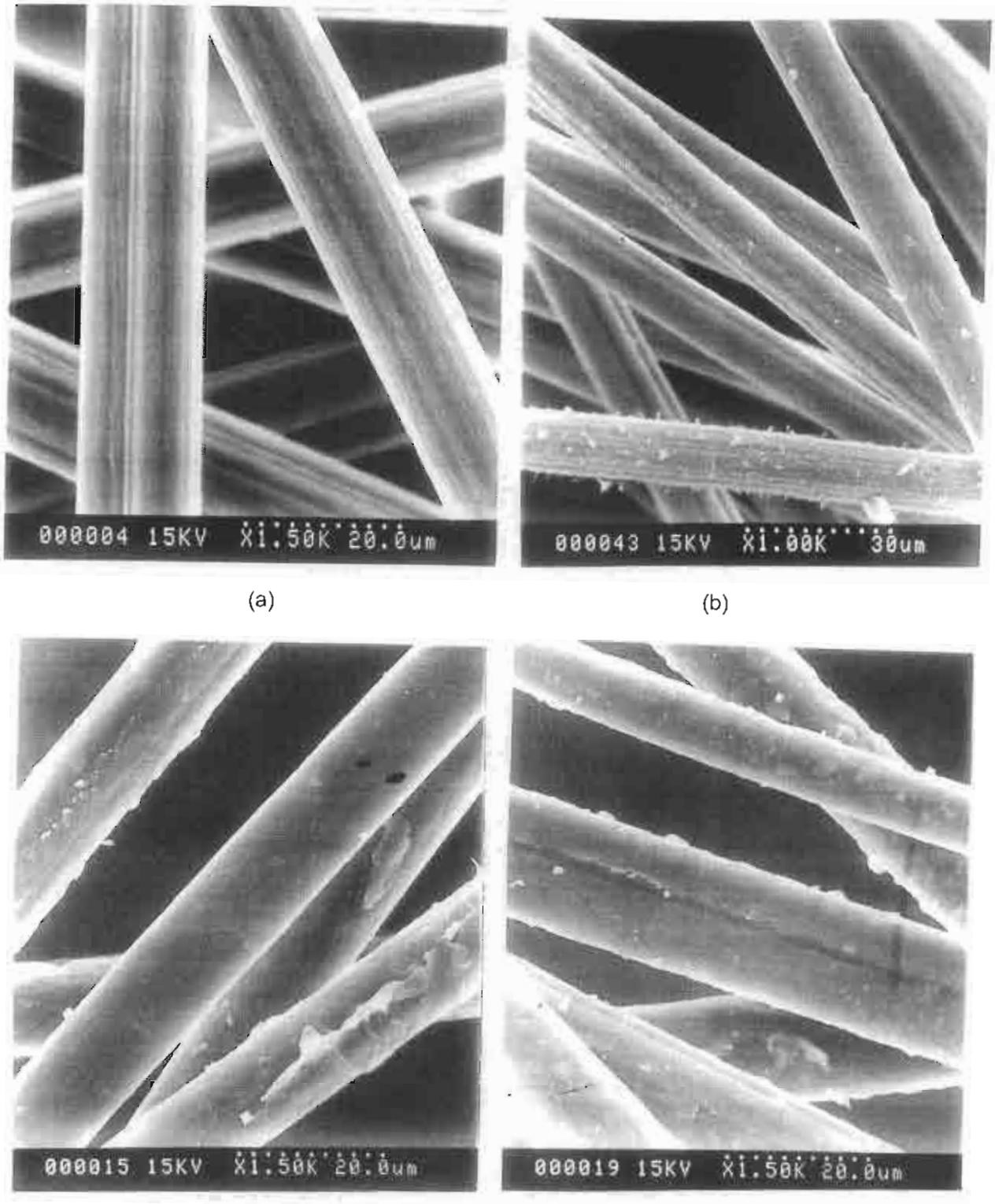

(a) (b)

(c) (d)

รูปที่ 1.7 SEM micrographs ของ Conex short fiber (a) ก่อนปรับผิว (b) หลังปรับผิวด้วยวิธี hydrolysis (c) หลังปรับผิวด้วยวิธี N-heptylation และ (d) หลังปรับผิวด้วยวิธี N-dodecylation

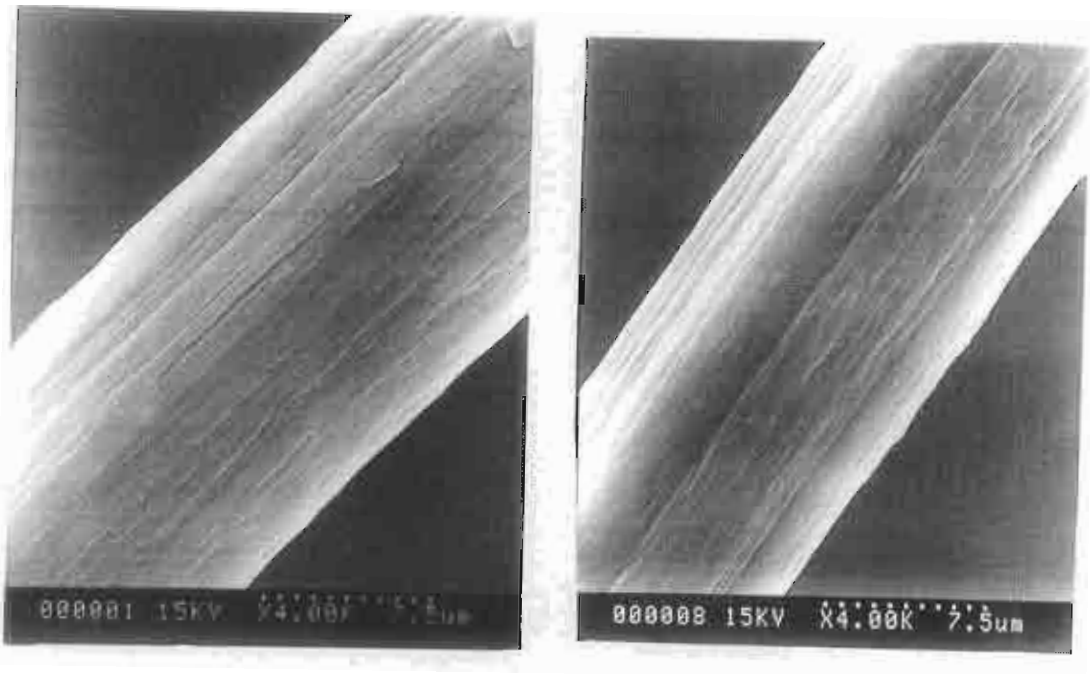

(a) (b)

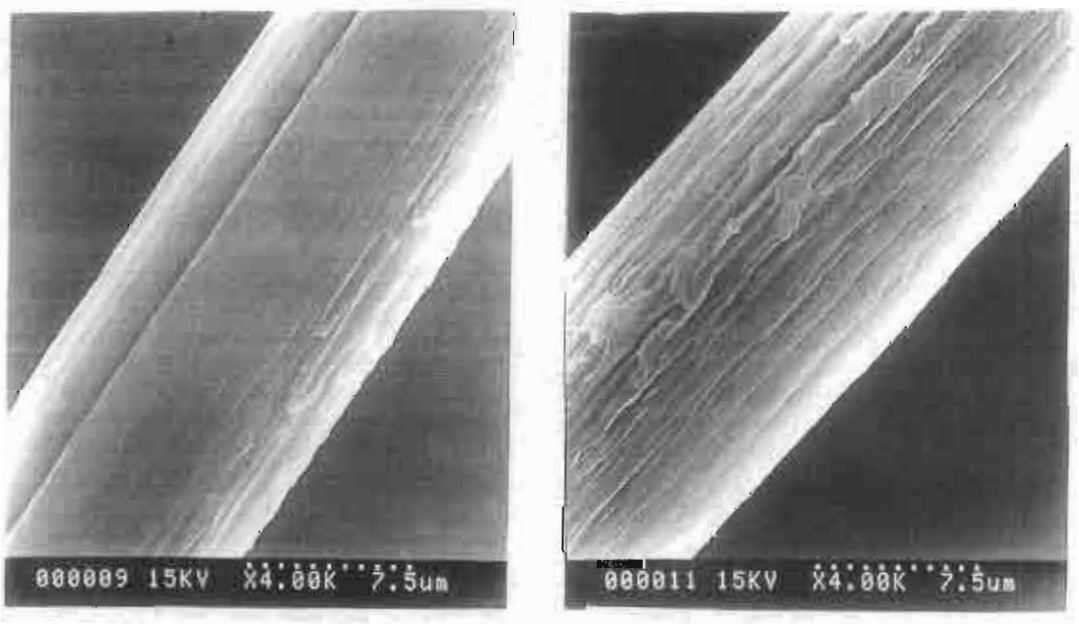

(c) (d)

รูป 1.8 ผลของการอาบออกซิเจนพลาสมาบนผิวของ Conex fiber ความดัน 0.1 torr, กำลัง 100W ที่เวลา (a) 0, (b) 5, (c) 10 และ (d) 15 นาที

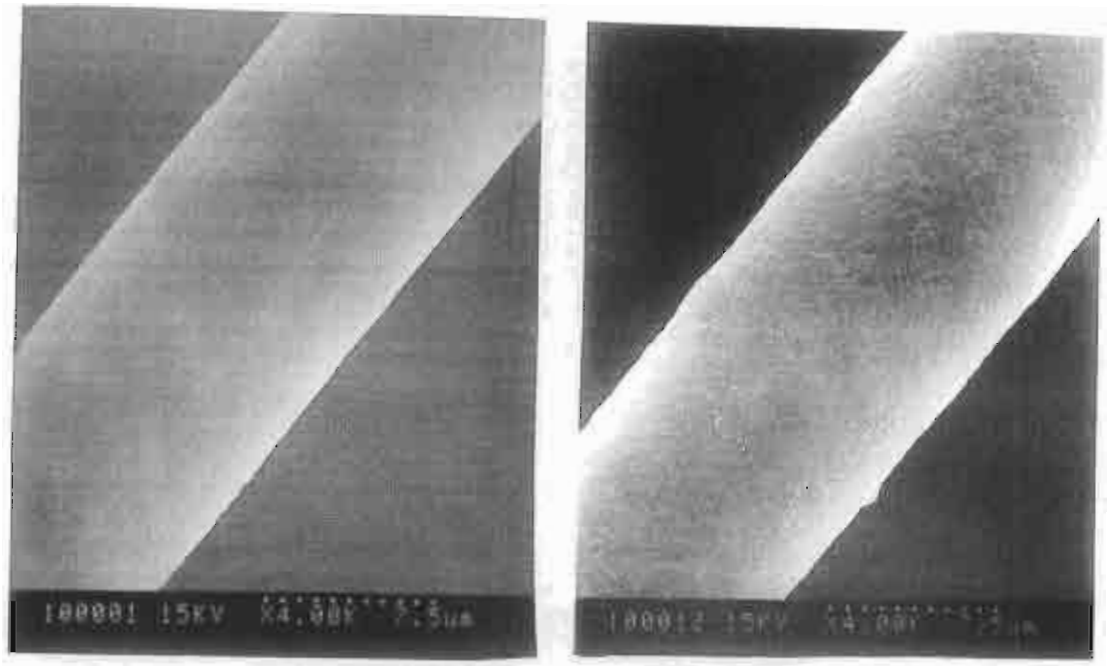

(a) (b)

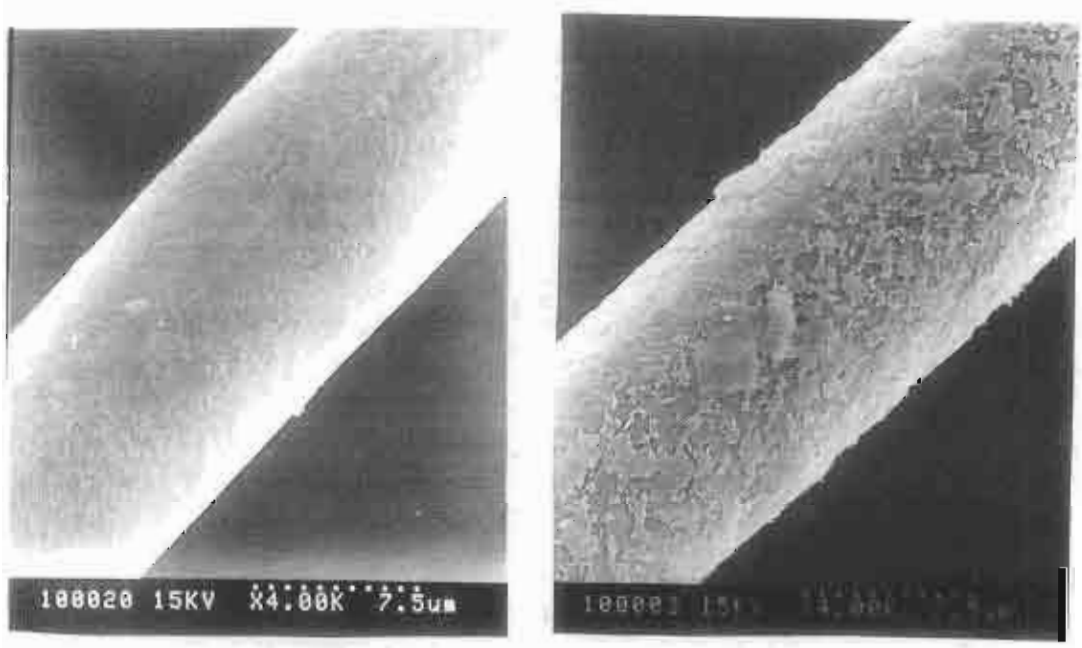

(c) (d)

รูปที่ 1.9 ผลของการอาบออกซิเจนพลาสมาบนผิวของ Technora fiber ความดัน 0.1 torr, กำลัง 60W ที่เวลา (a) 0, (b) 5, (c) 10 นาที และ (d) ที่กำลัง 100W เป็นเวลา 15 นาที

2. คอมพอสิตระหว่างเส้นใยอะรามิดกับเทอร์โมพลาสติกอีลาสโตเมอร์

2.1 คอมพอสิตระหว่างเส้นใย Kevlar, Conex และ Technora กับ SEBS matrix

ผลของปริมาณเส้นใยต่อค่าความทนต่อแรงดึง แสดงโดย stress-strain curves ดังรูปที่ 2.1 – 2.3 สำหรับ Kevlar/SEBS, Conex/SEBS และ Technora/SEBS composites ตามลำดับ แสดงให้เห็นว่า SEBS ซึ่งเป็นอีลาสโตเมอร์ที่มี strain crystallization effect สูง ทำนองเดียวกับ vulcanized rubber เมื่อเติม fiber ทำให้ strain crystallization effect ลดลง โดยที่ความยาวที่จุดขาดไม่เปลี่ยนในช่วงที่ปริมาณเส้นใยต่ำกว่า 5% แต่ค่า tensile strength ลดลง ในขณะที่เมื่อปริมาณเส้นใยมากกว่า 5% ค่าความยาวที่จุดขาดลดลง แต่ค่า tensile strength ไม่ต่างกันมาก

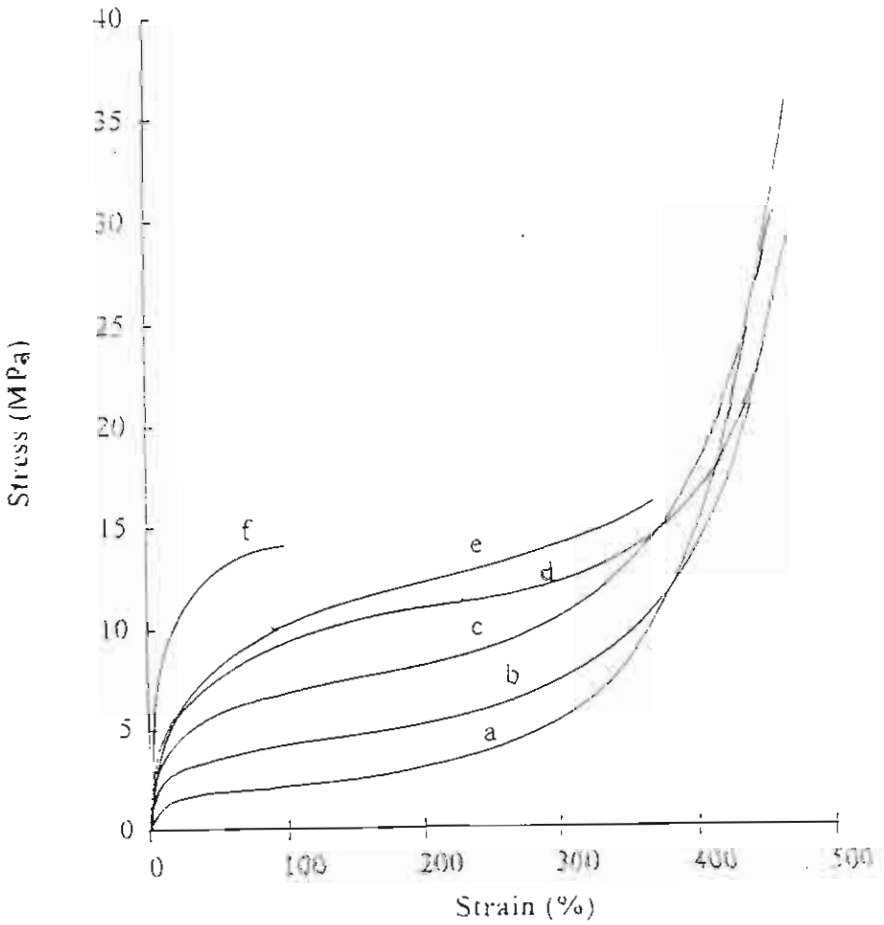

รูปที่ 2.1 Stress-strain curves ของ Kevlar pulp/SEBS composite ปริมาณเส้นใย (%wt) : a = 0, b = 1, c = 3, d = 5, e = 7 และ f = 10

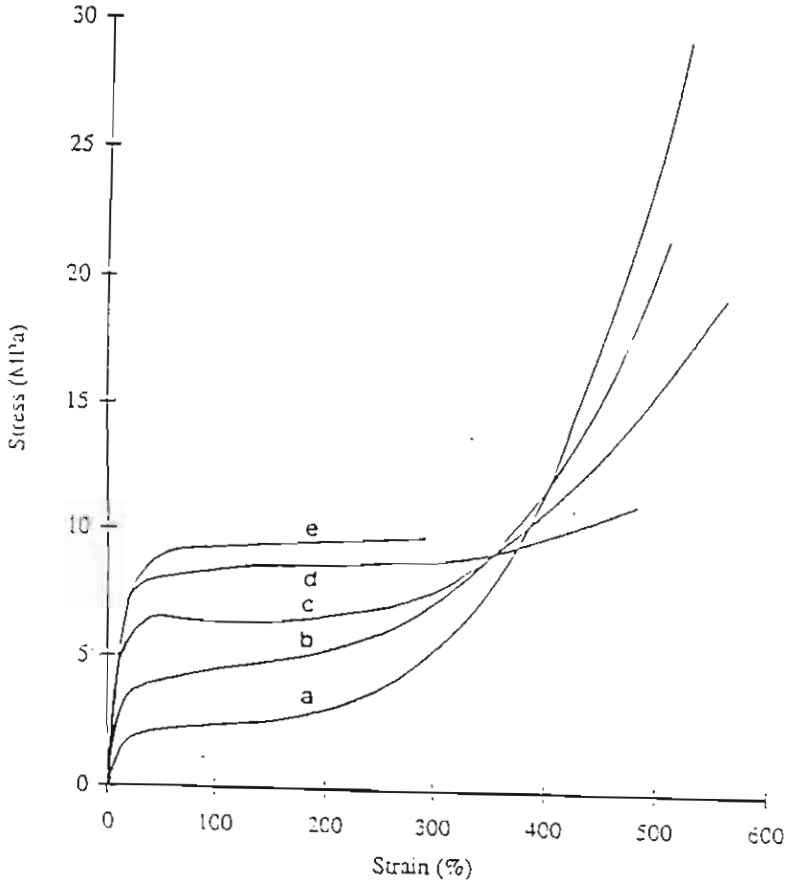

รูปที่ 2.2 Stress-strain curves ของ Conex short fiber/SEBS composite ปริมาณเส้นใย (%wt) : a = 0, b = 1, c = 3, d = 5, e = 7

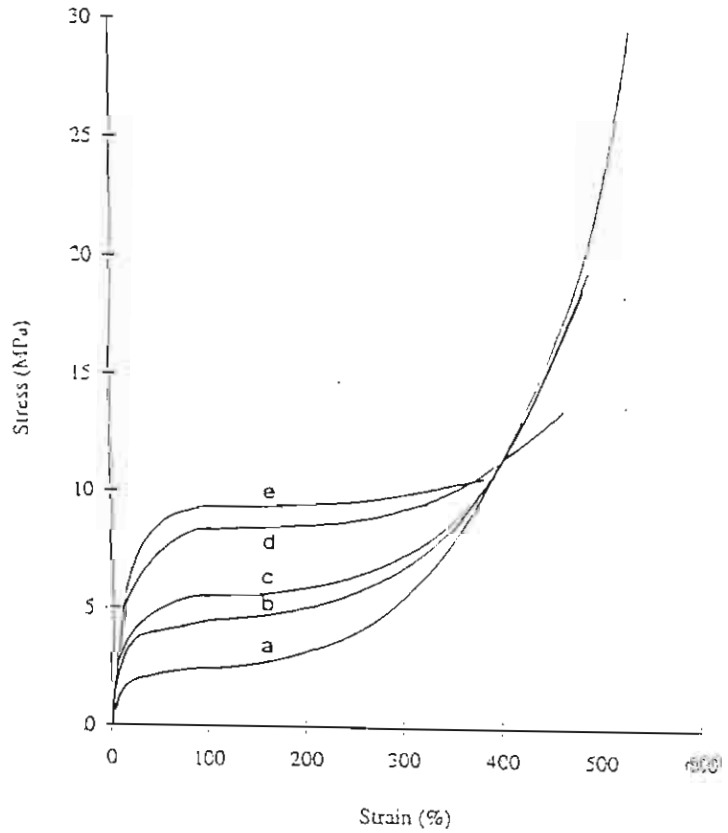

รูปที่ 2.3 Stress-strain curves ของ Technora short fiber/SEBS composite ปริมาณเส้นใย (%wt) : a = 0, b = 1, c = 3, d = 5, e = 7

เมื่อปรับผิวของเส้นใยทั้งสามชนิดด้วยวิธี hydrolysis แล้วเติมสารช่วยผสม MA-g-SEBS โดยแปรปริมาณจาก 0 ถึง 7 wt% แล้วนำคอมพอสิตไปวัด tensile properties ได้ผลดังแสดงในรูปที่ 2.4 (a) 100% modulus และ รูป 2.4 (b) tensile strength จะเห็นว่าค่า modulus ลดลงเล็กน้อยเมื่อปริมาณ MA-g-SEBS $\geq$ 5 % ส่วนค่า tensile strength ของhyd.-Kevlar/MA-g-SEBS/SEBS ลดลงเล็กน้อยเมื่อเพิ่มปริมาณ compatibilizer $\geq$ 5% ในขณะที่ tensile strength ของ hyd.-Conex/MA-g-SEBS/SEBS มีค่า เพิ่มขึ้นเมื่อเพิ่มปริมาณ MA-g-SEBS จนเท่ากับค่า tensile strength ของ ระบบ Kevlar composite ส่วนระบบ hyd.-Technora/MA-g-SEBS/SEBS มีค่า tensile strength ลดลงเมื่อเติม MA-g-SEBS 3 wt%

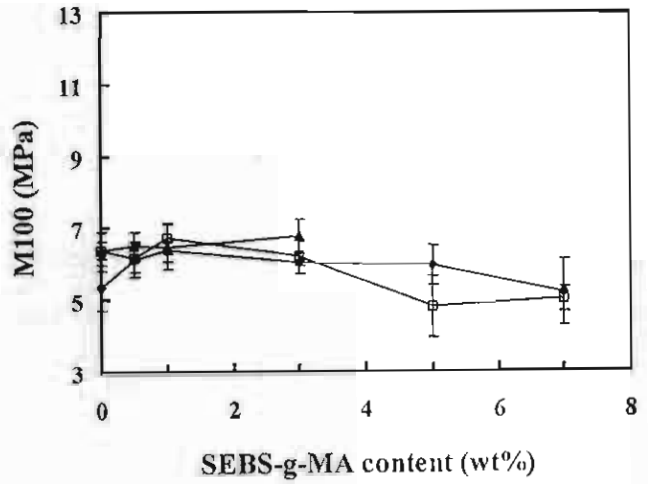

(a)

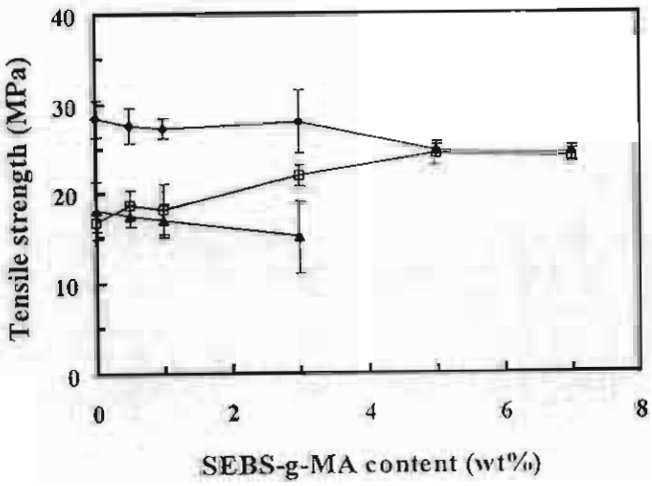

(b)

รูปที่ 2.4 Tensile properties ของ hydrolyed aramid fibre/MA-g-SEBS/SEBS composites
(◆ : Kevlar, □ : Conex, ▲ : Technora)
(a) Modulus at 100%, (b) Tensile strength

โครงสร้างสัณฐานของ fracture surface ของคอมพอสิตระบบ Kevlar/SEBS แสดงในรูปที่ 2.5 เปรียบเทียบระบบก่อนและหลังปรับผิวจะเห็นว่าก่อนการปรับผิวเส้นใยจะมีลักษณะยาวเหนือเมทริกซ์แสดงว่าการยึดเกาะระหว่างเส้นใยกับเมทริกซ์ไม่ดี แต่หลังการปรับผิวเส้นใยแล้วเติม compatibilizer พบว่า fracture surface มีลักษณะการหักของเส้นใยสั้นลง แสดงว่าการยึดเกาะระหว่างเส้นใยกับเมทริกซ์ดีขึ้น นอกจากนี้ ภาพ SEM ที่ได้จากเส้นใยหลังการสะกัดพอลิเมอร์เมทริกซ์ออกแสดงการติดของยางอยู่บนเส้นใยซึ่งสะกัดออกไม่ได้ เพราะอาจมีพันธะเคมีเกิดขึ้นระหว่างหมู่ MA ของ compatibilizer และหมู่ NH_2 บนผิวของเส้นใย

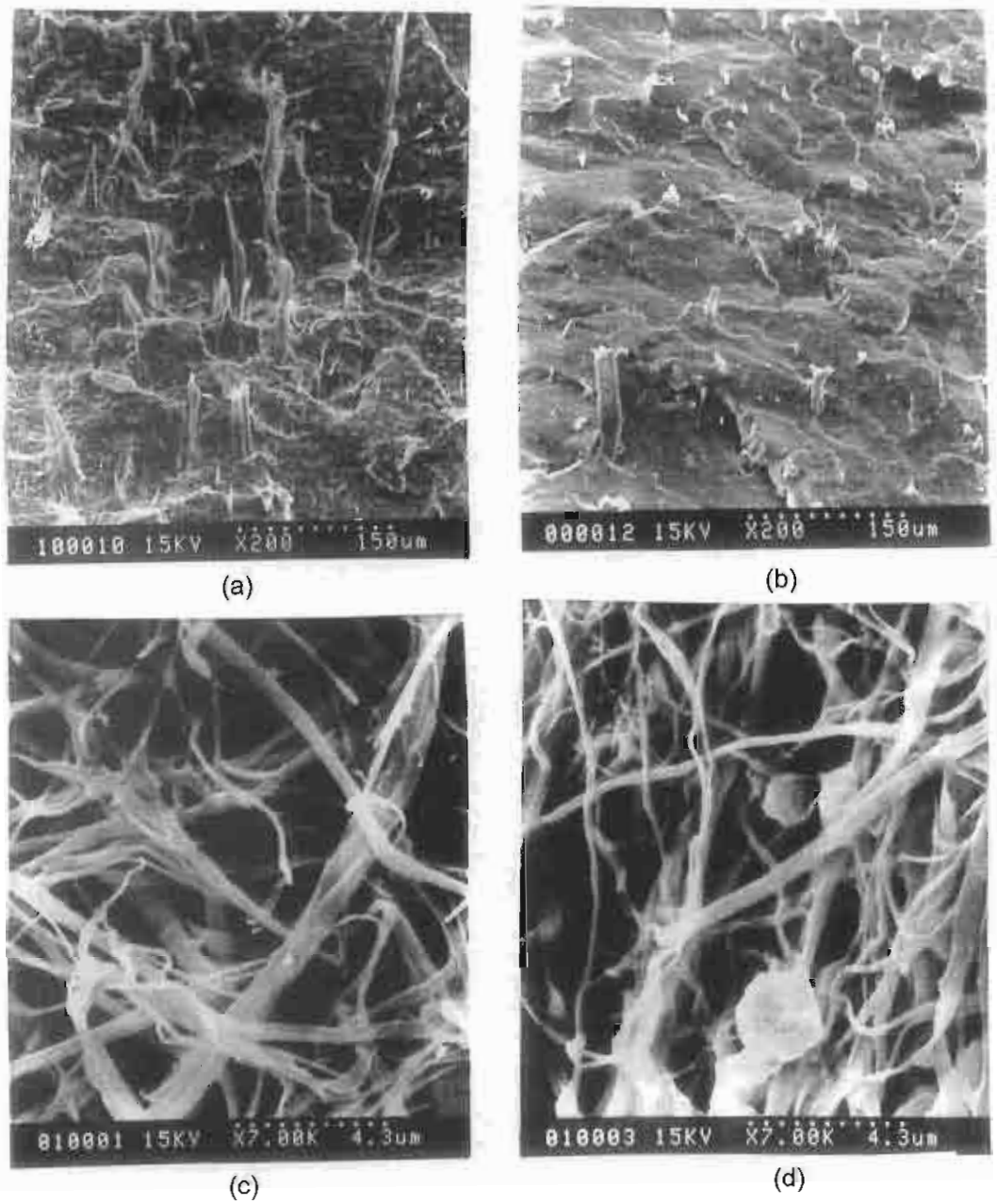

รูปที่ 2.5 SEM micrographs ของ fracture surface (a) Kevlar/SEBS
(b) hyd. Kevlar/MA-g-SEBS/SEBS (c) Extracted Kevlar from Kevlar/SEBS
(d) Extracted Kevlar from hyd. Kevlar/MA-g-SEBS/SEBS

fracture surface ของ Conex/SEBS แสดงในรูปที่ 2.6 (a) และ (b) เป็น unmodified Conex/SEBS กำลังขยาย 150 และ 2000 เท่าตามลำดับ แสดงให้เห็นลักษณะ fiber pull-out ซึ่งแสดงว่าการยึดเกาะระหว่างเส้นใยกับเมทริกซ์ไม่ดี ส่วนรูป 2.6 (c) และ (d) hydrolyzed Conex/MA-g-SEBS/SEBS กำลังขยาย 150 และ 2000 เท่า ตามลำดับแสดงให้เห็น fiber breakage ซึ่งแสดงว่าการยึดเกาะระหว่างเส้นใยและเมทริกซ์ดีขึ้นเมื่อมีการปรับผิวของเส้นใย

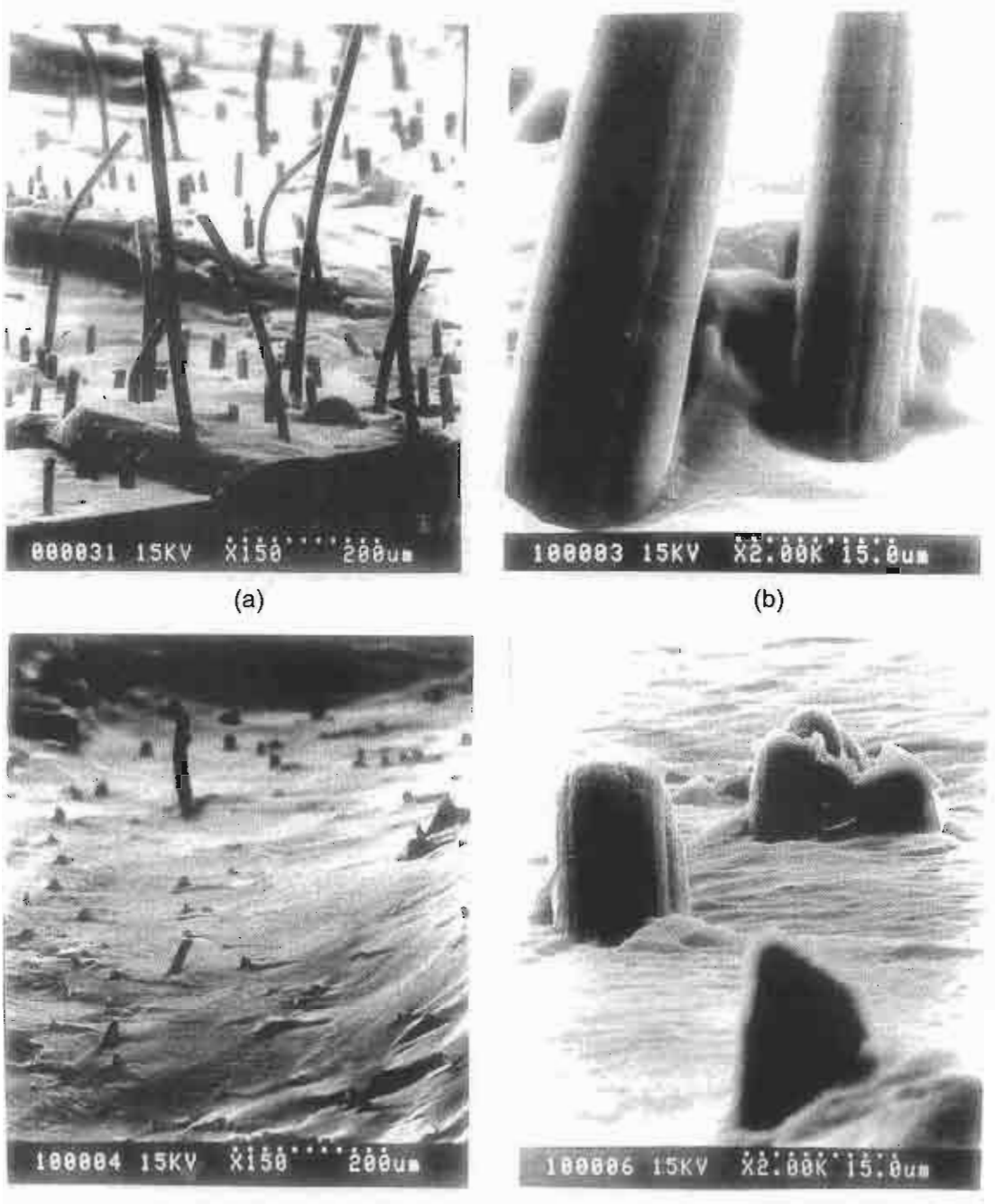

รูปที่ 2.6 SEM micrographs ของ fracture surface (a) Conex/SEBS กำลังขยาย 150 เท่า (b) Conex/SEBS กำลังขยาย 2000 เท่า (c) hyd. Conex/MA-g-SEBS/SEBS กำลังขยาย 150 เท่า (d) hyd. Conex/MA-g-SEBS/SEBS กำลังขยาย 2000 เท่า

fracture surface ของ Technora/SEBS แสดงในรูปที่ 2.7 (a) และ (b) เป็น unmodified Technora/SEBS กำลังขยาย 200 และ 2000 เท่าตามลำดับ แสดงให้เห็นลักษณะ fiber pull-out และรอยแยกที่โคนเส้นใยซึ่งแสดงว่าการยึดเกาะระหว่างเส้นใยกับเมทริกซ์ไม่ดี ส่วนรูป 2.7 (c) และ (d) hydrolyzed Technora/MA-g-SEBS/SEBS กำลังขยาย 204 และ 2000 เท่า ตามลำดับแสดงให้เห็น fiber breakage และการยึดติดที่โคนเส้นใย ซึ่งแสดงว่าการยึดเกาะระหว่างเส้นใยและเมทริกซ์ดีขึ้นเมื่อมีการปรับผิวของเส้นใย

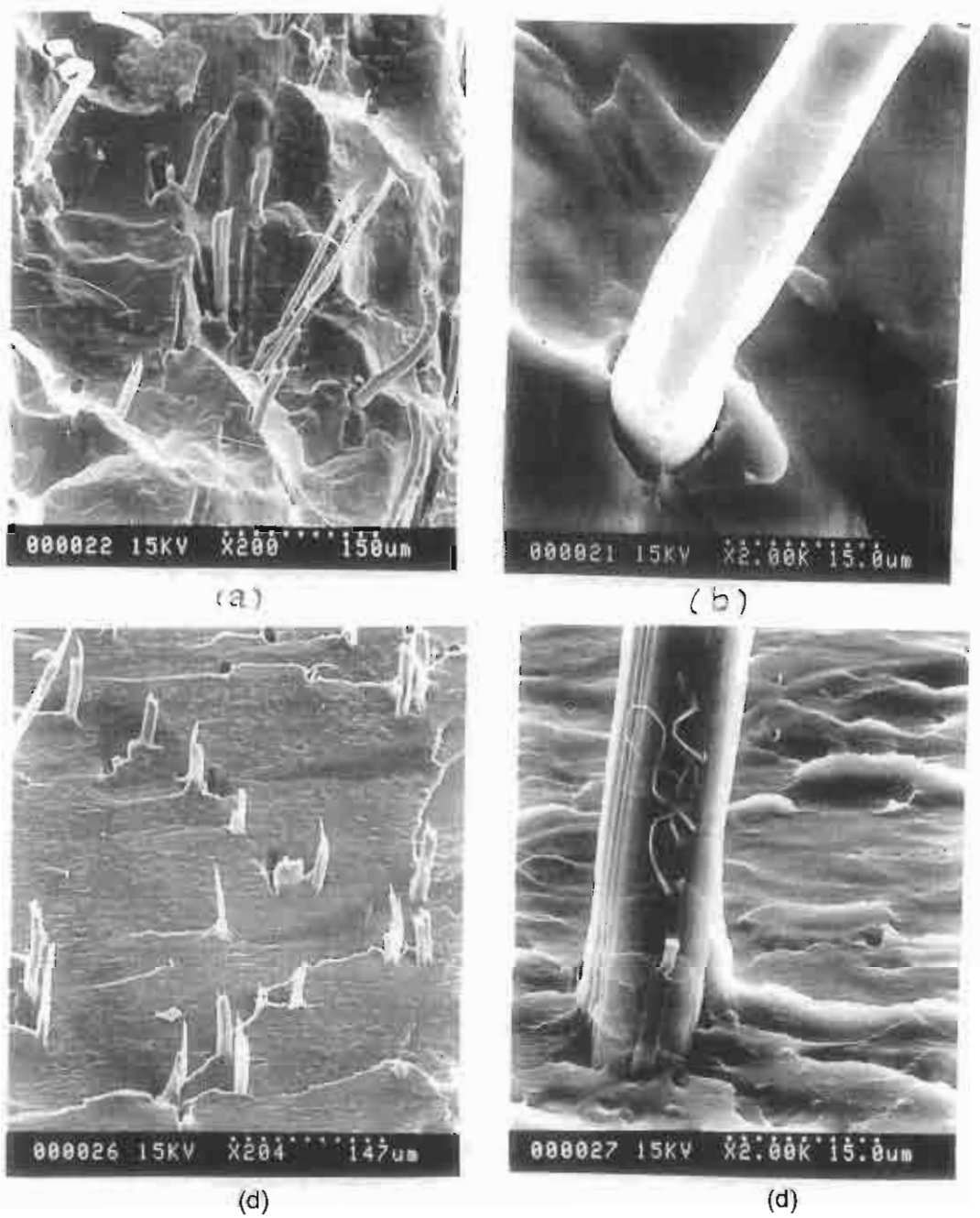

รูปที่ 2.7 SEM micrographs ของ fracture surface (a) Technora/SEBS ขยาย 200 เท่า (b) Technora/SEBS ขยาย 2000 เท่า (c) hyd. Technora/MA-g-SEBS/SEBS ขยาย 200 เท่า (d) hyd. Technora/MA-g-SEBS/SEBS ขยาย 2000 เท่า

สรุปผลการทดลองของทั้ง 3 ระบบ คือ Kevlar/SEBS, Conex/SEBS และ Technora/SEBS โดยการปรับผิวด้วยวิธี hydrolysis และใช้ MA-g-SEBS เป็นสารช่วยผสม จาก SEM micrographs ของ fracture surface แสดงว่ามีการยึดเกาะที่รอยต่อระหว่างเส้นใยกับเมทริกซ์ดีขึ้นทุกระบบ แต่ค่า tensile strength เพิ่มขึ้นระบบเดียวคือ Conex/SEBS ผลงานวิจัยทั้งสามระบบนี้ได้ตีพิมพ์เป็นบทความ 3 เรื่องลงในวารสาร J.Sci.Soc.Thailand **23** (1997) 101-114 (output 1.1), Polymer **40** (1999) 2993-2999 (output 1.3) และ Mahidol J. **5** (1998) 115-120 (output 2.1)

2.2 พอลิเมอร์ผสมระหว่างเส้นใย Kevlar และ Conex กับ SEBS matrix ปรับผิวเส้นใย โดยวิธี N-alkylation

ผลของการปรับผิวเส้นใยโดยวิธี N-alkylation ที่มีต่อสมบัติการทนต่อแรงดึงของ Conex/SEBS composites แสดงในรูปที่ 2.8 เป็น stress-strain curves ของ (a) neat SEBS, (b) 5 wt% unmodified Conex/SEBS, (c) 5 wt% heptylated conex/SEBS และ (d) 5 wt% dodecylated conex/SEBS จะเห็นว่า modulus ที่ strain ต่ำ มีค่าเพิ่มขึ้นประมาณ 3 เท่าเมื่อเติมเส้นใย ส่วนค่าความยาวที่จุดขาดไม่ต่างกันทั้ง 4 ตัวอย่าง พบว่าค่าความทนต่อแรงดึงที่จุดขาด (tensile strength) ของ SEBS (curve a) ลดลงมากเมื่อเติม Conex 5% (curve b) แต่เมื่อปรับผิวเส้นใย Conex โดยมีหมู่ heptyl และ dodecyl ทำให้ผิวของเส้นใยลดความมีขั้วลงและสามารถยึดเกาะกับ SEBS matrix ซึ่งเป็นพอลิเมอร์ที่ไม่มีขั้วได้ดีขึ้นจึงทำให้ค่า tensile strength สูงขึ้น (curves c และ d)

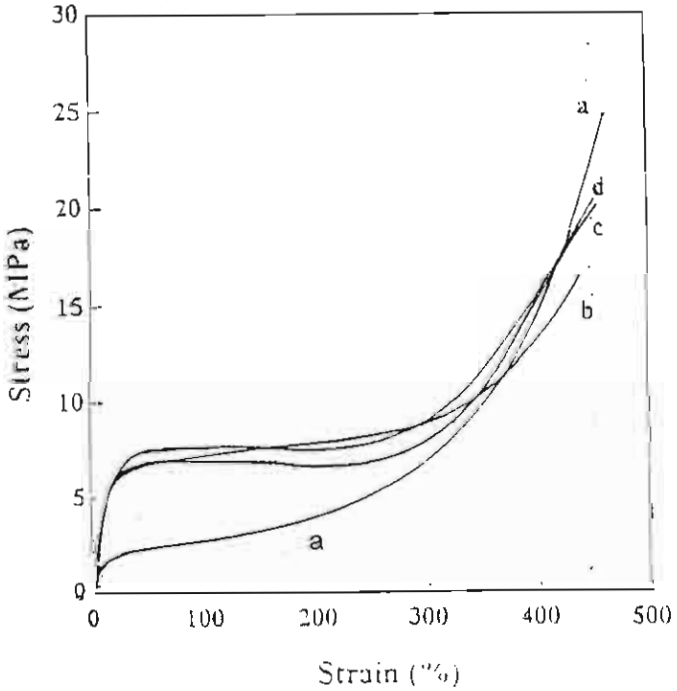

รูปที่ 2.8 Stress-strain curves ของ (a) neat SEBS, (b) 5 wt% unmodified Conex/SEBS, (c) 5 wt% heptylated Conex/SEBS และ (d) 5 wt% dodecylated Conex/SEBS

ซึ่งจะเห็นได้จาก SEM micrographs ของ fracture surface ในรูปที่ 2.9 แสดงให้เห็นว่าหลังการปรับผิวของเส้นใยมี fiber breakage (รูป 2.9 c) เมื่อเทียบกับก่อนปรับผิวเส้นใยจะเป็น fiber pull-out ดังในรูป 2.9 a ที่กำลังขยายสูงจะเห็น matrix เกาะติดและเคลือบบนผิวและยึดที่โคนเส้นใย (รูป 2.9 d) เมื่อเทียบกับรูป 2.9 b ซึ่งเป็นเส้นใยที่ไม่ได้ปรับผิวจะเห็นร่องและรอยแตกบนผิวของเส้นใย แสดงว่าหมู่ alkyl บนผิวเส้นใยช่วยให้การติดของ matrix เกิดได้ดีมากจึงส่งผลให้ค่าความทนต่อแรงดึงเพิ่มขึ้นดังกล่าว (ผลงานวิจัยระบบนี้ส่งดีพิมพ์ในวารสาร J. Appl. Polym. Sci. คาดว่าจะออกในปลายปีนี้, research output 1.5)

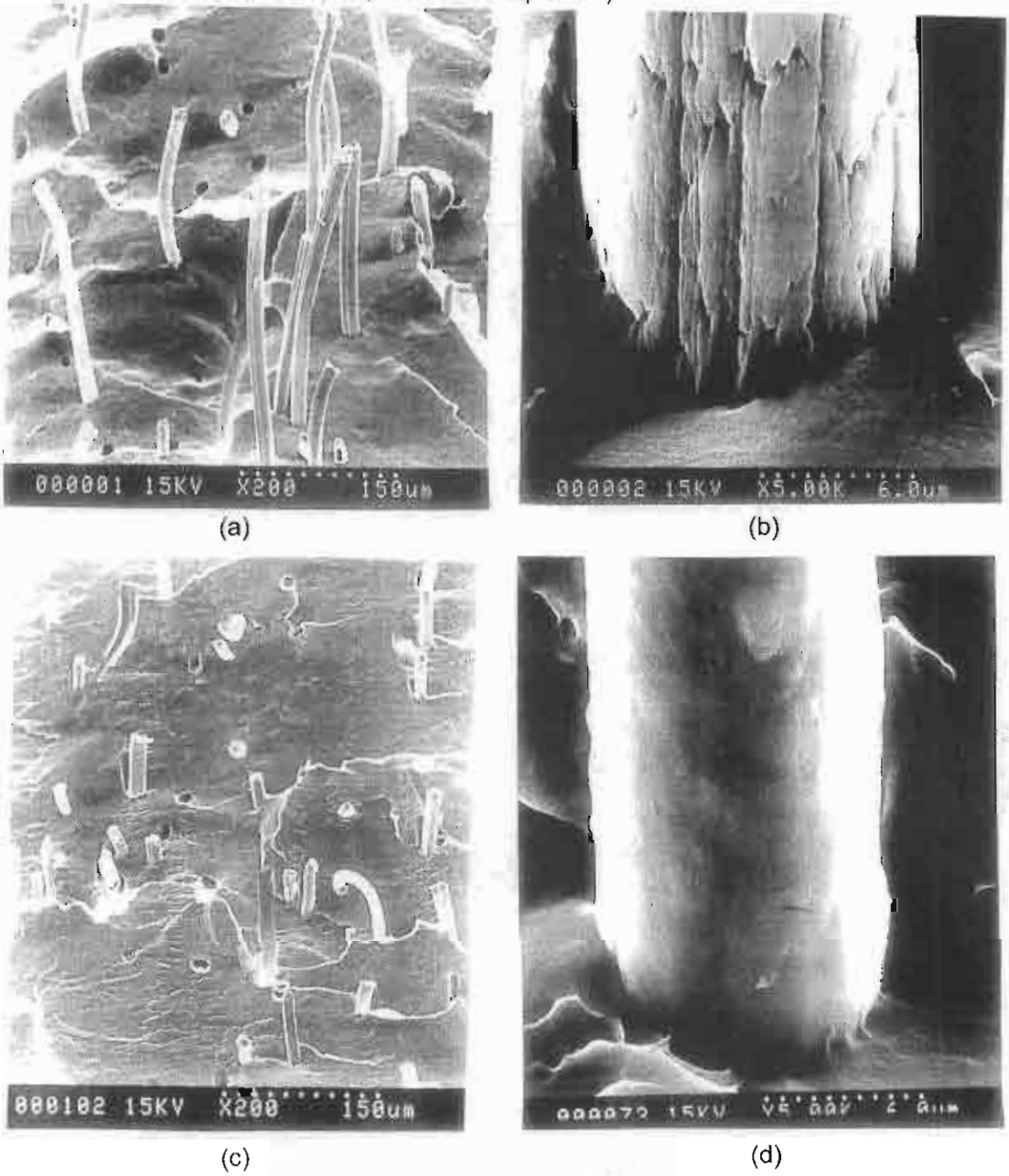

รูปที่ 2.9 SEM fracture surface ของ (a) Conex/SEBS กำลังขยาย 200 เท่า (b) Conex/SEBS กำลังขยาย 5,000 เท่า (c) heptylated Conex/SEBS กำลังขยาย 200 เท่า (d) heptylated Conex/SEBS กำลังขยาย 5,000 เท่า

ทำนองเดียวกัน fracture surface ของ Kevlar/SEBS composites ที่ปรับผิวโดยวิธี N-alkylation ก็ให้ fiber breakage มากขึ้นกว่าเส้นใยที่ก่อนการปรับผิว ซึ่งแสดงว่ามีแรงยึดเหนี่ยวที่ interface เพิ่มขึ้น ดังแสดงในรูปที่ 2.10 แต่ในระบบนี้ค่า tensile strength ไม่เพิ่มขึ้น

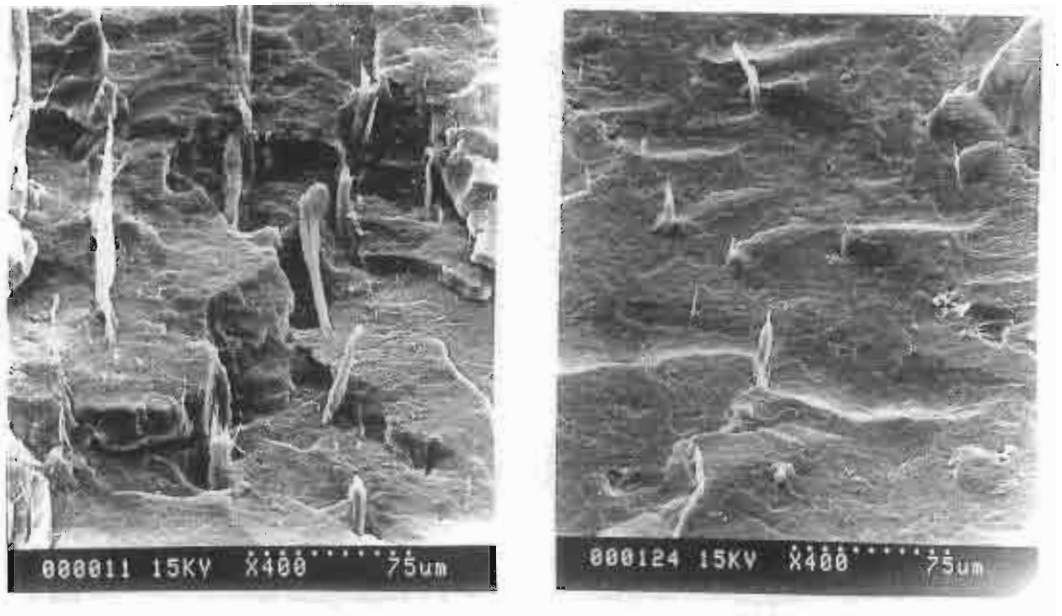

(a) (b)

(c)

รูปที่ 2.10 SEM fracture surface ของ Kevlar/SEBS composites โดยใช้เส้นใย Kevlar pulp (a) unmodified Kevlar (b) pentylated Kevlar (c) dodecylated Kevlar

2.3 พอลิเมอร์ผสมระหว่างเส้นใย Kevlar และ Conex กับ Santoprene matrix ปรับผิวเส้นใย โดยวิธี hydrolysis และ N-alkylation

Santoprene เป็น thermoplastic elastomer ที่ประกอบด้วย hard phase คือ polypropylene และ soft phase คือ EPDM (ethylene propylene diene monomer) ไม่มี covalent bond ระหว่าง hard phase และ soft phase ซึ่งต่างจาก SEBS thermoplastic elastomer ดังนั้น stress-strain curve ของระบบนี้จึงไม่มี strain crystallization effect แบบระบบ SEBS (ดูรูป 2.11) เมื่อเติมเส้นใย Conex ลงใน Santoprene จึงทำให้ค่า elongation at break ลดลงไปเรื่อยๆ ค่า modulus สูงขึ้นคามที่ควรจะเป็นเมื่อเติมเส้นใยที่มีความแข็งแรงสูงกว่าเมทริกซ์ ส่วนค่าแรงดึงที่จุดขาดเพิ่มขึ้นเมื่อเติมเส้นใย 3 wt% แต่ไม่เพิ่มต่อเมื่อเติมเส้นใยมากขึ้น

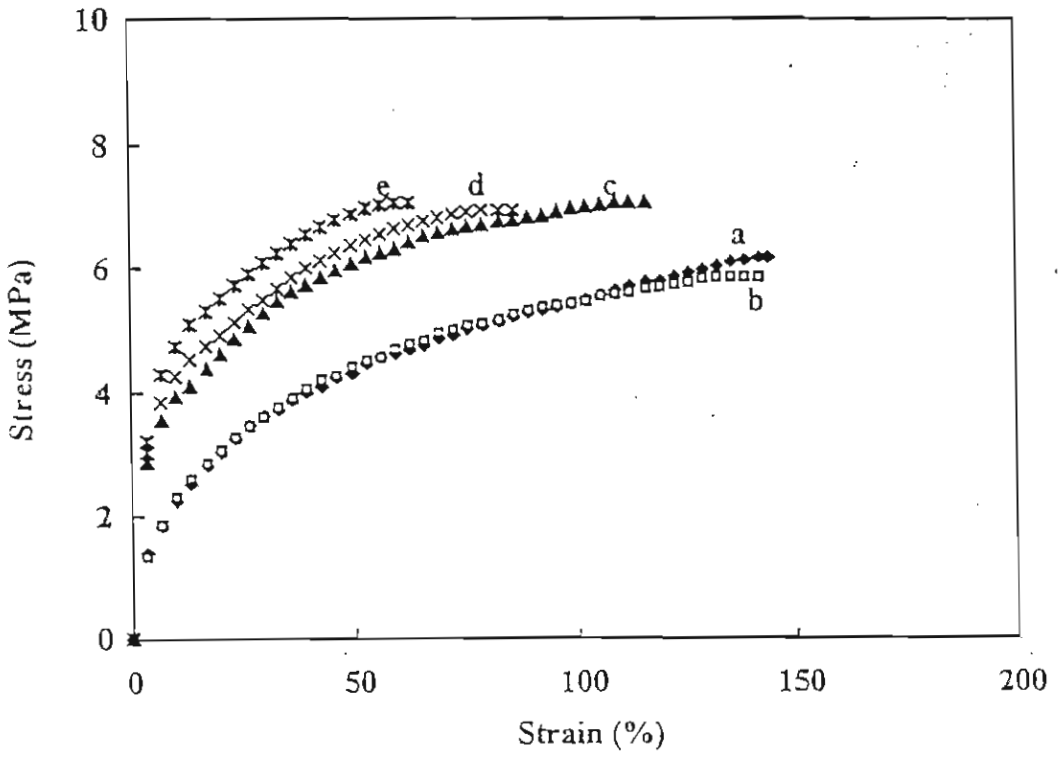

รูปที่ 2.11 Stress-strain curves ของ Conex/Santoprene composites เมื่อเติมเส้นใย Conex (wt%) (a) 0, (b) 1, (c) 3, (d) 5 และ (e) 7

ผลของการปรับผิวเส้นใยโดยวิธี hydrolysis และเติม MA-g-PP ระบบที่ได้ผลดีมาก ทำให้ค่า tensile strength เพิ่มขึ้นคือ hydrolysed Kevlar/Santoprene โดยเติม MA-g-PP เป็นสารช่วยผสม ดังแสดงในรูปที่ 2.12 เมื่อเติมเส้นใย 3 wt% ทำให้ค่า modulus เพิ่มขึ้นประมาณ 2 เท่า ส่วนค่า tensile strength เพิ่มขึ้นเล็กน้อย แต่ค่า elongation at break ลดลงมาก (curve b เทียบกับ curve a) แต่เมื่อนำเส้นใยไป hydrolysed ทำให้มีหมู่ที่ไวต่อการทำปฏิกิริยากับ matrix เพิ่มขึ้นซึ่งทำให้เกิดพันธะเคมีช่วยให้เส้นใยและเมทริกซ์ยึดติดกันดีขึ้น จึงทำให้ค่า tensile strength และ elongation at break เพิ่มขึ้นดังแสดงใน curve c และเมื่อเติมสารช่วยผสม MA-g-PP 3 wt% ยิ่งทำให้สมบัติดีขึ้นอีกทั้ง modulus และ tensile strength (curve d)

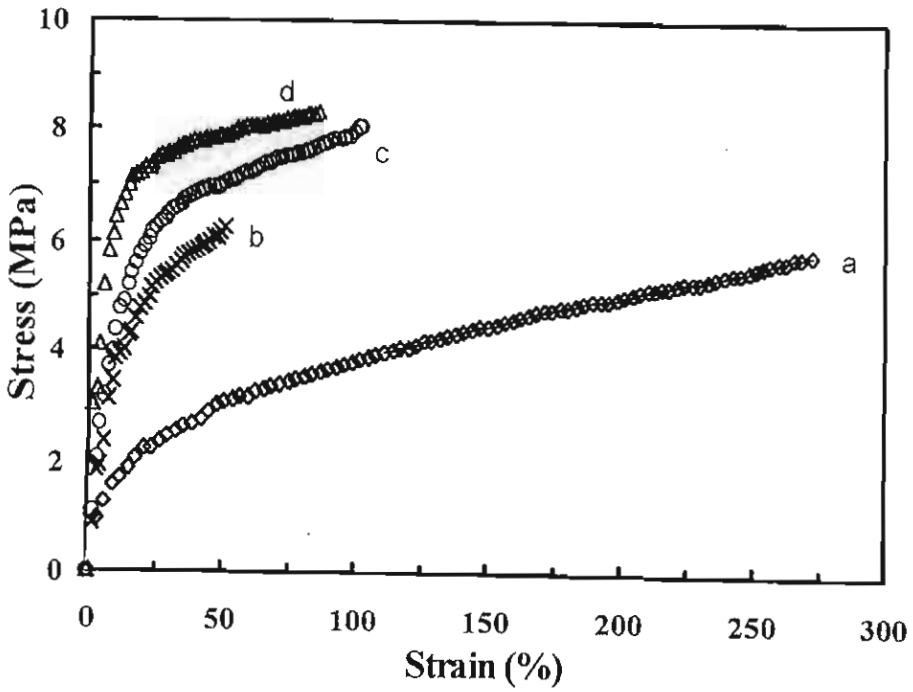

รูปที่ 2.12 stress-strain curves ของ (a) neat Santoprene,
(b) 3 wt% Kevlar/Santropene, (c) 3 wt% hydrolysed Kevlar/Santoprene
(d) 3 wt% hydrolysed Kevlar/Santoprene/3 wt% MA-g-PP

นอกจากนี้ได้วัด dynamic mechanical properties ของ Kevlar/Santoprene เพื่อศึกษาผลของ MA-g-PP ที่มีต่อ interfacial adhesion ของคอมพอสิต ได้ผลของ storage modulus ดังแสดงในรูปที่ 2.13 (a) พบว่าค่า storage modulus ของ 3 wt% hydrolysed Kevlar/3 wt% MA-g-PP/Santoprene มีค่าสูงที่สุดตลอดช่วงอุณหภูมิเหนือ T_g (-40°C) ส่วนรูป 2.13 (b) แสดงค่า tanδ ซึ่งมี peak ที่ประมาณ –40°C คือค่า T_g ของ EPDM ส่วน peak ที่ประมาณ 0°C คือค่า T_g ของ PP จะเห็นว่าค่า T_g ของ PP ขยับไปที่อุณหภูมิสูงขึ้นเล็กน้อยและ tanδ มีขนาดเล็กลง เมื่อเติม MA-g-PP แสดงให้เห็นว่าการเคลื่อนที่ของ PP chain ถูกจำกัดโดย compatibilizer ซึ่งหมายความว่าการยึดติดที่ interface ดีขึ้น

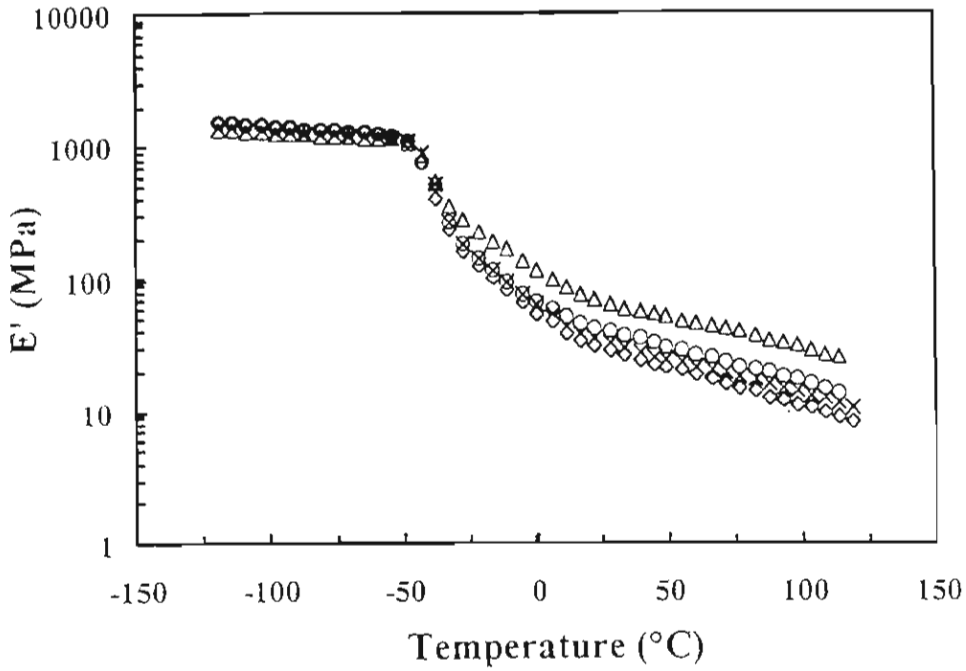

(a)

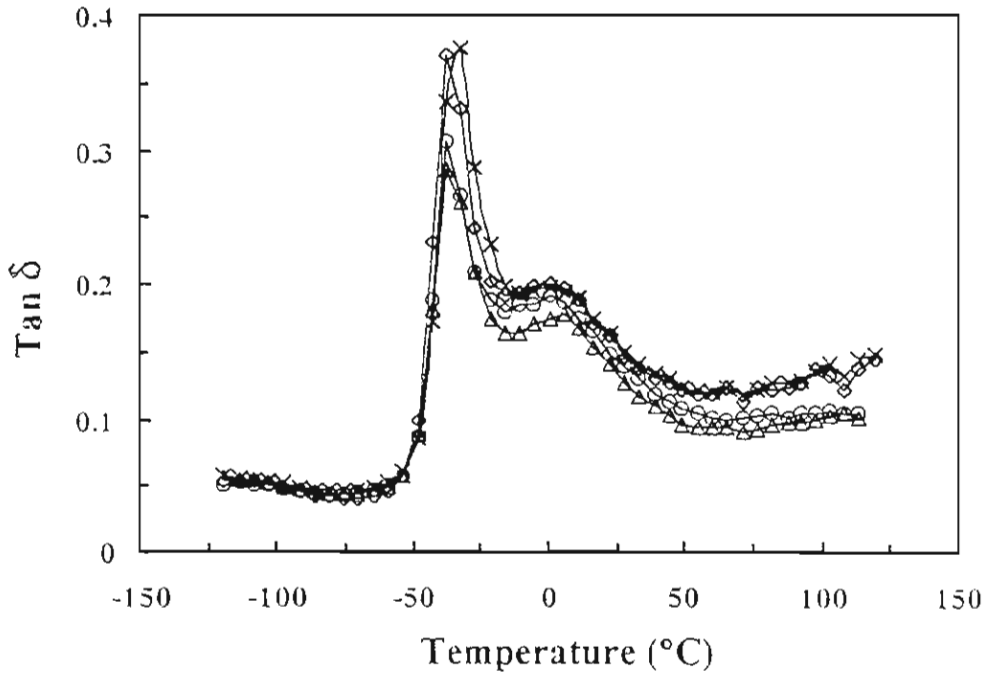

(b)

รูปที่ 2.13 (a) Storage modulus (E') และ (b) tanδ ของ Kevlar/Santoprene composites
3 wt% hydrolysed Kevlar/3 wt% MA-g-PP/Santoprene (Δ),
3 wt% untreated Kevlar/Santoprene (×),
3 wt% hydrolysed Kevlar/3 wt% PP/Santoprene (○),
Santoprene (◇).

ภาพ SEM ของ fracture surface ของระบบ Kevlar/Santoprene composites ซึ่งปรับผิวโดยวิธี hydrolysed แล้วเติม MA-g-PP และโดยวิธี dodecylation แสดงในรูปที่ 2.14 จะเห็นว่า ก่อนการปรับผิวเส้นใยจะโผล่เหนือ matrix ยาว (pull-out) เมื่อเทียบกับเส้นใยที่ปรับผิวแล้ว โดยเฉพาะอย่างยิ่ง hydrolysed Kevlar/MA-g-PP/Santoprene (รูป 2.14 c) เส้นหักสั้นติด matrix แสดงว่าการยึดเกาะระหว่างเส้นใยกับ matrix ดีมากจึงมีผลทำให้ tensile strength เพิ่มขึ้นดังที่กล่าวแล้ว

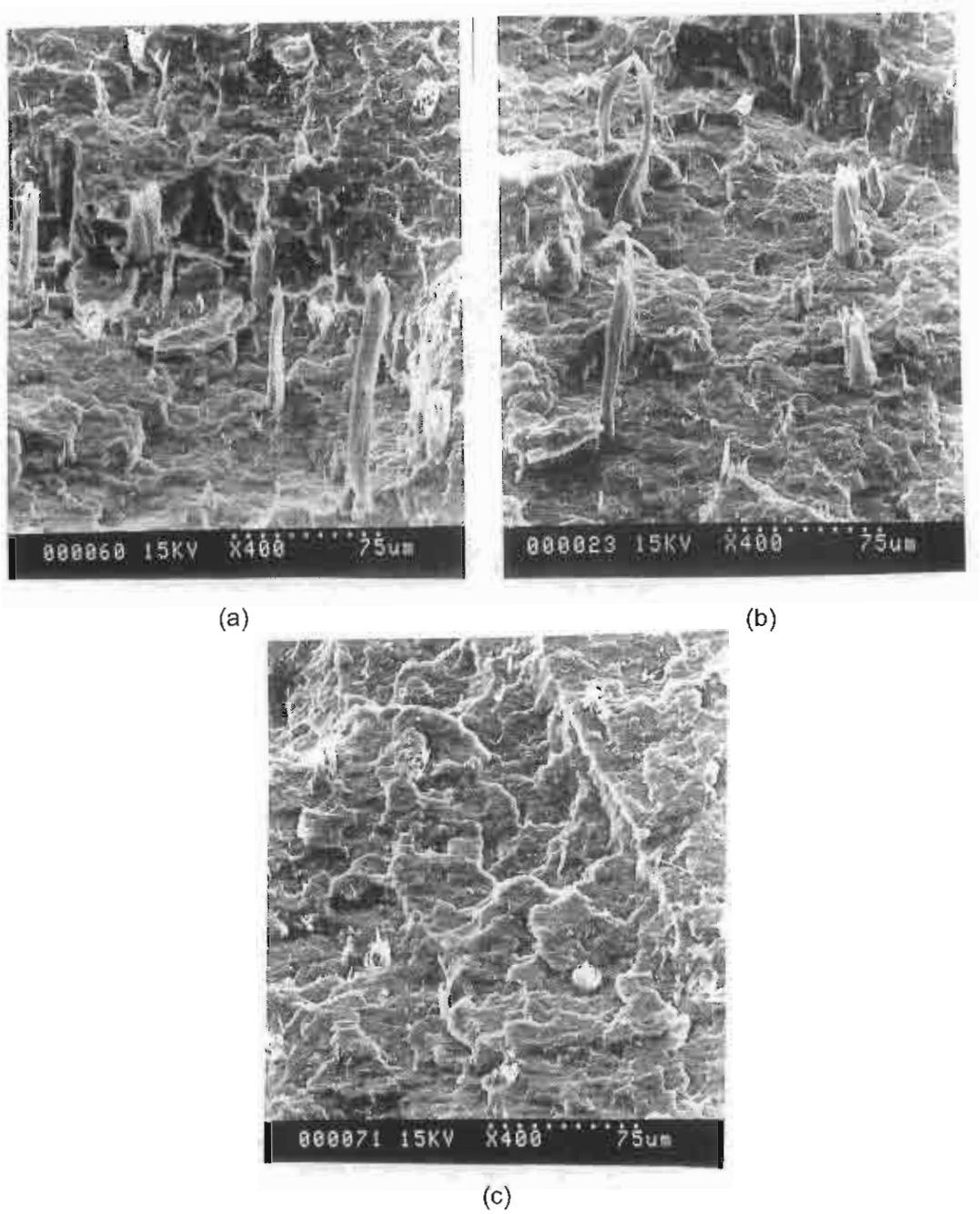

(a) (b)

(c)

รูปที่ 2.14 SEM micrographs 3 wt% Kevlar/Santoprene composites
(a) unmodified Kevlar, (b) dodecylated Kevlar (c) hydrolysed Kevlar และเติม 3 wt% MA-g-PP

สำหรับระบบ Conex/Santoprene พบว่าให้ค่า tensile strength สูงขึ้นโดยเติม MA-g-PP แต่ไม่ต้อง hydrolysed เส้นใย จะได้ผลดีกว่า

สำหรับระบบ N-alkylated Conex/Santoprene ก็ให้ค่า tensile strength สูงขึ้นเช่นเดียวกัน ดังแสดงในรูปที่ 2.15 stress-strain curve a คือ neat Santoprene, curve b ตือ 3 wt% Conex/Santoprene ซึ่งให้ค่า modulus และ tensile strength สูงกว่า neat Santoprene และเมื่อนำเส้นใย Conex ไปทำ N-heptylation ทำให้ได้ stress-strain curve c ซึ่งมีค่า modulus และ tensile strength สูงขึ้นกว่า curve b แต่ค่า elongation at break ต่ำลง

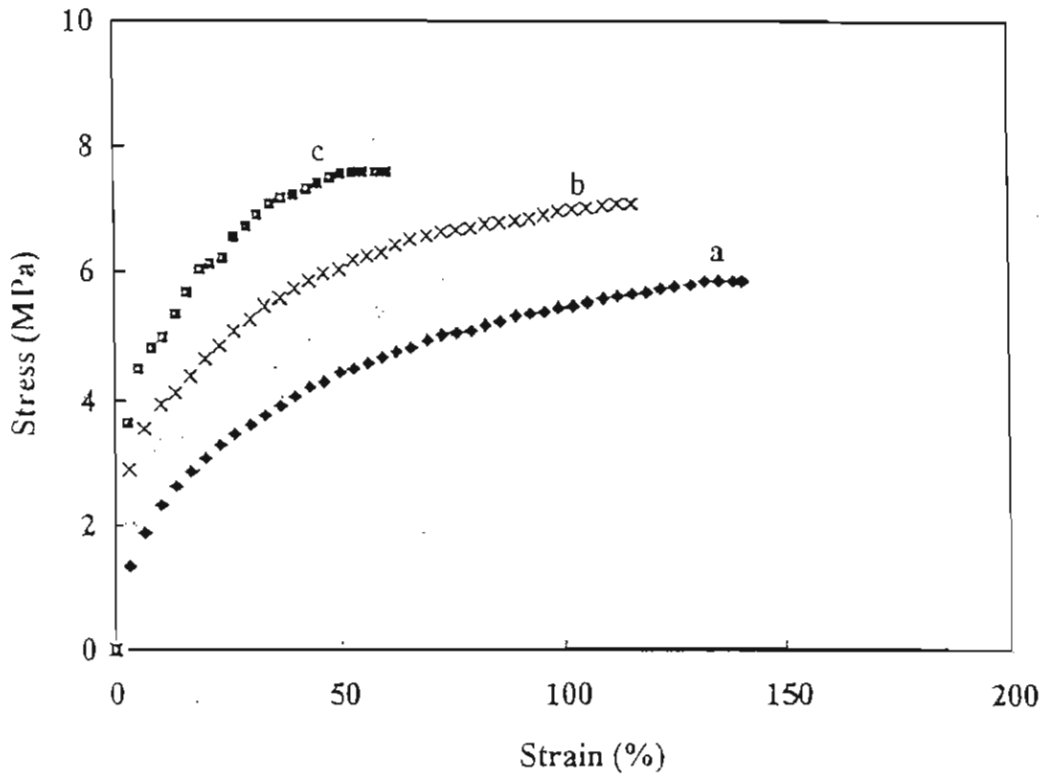

รูปที่ 2.15 Stress-strain curves (a) neat Santoprene, (b) 3 wt% conex/Santoprene (c) 3 wt% heptylated Conex/Santoprene

Morphology ของ Conex/Santoprene composites แสดงในรูปที่ 2.16 ทั้งเส้นใยก่อนการปรับผิวและหลังการปรับผิวด้วยวิธี hydrolysed แล้วเติม MA-g-PP และเส้นใยที่ปรับผิวด้วยวิธี N-alkylation จะเห็นว่าเส้นใยหักค่อนข้างสั้นพอๆกัน แสดงให้เห็นว่าการยึดเกาะระหว่างเส้นใยกับ matrix ค่อนข้างดี แต่ถ้าสังเกตที่ผิวของเส้นใยจะเห็น matrix เกาะติดอยู่มากกว่ากรณีที่ใช้เส้นใยที่ไม่ได้ปรับผิว

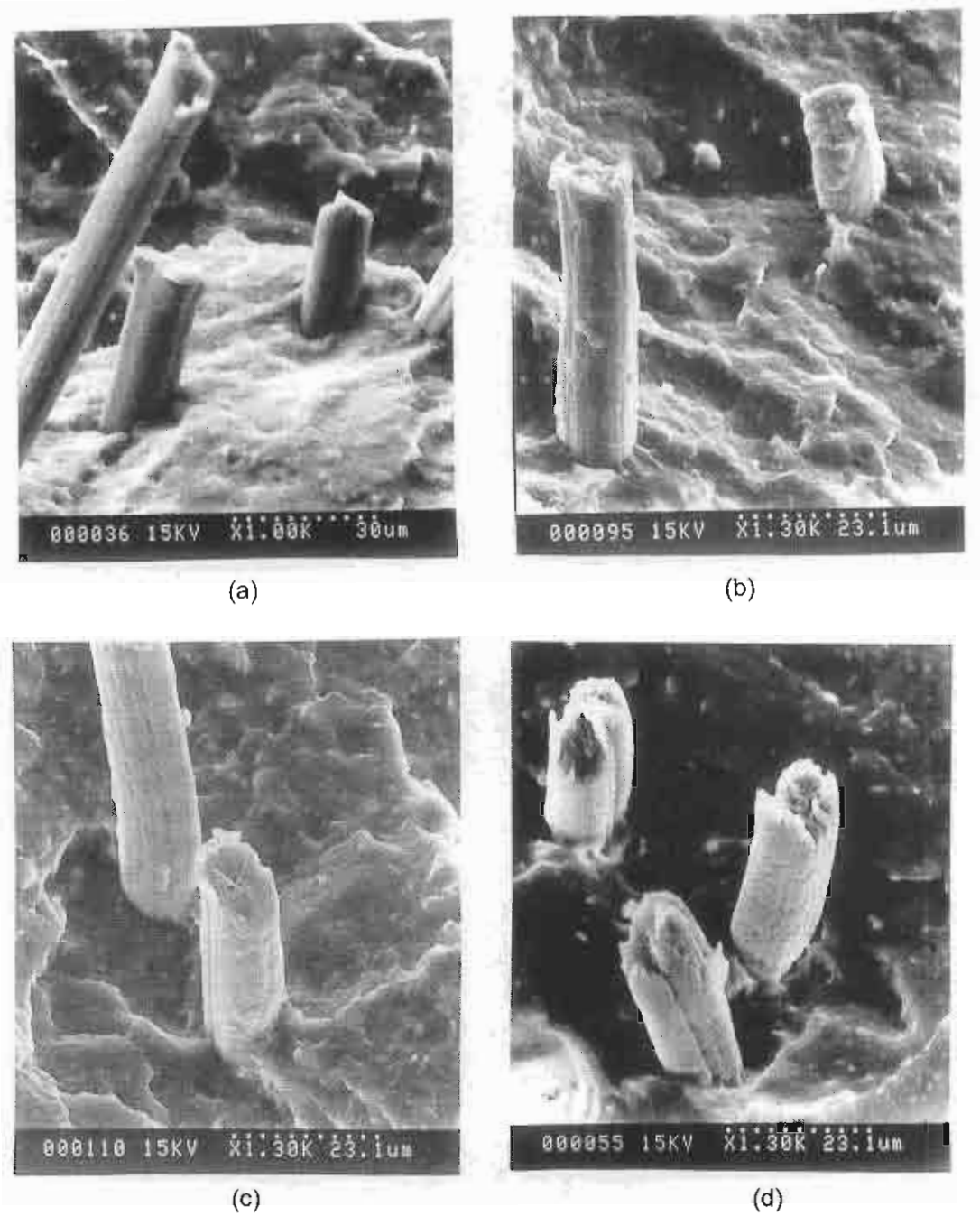

(a) (b)

(c) (d)

รูปที่ 2.16 SEM micrographs ของ 3 wt% Conex/Santoprene composites กรณีที่ใช้เส้นใย
(a) unmodified, (b) heptylated Conex, (c) dodecylated Conex
(d) hydrolysed Conex และ 3 wt% MA-g-PP

สรุปผลของ composites ที่ใช้ Santoprene เป็น matrix พบว่าระบบที่ให้ค่า tensile strength เพิ่มขึ้น สอดคล้องกับภาพจาก SEM ที่เกิด fiber breakage และ matrix เกาะติดที่ผิวของเส้นใยซึ่งแสดงว่าการยึดเกาะที่ interface ดี ได้แก่ระบบ Conex/MA-g-PP/Santoprene, alkylated Conex/Santoprene และ hydrolysed Kevlar/MA-g-PP/Santoprene (ส่งตีพิมพ์ในวารสาร Polymer **40**, 6437-6442 research output 1.4)

2.4 พอลิเมอร์ผสมระหว่าง Conex short fiber และ Thermoplastic Polyurethane Elastomer (TPU) ปรับผิวของเส้นใยด้วย Oxygen plasma และโดยวิธี hydrolysis

ได้ศึกษาสมบัติเชิงกลและโครงสร้างสัณฐานของพอลิเมอร์ผสมระหว่าง thermoplastic polyurethane elastomer (TPU) และ Conex short fiber ก่อนและหลังการปรับผิวของเส้นใยด้วยวิธี oxygen plasma treatment และ alkali hydrolysis ซึ่งจะทำให้เกิดหมู่ที่ไวต่อการทำปฏิกิริยา เช่น $-NH_2$, -COOH ที่ผิวของเส้นใยเพิ่มขึ้นและทำให้ผิวเส้นใยขรุขระมากขึ้น ซึ่งจะช่วยให้การยึดติดระหว่างเส้นใยกับ matrix ดีขึ้น

ผลของการวัดสมบัติ Tensile ของ untreated Conex/TPU composite เมื่อแปรปริมาณเส้นใยแสดง stress-strain behavior ของ untreated Conex/TPU composite เมื่อแปรปริมาณเส้นใย 1-10 wt% แสดงในรูปที่ 2.17 พบว่า TPU แสดงลักษณะเฉพาะของยางที่มี strain hardening effect คือที่ strain สูงๆ ค่า tensile strength สูงมาก ลักษณะเช่นนี้ปรากฏเมื่อผสมเส้นใยจนถึง 5% โดยน้ำหนัก แต่เมื่อปริมาณ Conex สูงมากกว่า 5% จะเกิด yield พบว่า เมื่อปริมาณ Conex เพิ่มขึ้นจนถึง 10% ค่า modulus ที่ 10% strain มีค่าเพิ่มขึ้นเป็น 5 เท่าของ unfilled TPU ส่วนค่า tensile strength ลดลงอย่างมากเมื่อปริมาณ Conex เพิ่มขึ้นเป็น 7% แต่กลับเพิ่มขึ้นอีกครั้งเมื่อปริมาณ Conex เพิ่มเป็น 10% พบว่า pure TPU และ composite ที่ประกอบด้วยเส้นใย ≤ 5 wt% จะมีค่า elongation at break พอๆกันคือมากกว่า 700% และจะลดลงอย่างรวดเร็วเหลือประมาณ 50% เมื่อมีปริมาณ Conex มากกว่า 7 wt%

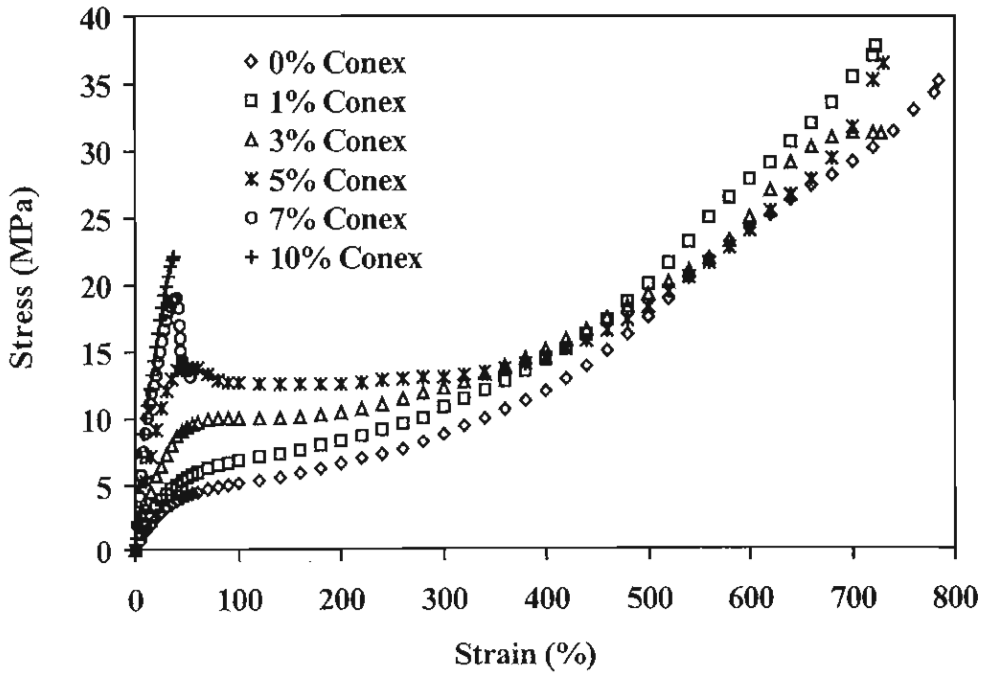

รูปที่ 2.17 Stress-strain curves ของ untreated Conex /TPU composites เมื่อแปรปริมาณเส้นใย จาก 0 – 10 wt%

หลังจาก treat surface ของ Conex fiber ด้วย oxygen plasma โดยใช้กำลัง 100 W เป็นเวลานาน 3, 5, 10 และ 15 นาที และ treat ผิวเส้นใยโดยใช้วิธี hydrolysis นำไปผสมกับ TPU โดยใช้ปริมาณ Conex 7 wt% คงที่ แล้วนำ composites มาวัดสมบัติ tensile ผลที่ได้แสดงดังรูปที่ 2.18 จะเห็นว่าการทำ plasma treatment และ hydrolysis ไม่ทำให้ค่า modulus ของ composite เปลี่ยนแปลงไปจาก untreated Conex ส่วนค่า yield stress และ tensile strength ของ composite ที่ได้จากเส้นใยที่ทำ plasma treatment เป็นเวลา 3 นาที และ hydrolysis มีค่าเพิ่มขึ้นเล็กน้อย

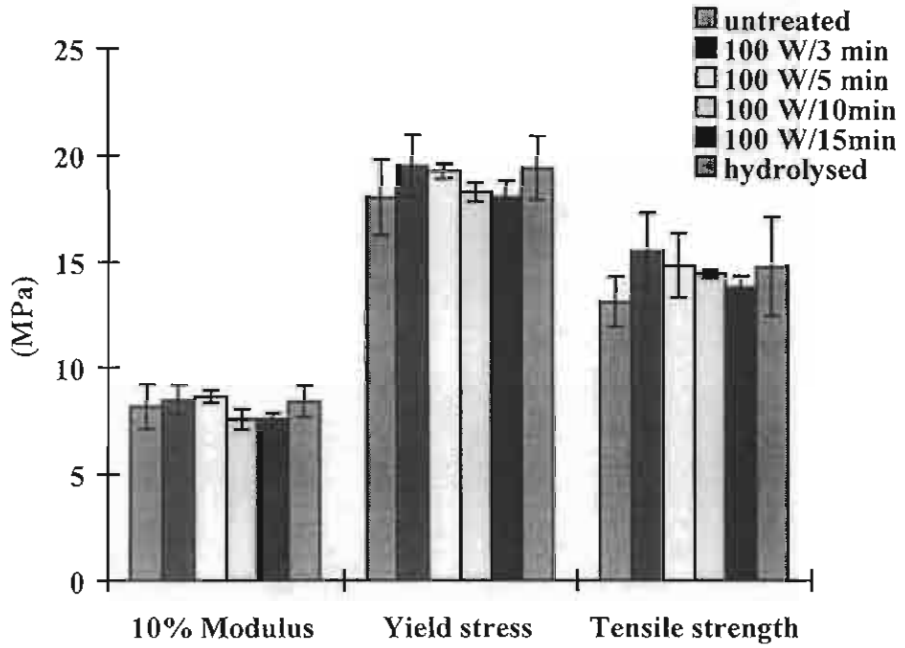

รูปที่ 2.18 แสดงสมบัติ tensile ของ untreated Conex และ treated Conex/TPU composites

นอกจากนี้ได้วัด dynamic mechanical properties ของพอลิเมอร์ผสม โดยใช้ bending mode ที่ frequency 3 Hz, 64 μm peak to peak displacement วัดในช่วงอุณหภูมิที่ใช้จาก –60 ถึง 100°C โดยใช้ heating rate 5°C/min ผลที่ได้ของ untreated Conex/TPU composites ที่แปรปริมาณเส้นใย 0 - 10 % แสดงในรูปที่ 2.19 (a) คือค่า storage modulus (E′) พบว่า E' มีค่าเพิ่มขึ้น เมื่อปริมาณเส้นใยเพิ่มขึ้น ในช่วงอุณหภูมิเหนือ T_g (-11°C) ซึ่งผลที่ได้นี้สอดคล้องกับค่า tensile modulus ที่เพิ่มขึ้น

สำหรับค่า loss tangent (tanδ) แสดงในรูปที่ 2.19 (b) พบว่าเมื่อปริมาณเส้นใยเพิ่มขึ้นจาก 0 เป็น 10 wt% T_g มีค่าสูงขึ้นจาก -11°C เป็น -9°C (เนื่องจากการเคลื่อนไหวของ polymer chain ถูกจำกัดเพราะติดกับเส้นใย) นอกจากนี้พบว่า $\tan\delta_{max}$ มีค่าลดลงเมื่อปริมาณเส้นใยเพิ่มขึ้น แสดงให้เห็นถึง damping characteristic ที่ดีขึ้น คือสามารถส่งผ่านแรงจาก polymer matrix ไปสู่ fiber ได้ดีขึ้น แสดงว่าการยึดติดระหว่างเส้นใยกับเมทริกซ์ดี

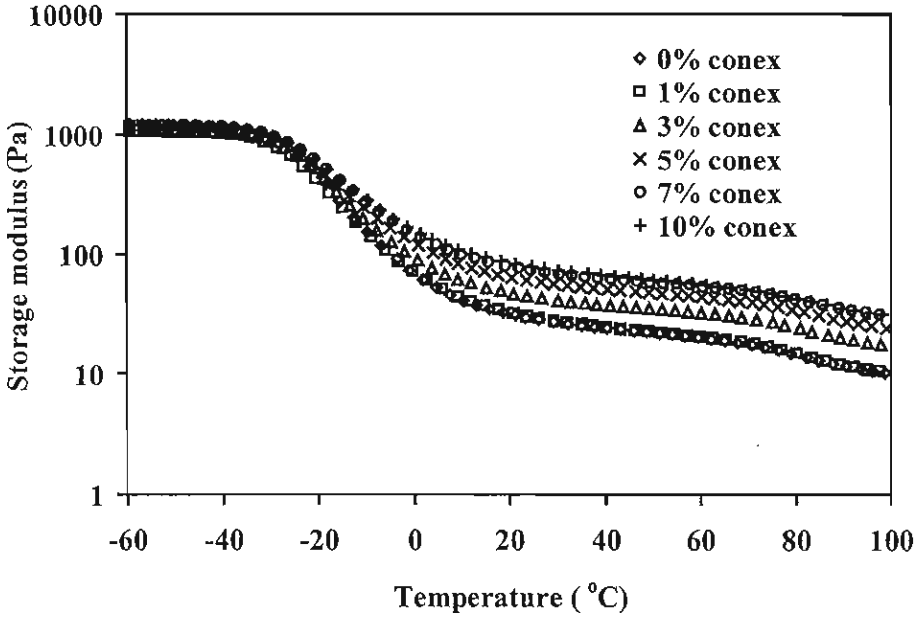

(a)

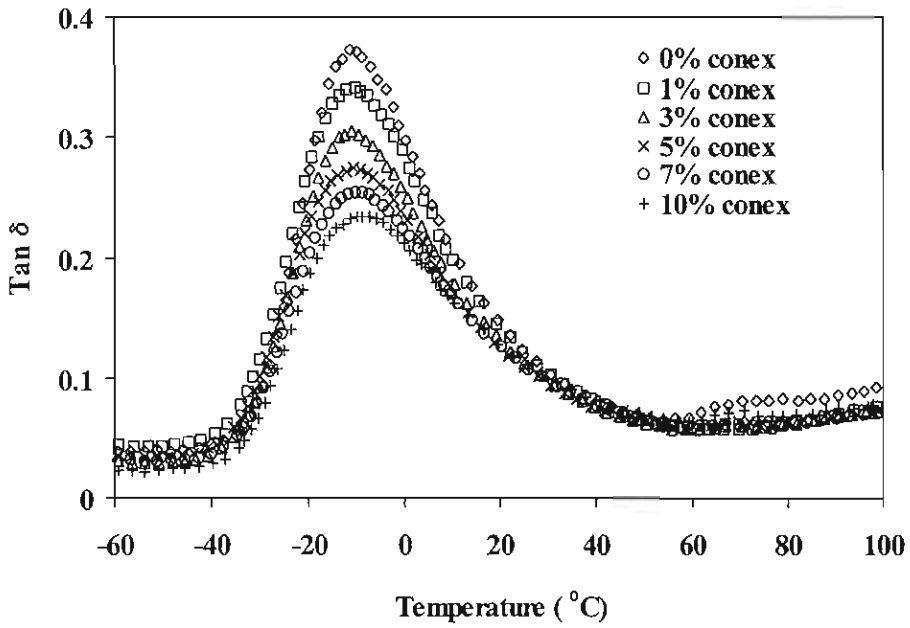

(b)

รูปที่ 2.19 (a) storage modulus (E′) และ (b) loss tangent ของ untreated Conex/TPU composites เมื่อแปรปริมาณเส้นใย

morphology ของ fracture surfaces ของ untreated และ treated Conex/TPU composites แสดงในรูปที่ 2.20 เป็น SEM micrographs ที่กำลังขยาย 200 เท่า จะเห็นว่าทั้งเส้นใย untreated และ treated Conex มีลักษณะหักสั้นเหมือนกัน ส่วนรูปที่กำลังขยาย 4000 เท่า จะเห็นว่าบริเวณ interface ระหว่าง fiber และ matrix มีการยึดติดกันดี แสดงให้เห็นว่า

Conex fiber และ TPU มีการยึดเกาะกันดี ซึ่งผลการทดลองส่วนนี้สอดคล้องกับผลที่ได้จาก tensile properties และ dynamic mechanical properties ของ composite

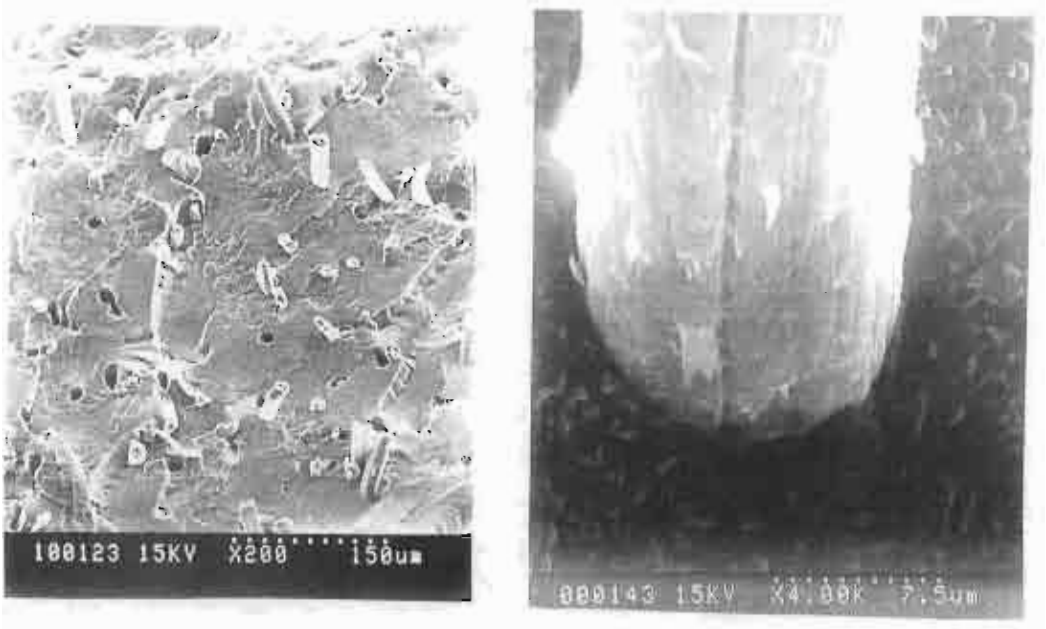

(a) (b)

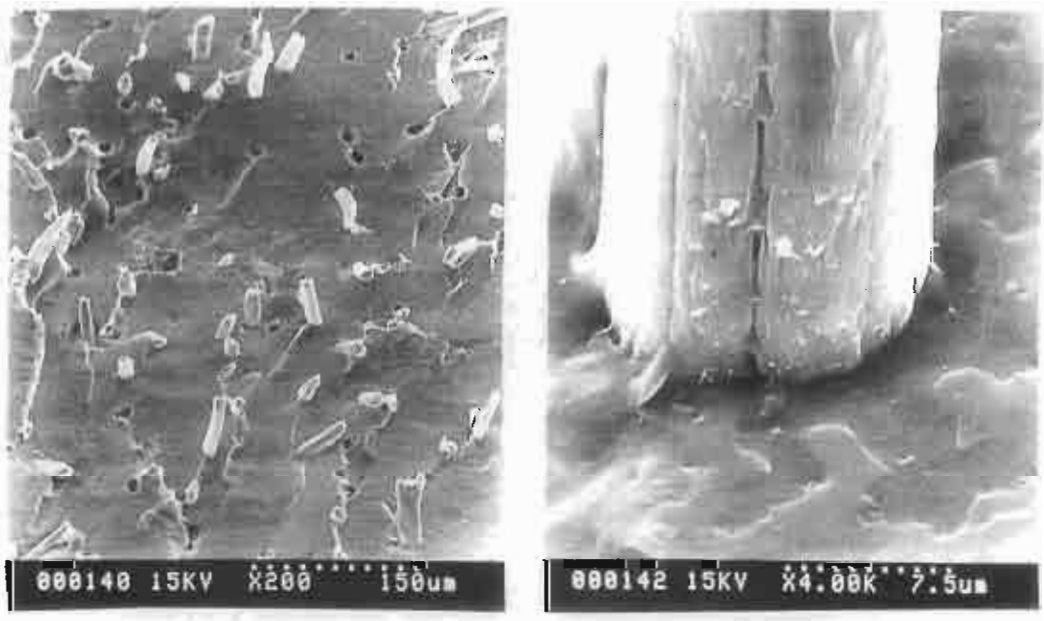

(a) (d)

รูปที่ 2.20 SEM micrographs ของ Conex/Polyurethane fracture surfaces

(a) untreated fiber กำลังขยาย 200 เท่า (b) untreated fiber กำลังขยาย 4,000 เท่า

(c) 5 min O_2-plasma treated fiber กำลังขยาย 200 เท่า

(d) 5 min O_2-plasma treated fiber กำลังขยาย 4,000 เท่า

3. พอลิเมอร์ผสมระหว่างพอลิเมอร์ผลึกเหลวเทอร์โมโทรปิกกับเทอร์โมพลาสติก

3.1 พอลิเมอร์ผสมระหว่าง Polypropylene และ Rodrun LC3000

เตรียมพอลิเมอร์ผสม (*in-situ* composite) ระหว่างพอลิพรอพิลีน (polypropylene, PP) กับ Rodrun LC3000 (copolymer ของ hydroxy benzoic acid และ ethylene terephthalate สัดส่วน 60/40 mole)ซึ่งเป็นพอลิเมอร์ผลึกเหลวชนิดเทอร์โมโทรปิก (Thermotropic Liquid Crystalline Polymer, TLCP) โดยศึกษาสภาวะการผสม การขึ้นรูปเป็นฟิล์ม ใช้ PP matrix ที่ มีความหนืดต่างๆ (แปรค่า melt flow rate) และใช้ สารช่วยผสม เช่น SEBS, MA-g-SEBS (1.8 wt% MA) , MA-g-PP (0.1 และ 0.5 wt% MA), EPDM, MA-g-EPDM (1 wt% MA) เป็นสารช่วยผสม โดยขึ้นรูปเป็นฟิล์มบาง

เนื่องจาก TLCP และ PP ไม่ผสมเข้าเป็นเนื้อเดียวกันจะได้พอลิเมอร์ผสมที่มี TLCP เป็นหยดเล็กๆกระจายอยู่ใน PP matrix และเมื่อได้รับแรงเฉือนและแรงดึงจากการขึ้นรูปโดยการฉีดหรือรีดทำให้ TLCP ยืดออกเป็นเส้น และเมื่อทำให้ของผสมนี้เย็นตัวลงโดยเร็วจะได้ฟิล์มที่มีลักษณะเป็นเหมือน short fiber reinforced plastics ดังแผนภาพที่แสดงในรูป 3.1

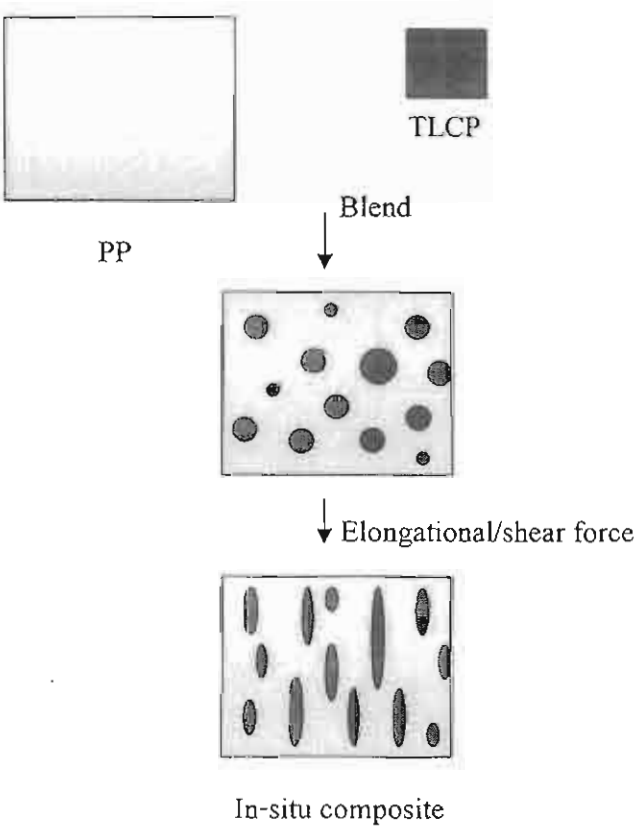

รูป 3.1 schematic diagram แสดงการเกิด *in-situ* compoaite

3.1.1 ผลของ draw ratio ที่มีต่อโครงสร้างสัณฐาน ความเป็นระเบียบของโมเลกุล (order parameter) และสมบัติ tensile

เมื่อเพิ่ม draw ratio ของฟิล์ม in-situ composite (ความกว้างของ slit die ต่อความหนาของฟิล์ม) จาก 9 เป็น 19 และ 33 จะเห็นว่าการยืดของเส้นใย TLCP ยาวขึ้น ดังแสดงในรูปที่ 3.2 ในฟิล์มที่ผลิตด้วย draw ratio 9 จะเห็นว่ามีลวดลายภายในเส้นใยมากเป็นแบบที่เรียกว่า schlieren texture ซึ่งแสดงว่าโมเลกุลเรียงตัวไม่เป็นระเบียบนัก แต่เมื่อเพิ่ม draw ratio จะได้เส้นใยที่ texture มีความสม่ำเสมอมากขึ้น แสดงว่าโมเลกุลเรียงเป็นระเบียบมากขึ้น ซึ่งสอดคล้องกับค่า order parameter ซึ่งคำนวณจาก dichroism ของ FTIR spectra ดังแสดงในรูปที่ 3.3

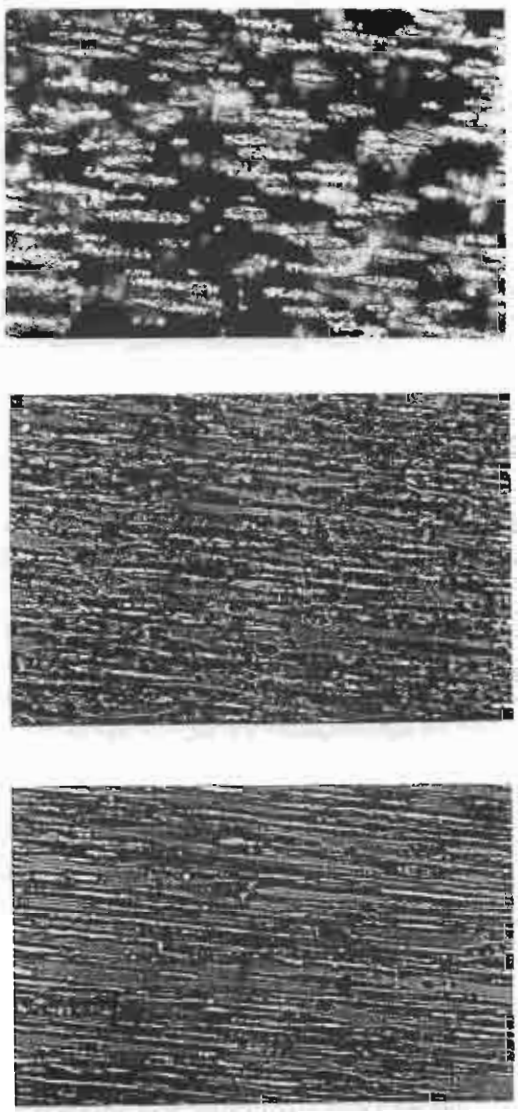

รูปที่ 3.2 ภาพจากกล้องจุลทรรศน์ของฟิล์ม 10 wt% TLCP/PP in-situ composite ที่ draw ratio (a) 9 (b) 19 (c) 33

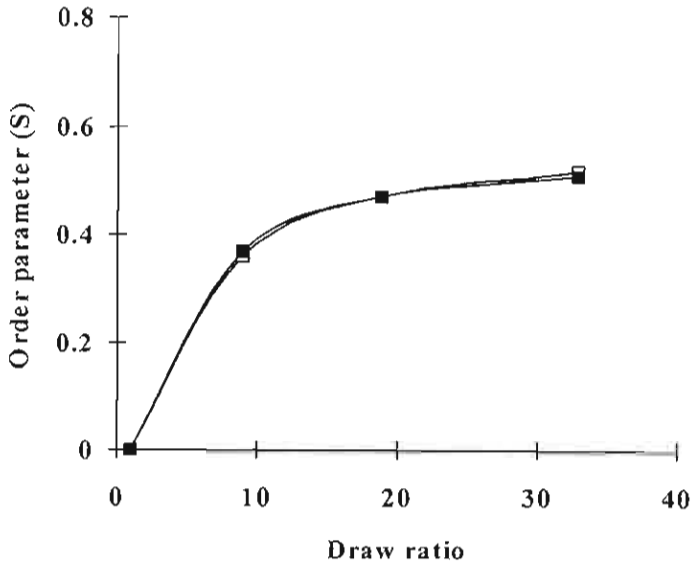

รูปที่ 3.3 order parameter ของ TLCP phase ในTLCP/PP composite film แปรผันกับค่า draw ratio คำนวณโดยใช้ peak 1601 cm^{-1} (—ι —) และ 726 cm^{-1} (—■—).

ค่า order parameter, S คำนวณโดยใช้ peak ที่ตำแหน่ง 1601 cm^{-1} และ 726 cm^{-1} ให้ผลใกล้เคียงกันมาก ที่จุด draw ratio = 1 คือจุดที่ไม่มีการดึงฟิล์มในทางทฤษฎีค่า S = 0 (ไม่ได้วัด) ความเป็นระเบียบของโมเลกุลในวัฏภาค TLCP เพิ่มเสมือนกับว่าเส้นใยของแข็ง TLCP มีความเป็นผลึกเพิ่ม ควรจะทำให้เส้นใย TLCP มีความแข็งแรงเพิ่ม (fiber modulus เพิ่ม) ซึ่งน่าจะส่งผลให้ modulus ของ composite เพิ่มด้วย

เมื่อนำฟิล์มที่ได้จากการแปร draw ratio ไปวัดสมบัติ tensile (รูปที่ 3.4) พบว่าค่า modulus ของ pure PP วัดในทิศขนานกับการฉีดฟิล์ม (machine direction, MD) และ modulus ในทิศตั้งฉาก (transverse direction, TD) ไม่แตกต่างกัน (isotropic) ส่วนค่า MD modulus ของ composite มีค่าสูงขึ้นมากเมื่อเพิ่มฟิล์ม draw ratio โดยเฉพาะที่ draw ratio 33 ค่า MD modulus เพิ่มขึ้นถึง 77% เมื่อเทียบกับ pure PP ส่วนค่า TD modulus ของ composite film มีค่าเกือบคงที่เมื่อเพิ่ม draw ratio (anisotropic) ทำนองเดียวกัน ค่า yield stress ของ composite ในทิศ MD เพิ่มขึ้นเมื่อเพิ่ม draw ratio เพียงแต่ไม่มากเท่ากรณีของ modulus ส่วนค่า yield stress ในทิศ TD ไม่เปลี่ยนแปลงมาก

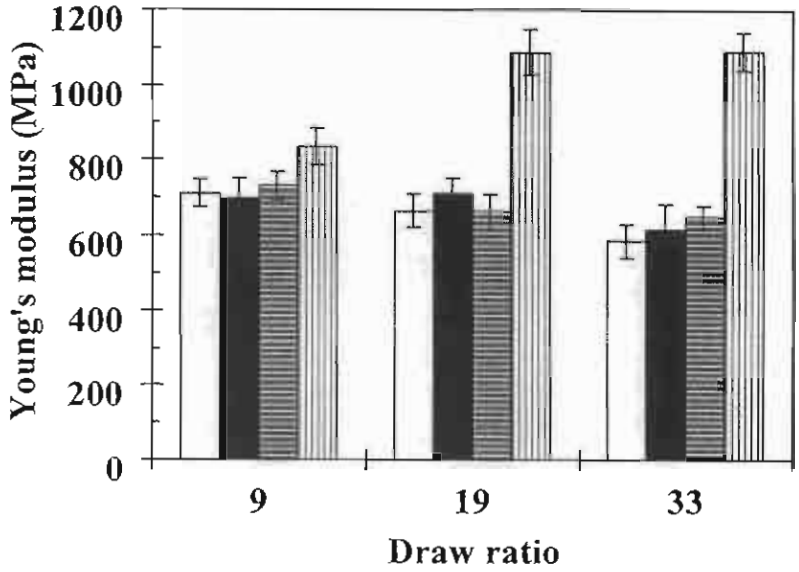

(a)

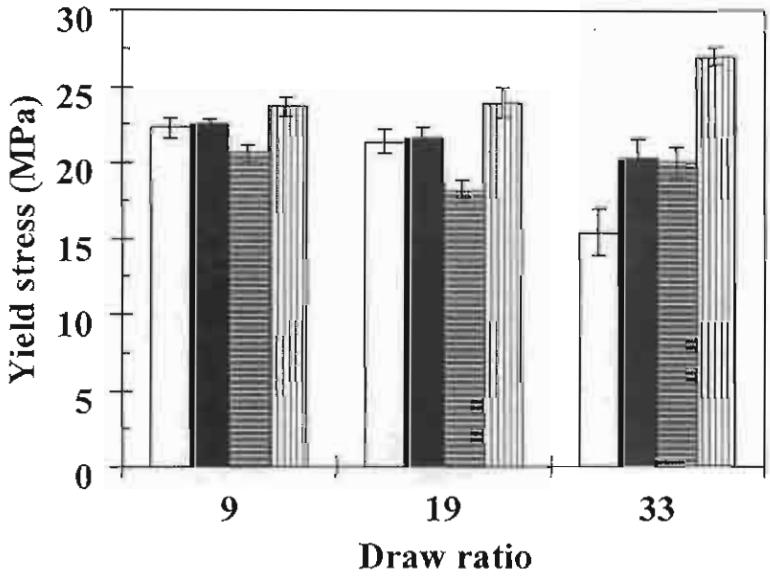

(b)

รูปที่ 3.4 (s) modulus และ (b) yield stress ของ pure PP และ 10 wt% TLCP/PP composite ที่ draw ratio 9, 19 และ 33

□ PP(TD) ■ PP(MD) □ TLCP/ PP(TD) □ TLCP/ PP(MD)

3.1.2 ผลของการเติม compatibilizer ที่มีต่อโครงสร้างสัณฐานและสมบัติของฟิล์ม *in-situ* composites

ได้ทดลองใช้ compatibilizer 3 ชนิด ได้แก่ MA-g-PP , SEBS และ MA-g-SEBS โดยแปรปริมาณจาก 0 - 8 wt% สารช่วยผสมเหล่านี้คาดว่าจะช่วยให้การกระจายตัวของ TLCP ดีขึ้นโดยที่สารเหล่านี้จะไปอยู่ที่รอยต่อระหว่างวัฏภาค (interface) ของ TLCP และ PP เช่นกรณี SEBS ประกอบด้วย styrene block ที่ปลายทั้งสองซึ่งเป็นสารอะโรเมติกผสมเข้ากันได้ดีกับ TLCP ส่วน ethylene butylene block ซึ่งอยู่ตรงกลางเป็นสารประเภทอัลเคนผสมเข้ากันได้ดีกับ PP matrix ดังนั้น SEBS จึงน่าจะไปอยู่ที่รอยต่อระหว่าง phase และช่วยยึดที่รอยต่อนี้ได้ดีขึ้น ส่วนสารที่มีหมู่ maleic anhydride จะสามารถทำปฏิกิริยากับหมู่ที่เป็นเบสได้หรืออาจเกิดพันธะไฮโดรเจนได้ ซึ่งจะสารเหล่านี้ไปอยู่ที่ interface และช่วยให้เกิดการกระจายได้ดีขึ้น เช่นกรณี MA-g-PP ก็มีผู้พบว่าสามารถเกิดพันธะไฮโดรเจนกับ TLCP และช่วยให้ TLCP กระจายใน PP ได้ดีขึ้น (16)

เมื่อนำฟิล์มที่ผสมสารช่วยผสมไปวัดค่า modulus และ yield stress ได้ผลดังแสดงในรูปที่ 3.5 จะเห็นว่า 3 wt% SEBS ให้ค่า modulus สูงที่สุด (1,592 MPa) เมื่อเทียบกับก่อนใส่สารช่วยผสม (1,091 MPa) เพิ่มขึ้นถึง 46% รองลงมาคือ 1.5 wt% MA-g-SEBS ให้ค่า modulus เพิ่มขึ้นประมาณ 21% และ MA-g-PP ให้ค่า modulus เพิ่มขึ้นเพียงเล็กน้อย ผลที่ได้นี้เป็นที่น่าประหลาดใจมาก เมื่อเติมยางซึ่งเป็นวัสดุที่อ่อนลงในพลาสติกยิ่งกลับทำให้พลาสติกแข็งมากขึ้นอีก เมื่อวิเคราะห์โครงสร้างสัณฐานของฟิล์มด้วยกล้องจุลทรรศน์อิเล็กตรอนแบบกวาด (รูปที่ 3.6) จะเห็นว่า สารช่วยผสมเหล่านี้ช่วยให้การกระจายตัวของ TLCP ดีขึ้น ได้เส้นใยจำนวนมากขึ้น และเส้นบางลง นั่นคือมีค่า fiber aspect ratio (ความยาวต่อเส้นผ่าศูนย์กลางของเส้นใย) สูงขึ้น จึงมีผลทำให้ค่า modulus สูงขึ้นนั่นเอง นอกจากนี้จะเห็นผิวของเส้นใยที่แตกต่างกัน สารช่วยผสมที่เป็นยางคือ SEBS และ MA-g-SEBS ทำให้ผิวของเส้นใยขรุขระ แสดงว่าขณะที่เส้นใยยืดตัวจากการดึง การยืดหยุ่นตัวของยางซึ่งอยู่ที่รอยต่อระหว่างวัฏภาคทำให้เกิดความขรุขระที่ผิว และทำให้พื้นที่ผิวตรงรอยต่อระหว่างวัฏภาคเพิ่มขึ้น จึงมีส่วนทำให้การยึดเกาะมีประสิทธิภาพมากขึ้น นอกจากนี้ผลการวิจัยนี้ยังเป็นการพบเป็นครั้งแรกว่าสารช่วยผสมที่ไม่มีหมู่ที่ไวต่อการทำปฏิกิริยา (maleic anhydride, MA) คือ SEBS กลับให้ผลดีกว่าสารช่วยผสมที่มีหมู่ MA คือ MA-g-SEBS ทั้งนี้อาจเป็นเพราะสารช่วยผสมที่มีหมู่ MA ทำให้เกิดพันธะเคมีหรือพันธะไฮโดรเจนที่รอยต่อระหว่างวัฏภาคซึ่งขัดขวางการยืดตัวของเส้นใย TLCP

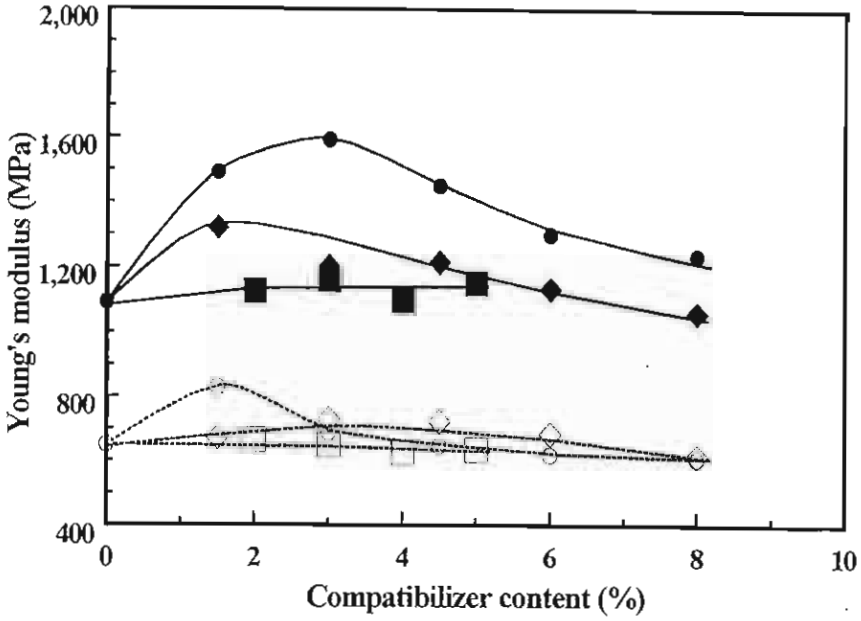

(a)

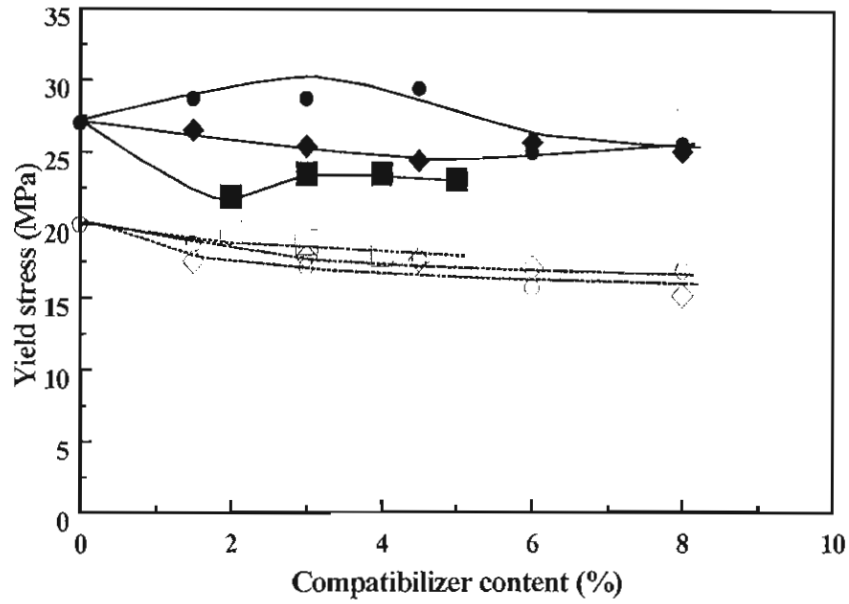

(b)

รูปที่ 3.5 ผลของ compatibilizers ที่มีต่อค่า (a) Young's Modulus และ (b) yield stress ของ TLCP/PP composite films.(●, ○ : SEBS; ◆, ◊ : MA-g-SEBS และ ■, □ : MA-g-PP; MD filled and TD : unfilled)

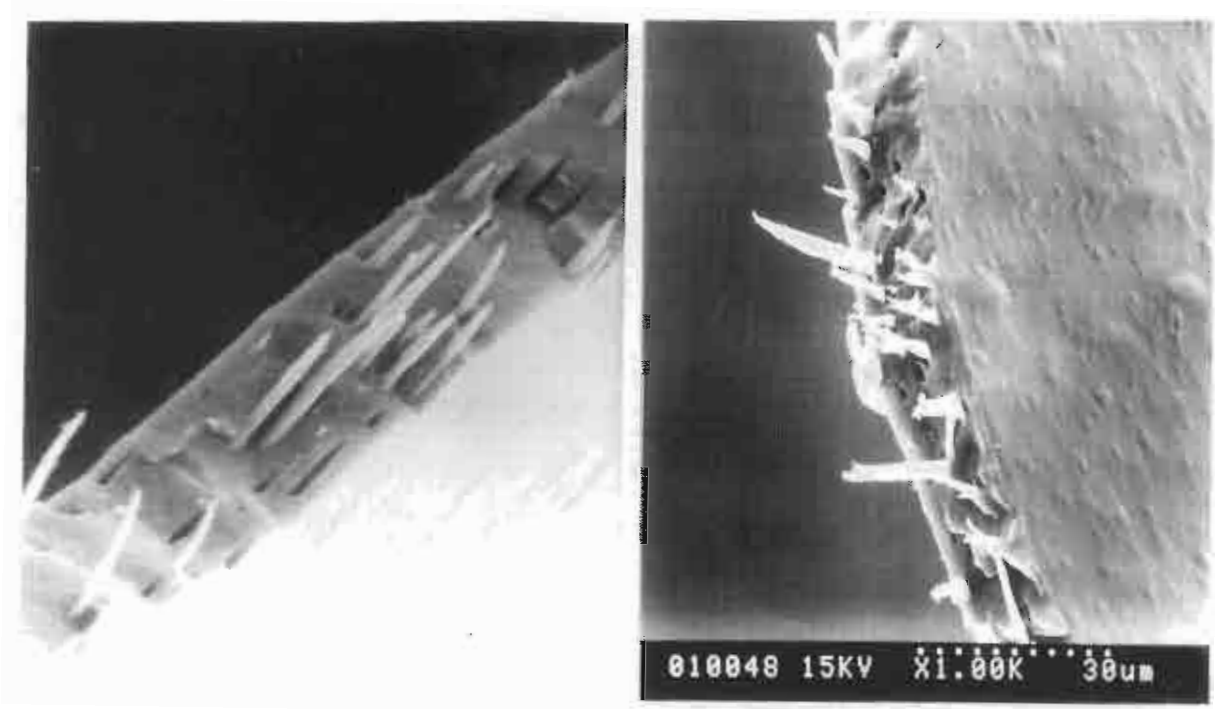

(a) (b)

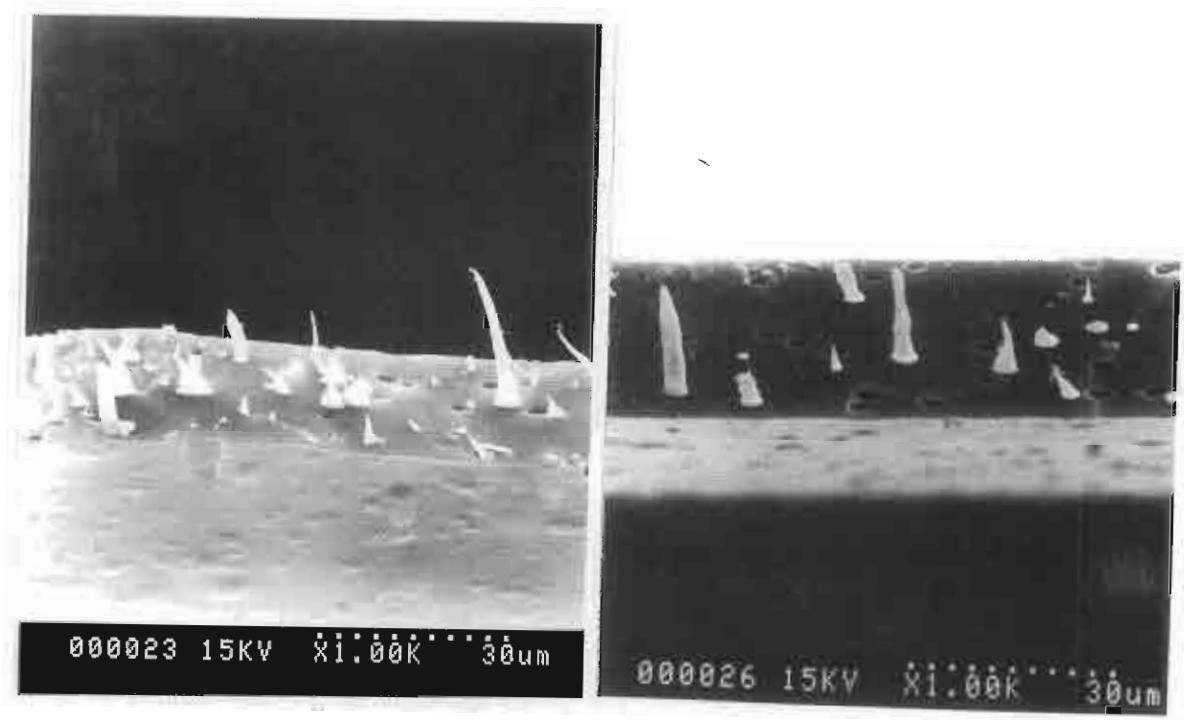

(c) (d)

รูปที่ 3.6 ภาพจาก SEM ของ 10 wt% TLCP/PP (a) ไม่มีสารช่วยผสม
(b) เติม 3 wt% SEBS, (c) 1.5 wt% MA-g-SEBS และ (d) 3 wt% MA-g-PP

เนื่องจาก *in-situ* composite เป็นพอลิเมอร์ผสมที่มีการแยกวัฏภาคจึงมีจุดอ่อนที่รอยต่อระหว่างวัฏภาคซึ่งมีแรงยึดเหนี่ยวต่ำทำให้สมบัติการทนต่อแรงกระแทกไม่ดี การเติม SEBS และ MA-g-SEBS ซึ่งเป็นยางจะสามารถทำหน้าที่ช่วยเพิ่มสมบัติการทนต่อแรงกระแทกได้ด้วย เนื่องจากยางทำหน้าที่เป็น impact modifier ได้ จึงวัด impact strength ของฟิล์มได้ผลดังแสดงในรูปที่ 3.7

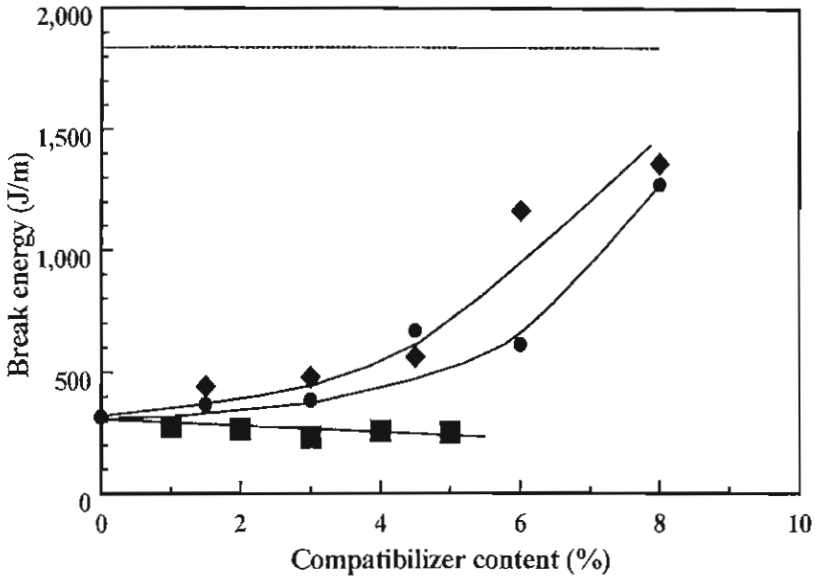

รูปที่ 3.7 ผลของ compatibilizers ที่มีต่อค่า impact strength ของ TLCP/PP composite films ● : SEBS; ◆: MA-g-SEBS and ■ : MA-g-PP; เส้นประคือค่าของ pure PP.

จะเห็นว่าค่า impact strength ของฟิล์มของพอลิเมอร์ผสมต่ำลงมากเมื่อเทียบกับ pure PP (เส้นประ) แต่เมื่อเติมสารช่วยผสมที่เป็นยาง (SEBS และ MA-g-SEBS) ทำให้ค่า impact strength กลับสูงขึ้นมาเกือบเท่าเดิมเมื่อเติมยาง 8% ซึ่งที่ปริมาณยางมากขนาดนี้ก็ยังให้ค่า modulus สูงกว่ากรณีที่ไม่เติมสารช่วยผสม (เปรียบเทียบรูป 3.5) ส่วน MA-g-PP ไม่มีผลต่อค่า impact strength เนื่องจากเป็นพลาสติก

3.1.3 ความหนืดของเมทริกซ์ PP อัตราส่วนความหนืด และผลที่มีต่อโครงสร้างสัณฐานและสมบัติของฟิล์ม *in-situ* composites

ได้แปรความหนืดของ PP โดยเลือกใช้ PP ที่มีค่า MFR 5, 9, 14, 28 ผสมกับ TLCP 10 wt% ความหนืดของพอลิเมอร์ทั้งหมดวัดโดยใช้ capillary rheometer โดยแปร shear rate ในช่วง 60 – 10^4 s^{-1} วัดที่อุณหภูมิ 240 และ 255°C ได้ผลดังแสดงในรูปที่ 3.8 จะเห็นว่าความหนืดของ TLCP ต่ำมากเมื่อเทียบกับ PP matrix ส่วนความหนืดของ PP มีค่าจากมากไปหาน้อยคือ PP5 > PP9 > PP14 > PP28 ตามที่ควรจะเป็น พอลิเมอร์ทุกตัวมีค่าความหนืดลดลงเมื่อเพิ่ม shear rate ปรากฏการณ์นี้เรียกว่า shear thinning effect เนื่องจาก shear rate สูงทำให้ entanglement ของโมเลกุลพอลิเมอร์ลดลง

อัตราส่วนระหว่างความหนืดของ TLCP ต่อความหนืดของ PP เป็นค่าที่บอกให้รู้ว่าการยืดของ TLCP phase เกิดได้หรือไม่ ถ้าอัตราส่วนความหนืดน้อยกว่า 1 จึงจะเกิดการยืดได้ กรณี TLCP/PP มีผู้ศึกษาโดยการเตรียมตัวอย่างเป็น extruded strand และ injection molded พบว่าค่าสัดส่วนความหนืดควรอยู่ในช่วง 0.5 – 1 (22) แต่ในการทดลองนี้พบว่าค่าอัตราส่วนความหนืดต่ำมากคือที่อุณหภูมิ 255°C อยู่ในช่วง 0.04 – 0.15 และที่อุณหภูมิ 255°C อยู่ในช่วง 0.07 – 0.23 (รูปที่ 3.9) ก็เกิด fibrillation ของ TLCP ได้ดีถ้าดึงฟิล์มด้วย draw ratio สูงถึงประมาณ 30 (รูปที่ 3.10)

พอลิเมอร์ผสมที่เตรียมจาก 10 wt% TLCP/PP โดยแปรค่า MFR ของ PPได้ฟิล์มที่มีโครงสร้างสัณฐานดังแสดงในรูปที่ 3.10 โดยที่เตรียมฟิล์มด้วย draw ratio 30 เท่ากัน ถ่ายรูปจากกล้องจุลทรรศน์โดยตรง (แถวซ้าย) และ นำฟิล์มมาสกัด PP ออกด้วย xylene เพื่อให้เห็นขนาดของเส้นใย TLCP ชัดเจนยิ่งขึ้น (แถวขวา) จะเห็นว่าเส้นใย TLCP ยืดยาวขึ้นเมื่อใช้ PP ที่มีความหนืดสูงขึ้นเป็น matrix ทั้งนี้เป็นเพราะ matrix ที่มีความหนืดสูงสามารถส่งผ่านแรงไปยัง TLCP ได้มากทำให้เส้น TLCP ยืดออกบางมากขึ้น นั่นคือมีค่า fiber aspect ratio สูงขึ้น ซึ่งจะทำให้ได้ค่า modulus เพิ่มขึ้น ดังแสดงในรูปที่ 3.11 จะเห็นว่า PP ที่มีค่า MFR = 5 คือมีความหนืดมากที่สุดจะให้ค่า modulus สูงที่สุด และค่า MD modulus เพิ่มขึ้นเมื่อเพิ่ม draw ratio ส่วนค่า MD yield stress ไม่ขึ้นกับค่า MFR ของ PP matrix แต่ขึ้นกับค่า draw ratio ของฟิล์ม คือเมื่อเพิ่ม draw ratio ค่า yield stress จะเพิ่มขึ้น

โดยสรุปงานวิจัยเรื่องนี้ให้ความรู้ใหม่เกี่ยวกับการขึ้นรูปฟิล์ม in-situ composite ว่าการดึงฟิล์มขณะที่พอลิเมอร์เหลวเพิ่งพ้นจากหัว die มีความสำคัญมากในการทำให้ได้ TLCP fibrills ยาว ซึ่งทำให้ได้ค่า modulus สูง สำคัญกว่าการเลือกสัดส่วนความหนืดของคู่ matrix/TLCP ดังที่มีผู้รายงานมาก่อนหน้านี้ นอกจากนี้ยังแสดงให้เห็นว่าสารช่วยผสมที่ใช้ควรเป็น elastomer ซึ่งจะช่วยเพิ่มทั้งสมบัติ tensile และ impact strength และยังเป็นการค้นพบเป็นครั้งแรกว่าสารที่ช่วยผสมนี้ไม่จำเป็นต้องมีหมู่ที่ไวต่อการทำปฏิกิริยาที่รอยต่อระหว่างวัฏภาคตามที่เคยเข้าใจกันมาก่อนหน้านี้ เนื่องจากกรณีนี้ต้องการให้มีการยืดตัวของ TLCP domain ถ้ามีหมู่ที่ทำให้เกิดพันธะทางเคมีหรือพันธะไฮโดรเจนยิ่งจะไปขัดขวางการยืดตัวของ TLCP phase

ผลงานวิจัยเรื่อง TLCP/PP นี้ได้ส่งตีพิมพ์ 3 เรื่อง ใน Polym. Eng. Sci. (1999) **39**, 312-320 (output 1.2), ScienceAsia (in press) (output 1.6) และ Rheol. Acta (submitted) (output 1.7)

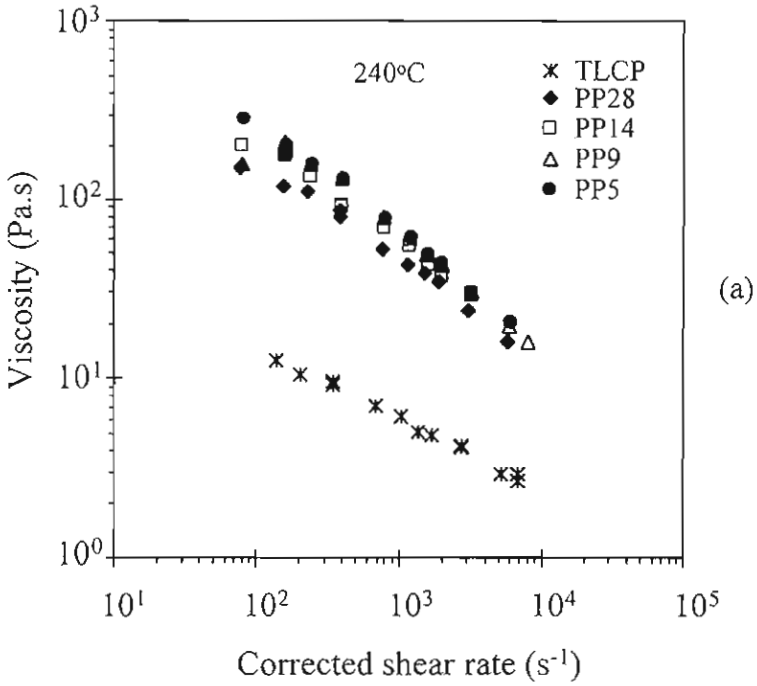

รูปที่ 3.8 ความหนืดที่ค่าอัตราเฉือนต่างๆของ TLCP และ PP ที่มีค่า MFR 5, 9, 14 และ 28 วัดที่อุณหภูมิ (a) 240°C และ (b) 255°C

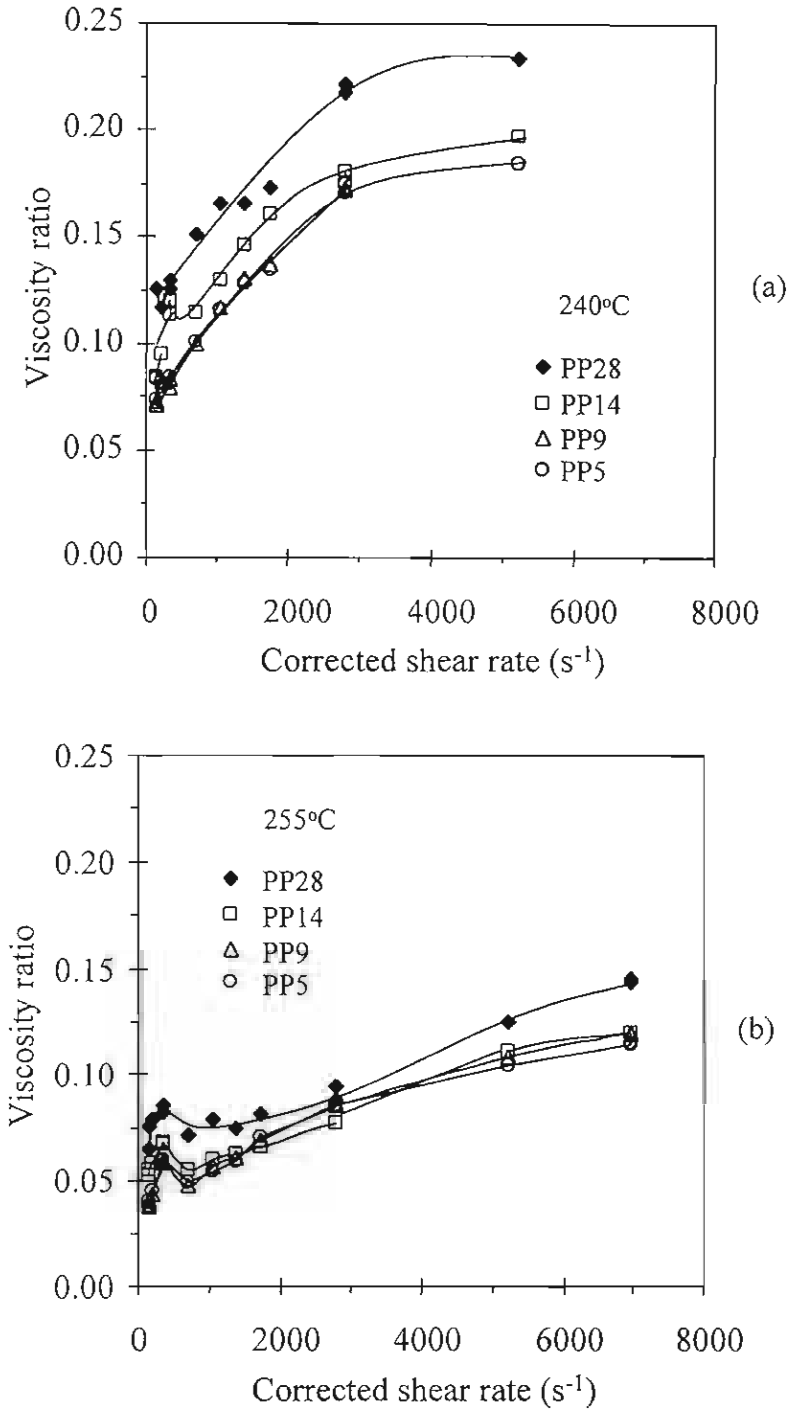

รูปที่ 3.9 Viscosity ratio ระหว่าง TLCP และ PP ที่ค่า shear rate ต่างๆ วัดที่ (a) 240°C และ (b) 255°C

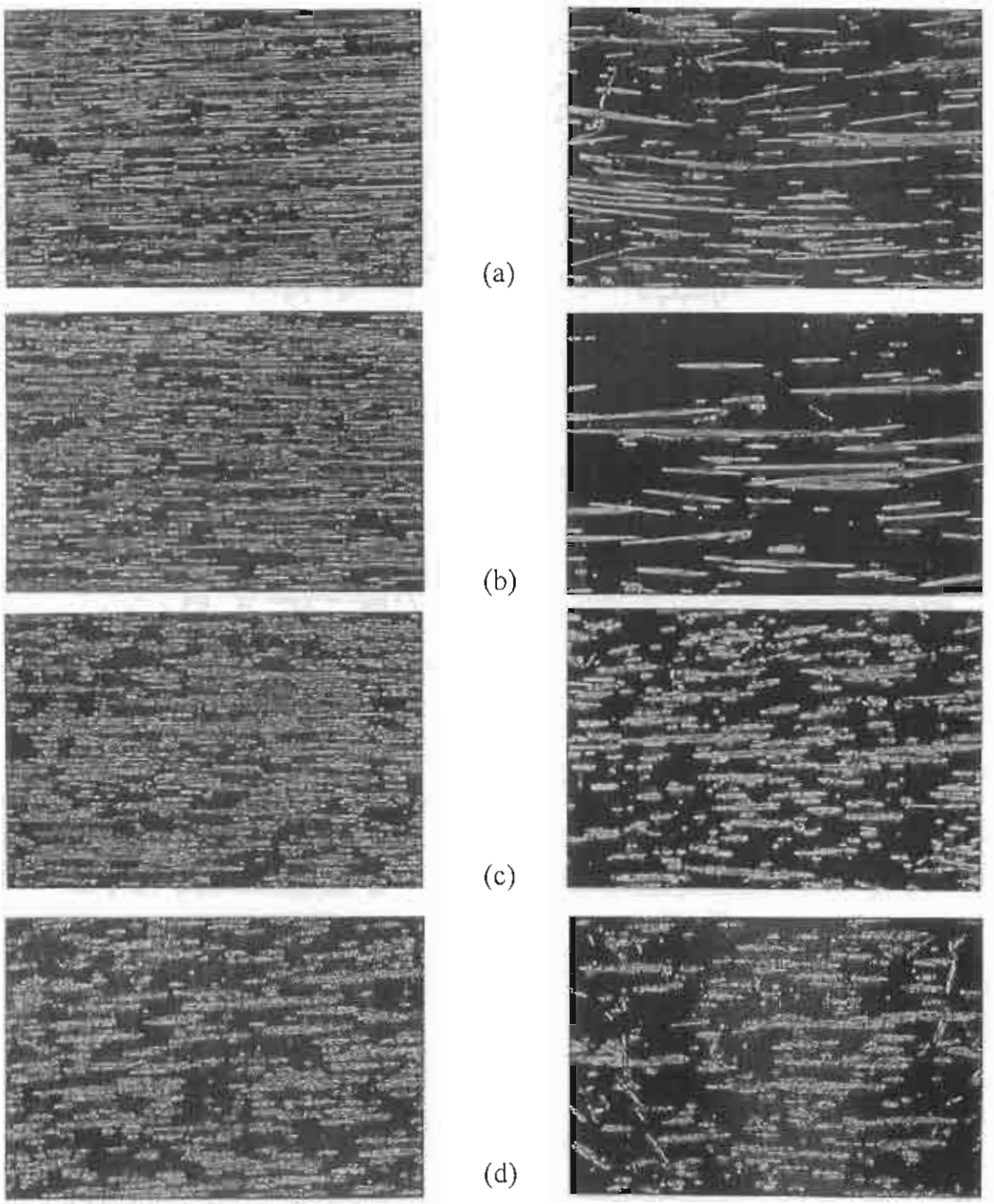

รูปที่ 3.10 แสดงภาพถ่ายจากกล้องจุลทรรศน์ ของ PP/TLCP ฟิล์ม ที่มีค่า Draw ratio 30 กำลังขยาย 200 เท่า ขึ้นรูปที่อุณหภูมิ 255°C เตรียมจาก PP ที่มีค่า MFI (a) 5 (b) 9 (c) 14 และ (d) 28 g/10 min โดยที่แถวซ้ายมือถ่ายจากฟิล์มโดยตรง และภาพแถวขวามือถ่ายหลังสกัด PP ออกด้วย xylene

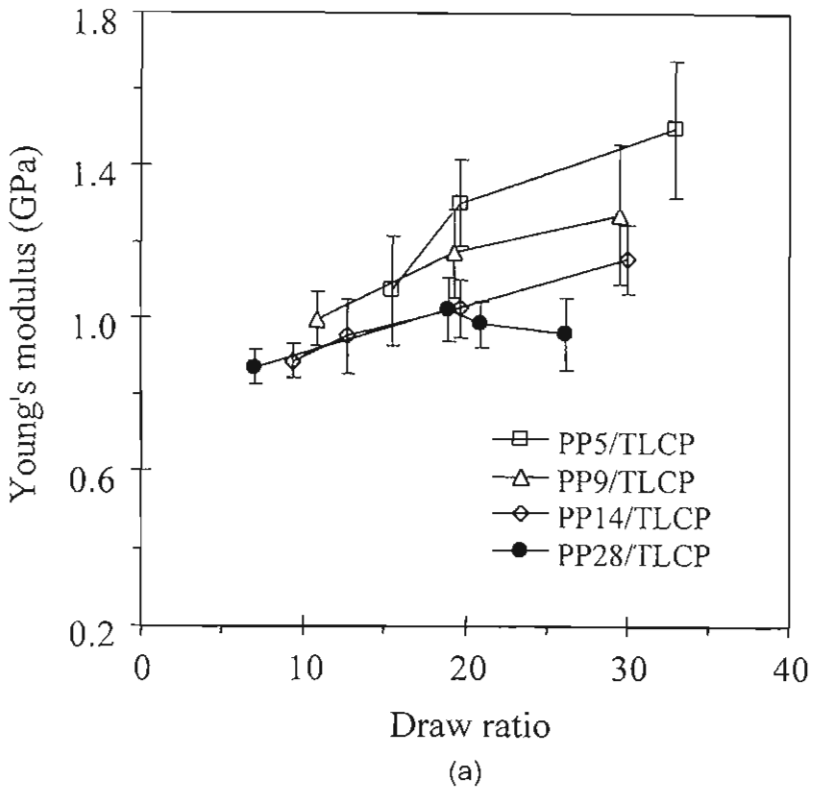

(a)

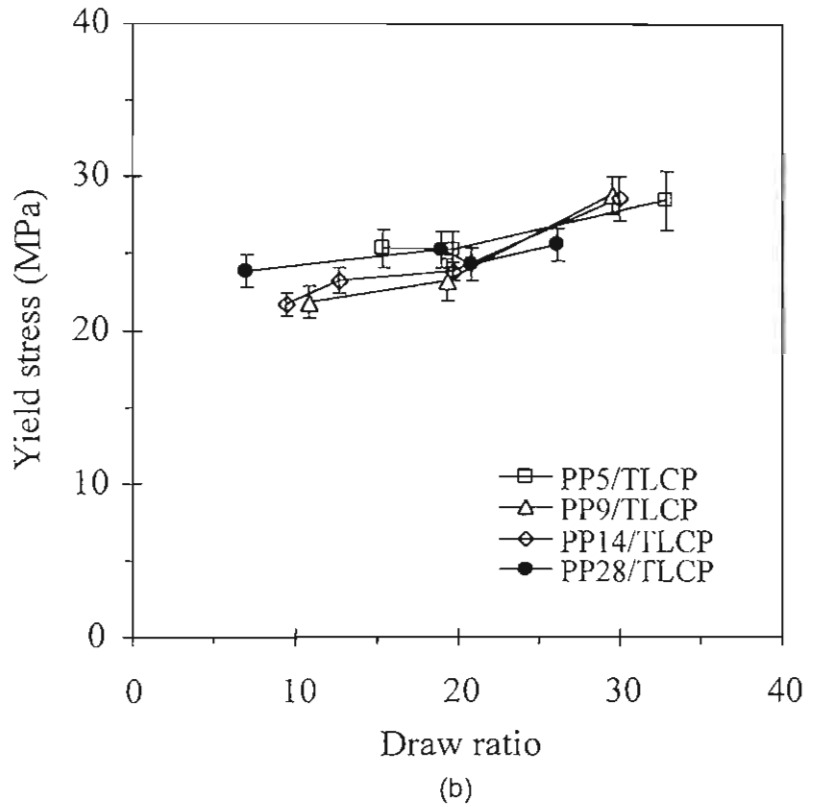

(b)

รูปที่ 3.11 แสดงค่า (a) MD Young's modulus และ (b) MD yield stress ของ TLCP/PP (vary MFR) โดยเตรียมฟิล์ม ที่ draw ratio ต่างๆ

3.2 พอลิเมอร์ผสมระหว่าง Polyethylene และ Rodrun LC3000

เตรียมพอลิเมอร์ผสม (*in-situ* composite) ระหว่างพอลิเอทธิลีนความหนาแน่นต่ำ (low density polyethylene, LDPE) กับ Rodrun LC3000 ซึ่งเป็นพอลิเมอร์ผลึกเหลวชนิดเทอร์โมโทรปิก (Thermotropic Liquid Crystalline Polymer, TLCP) และใช้ SEBS, MA-g-SEBS , EPDM, MA-g-EPDM เป็นสารช่วยผสม โดยขึ้นรูปเป็นฟิล์มบาง

3.1.1 ผลของการแปร draw ratio ที่มีต่อสมบัติ tensile ของ pure LDPE และพอลิเมอร์ผสม LDPE/TLCP แสดงในรูปที่ 3.12

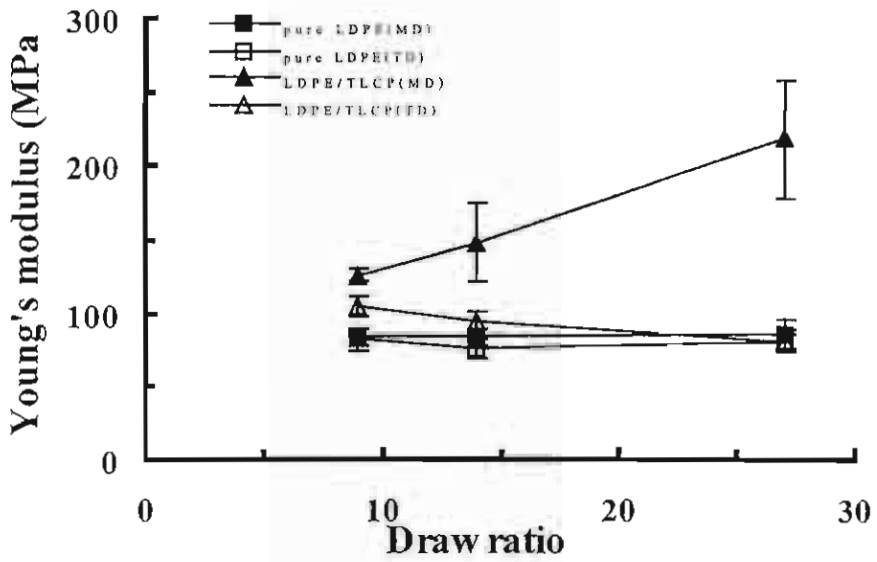

รูปที่ 3.12 Young's modulus ของฟิล์ม LDPE และ 10 wt% TLCP/LDPE ที่ค่า draw ratio ต่างๆ วัดในทิศการฉีดฟิล์ม (MD) และวัดในทิศตั้งฉาก (TD)

ผลจากรูปที่ 3.12 แสดงให้เห็นว่าค่า Young's modulus ของ composite film TLCP/LDPE ในทิศ MD มีค่าเพิ่มขึ้นประมาณ 2 เท่า เมื่อค่า Draw ratio สูงขึ้นจาก 9 เป็น 27 ส่วนค่า modulus ในทิศ TD จะมีค่าลดลงเล็กน้อย ผลที่ได้นี้สอดคล้องกับภาพที่เห็นจากกล้องจุลทรรศน์คือเส้นใย TLCP ยาวขึ้นเมื่อ draw ratio มีค่าสูงขึ้น ส่วนในกรณี neat LDPE พบว่าการแปร draw ratio ไม่มีผลต่อค่า Modulus ทั้งสองทิศทางแสดงว่าการดึงฟิล์มถึง draw ratio 27 ไม่มีผลต่อการเรียงตัวของโมเลกุลใน LDPE

3.2.2 ผลของการแปรปริมาณของ TLCP ที่มีต่อสมบัติ tensile modulus ที่ได้จากการวัดทั้งในทิศ MD และในทิศ TD ของ composite TLCP/LDPE ผลที่ได้แสดงในรูปที่ 3.13

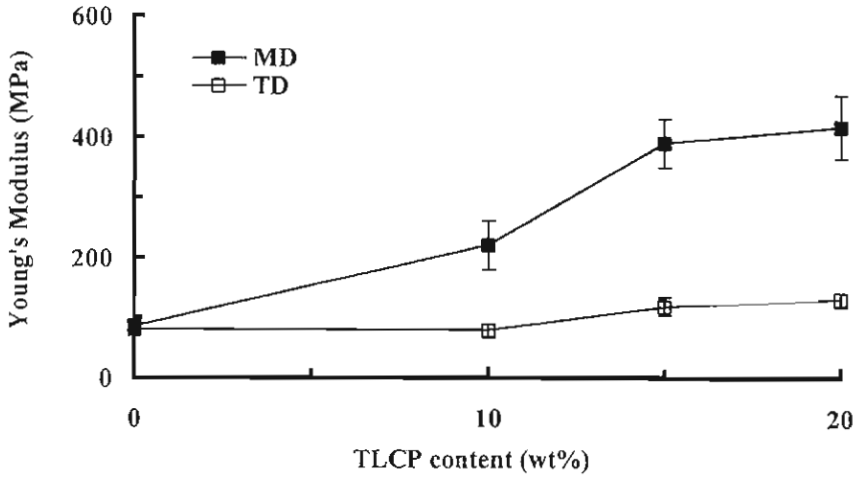

รูปที่ 3.13 ผลของปริมาณ TLCP ที่มีต่อค่า Young's modulus ของ composites LDPE/TLCP ที่วัดในทิศ MD และทิศ TD

พบว่าเมื่อเพิ่มปริมาณของ TLCP ค่า modulus ในทิศ MD มีค่าเพิ่มขึ้นมาก โดยที่ค่า modulus ของฟิล์มที่มี TLCP 10, 15, และ 20 wt% มีค่าสูงขึ้นเป็น 158, 356, และ 390 % เมื่อเปรียบเทียบกับ pure LDPE ตามลำดับ เนื่องจากการเติม TLCP ทำให้ได้ปริมาณของเส้นใย TLCP เพิ่มมากขึ้น แต่จากการส่องดูโครงสร้างสัณฐานด้วยกล้องจุลทรรศน์จะเห็นว่าความยาวของเส้นใยที่ได้ไม่ต่างกันมาก ส่วนค่า modulus ในแนว TD มีค่าเพิ่มขึ้นเล็กน้อยเมื่อเพิ่มปริมาณ TLCP

3.2.3 ผลของการเติมสารช่วยผสมที่มีต่อ tensile modulus ของฟิล์ม 10 wt%TLCP/LDPE โดยการเติม 3 wt% ของสารช่วยผสม SEBS, MA-g-SEBS, EPDM, และ MA-g-EPDM ได้ผลดังแสดงในรูปที่ 3.14 พบว่าค่า Modulus ในทิศ MD ลดลงหลังจากเติมสารช่วยผสม ส่วนค่า modulus ในทิศ TD มีค่าเพิ่มขึ้นเล็กน้อย ผลที่ได้นี้สอดคล้องกับภาพจากกล้องจุลทรรศน์ซึ่งจะเห็นว่าเส้นใยภายในฟิล์มที่เติมสารช่วยผสมมีขนาดสั้นกว่าเส้นใย TLCP ในคอมพอสิตที่ไม่ได้เติมสารช่วยผสม ทั้งนี้อาจเป็นเพราะสารช่วยผสมจะไปทำให้การกระจายตัวของหยด TLCP ดีขึ้น ทำให้ได้เส้นใยขนาดบางมากขึ้นและเมื่อได้รับแรงเฉือนจะทำเส้นใยขาด จึงได้เส้นใยขนาดเล็กและสั้นลง และส่งผลให้ค่า modulus ลดลง

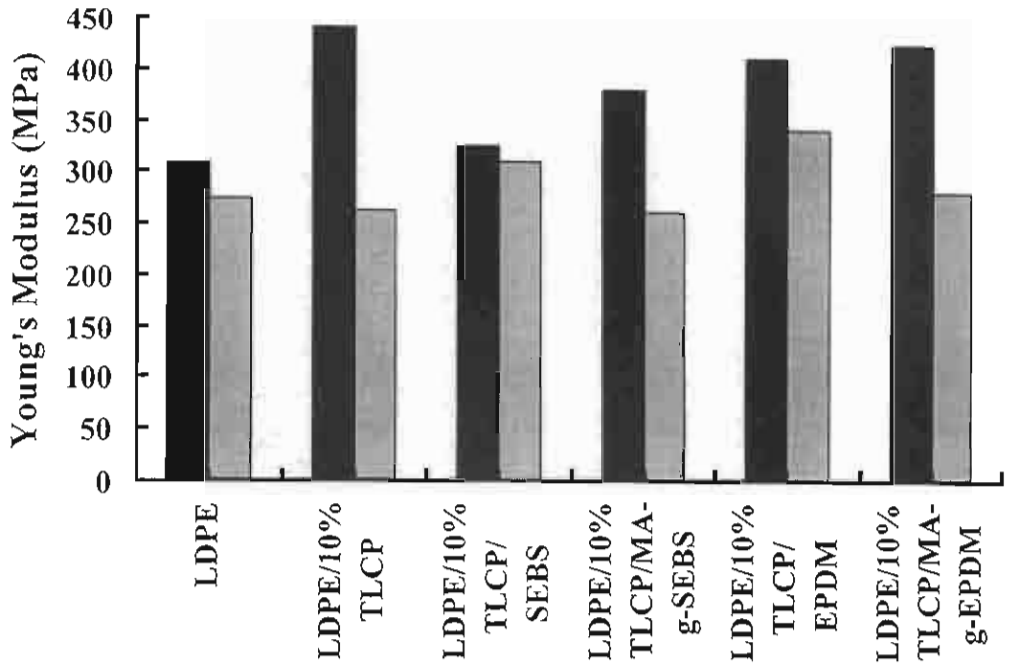

รูปที่ 3.14 Young's modulus ของฟิล์ม 10 wt%TLCP/LDPE ที่ผสมสารช่วยผสมต่างๆ 3 wt% วัดในทิศ MD (ดำ) และทิศ TD (เทา)

3.2.4 ผลของการวัดความหนืดของ LDPE และพอลิเมอร์ผสม ด้วยเครื่อง Capillary Rheometer ที่อุณหภูมิ 240°C และแปรอัตราการเฉือนตั้งแต่ 100 ถึง 10,000 s^{-1} แสดงในรูปที่ 3.15

ค่าความหนืดที่อัตราการเฉือนต่างๆของพอลิเมอร์ผสม TLCP/LDPE จะมีค่าต่ำลงเมื่อปริมาณ TLCP มากขึ้น เนื่องมาจาก TLCP มีค่าความหนืดต่ำมากเมื่อเทียบกับ LDPE ดังนั้นเมื่อปริมาณ TLCP มากขึ้นก็ส่งผลให้ค่าความหนืดของพอลิเมอร์ผสมมีค่าลดลง (TLCP ทำหน้าที่เป็น processing aid) นอกจากนี้พบว่าความหนืดของพอลิเมอร์ทุกตัวลดลงเมื่อเพิ่ม shear rate (shear thinning effect) ซึ่งเป็นลักษณะปกติซึ่งเกิดจากการพันการคล้องกันของโมเลกุลลดลงเมื่อได้แรงเฉือนมากขึ้น (disentanglement)

เมื่อนำค่าความหนืดของ TLCP และ LDPE มาคำนวณหาอัตราส่วนระหว่างความหนืดของ TLCP ต่อความหนืดของ LDPE จะได้ค่าอยู่ในช่วง 0.06 ถึง 0.1 ขึ้นกับ shear rate ค่าอัตราส่วนความหนืดนี้เป็นตัวแปรสำคัญที่จะบอกว่าในการผสม TLCP กับ matrix จะเกิดเป็น TLCP fiber หรือไม่ โดยที่ TLCP จะเกิดเป็น fiber ได้ก็ต่อเมื่ออัตราส่วนความหนืดมีค่าน้อยกว่าหนึ่ง เมื่อพอลิเมอร์เมทริกซ์ได้รับแรงจากภายนอกจะส่งแรงผ่านไปยังวัฏภาคของ TLCP ทำให้ TLCP เปลี่ยนรูปร่างจาก droplet ยืดออกเป็นเส้นใย

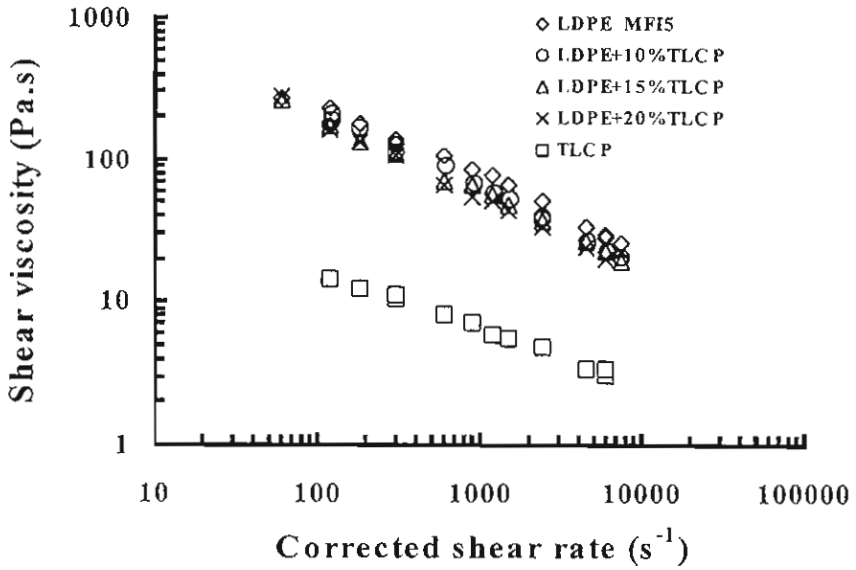

รูปที่ 3.15 ความหนืดที่ค่า shear rate ต่างๆ ของ TLCP, LDPE และ TLCP/LDPE blends โดยแปรปริมาณของ TLCP

3.2.5 โครงสร้างสัณฐาน (Morphology) ของฟิล์มวิเคราะห์โดยใช้กล้องจุลทรรศน์ (polarized optical microscope, OM) แสดงในรูปที่ 3.16 คือเส้นใย TLCP ที่ได้จากการสกัด film TLCP/LDPE ด้วย xylene รูปนี้แสดงผลของการดึงฟิล์มด้วย draw ratio 9, 14 และ 27 ที่มีต่อขนาดของเส้นใย จะเห็นว่าเส้นใย TLCP ยาวขึ้นเมื่อเพิ่ม draw ratio

รูปที่ 3.17 คือฟิล์ม TLCP/LDPE composite ที่แปรปริมาณของ TLCP จะเห็นว่าขนาดของเส้นใยไม่ต่างกัน เพียงแต่จำนวนเส้นใยเพิ่มขึ้นเมื่อเพิ่มปริมาณ TLCP จึงส่งผลให้ค่า modulus สูงขึ้นดังกล่าวแล้ว

รูปที่ 3.18 แสดงฟิล์ม 10 wt%TLCP/LDPE ที่ผสมสารช่วยผสม SEBS, MA-g-SEBS, EPDM, MA-g-EPDM จะเห็นว่าเส้นใย TLCP มีขนาดสั้นลงเพราะสารช่วยผสมไปทำให้การกระจายตัวของ TLCP ดีขึ้น ได้ขนาดของหยด TLCP เล็กลงเมื่อได้รับแรงเฉือนจากเครื่อง extruder เส้นใย TLCP จึงขาด มีขนาดเล็กและสั้นลง

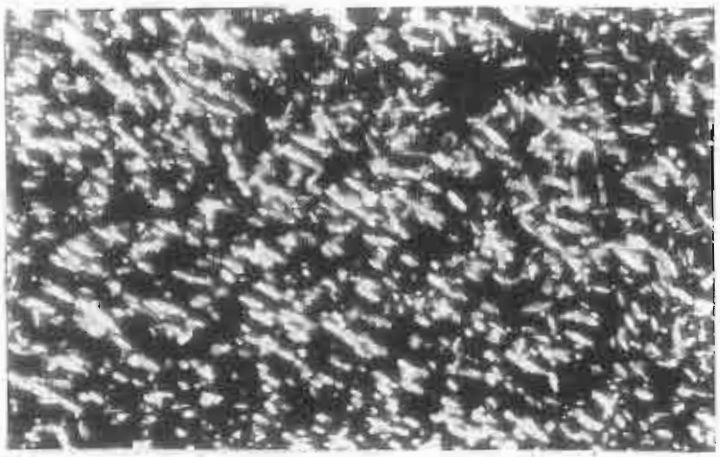

(a)

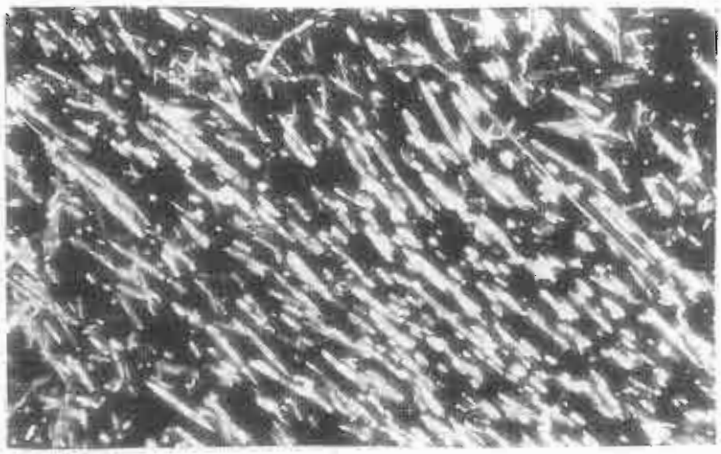

(b)

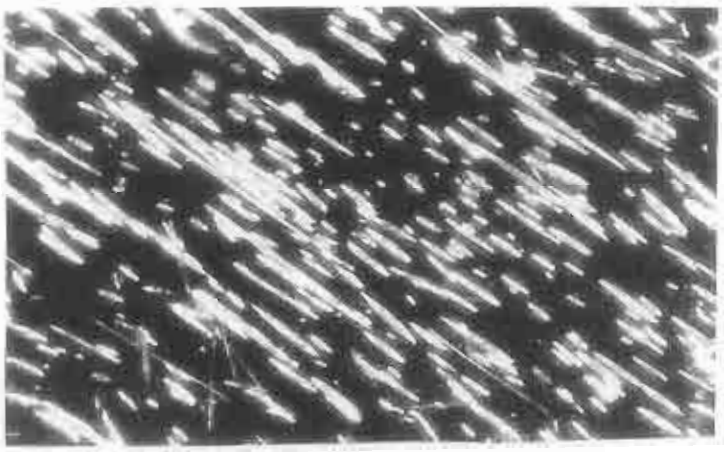

(c)

รูปที่ 3.16 TLCP fiber สกัดจาก ฟิล์ม LDPE/10 wt%TLCP ที่ได้จากการดึงด้วย draw ratio (a) 9 (b) 14 (c) 27 (กำลังขยาย 200 เท่า)

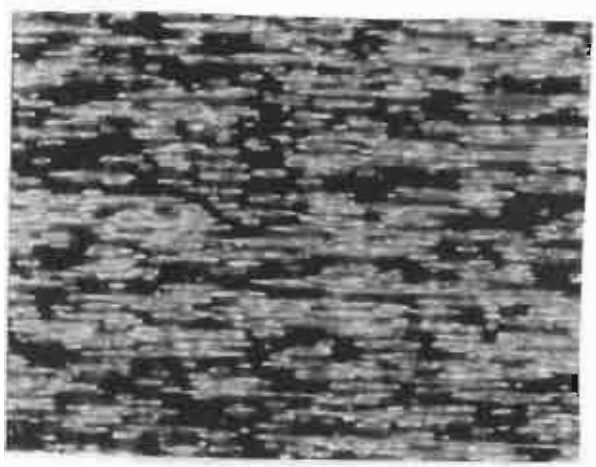

(a)

(b)

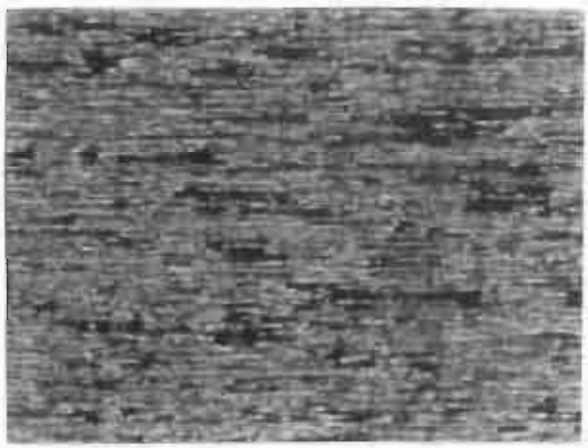

(c)

รูปที่ 3.17 ฟิล์ม TLCP/LDPE ที่ผสม TLCP 10, 15, 20 wt% กำลังขยาย 200 เท่า

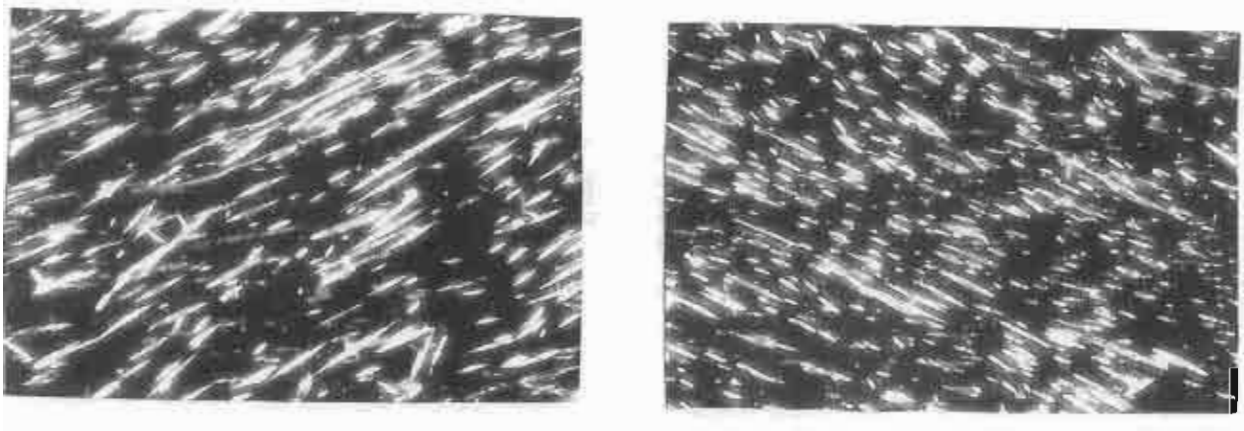

(a) (b)

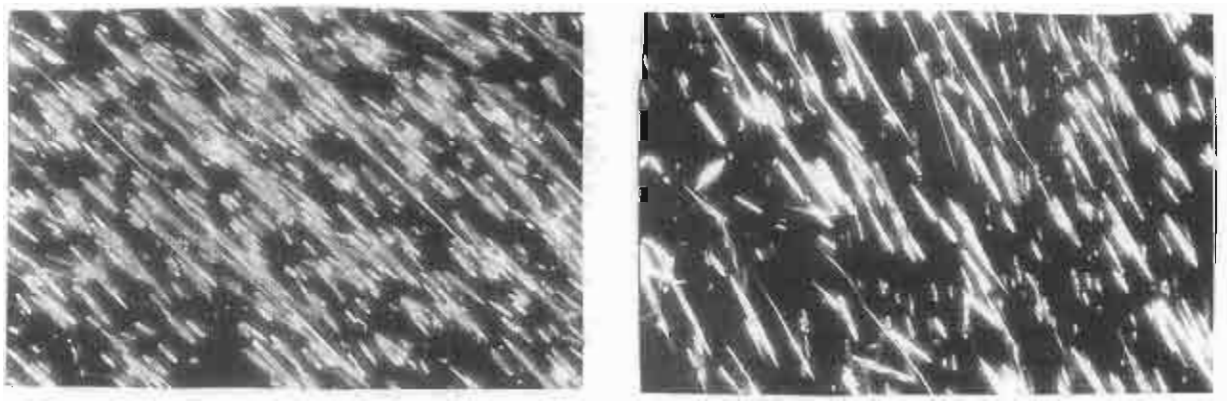

(c) (d)

รูปที่ 3.18 ฟิล์ม 10 wt%TLCP/LDPE ที่มีสารช่วยผสม (a) SEBS (b) MA-g-SEBS (c) EPDM (d) MA-g-EPDM (กำลังขยาย 200 เท่า)

ผลการศึกษาโครงสร้างสัณฐาน (Morphology) ของฟิล์มโดยใช้กล้องจุลทรรศน์อิเล็กตรอนแบบกวาด (Scanning electron microscope, SEM)

รูปที่ 3.20 เปรียบเทียบ fracture surface ที่ได้จาก composites TLCP/LDPE ที่เติมและไม่เติมสารช่วยผสมจะเห็นว่าในภาพ (a) เส้นใย TLCP มีผิวเรียบ ยาว ขนาดใหญ่และแสดงการหลุดแบบถอดออก (pull-out) ซึ่งแสดงว่าการยึดเกาะที่ผิวไม่ดี ในขณะที่ภาพ (b) – (e) ได้จากการเติมสารช่วยผสม ทำให้เส้นใย TLCP ที่ได้มีขนาดเล็กลง มีปลายแหลม แสดงว่า TLCP มีการกระจายตัวมากขึ้นทำให้เส้นมีขนาดเล็ก เมื่อเกิดการยืดและขาดจึงมีลักษณะปลายแหลม ส่งผลให้สมบัติ tensile ไม่ดีขึ้นดังที่กล่าวมาแล้ว

สรุปผลการทดลอง

in-situ compositss film TLCP/LDPE มีค่า modulus ในทิศ MD สูงขึ้นเมื่อค่า draw ratio สูงขึ้น และมีค่า modulus ในทิศ MD สูงขึ้นเมื่อเพิ่มปริมาณ TLCP นอกจากนี้พบว่า elastomeric compatibiliser ที่ใช้ในการทดลองนี้ไม่ช่วยให้ modulus เพิ่มขึ้น ซึ่งต่างจากระบบ TLCP/PP composites ทั้งๆที่ PP และ LDPE เป็น polyolefin เหมือนกัน ความไม่มีชั้วใกล้เคียงกัน แต่สิ่งที่ต่างกันคือ ความสามารถในการเรียงอัดตัวของโมเลกุล แม้ว่า LDPE จะมี branching บ้างแต่ก็ไม่มีหมู่เมทิลห้อยด้านข้างมากแบบ PP (ทำให้ความหนาแน่นของ PP ต่ำกว่า LDPE) ดังนั้นการเรียงตัวและอัดตัวของโมเลกุลเมื่อถูกดึงจึงเกิดใน LDPE ได้มากกว่าใน PP เมื่อใช้สภาวะการผสมและการเตรียมตัวอย่างเหมือนกันจึงได้เส้นใย TLCP ใน LDPE matrix เล็กและบางกว่าใน PP matrix มาก เนื่องจากเกิดแรงอัดด้านข้างได้มากกว่า ทำให้ความเสถียรของเส้นใย TLCP ใน LDPE มีน้อยกว่าจึงขาดง่าย

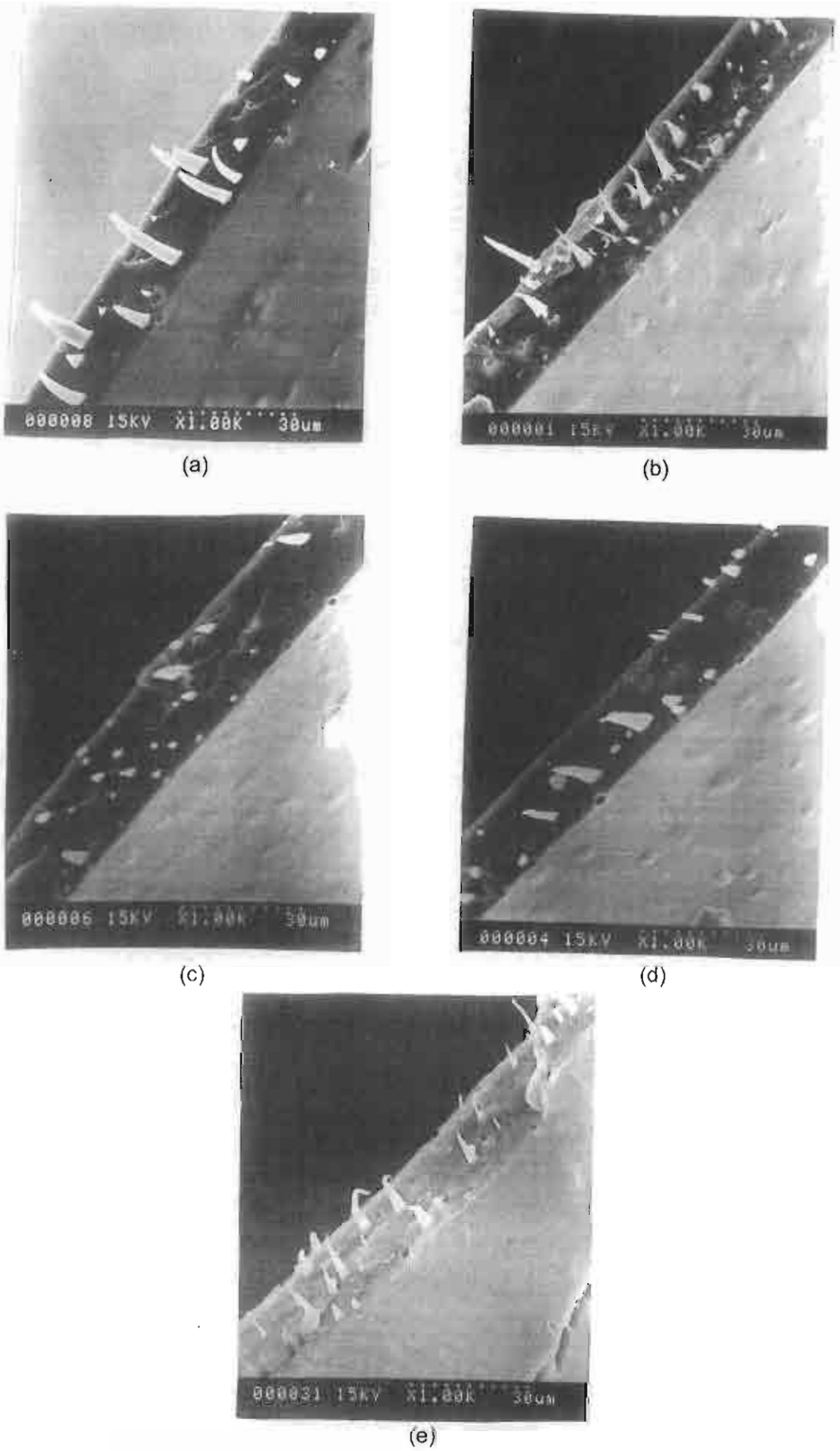

รูปที่ 3.20 แสดงภาพถ่ายจาก SEM ของ 10 wt% TLCP/LDPE กำลังขยาย 1000 เท่า
(a) ไม่เติมสารช่วยผสม (b) เติม 3 wt% SEBS (c) เติม 3 wt% SEBS-g-MA
(d) 3 wt% EPDM (e) 3 wt% EPDM-g-MA

References

1. Foldi, A. P. in Vigo, T. L. and Kinzig, B. L. editors (1992) Composite Applications: The role of matrix, fiber and interface, VCH publisher, New York, pp 133-177
2. Brown, C. S. and Alder, P. T. (1993) in Polymer Blends and Alloys, M. J. and Hope, P. S. editors, Blackie Academic & Professional, Glasgow, pp 195-227
3. Nando, G. B. and Gupta, B. R. (1996) in Short Fiber-Polymer Composites, S. K. De and J. R. White, editors, Woodhead Publisher, Cambridge, pp 84-115
4. Kutty, S. K. N. and Nando, G. B. (1992) *J. Appl. Polym Sci.*, **46**, 471
5. Chiao, C. C. and Chiao, T. T. in Lubin, G. editor (1982) Handbook of Composites, van Nostrand Reinhold Company, New York, pp272-317
6. Garbassi, F., Morra, M. and Occheillo, E., (1994) Polymer Srufaces, From Physics to Technology, John Wiley & Sons Lid, Chichester
7. Vaughan D.J. (1978) The Use of Coupling Agents to enhance the Performance of Aramid Reinforced Composites *Polym Eng Sci* **18**, 167-169
8. Takayanaki M., Kajiyama T. and Katayose T. (1982) Surface-Modified Kevlar Fiber-Reinforced Polyethylene and Ionomer *J Appl Polym Sci* **27**, 3903-3917
9. Breznick M., Banbaji J., Guttmann H. and Marom G. (1987) Surface T reatment Technique for Aramid Fibres *Polym Commun* **28**, 55-56
10. Andreopoulos A. G. (1989) A New Coupling Agent for Aramid Fibre *J Appl. Polym. Sci* **38**, 1053-1064
11. Kiss, G. (1987) *In situ* composites: blends of isotropic polymers and thermotropic liquid crystalline polymers. *Polym. Eng. Sci.*, **27**, 410
12. Dutta, D., Fruitwala, H. , Kohli, A. and Weiss, R. A. (1990) Polymer blends containing liquid crystals: a review. *Polym. Eng. Sci.*, **30**, 1005
13. Handlos, A. A. and Baird, D. G. (1995) Processing and associated properties of *in situ* composites based on thermotropic liquid crystalline polymers and thermoplastics.. *J. M. S. Rev. Macromol. Chem. Phys.*, **C35**, 183-238
14. Hull, J. B. and Jones, A. R. (1996) in *Rheology and Processing of Liquid Crystalline Polymers,* Arcierno, D. and Collyer, A. A, editors Chapman & Hall, London, pp 218-250
15. Datta, A. and Baird, D. G. (1995) Compatibilization of Thermoplastic Composites Based on Blends of Polypropylene with Two Liquid Crystalline Polymers. *Polymer* **36**, 505-514

16. O'Donnell, H. J. and Baird, D. G. (1995) *In-Situ* Reinforcment of Polyproplene with Liquid Crystalline Polymers: Effect of Maleic Anhydride-Grafted Polypropylene. *Polymer* **36,** 3113-3126

17. Seo, Y.J. (1997) Interfacial Adhesion and Deformation of Thermotropic Liquid Crystal Polymers in Engineering Thermoplastics: Blends of a Poly(ester amide) with Nylon 6 and a Polyester with PBT *J. Appl. Polym. Sci.* **64,** 359

18. Engberg K., Knuttson A. and Werner P.-E. *et al.* (1990) Knit Line Features in Injection Molded Liquid Crystalline Polymer *Polym. Eng. Sci.* **30,** 1620-9

19. Crevecoeur, G. and Groeninckx, G. (1993) Sheet extrusion of *in-situ* composites : influene of processing parameters. *Polym. Eng. Sci.*, **33**, 937-943

20. Hsu, T. C. Lichkus, A. M. and Harrison, I. R. (1993) Liquid crystal polymer/polyethylene blends for thin film applications. *Polym. Eng. Sci.*, **33**, 860-862

21. Chinsirikul, W. Hsu, T. C. and Harrison, I. R. (1996) Liquid crystalline polymer (LCP) reinforced polyethylene blend blown film: effect of counter-rotating die on fiber orientation and film properties. *Polym. Eng. Sci.*, **36**, 2708-2717

22. Heino MT, Hietaoja PT, Vainio TP and Seppala JV (1994) Effect of Viscosity Ratio and Processing Conditions on the Morphology of Blends of Liquid Crystalline Polymer and Polypropylene. *J Appl Polym Sci* **51**, 259-270

Research Output จากทุนเมธีวิจัยอาวุโส-สกว เสาวรภย์ บัวเล็ก-ลิ้มเจริญ (RTA3880009)

1. ผลงานตีพิมพ์ในวารสารวิชาการนานาชาติ

1.1 S. Bualek-Limcharoen, T. Nakinpong, T. Amornsakchai and W. Meesiri, Kevlar Pulp-Thermoplastic Elastomer Composites : Morphology and Mechanical Properties, *J. Sci. Soc. Thailand* **23** (1997)101-114

1.2 S. Bualek-Limcharoen, J. Samran, T. Amornsakchai and W. Meesiri, Effect of Compatibilizers on Mechanical Properties and Morphology of *In-Situ* Composite Film of Thermotropic Liquid Crystalline Polymer/Polypropylene, *Polym. Eng. Sci.* **39** (1999)312-320

1.3 T. Amornsakchai, B. Sinpatanapan, S. Bualek-Limcharoen and W. Meesiri, Composite of Aramid Fibre (Poly-m-phenylene isophthalamide)-Thermoplastic Elastomer (SEBS) : Enhancement of Tensile Properties by Maleated-SEBS Compatibiliser, *Polymer.* **40** (1999)2993-2999

1.4 S. Saikrasun, T. Amornsakchai, C. Sirisinha, W. Meesiri and S. Bualek-Limcharoen, Kevlar Reinforcement of Polyolefin-Based Thermoplastic Elastomer, *Polymer* **40**, (1999) 6437-6442

1.5 A. Chantaratcharoen, C. Sirisinha, T. Amornsakchai, S. Bualek-Limcharoen and W. Meesiri, Improvement of Interfacial Adhesion of Poly-(m-phenylene isophthalamide) short fibre-Thermoplastic Elastomer(SEBS) Composites by N-Alkylation on Fiber Surface, *J. Appl. Polym. Sci.* **74** (1999) 2414-2422

1.6 J. Samran, W. Meesiri, S. Bualek-Limcharoen and T. Amornsakchai, In-situ Composite Film of Thermotropic Liquid Crystalline Polymer/Polypropylene : Effect of Film Drawing on Molecular Orientation and Properties, *ScienceAsia* **25** (1999) 91-97.

1.7 B. Wanno, J. Samran and S. Bualek-Limcharoen, Effect of Melt Viscosity of Polypropylene on Fibrillation of Thermotropic Liquid Crystalline Polymer in In-situ Composite Film, Rheologica Acta (submitted).

1.8 S. Bualek-Limcharoen, B. Wanno, W. Meesiri, C. Sirisinha and T. Amornsakchai, Effect of Processing Condition, Melt Viscosity and Compatibilizer on Tensile Properties and Morphology of Liquid Crystalline Polymer (60/40 HBA/PET)-Polypropylene *In-Situ* Composite Films (in preparation).

1.9 C. Vajrasthira, S. Bualek-Limcharoen, T. Amornsakchai and C. Sirisinha, Mechanical Properties and Morphology of Poly-(m-phenylene isophthalamide) Short Fiber-Polyurethane Thermoplastic Elastomer Composite (in preparation).

2 ผลงานตีพิมพ์ในวารสารวิชาการในประเทศไทย

2.1 T. Nakinpong, B. Sinpatanapan, W. Meesiri, T. Amornsakchai and S. Bualek-Limcharoen, Aramid Fibres-Thermoplastic Elastomer (SEBS) Composites: Effect of Maleic Anhydride Grafted Compatibiliser on Mechanical Properties, *Mahidol J.* **5**, (1998) 115-120

3 หนังสือ -

4 การจดทะเบียนสิทธิบัตร -

5 การเสนอผลงานในที่ประชุมวิชาการนานาชาติ

5.1 T. Nakinpong, T. Amornsakchai, W. Meesiri and S. Bualek, Effect of Surface Treatment on Mechanical Properties of Aramid Pulp-Thermoplastic Elastomer Composites, Proceeding of The International Conference on Materials Technology: Recent Development and Future Potential p343-352, 9-10 January 1997, Chaing Mai

5.2 S. Bualek-Limcharoen, J. Samran, W. Meesiri and T. Amornsakchai, Thermoplastics-Liquid Crystalline Polymer Blends: Processing, Characterisation and Properties of *In-Situ* Composite Films, Proceeding of the Conference: Polymer Blends Toward 2000, 18-20 Auguest 1997, Kasetsart University, p95-105

5.3 T. Amornsakchai, W. Meesiri, T. Nakinpong, B. Sinpatanapan and S. Bualek-Limcharoen, Aramid Fibers-Thermoplastic Elastomer Composites: Properties of Composites Using Maleic Anhydride Grafted Compatibilizer, 7 pages in the Proceeding of the International Rubber Conference 18-20 October 1997, Kuala Lumpur, Malaysia

5.4 S. Bualek-Limcharoen, T. Amornsakchai and J. Samran, In-Situ Composites PP/LCP : Enhancement of Modulus and Impact Strength by Compatibilizers, IUPAC World Polymer Congress, 37th International Symposium on Macromolecules, 12-17 July 1998, Gold Coast, Australia

5.5 S. Bualek-Limcharoen, Composites of Aramid Fibers-Thermoplastic Elastomers : Improvement of Interfacial Adhesion by Chemical Modifications of Fiber Surface, 7th International Seminar on Elastomer, 16-17 December 1998, Bangkok, Thailand

5.6 B. Wanno, J. Samran and S. Bualek-Limcharoen, Effect of Melt Viscosity of Polypropylene on Fibrillation of Thermotropic Liquid Crystalline Polymer in In-situ Composite Film, Eurorheo 99-1 and Europhysics Conference, 3-7 May 1999, Sophia-Antipolis (Nice), France

5.7 S. Bualek-Limcharoen, S. Saikrasun and A. Chantaratcharoen, Chemical Treatments of Aramid Fibers to Improve Adhesion with Non-Polar Polymer Matrices, The 5th Asian Textile Conference, Sept, 30 to Oct. 2 1999, Kyoto, International Conference on Advanced Fiber Materials, Oct. 4-5, 1999, Ueda and The 48th SPSJ Symposium on Macromolecules , 6-8 October 1999, Niigaka, Japan, invited speaker

5.8 I. Jangchud, B. Sukying and S. Bualek-Limcharoen, Plasma Surface Modification of Kevlar Short Fiber/ABS Composites, Innovation Polymer Processing, 1-3 Dec. 1999, Bangkok

6 การเสนอผลงานในที่ประชุมวิชาการในประเทศไทย (โปสเตอร์)

6.1 T. Nakinpong, T. Amornsakchai, W. Meesiri and S. Bualek, Composite of Kevlar Pulp and Thermoplastic Elastomer: Mechanical Properties and Compatibilisation, การประชุมวิทยาศาสตร์และเทคโนโลยีแห่งประเทศไทยครั้งที่ 22 เซ็นทรัลพลาซ่า ลาดพร้าว 16-18 ตุลาคม 2539, 732–733

6.2 W. Chawalitamporn, T. Amornsakchai, W. Meesiri and S. Bualek, Machanical Properties of Aramid Pulp-Polypropylene Composites, การประชุมวิทยาศาสตร์และเทคโนโลยีแห่งประเทศไทยครั้งที่ 22 เซ็นทรัลพลาซ่า ลาดพร้าว 16-18 ตุลาคม 2539, 734–735

6.3 J. Samran, W. Meesiri, T. Amornsakchai and S. Bualek-Limcharoen, Effect of Compatibilisers on Mechanical Properties and Morphology of Polypropylene/ Liquid Crystalline Polymer in situ Composite Films, การประชุมวิทยาศาสตร์และเทคโนโลยีแห่งประเทศไทยครั้งที่ 23 เชียงใหม่ 20-22 ตุลาคม 2540, 300-302

6.4 S. Saikrasun, T. Amornsakchai, W. Meesiri and S. Bualek-Limcharoen, Mechanical Properties of N-Alkylated Kevlar-Pulp/Styrene (Ethylene Butylene) Styrene Thermoplastic Elastomer Composite, การประชุมวิทยาศาสตร์และเทคโนโลยีแห่งประเทศไทยครั้งที่ 23 เชียงใหม่ 20-22 ตุลาคม 2540, 302-303

6.5 A. Chantaratcharoen, T. Amornsakchai, W. Meesiri and S. Bualek-Limcharoen, Properties of Alkylated Conex Fibre-Styrene Ethylene Butylene Styrene Thermoplastic Elastomer, การประชุมวิทยาศาสตร์และเทคโนโลยีแห่งประเทศไทยครั้งที่ 23 เชียงใหม่ 20-22 ตุลาคม 2540, p976-977

6.6 S. Saikrasun, T. Amornsakchai, C. Sirisinha, W. Meesiri and S. Bualek-Limcharoen, Chemically Modified Kevlar Fibre-Thermoplastic Elastomer (Santoprene) Composites : Mechanical Properties and Morphology, การประชุมวิทยาศาสตร์และเทคโนโลยีแห่งประเทศไทยครั้งที่ 24 ศูนย์ประชุมสิริกิติ์ กรุงเทพฯ 19-21 ตุลาคม 2541, p154-155

6.7 B. Wanno, T. Amornsakchai, C. Sirisinha, W. Meesiri and S. Bualek-Limcharoen, Effect of Polymer Melt Viscosity on Fibrillation of Thermoplastic Liquid Crystalline Polymer in *In-Situ* Composite Films, การประชุมวิทยาศาสตร์และเทคโนโลยีแห่งประเทศไทยครั้งที่ 24 ศูนย์ประชุมสิริกิติ์ กรุงเทพฯ 19-21 ตุลาคม 2541, p168-169

6.8 A. Chantaratcharoen, S. Bualek-Limcharoen, T. Amornsakchai, C. Sirisinha and W.Meesiri, Morphology and Mechanical Properties of Chemically Modified Conex Fibre and Thermoplastic Elastomer Composites, การประชุมวิทยาศาสตร์และเทคโนโลยีแห่งประเทศไทยครั้งที่ 24 ศูนย์ประชุมสิริกิติ์ กรุงเทพฯ 19-21 ตุลาคม 2541, p910-911

6.9 T. Nakinpong, S. Bualek-Limcharoen, C. Sirisinha and W. Meesiri, Study of Liquid Crystalline Polymer and Low Density Polyethylene Blend, การประชุมวิทยาศาสตร์และเทคโนโลยีแห่งประเทศไทยครั้งที่ 25 พิษณุโลก 20-22 ตุลาคม 2542

6.10 C. Vajrasthira, S. Bualek-Limcharoen, C. Sirisinha and T. Amornsakchai, Mechanical Properties and Morphology of Aramid Short Fibers-Thermoplastic Polyurethane Elastomer Composites, การประชุมวิทยาศาสตร์และเทคโนโลยีแห่งประเทศไทยครั้งที่ 25 พิษณุโลก 20-22 ตุลาคม 2542

6.11 B. Wanno, J. Samran, C. Sirisinha, T. Amornsakchai, W. Meesiri and S. Bualek-Limcharoen, Effect of Melt Viscosity of Polypropylene and Compatibilizer on Fibrillation of Thermotropic Liquid Crystalline Polymer in In-Situ Composite ประชุมวิทยาศาสตร์และเทคโนโลยีแห่งประเทศไทยครั้งที่ 25 พิษณุโลก 20-22 ตุลาคม 2542

7 ผลงานอื่น ๆ

(1) จัดประชุมประจำปี เรื่อง Liquid Crystalline Polymer Blends and Composites เพื่อเสนอผลงานของกลุ่มและงานของผู้อื่นที่เกี่ยวข้องเมื่อวันที่ 27 พฤศจิกายน 2539

(2) จัดประชุมประจำปี Liquid Crystalline Polymer Blends and Composites เพื่อเสนองานของกลุ่มและงานของผู้อื่นที่เกี่ยวข้องเมื่อวันที่ 5 พฤศจิกายน 2540

(3) แสดงโปสเตอร์ผลงานวิจัยทั้งหมดในงานวันวิทยาศาสตร์แห่งชาติ ที่ศูนย์ประชุมสิริกิติ์ กรุงเทพฯ 18-22 สิงหาคม 2541

รายชื่อผู้ทำงานในโครงการวิจัย ทุนเมธีวิจัยอาวุโส-สกว เสาวรภย์ บัวเล็ก-ลิ้มเจริญ

ชื่อ-นามสกุล	ตำแหน่งวิชาการ		ต้นสังกัด			ตำแหน่งในโครงการ	สถานภาพปัจจุบัน
	เมื่อเริ่มเข้าโครงการ	ปัจจุบัน	ภาควิชา	คณะ	มหาวิทยาลัย		
1 เสาวรภย์ บัวเล็ก-ลิ้มเจริญ	ศาสตราจารย์	ศาสตราจารย์	เคมี	วิทยาศาสตร์	มหิดล	หัวหน้าโครงการ	
2 ทวีชัย อมรศักดิ์ชัย	อาจารย์	ผู้ช่วยศาสตราจารย์	เคมี	วิทยาศาสตร์	มหิดล	ผู้ร่วมวิจัย	
3 วิริยะ มีศิริ	นาวาอากาศเอก	นาวาอากาศเอก		กองสรรพาวุธ	กองทัพอากาศ	ผู้ร่วมวิจัย	
4 ปราณี ภิญโญชีพ	ผู้ช่วยศาสตราจารย์	ผู้ช่วยศาสตราจารย์	เคมี	วิทยาศาสตร์	มหิดล	ผู้ร่วมวิจัย	
5 อิทธิพล แจ้งชัด	อาจารย์	อาจารย์	เคมีอุตสาหกรรม	วิทยาศาสตร์	สถาบันพระจอมเกล้าเจ้าคุณทหารลาดกระบัง	ผู้ร่วมวิจัย	
6 ชาคริต สิริสิงห	อาจารย์	ผู้ช่วยศาสตราจารย์	เคมี	วิทยาศาสตร์	มหิดล	ผู้ร่วมวิจัย	
7 บุษพร สินพัฒนพันธุ์			เคมี	วิทยาศาสตร์	มหิดล	ผู้ช่วยวิจัย	นักวิชาการ สวทช
8 ธีรวุฒิ นคินพงษ์			เคมี	วิทยาศาสตร์	มหิดล	นักศึกษาปริญญาโท	บริษัท TPI
9 วรพงษ์ ชวลิตอัมพร			เคมี	วิทยาศาสตร์	มหิดล	นักศึกษาปริญญาโท	โรงเรียนศรีวิกรม์
10 จรีรัตน์ สำราญ			เคมี	วิทยาศาสตร์	มหิดล	นักศึกษาปริญญาโท	มหาวิทยาลัยสงขลานครินทร์, ปัตตานี
11 สุนันท์ สายกระสุน			เคมี	วิทยาศาสตร์	มหิดล	นักศึกษาปริญญาโท	มหาวิทยาลัยมหาสารคาม
12 อนงค์นุช จันทรัตน์เจริญ			เคมี	วิทยาศาสตร์	มหิดล	นักศึกษาปริญญาโท	บริษัท Bang Trading
13 บรรจบ วันโน			เคมี	วิทยาศาสตร์	มหิดล	นักศึกษาปริญญาโท	มหาวิทยาลัยมหาสารคาม
14 ธีรนันท์ นคินพงษ์			เคมี	วิทยาศาสตร์	มหิดล	นักศึกษาปริญญาโท	
15 จันทร์ทิพา วัชรเสถียร			เคมี	วิทยาศาสตร์	มหิดล	นักศึกษาปริญญาโท	
16 ยอดพันธุ์ บุญสนอง			เคมี	วิทยาศาสตร์	มหิดล	นักศึกษาปริญญาโท	
17 สายันต์ แสงสุวรรณ			เคมี	วิทยาศาสตร์	มหิดล	นักศึกษาปริญญาเอก	
18 ภัควดี สุขอนันต์			เคมี	วิทยาศาสตร์	มหิดล	นักศึกษาปริญญาเอก	

4. Reprints

4.1 S. Bualek-Limcharoen, T. Nakinpong, T. Amornsakchai and W. Meesiri, Kevlar Pulp-Thermoplastic Elastomer Composites : Morphology and Mechanical Properties, *J. Sci. Soc. Thailand* **23** (1997) 101-114

4.2 T. Nakinpong, B. Sinpatanapan, W. Meesiri, T. Amornsakchai and S. Bualek-Limcharoen, Aramid Fibres-Thermoplastic Elastomer (SEBS) Composites: Effect of Maleic Anhydride Grafted Compatibiliser on Mechanical Properties, *Mahidol J.* **5**, (1998) 115-120

4.3 S. Bualek-Limcharoen, J. Samran, T. Amornsakchai and W. Meesiri, Effect of Compatibilizers on Mechanical Properties and Morphology of *In-Situ* Composite Film of Thermotropic Liquid Crystalline Polymer/Polypropylene, *Polym. Eng. Sci.* **39** (1999) 312-320

4.4 T. Amornsakchai, B. Sinpatanapan, S. Bualek-Limcharoen and W. Meesiri, Composite of Aramid Fibre (Poly-m-phenylene isophthalamide)-Thermoplastic Elastomer (SEBS) : Enhancement of Tensile Properties by Maleated-SEBS Compatibiliser, *Polymer.* **40** (1999) 2993-2999

4.5 S. Saikrasun, T. Amornsakchai, C. Sirisinha, W. Meesiri and S. Bualek-Limcharoen, Kevlar Reinforcement of Polyolefin-Based Thermoplastic Elastomer, *Polymer* **40**, (1999) 6437-6442

4.6 A. Chantaratcharoen, C. Sirisinha, T. Amornsakchai, S. Bualek-Limcharoen and W. Meesiri, Improvement of Interfacial Adhesion of Poly-(m-phenylene isophthalamide) short fibre-Thermoplastic Elastomer(SEBS) Composites by N-Alkylation on Fiber Surface, *J. Appl. Polym. Sci.* (in press)

4.7 J. Samran, W. Meesiri, S. Bualek-Limcharoen and T. Amornsakchai, In-situ Composite Film of Thermotropic Liquid Crystalline Polymer/Polypropylene: Effect of Film Drawing on Molecular Orientation and Properties, *ScienceAsia* **25** (1999) 91-97

4.8 preprint : B. Wanno, J. Samran and S. Bualek-Limcharoen, Effect of Melt Viscosity of Polypropylene on Fibrillation of Thermotropic Liquid Crystalline Polymer in In-situ Composite Film, Rheologica Acta (revised).

5. Manuscripts จากการประชุมนานาชาติ

5.1 T. Nakinpong, T. Amornsakchai, W. Meesiri and S. Bualek, Effect of Surface Treatment on Mechanical Properties of Aramid Pulp-Thermoplastic Elastomer Composites, Proceeding of The International Conference on Materials Technology: Recent Development and Future Potential p343-352, 9-10 January 1997, Chaing Mai

5.2 S. Bualek-Limcharoen, J. Samran, W. Meesiri and T. Amornsakchai, Thermoplastics- Liquid Crystalline Polymer Blends: Processing, Characterisation and Properties of *In-Situ* Composite Films, Proceeding of the Conference: Polymer Blends Toward 2000, 18-20 Auguest 1997, Kasetsart University, p95-105

5.3 T. Amornsakchai, W. Meesiri, T. Nakinpong, B. Sinpatanapan and S. Bualek-Limcharoen, Aramid Fibers-Thermoplastic Elastomer Composites: Properties of Composites Using Maleic Anhydride Grafted Compatibilizer, 7 pages in the Proceeding of the International Rubber Conference 18-20 October 1997, Kuala Lumpur, Malaysia

5.4 S. Bualek-Limcharoen, T. Amornsakchai and J. Samran, In-Situ Composites PP/LCP : Enhancement of Modulus and Impact Strength by Compatibilizers, IUPAC World Polymer Congress, 37th International Symposium on Macromolecules, 12-17 July 1998, Gold Coast, Australia

5.5 S. Bualek-Limcharoen, Composites of Aramid Fibers-Thermoplastic Elastomers : Improvement of Interfacial Adhesion by Chemical Modifications of Fiber Surface, 7th International Seminar on Elastomer, 16-17 December 1998, Bangkok, Thailand

5.6 B. Wanno, J. Samran and S. Bualek-Limcharoen, Effect of Melt Viscosity of Polypropylene on Fibrillation of Thermotropic Liquid Crystalline Polymer in In-situ Composite Film, Eurorheo 99-1 and Europhysics Conference, 3-7 May 1999, Sophia-Antipolis (Nice), France

5.7 S. Bualek-Limcharoen, S. Saikrasun and A. Chantaratcharoen, Chemical Treatments of Aramid Fibers to Improve Adhesion with Non-Polar Polymer Matrices, The 5th Asian Textile Conference, Sept, 30 to Oct. 2 1999, Kyoto, and The 48th SPSJ Symposium on Macromolecules , 6-8 October 1999, Niigaka, Japan, invited speaker

J.Sci.Soc.Thailand, 23(1997) 101-114

KEVLAR PULP-THERMOPLASTIC ELASTOMER COMPOSITES: MORPHOLOGY AND MECHANICAL PROPERTIES

SAUVAROP BUALEK-LIMCHAROEN,[a] TEERAVUT NAKINPONG,[a] TAWEECHAI AMORNSAKCHAI[a] AND WIRIYA MEESIRI[b]

[a] *Department of Chemistry, Faculty of Science, Mahidol University, Rama 6 Road, Bangkok 10400*

[b] *Directorate of Armament, Royal Thai Air Force, Donmuang, Bangkok 10210*

(Received May 10, 1997)

ABSTRACT

Reinforcement of Styrene (Ethylene Butylene) Styrene thermoplastic elastomer (SEBS) with Kevlar pulp was investigated. Surface treatment of the fibre was carried out by alkali hydrolysis in order to increase the number of reactive groups. Maleic anhydride-grafted-SEBS was used as a compatibiliser. The composites were prepared by a one step process in an internal mixer. Mechanical properties of the composites were assessed using a tensile testing machine. The results suggested that as the loading of Kevlar pulp increased, tensile modulus increased but tensile strength and elongation at break decreased. The fracture surface of the composites observed under Scanning Electron Microscope (SEM) revealed fibre pull-out in the composite without compatibiliser and more fibre breakage were observed in the samples containing compatibiliser. Quantitative analysis of the adsorbed elastomer on the fibre surface using gravimetric, diffuse reflectance FTIR (DRIFT) techniques and observation of SEM micrographs of extracted pulp showed that in the presence of compatibiliser, a large amount of elastomer was adsorbed. However, SEBS-g-MA showed no remarkable effect on the tensile properties of the composites and this might be due to uneven adsorption of rubber particles.

INTRODUCTION

The excellent thermal and mechanical properties of poly (*p*-phenylene terephthalamide) (aramid) fibre make it a good candidate as reinforcement fibre in polymer composites. The main problem due to poor adhesion between the fibre and a polymer matrix, however, does exist and continues to pose a challenge to researchers. Vaughan[1] applied various commercial coupling agents and obtained some improvement on adhesion. Other efforts to modify the fibre by dispersion of fibre in an ionomer matrix seemed to be very effective[2,3]. Marom *et al.*[4] proposed a surface treatment technique using bromine water which led to surface roughening and resulted in improvement of interlaminar shear strength. Andreopoulos[5] used various compounds to promote adhesion of Kevlar fibre and pulp with unsaturated polyester. Treatment of fibre with methacryloyl chloride resulted in considerably high tensile strength compared to that of composites incorporating untreated fibre. Wang *et al.*[6] prepared plasma treated aramid fibre-polyethylene composites. The reactive groups such as -COOH, -OH, $-NH_2$ were generated on the aramid fibre surface using oxygen plasma. These groups were used to chemically anchor Ziegler-Natta catalyst to the fibre surface, which was then followed by ethylene polymerisation on the surface. This type of composites exhibit higher tensile strength both in parallel and transverse to the fibre direction. Yu *et al.*[7] studied nylon/Kevlar composites and found that Kevlar could be used to reinforce nylon. The effect of various surface treatment methods, *e.g.* hydrolysis and hydrolysis followed by chemical grafting with acid chloride, were also studied. It was found that the mechanical properties of the composite could be improved by appropriate fibre treatment.

Recently, short-fibre reinforced elastomers have increasingly attracted more attentions by several researchers.[8-12] Reinforcements for such system mainly involved using conventional fibres like poly (ethylene terephthalate) (PET) and nylon. Consequently, the use of Kevlar fibre as a reinforcement in thermoplastics have become an interesting application of this high performance fibre.

The present work involved the studies of Kevlar pulp reinforced styrene (ethylene butylene) styrene (SEBS) thermoplastic elastomer. SEBS represented a model thermoplastic elastomer matrix to be reinforced by an organic fibre. From a molecular structure point of view, the two components are quite incompatible. Kevlar is a highly hydrogen-bonded polyamide while SEBS containing olefinic and styrenic blocks is relatively nonpolar. In order to obtain compatibility, chemical bonding was introduced by partially hydrolysing the amide bonds on Kevlar fibre surface followed by the addition of SEBS-grafted-maleic anhydride (SEBS-g-MA), a compatibiliser for this system. The formation of imide groups from the reaction of maleic anhydride and amine end groups on the fibre surface was expected[13]. This should be able to improve the adhesion of fibres and rubber matrix

EXPERIMENTAL

Materials

Styrene-(ethylene-co-butylene)-styrene (SEBS) triblock copolymer (Kraton G1652, Mn ≈ 83,700) and Maleated SEBS (Kraton FG1901x, Mn ≈ 85,000) were provided by Shell Chemical Co. Poly(*p*-Phenylene Terephthalamide) pulp (Kevlar 49) was provided by E.I. Du Pont .

Hydrolysis of Kevlar 49 pulp

Kevlar 49 pulp was first washed with acetone and distilled water in order to remove the possible surface impurities such as lubricating agents and dried in vacuum oven at 50°C . Ten grams of Kevlar pulp was dispersed in 400 ml 10 wt% aqueous NaOH solution at ambient temperature for 20 minutes. Following the hydrolysis, Kevlar 49 pulp was throughly washed with distilled water and toluene, dried in vacuum oven at 50°C for 48 hours and kept in desiccator.

Spectroscopic characterisation

Diffuse Reflectance Infrared Fourier Transform (DRIFT) spectrometer (Perkin Elmer FTIR 2000) was used to characterise the surface of Kevlar 49 pulp. Two hundred scans at a resolution 4 cm^{-1} and throughout the range 4,000-600 cm^{-1} were usually required to obtain a decent spectrum.

Preparation of SEBS/Kevlar 49 pulp composites

Pulp was first opened by using a Moulinex blender for half a minute, then it was put in the internal mixer, Haake Rheocord 90, together with SEBS and compatibiliser. Samples weight 50 grams of various Kevlar pulp/SEBS composites were blended at 165°C, rotor speed 90 rpm for 10 minutes and passed through a two-roll mill twice. The composites were collected promptly and kept in a desiccator in order to mininize moisture adsorption.

Loading of Kevlar pulp was varied from 0 - 10% by weight. The effect of compatibiliser was studied in a composite of 3wt% of Kevlar in SEBS. The amount of SEBS-g-MA varied from 0 - 10% by weight was added to the composites using the same mixing condition.

Extraction of the composites

A known weight of the composite was extracted in Soxhlet apparatus using toluene as a solvent for 72 hours. The sample was then dried in a vacuum oven at 50°C. The amount of the bound rubber can be calculated by gravimetric method. The extracted pulp was also characterised by DRIFT and SEM.

Mechanical properties of the composites

Kevlar 49 pulp/SEBS composites were compression moulded at 180°C for 10 minutes under a pressure of 15 MPa and quenched with cold water. After conditioned for at least 24 hours, tensile specimens were cut with dumbell-shape die of size 115 x 6 x 1 mm parallel and transverse to the direction passing through the two-roll mill. Testing was carried out on an Instron testing machine model 4301 in accordance with ASTM D638 at a cross head speed of 500 mm/min with a full scale load cell at 100 kg.

Scanning electron microscopy (SEM)

Observation of fibre surface and fracture surfaces of the composite were performed on Hitachi S2500. A thin layer of palladium was coated by Hitachi E102 ion sputter on the specimen to prevent charging on the surface. SEM was operated at 15 kV.

Fracture surface of the composites was prepared by freezing the composite in liquid nitrogen for 5 minutes and then broken rapidly above the surface of liquid nitrogen.

Optical microscopy

Orientation and fibre length in the composite were observed under an optical microscope (Nikon 70562). The sample was prepared by melt-press between slide glasses. The fibre aspect ratio (length to diameter ratio) was evaluated from the photographs taken at various points.

RESULTS AND DISCUSSION

Hydrolysis of Kevlar surface

It is generally known that Kevlar aramid is poly (*p*-phenylene terephthalamide) or PPTA. In this study, Kevlar pulp was partially hydrolysed on the surface by using 10% NaOH for 20 minutes to create more -NH_2 and -COOH end groups as indicated in the following reaction.

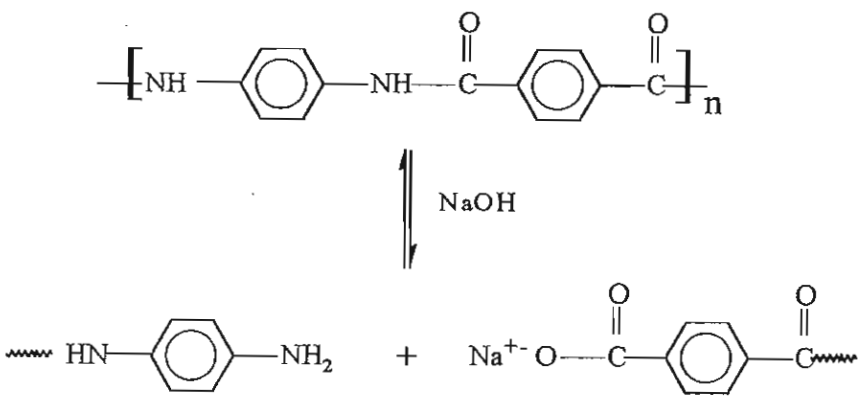

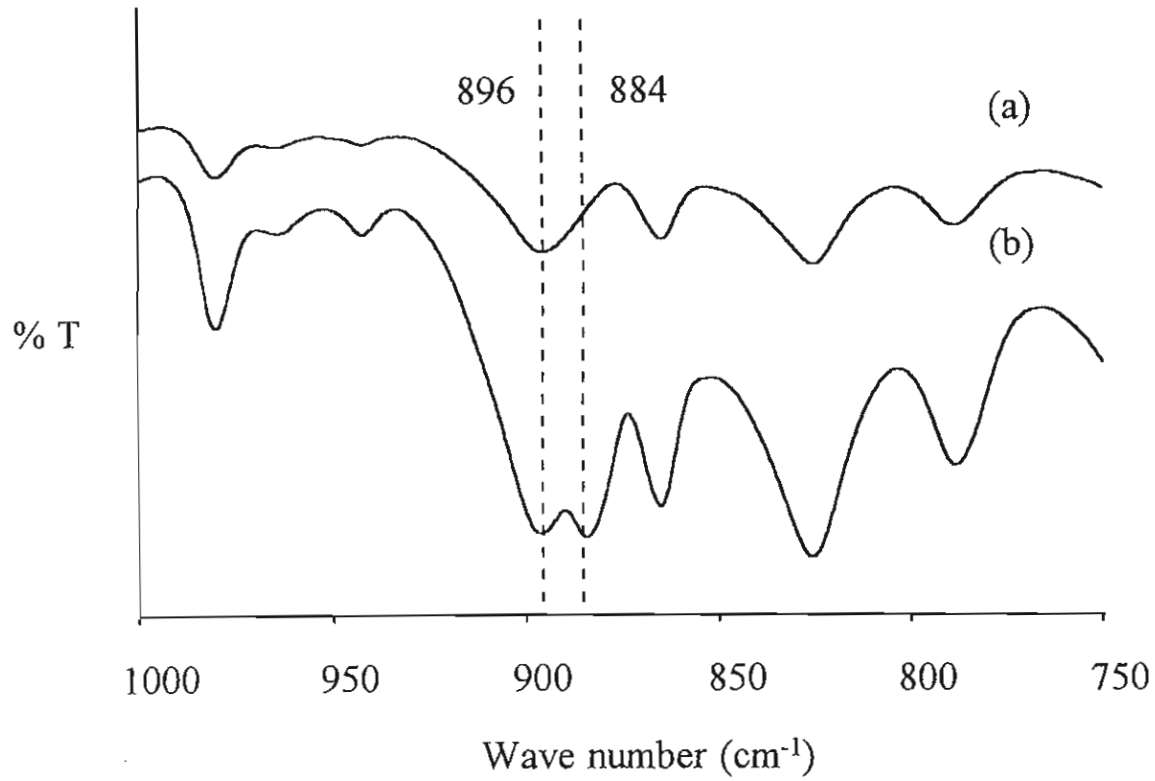

Fig.1. Infrared spectra of Kevlar surface (a) before and (b) after hydrolysis (without washing with water).

Fig.2. Optical micrograph of Kevlar pulp/SEBS composite pressed between slide glasses.

Figure 1 shows infrared spectra of Kevlar pulp before and after hydrolysis using DRIFT technique. It can be seen that a new peak appears at 884 cm^{-1}. The peak is associated with the C-H out of plane bending of aromatic ring next to $-COO^-Na^+$ substituent as reported by Chatzi[14-15]. The pulp was throughly washed with distilled water, followed by toluene and dried to constant weight at 50°C under vacuum. The resulting pulp had a pale yellow colour. At this stage the 884 cm^{-1} peak disappeared. This can be explained by the fact that washing the pulp with distilled water would change $-COO^-Na^+$ to -COOH. It was found that the washing step was very important. If care was not taken the resulting pulp would turn dark yellow to brown after storage for a few days. Blending of this dark colour pulp with SEBS elastomer gave rise to a composite with very poor tensile properties.

Optical microscopic observation

Figure 2 shows the optical micrograph of the thin layer of the composite SEBS/Kevlar pulp. Two features of fibre can be seen, namely, long fibres and small fibrils which split from the long one, since pulp is a highly fibrilated form of fibre. According to the compressive force applied on the slide glasses the direction of orientation of these small fibrils are therfore perpendicular to the long ones. The similar orientation behaviour should also be found in the compression moulded specimen prepared for the tensile measurement. It should be noted here that the measurement of tensile properties of the specimens prepared in this experiment and cut in the direction parallel and perpendicular to the direction of passing through the two-roll mill were found to be approximately the same. This should be due to the biaxial orientation of these two types of fibre.

The average length of fibre before and after mixing was about 1.8 mm and 0.5 mm, respectively. Distribution of the aspect ratio of fibres after mixing evaluated from optical micrographs is shown in Figure 3. It can be seen that most of the fibre has aspect ratio of 22-38.

Mechanical properties

Fibre reinforced composites generally exhibit anisotropic properties. Mechanical properties in the machine direction are normally higher than those measured in the transverse direction (cross-machine direction). Our preliminary results showed that the mechanical properties in the two directions were not much different. This is probably due to biaxial orientation of the fibre and fibril as discussed above. However, the results to be followed are measured in the machine direction.

Stress-strain behaviour of SEBS/Kevlar pulp composites is shown in Figure 4. SEBS exhibits a typical characteristic of rubber with strain hardening effect at very high strain. This effect leads to a very high ultimate tensile strength. Addition of Kevlar up to 5% did not affect the shape of the curves to a great extent, ie. the composites still show strain hardening effect. Beyond 5 % of Kevlar, the composites failed at strain below the point which strain hardening effect was observed. The reinforcement effect of Kevlar can be clearly seen in all samples. However, the composites broke at relatively low strain when more Kevlar was added. This is probably due to debonding of the Kevlar from SEBS as indicated by whitening of the samples. Such debonding would leave certain imperfection on SEBS surface and cause premature failure. The other reason for premature failure would be due to poor dispersion of Kevlar pulp at high loading.

Tensile properties of Kevlar reinforced SEBS are shown in Figure 5. It can be seen that as the Kevlar loading is increased the tensile strength of the composite decreases. Modulus at

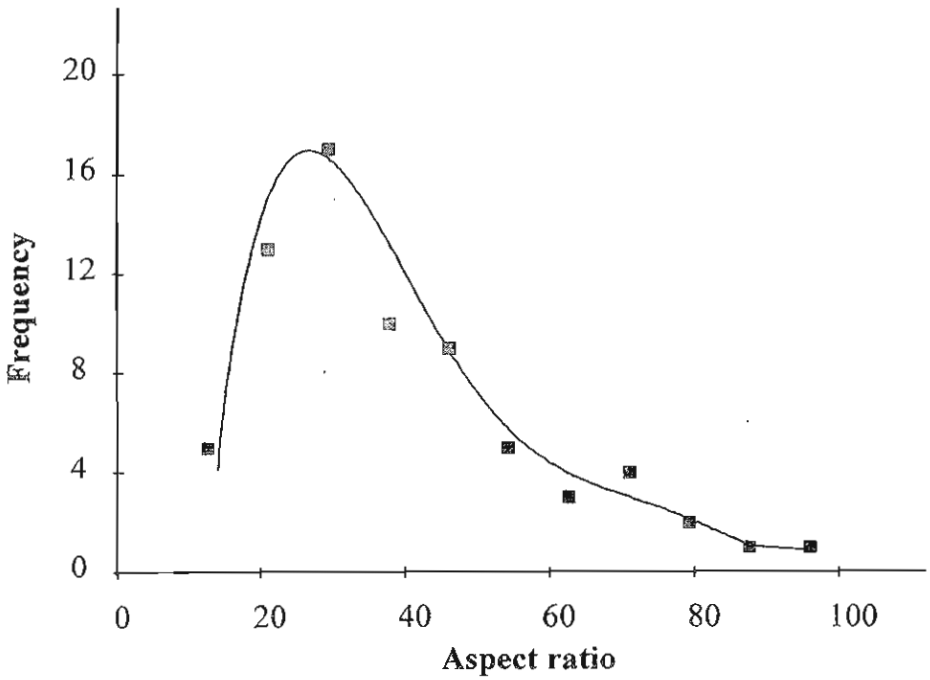

Fig.3. Distribution of aspect ratio of fibre after mixing.

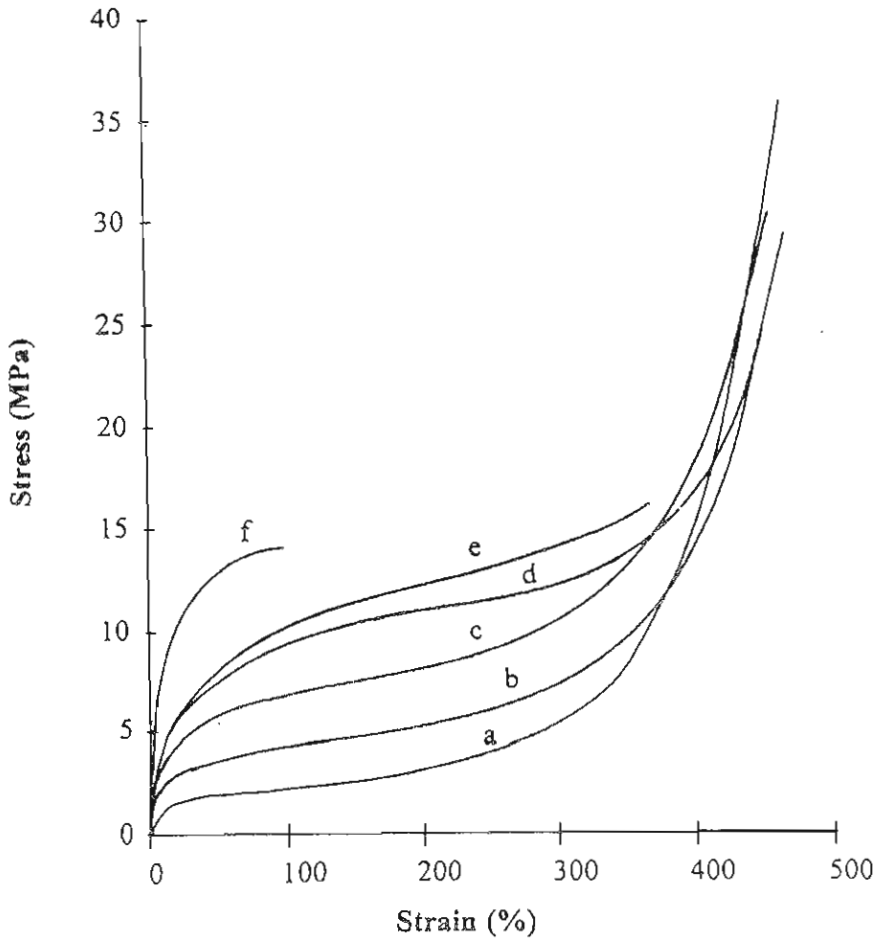

Fig.4. Stress-strain curves of Kevlar pulp/SEBS composites at fibre loading (wt%) a = 0, b = 1, c = 3, d = 5, e = 7 and f = 10.

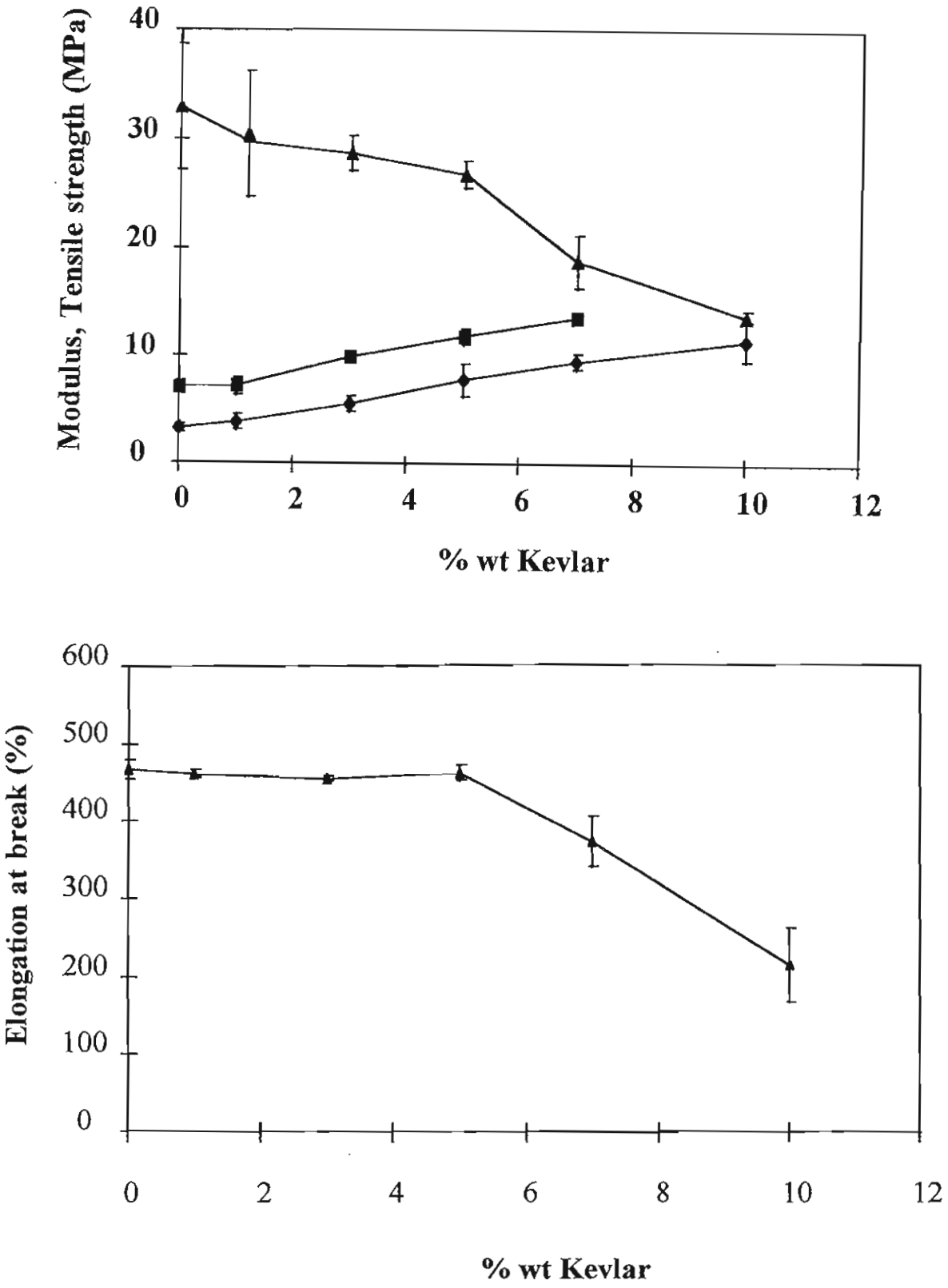

Fig.5. Shows a) Modulus at 100% (◆), 300% (■) and Tensile strength (▲) and b) Elongation at break of Untreated Kevlar/SEBS composite.

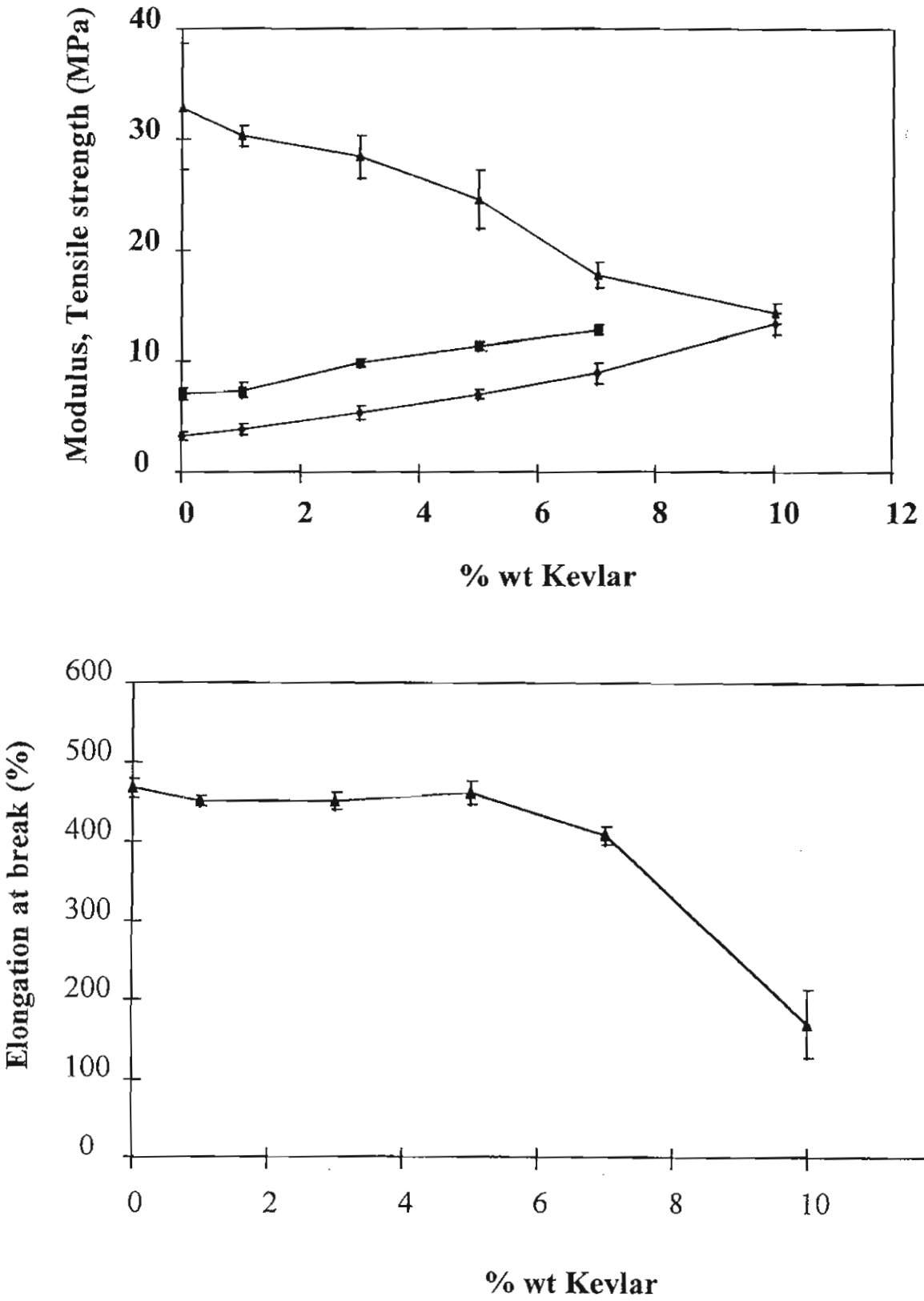

Fig.6. Shows a) Modulus at 100% (◆), 300% (■) and Tensile strength (▲) and b) Elongation at break of Treated Kevlar/SEBS composite.

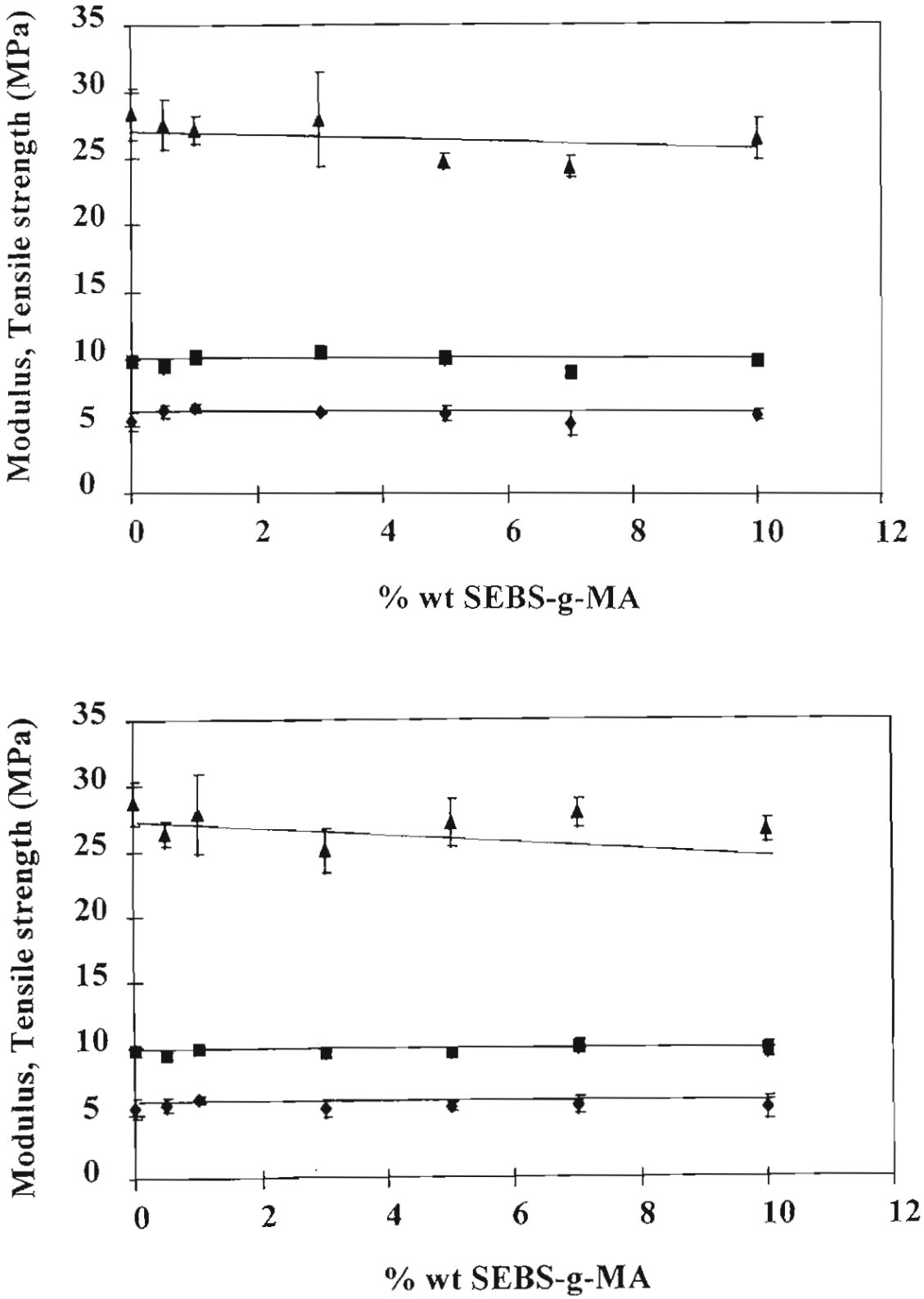

Fig.7. Shows effect of SEBS-g-MA on modulus at 100% (◆), 300% (■) and Tensile strength (▲) of (a) Untreated Kevlar/SEBS composite and (b) Treated Kevlar/SEBS composite.

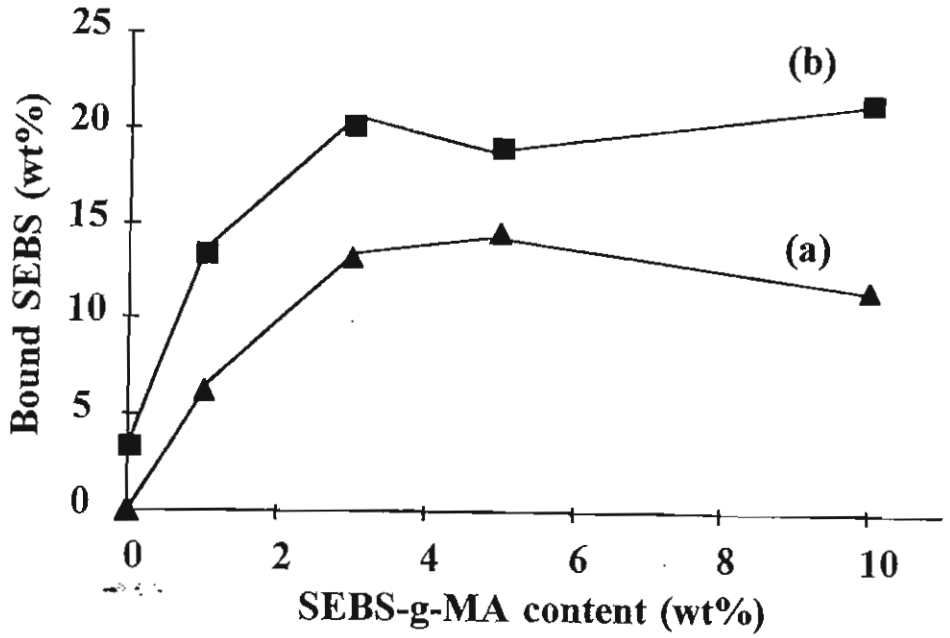

Fig.8. Bound SEBS (wt%) on extracted Kevlar pulp (a = as received, b = treated) obtained from composites containing various SEBS-g-MA contents.

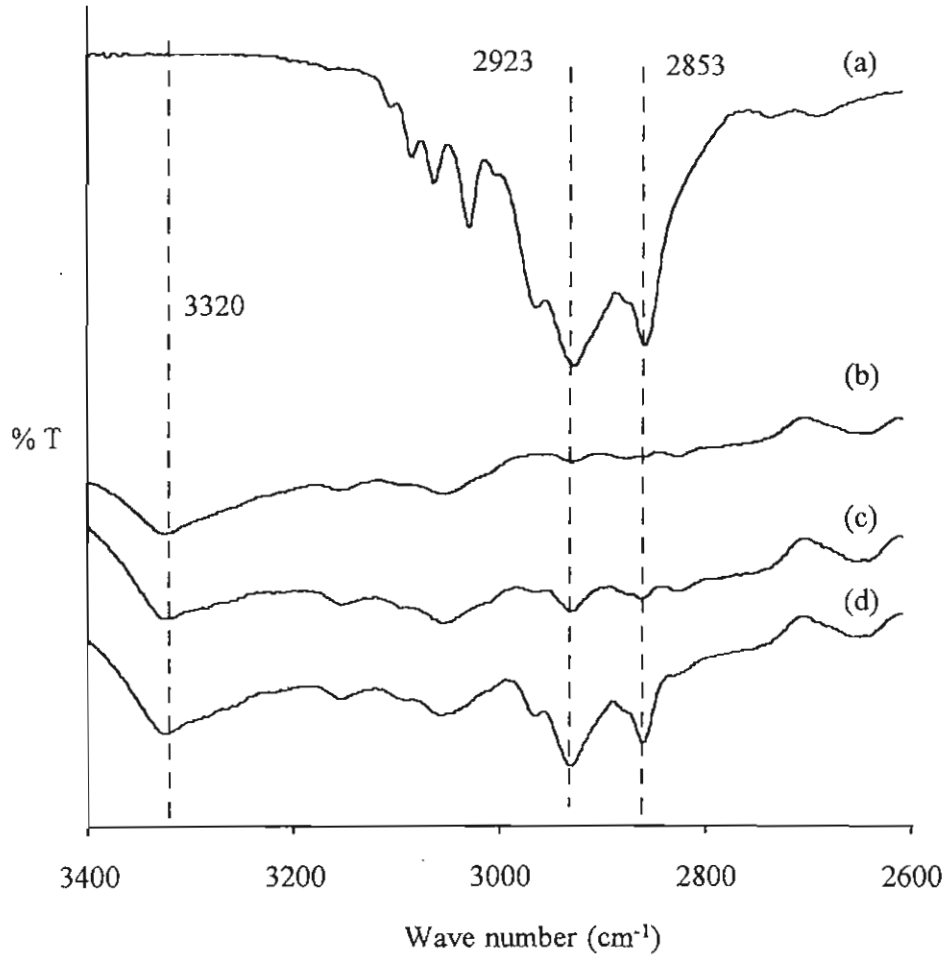

Fig.9. Spectra of extracted samples of (a) SEBS pure, (b) Kevlar, (c) Kevlar/SEBS (3/97) and (d) Kevlar/SEBS-g-MA/ SEBS (3/1/96).

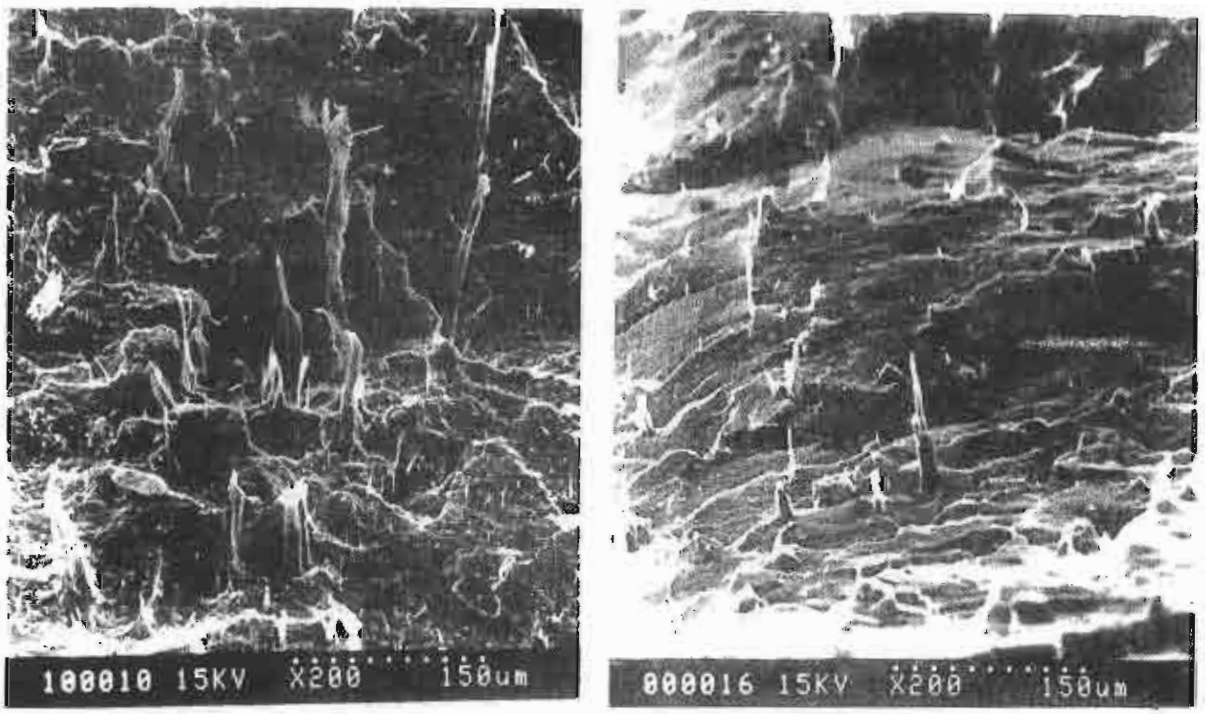

a b

Fig.10. SEM micrographs of
(a) Kevlar/SEBS (3/97).
(b) Kevlar/SEBS-g-MA/SEBS (3/1/96).

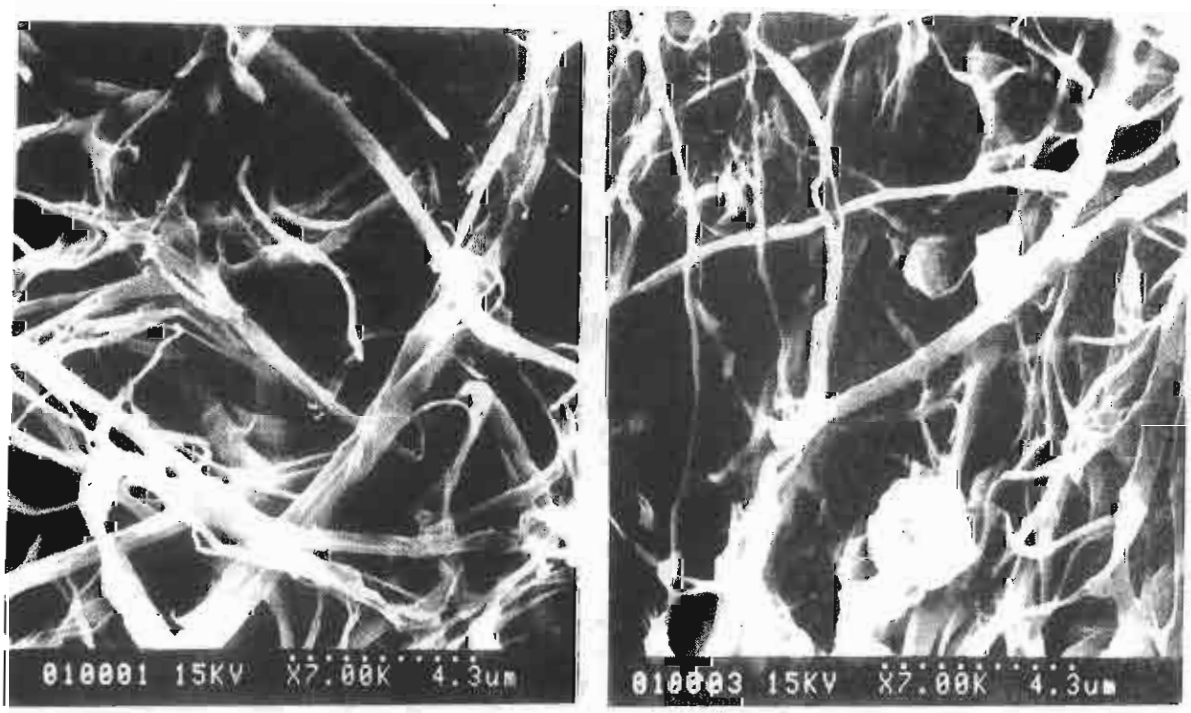

a b

Fig.11. SEM micrographs of extracted pulp from
(a) composite without SEBS-g-MA.
(b) composite with 1 wt% SEBS-g-MA.

100 and 300%, on the other hand, increases with increasing Kevlar loading. Elongation at break of the composite was found to drop slightly when Kevlar loading was increased. Beyond 10% Kevlar the elongation at break drops sharply. This was found to coincide with the observation of poorly dispersed Kevlar in SEBS.

An increase in modulus at both 100 and 300% was as expected when pulp of very high modulus like Kevlar was incorporated into SEBS elastomer matrix. A monotonic decrease in tensile strength with pulp loading was due to the fact that SEBS could be strain hardened at very high strain. Incorporation of Kevlar pulp could reduce such effect and/or impart weak points, which, at relatively low strain, may induce cracks.

Hydrolysis of Kevlar surface was found to have negligible effect on mechanical properties of the composites, as can be seen from Figures 6a and 6b. This indicates that only slight modification, either chemically or physically, had been done.

Effect of compatibiliser, SEBS-g-MA, on a composite containing 3% wt. Kevlar can be seen from Figures 7a and 7b. Two sets of Kevlar were studied, i.e. as received Kevlar and surface hydrolysed Kevlar. It was found that surface hydrolysed Kevlar resulted in a composite with approximately the same mechanical properties as that of untreated Kevlar.

In order to determine how SEBS was adsorbed on Kevlar surface the blends were subjected to extraction with toluene. Since SEBS can be dissolved in toluene at room temperature, it should be completely leached out after extraction for 72 hours at boiling temperature of toluene. Solvent extraction of the composite shows that the amount of bound (unextractable) rubber increases as SEBS-g-MA was added, as can be seen in Figure 8 from gravimetric measurement. Curves (a) and (b) are results from untreated and treated Kevlar, respectively. This figure clearly shows the effect of hydrolysis on the efficiency of adsorption. This suggests that SEBS-g-MA reacted with active group on the surface of Kevlar. The amount of bound rubber calculated base on the weight of fibre is, however, less than the amount of added SEBS-g-MA. The rest of SEBS-g-MA (unreacted) is likely to disperse in SEBS matrix and could weaken the composite if phase-separation occurs.

Figure 9a shows Infrared spectra (DRIFT) of pure SEBS in the range 2600-3400 cm^{-1}. Peaks at 2923 and 2853 cm^{-1} correspond to asymmetric and symmetric stretchings, respectively, of the $-CH_2-$ groups from ethylene block of SEBS. Figure 9b displays Infrared spectrum of as-received Kevlar pulp in the same region. It can be seen that there is a peak at 3320 cm^{-1} which corresponds to intermolecular hydrogen bonding in Kevlar. The Infrared spectra of the extracted pulp from specimens without and with SEBS-g-MA, shown in Figures 9c and 9d, respectively, display both typical peaks of SEBS and Kevlar. The ratio of the peak at two positions clearly shows the higher percentage of SEBS on the Kevlar surface as SEBS-g-MA was added.

Solvent extraction and spectroscopic evidences clearly suggest that the compatibiliser, SEBS-g-MA, reacted with Kevlar. The tensile strength of the blends are, however, not improved. Ishihara *et al.*[16]. reported that, for poly(ethylene terephthalate)-hydrogenated styrene-isoprene-styrene triblock copolymer (PET-SIPS) composite, treatment of PET fibre improved tensile strength in the fibre direction significantly. Tensile strength in the transverse direction was, however, not affected.

Morphology

Fracture surfaces of composites with and without compatibiliser are shown in Figures 10a and 10b, respectively. Detailed investigation of the photographs reveals very much different

fracture characteristics betweeen the two systems. Composite with compatibiliser, Figure 10b, exhibits mostly fibre breakage, whereas composite without compatibiliser exhibits both fibre pull out and fibre breakage (Figure 10a). Fibre pull out in the latter case seems to dominate. This evidence confirms that the compatibiliser, SEBS-g-MA, improves the adhesion between fibre and matrix.

Figures 11a and 11b are SEM micrographs taken from extracted fibre from the composites without and with compatibiliser, respectively. No adsorption of rubber can be seen in the first case whereas a few rubber particles adsorbed on fibre surface in the latter one. These particles of rubber might cause voids between the fibre surface and the rubber matrix, which led to poor contact at the interface, and hence no improvement of mechanical properties could be obtained even though larger amount of bound rubber on the fibre surface was found.

CONCLUSIONS

The above results can lead to the following conclusions:

1. Creation of reactive groups on Kevlar pulp by surface hydrolysis in this work does not lead to deterioration of its mechanical properties.

2. Moduli at 100 and 300% of the composites increase, tensile strength slightly decreases, and there is no significant change of elongation at break, as the loading of Kevlar is increased upto 5 wt%. However, beyond 10%wt of Kevlar loading, the dispersion is poor, and as a result tensile strength and the elongation at break drop sharply.

3. From gravimetric measurement and DRIFT technique, it is found that higher amount of SEBS adhered at the surface of Kevlar pulp as SEBS-g-MA is added.

4. In the presence of compatibiliser, SEM micrograph of fracture surface of the composite shows fibre breakage and the micrograph of extracted pulp shows adsorption of rubber particles on pulp surface, which are evidences of improvement of fibre-matrix adsorption.

5. Tensile strength of the composite containing SEBS-g-MA is, however, not improved. This might be due to uneven adsorption of rubber particles which probably cause some voids at the interface giving rise to the weak points.

ACKNOWLEDGEMENTS

Support of this work by The Thailand Research Fund is gratefully acknowledged. The authors also would like to thank the Shell Chemical Co. and E.I. Du Pont Co. for supplying SEBS and Kevlar pulp, respectively.

REFERENCES

1. D.J. Vaughan, *Polym. Eng. Sci.*, **18**, 167-169 (1978)
2. M. Takayanaki, T. Kajiyama and T. Katayose, *J. Appl. Polym. Sci.*, **27**, 3903-3917 (1982)
3. M. Takayanaki and T. Katayose, *Polym. Eng. Sci.*, **24**, 1047-1050 (1984)
4. M. Breznick, J. Banhaji, H. Guttmann and G. Marom, *Polym. Commun.*, **28**, 55-56 (1987)
5. A.G. Andreopoulos, *J. Appl. Polym. Sci.*, **38**, 1053-1064 (1989)
6. Q. Wang, S. Kaliaguine and A. Ait-Kadi, *J. Appl. Polym. Sci.*, **48**, 121-136 (1993)
7. Z. Yu, A. Ait-Kadi and J. Brisson, *Polym. Eng. Sci.*, **31**, 1222-1227 (1991)
8 W. Guo and M. Ashida, *J. Appl. Polym. Sci.*, **49**, 1081-1091 (1993)
9. M. Ashida and T. Noguchi, *J. Appl. Polym. Sci.*, **29**, 4107-4114 (1984)
10. M. Ashida and T. Noguchi, *J. Appl. Polym. Sci.*, **29**, 661-670 (1984)
11. M. Ashida, T. Noguchi and S. Mashimo, *J. Appl. Polym. Sci.*, **30**, 1011-1021 (1985)
12 A.P.Folgi, in Composite Applications: The Role of Matrix, Fiber and Interfaces, T L.Vigo and B.J. Kinzig (Eds.) Verlag Chemie, Weinheim, 1992
13. M. J. Modic and L.A. Pottick, *Polym. Eng. Sci.*, **33**, 819-826 (1993)
14. E.G. Chatzi, S.L. Tidrick and J.L. Koenig, *J. Polym. Sci.* **B26**, 1585-1593 (1988)
15. F.Garbassi, M.Morra and E.Occhiello, Polymer Surfaces: From Physics to Technology, John Wiley & Sons Ltd. Chichester, 1994
16. M. Ishihara, A. Nagatani, M. Mori, J. Okumura and K.Yamaguchi, Proceeding of International Rubber Conference, IRC95, p319-322, 23-27 Oct.1995, Kobe, Japan

บทคัดย่อ

งานวิจัยนี้เป็นการศึกษาการเสริมแรงยางเทอร์โมพลาสติกสไตรีนเอทธิลีนบิวธิลีนสไตรีน (SEBS) ด้วยเยื่อเคฟล่าร์(Kevlar pulp) ซึ่งปรับปรุงผิวเพื่อเพิ่มหมู่ที่ไวต่อการทำปฏิกิริยาด้วยวิธีไฮโดรไลซ์ด้วยเบส และใช้ SEBS ที่มีหมู่มาเลอิกแอนไฮดรายด์ต่อด้านข้าง (maleic anhydride grafted SEBS) เป็นสารช่วยผสม การผสมคอมพอสิทนี้ทำโดยใช้เครื่องผสมภายในโดยวิธีขั้นตอนเดียว แล้วนำไปวัดสมบัติการทนต่อแรงดึง พบว่าเมื่อเพิ่มปริมาณของเยื่อเคฟล่าร์ทำให้ค่ามอดูลัสของยางผสมนี้สูงขึ้นมาก แต่ค่าความทนต่อแรงดึงที่จุดขาดและความยาวที่จุดขาดลดลง ได้ใช้เทคนิค scanning electron microscopy (SEM) ศึกษาผิวของคอมพอสิทโดยการหักชิ้นงานในไนโตรเจนเหลว พบว่าเส้นใยมีลักษณะแบบหลุดออกจากเมทริกซ์เป็นส่วนใหญ่ แต่เมื่อมีสารช่วยผสมลักษณะของเส้นใยจะเป็นแบบขาดมากขึ้น และจากการสกัดเส้นใยจากคอมพอสิทแล้ววิเคราะห์ผิวโดยใช้อินฟราเรดสเปคโตรสโคปีและ SEM รวมทั้งโดยการชั่งน้ำหนัก พบว่ามียางเกาะที่ผิวของเส้นใยมากขึ้นเมื่อมีสารช่วยผสม อย่างไรก็ตาม จากการวัดสมบัติการทนต่อแรงดึงของคอมพอสิท พบว่าไม่เพิ่มขึ้น ซึ่งอาจเกิดจากการเกาะที่ไม่สม่ำเสมอ

Research Article

Aramid Fibres-Thermoplastic Elastomer (SEBS) Composites: Effect of Maleic Anhydride Grafted Compatibiliser on Mechanical Properties

Teeravut Nakinpong*, Budsaporn Sinpatanapan*, Wiriya Meesiri**, Taweechai Amornsakchai*, Sauvarop Bualek-Limcharoen*

Composites of styrene (ethylene butylene) styrene (SEBS) thermoplastic elastomer containing short aramid fibres were studied. Three types of fibres which include Kevlar, Conex and Technora, were used. Firstly, the fibres were used as-received. It was found that for all types of fibres, the modulus at 100% strain increased with increasing fibre content and there was no different between the type of loaded fibres. For modulus at 300% strain, a similar trend was still seen with Kevlar-SEBS exhibits approximately 50% higher moduli than those of Conex- and Technora-SEBS composites. Tensile strength of Kevlar-SEBS composites increased slightly with increasing fibre content and dropped off above 5%. Tensile strengths of Conex- and Technora-SEBS composites, however, decreased with increasing fibre content and were lower than that of Kevlar-SEBS composites at all compositions. Secondly, an attempt was made to improve the interfacial adhesion between fibres and matrix by modifying the fibre the surface using alkali hydrolysis to increase the number of active end groups on fibre surface. These active end groups could then react with anhydride grafted SEBS (SEBS-g-MA) which was used as a compatibiliser. It was found that surface hydrolysis and compatibiliser has little effect on moduli at 100 and 300% strain of the composites. Tensile strength of compatibilised Kevlar and Technora-SEBS decreased slightly with increasing the content of SEBS-g-MA. However, significant enhancement of tensile strength was observed for compatibilised Conex-SEBS composites. This result indicates improvement of the interfacial adhesion between fibre and the matrix.

Key words: aramid, composite, thermoplastic elastomer, fibre reinforcement

INTRODUCTION

Polymer composites using aramid fibres as reinforcement exhibit excellent thermal and mechanical properties. However, problems due to poor adhesion between the fibre and polymer matrix still remain to be solved. Researchers have used different techniques to obtain desired properties. Vaughan[1] applied various commercial coupling agents to composite mixtures and obtained improved adhesion. Other techniques involving modification of fibre reinforcement by dispersion in an ionomer matrix seemed to be very effective.[2,3] Marom *et al.*[4] proposed a technique using bromine water to roughen fibre surface which resulted in improved interlaminar shear strength. Andreopoulos[5] used methacryloyl chloride, an adhesion-promoting compound, to treat Kevlar fibre in an unsaturated polyester matrix and obtained higher tensile strength than the composite without such compound. In another surface modification technique, Wang *et al.*[6] prepared plasma-treated aramid fibre/polyethylene composites. Oxygen plasma was used to generate reactive groups such as -COOH, -OH, -NH_2 on the fibre surface. The reactive groups were used to chemically anchor Ziegler-Natta catalyst which in turn effected polymerization of polyethylene on the fibre surface. Yu *et al.*[7] reported works on nylon/Kevlar composites using various fibre surface treatment methods including hydrolysis, and hydrolysis followed by acid chloride grafting. The composites exhibited better mechanical properties compared to composites with unmodified fibre.

Short-fibre reinforced elastomer has attracted several researching groups.[8-11] Reinforcement used in these works involved conventional fibres like poly(ethylene terephthalate) (PET), and nylon. It is, therefore, quite logical to include such high-performance fibre like aramid in this type of composite.

In the present work, Styrene (Ethylene Butylene) Styrene (SEBS) represented a model thermoplastic elastomer to be reinforced by organic aramid fibres. Our work on composites containing Kevlar[12] and Conex[13] have been reported elsewhere. In this paper, another type of aramid fibre, Technora, will be reported in comparison with the previous results. On a molecular level, these fibres and SEBS are quite incompatible. The incompatibility arises from the relatively non-polar olefinic and styrenic blocks in SEBS and the highly polar hydrogen-bonded amide groups in aramid fibres. To improve compatibility, partial hydrolysis of fibre surface, followed by the addition of maleic anhydride grafted SEBS (SEBS-g-MA), a compatibiliser for this system, were carried out. The treatment should introduce chemical bonding due to the reaction of maleic anhydride and amine groups on the fibre surface, similar to that reported by Modic *et al.*[14] The resulted composites were expected to exhibit improved adhesion between the components and thus provide better mechanical properties.

EXPERIMENTAL

Materials

The materials used in this study are summarized in Table 1. Properties of the fibres are shown in Table 2.[15] Molecular structures of the three aramid fibres are given below.

* Department of Chemistry, Faculty of Science, Mahidol University, Rama 6 Road, Bangkok 10400, THAILAND.

** Directorate of Armament, Royal Thai Air Force, Bangkok, THAILAND.

Table 1 Materials used for this study.

Materials (Commercial designation)	Specification	Manufacturer
Styrene (Ethylene Butylene) Styrene Thermoplastic Elastomer (SEBS, Kraton G 1652)	29% styrene Mw S-block = 7,200 Mw EB-block = 37,500	Shell Chemical Co.
SEBS grafted with maleic anhydride (SEBS-g-MA, Kraton FG 1901x)	29% styrene 1.84 wt% MA	Shell Chemical Co.
Poly-*p*-phenylene terephthalamide (Kevlar)	pulp	DuPont Co.
Poly-*m*-phenylene isophthalamide (Conex)	short fibre	Teijin Ltd.
Poly-*p*-phenylene-3,4'-oxydiphenylene terephthalamide (Technora)	short fibre	Teijin Ltd.

Table 2 Properties of aramid fibres.[15]

Properties	Kevlar	Conex	Technora
Modulus (GPa)	24 - 25	8 - 10	20 - 21
Tensile strength (GPa)	1.8 - 2.1	0.5 - 0.6	3.0 - 3.2
Elongation at break (%)	3 - 4	35 - 45	5 - 7
Specific gravity	1.44	1.38	1.39
Fibre diameter (μm)	13	15	12
Fibre length (mm)	2	3	3

Kevlar

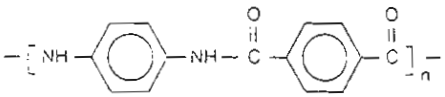

Conex

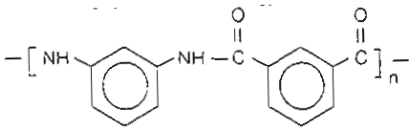

Technora

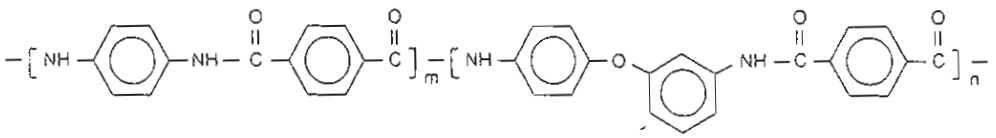

Hydrolysis of Aramid Fibre

The as-received aramid fibre was washed with distilled water, followed by acetone, and dried in a vacuum oven at 50°C for 24 h. Hydrolysis was carried out by dispersing about 10 grams of fibre in 400 ml of 10% sodium hydroxide aqueous solution at ambient temperature for 20 min. After hydrolysis, the fibre was thoroughly washed with distilled water, followed by toluene, and dried in a vacuum oven at 50°C for 48 h. The dried fibre was stored in a desiccator prior to use.

FTIR Characterisation

An FTIR spectrometer with a DRIFT attachment (Diffuse Reflectance Infrared Fourier Transform spectrometer, Perkin Elmer PE 2000) was used to probe the surface of fibre before and after hydrolysis. Each spectrum was obtained from 200 scans at 4 cm^{-1} resolution.

Preparation of Composites

Various compositions of aramid fibre/SEBS composite were prepared. The dried fibre was first pre-opened in a Moulinex blender for a few seconds, followed by blending for 0.5 min in an internal mixer (Haake Rheocord 90) with a rotor speed of 90 rpm at 175°C. The compatibiliser was then added and blended for another 0.5 min, and finally, SEBS was blended in for 9 min. The 50-gram batch composite was passed through a two-roll mill twice to obtain fibre orientation. The composite sheet was kept in a desiccator at room temperature for 24 h.

The effect of mixing condition on tensile properties of Kevlar-SEBS composites was investigated by Nakinpong.[16] The rotor speed at 90 rpm was found to give composites with the best tensile properties and mixing temperature within the range from 165 to185°C showed no effect on tensile properties.

Extraction of Composites

Extraction of composite specimen was carried out using a Soxhlet apparatus and toluene as a solvent. After extraction for 72 h, the sample was dried in a vacuum oven at 50°C for 24 h. The bound rubber on the extracted fibre was determined by DRIFT.

Mechanical Properties of Composites

The composite sheet was compression moulded at 185°C for 10 min under a pressure of 15 MPa, into a 1-mm thick sheet, followed by conditioning at room temperature for at least 24 h. Tensile specimen was die cut at the size of 115x6 mm with the long dimension parallel to the machine direction (direction passing through the two-roll mill). Testing was performed on an Instron testing machine model 4301, in accordance with ASTM D638 at a cross head speed of 500 mm/min with a full scale load cell at 100kg.

RESULTS AND DISCUSSION

Hydrolysis of Aramid Fibre Surface

Aramid fibres were partially hydrolysed to create more $-NH_2$ and -COOH end groups on the surface. Figure 1a, b and c show DRIFT spectra of untreated and treated Kevlar, Technora and Conex fibres, respectively. The peak at 880-884 cm^{-1} is due to C-H out-of-plane bending of the aromatic ring adjacent to $-COO^-Na^+$ as reported by Chatzi.[17] After washing with distilled water, followed by toluene, and dried, the peak disappeared, apparently due to the change from $-COO^-Na^+$ to -COOH. Without this washing step, sodium hydroxide would further hydrolyse to amide bonds on the fibre surface, resulting in a dark brown colour and reduced tensile properties of the composite.

Mechanical Properties of Composites

1. As-received fibres

Tensile properties of the aramid fibre/SEBS composites are shown in Figure 2. It is evident that for all composites Modulus at 100% (M100) increases linearly with increasing the amount of fibre loading and there is virtually no effect of fibre types on M100. An increase in M100 with fibre loading is due to incorporation of high modulus fibre in soft matrix. The fact that all type of fibres resulted in the same M100 would suggest that there is a saturation in M100 of the composites, regardless the mechanical properties and geometry of the reinforcing fibre. Similar effect of fibre loading are seen for Modulus at 300% (M300). In this case, however, Kevlar composites exhibit significantly higher M300 than Conex and Technora composites. Again, no difference was found between M300 of Conex and Technora composites. It appears that at this high strain (300%) stress transfer to Kevlar is greater than that to Conex and Technora. This would suggest that reinforcing element in pulp geometry is better than short cylindrical fibre.

Tensile strength of the composites are shown in Figure 2 (c). It can be seen that, for Kevlar composites, addition of fibre upto 5% slightly decreases the tensile strength of the composites. At higher fibre loading tensile strength drops sharply. This was found to coincide with the observation of poorly dispersed fibre in the matrix. For Conex and Technora composites, it can be seen that tensile strength linearly decreases with increasing fibre content. This can be understood as a debonding of fibre-matrix interface at very high strain which

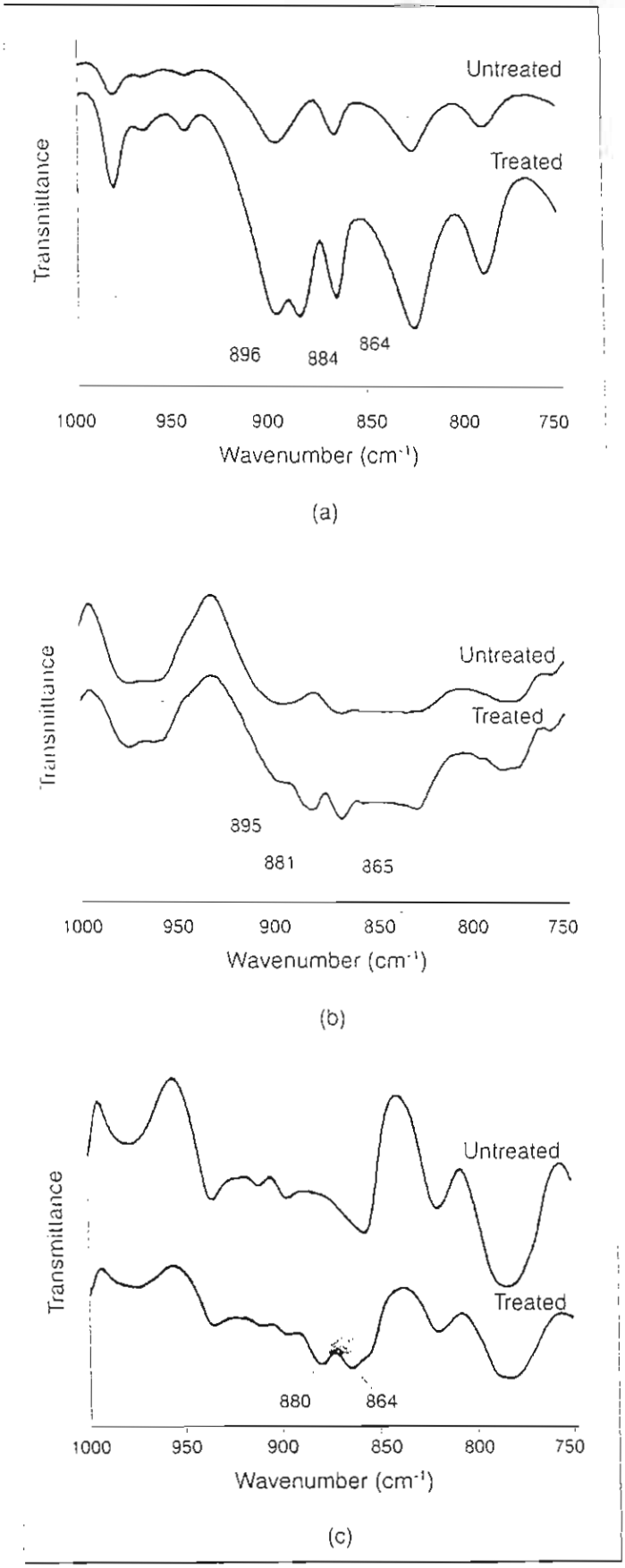

Fig. 1 Infrared spectra of untreated (as-received) and treated (surface hydrolysed) aramid fibres (a) Kevlar (b) Technora (c) Conex

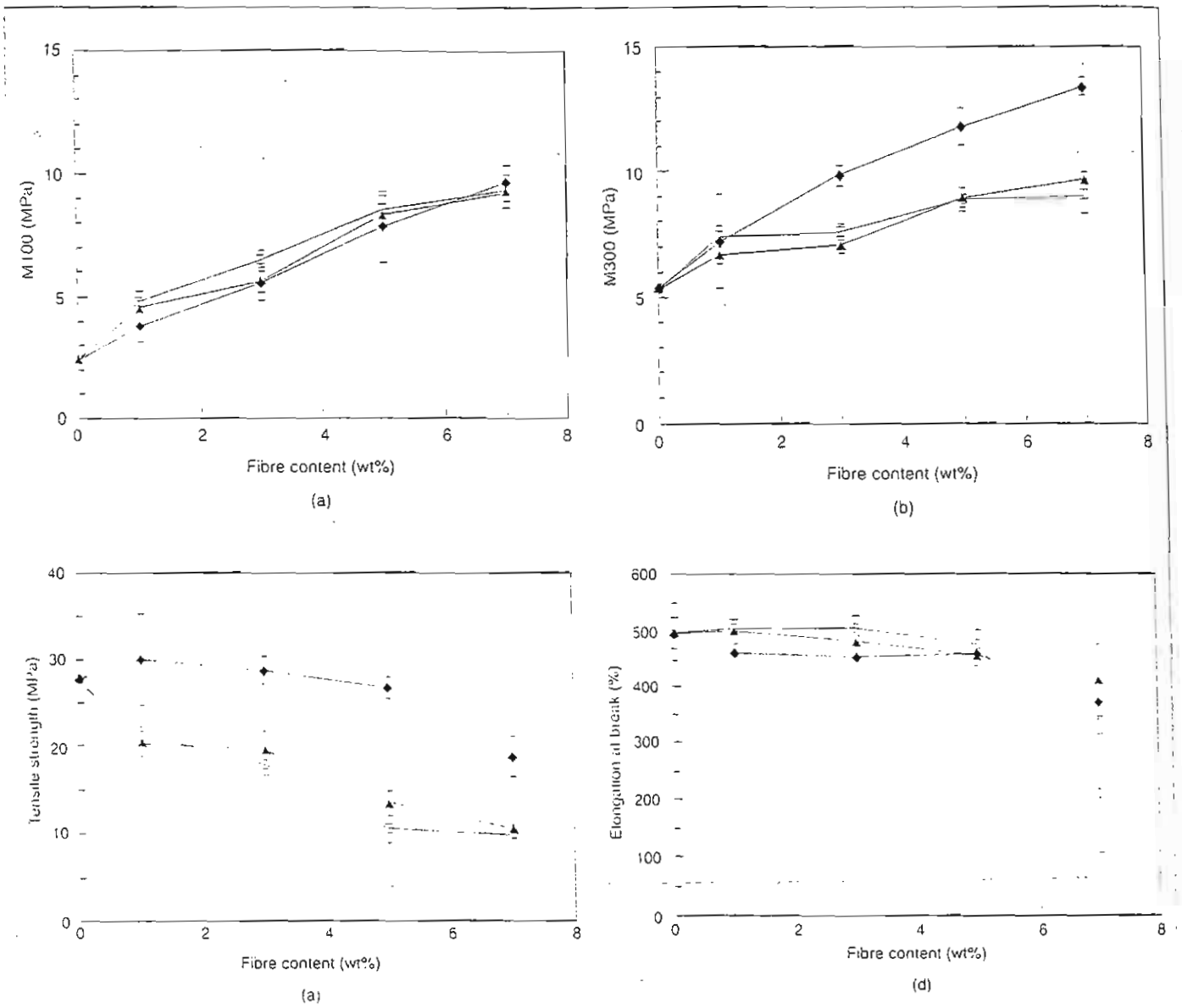

Fig. 2 Tensile properties of untreated aramid fibre/SEBS composite with various fibre loading (◆ : Kevlar, □ : Conex, ▲ : Technora) (a) Modulus at 100%, (b) Modulus at 300%, (c) Tensile strength, and (d) Elongation at break.

could be seen as specimen whitening. The specimens will therefore be weaken.

Elongation at break of all types of composites is virtually unchanged by increasing of fibre loading up to 5%. However, above 5% fibre content, elongation at break drops sharply. This is due to severe weakening of the interface debonding and poor dispersion of fibre at the high fibre content.

The results reported above were obtained from measurements of the specimens cut parallel to the machine direction (direction passing through the two-roll mill). In the case of Kevlar pulp-SEBS composite, tensile properties measured in the directions parallel and perpendicular to the machine direction were found to be approximately the same due to the biaxial orientation of the main fibre and the spitted small fibril as reported elsewhere.[12] The effect of fibre orientation was observed, however, in the case of composites with Conex and Technora short fibres. The properties of specimen measured in the direction perpendicular to the machine direction were about 10% less than those in the machine direction.

2. Surface-hydrolysed fibres

Surface hydrolysis of aramid fibre was carried out to increase the number of reactive end groups. These end groups could then react with SEBS-g-MA compatibiliser and modify surface properties of the fibres closer towards that of SEBS matrix.

Tensile properties of the composites containing 3% of treated fibres and compatibiliser are shown in Figure 3. It can be seen that compatibiliser content only slightly affects the properties of Kevlar and Technora composites. However, for Conex composites, it is clearly seen that the compatibiliser greatly improves the tensile strength of the composite. Tensile strength was found to increase with increasing compatibiliser content and approaching that of Kevlar composites at 5%. This

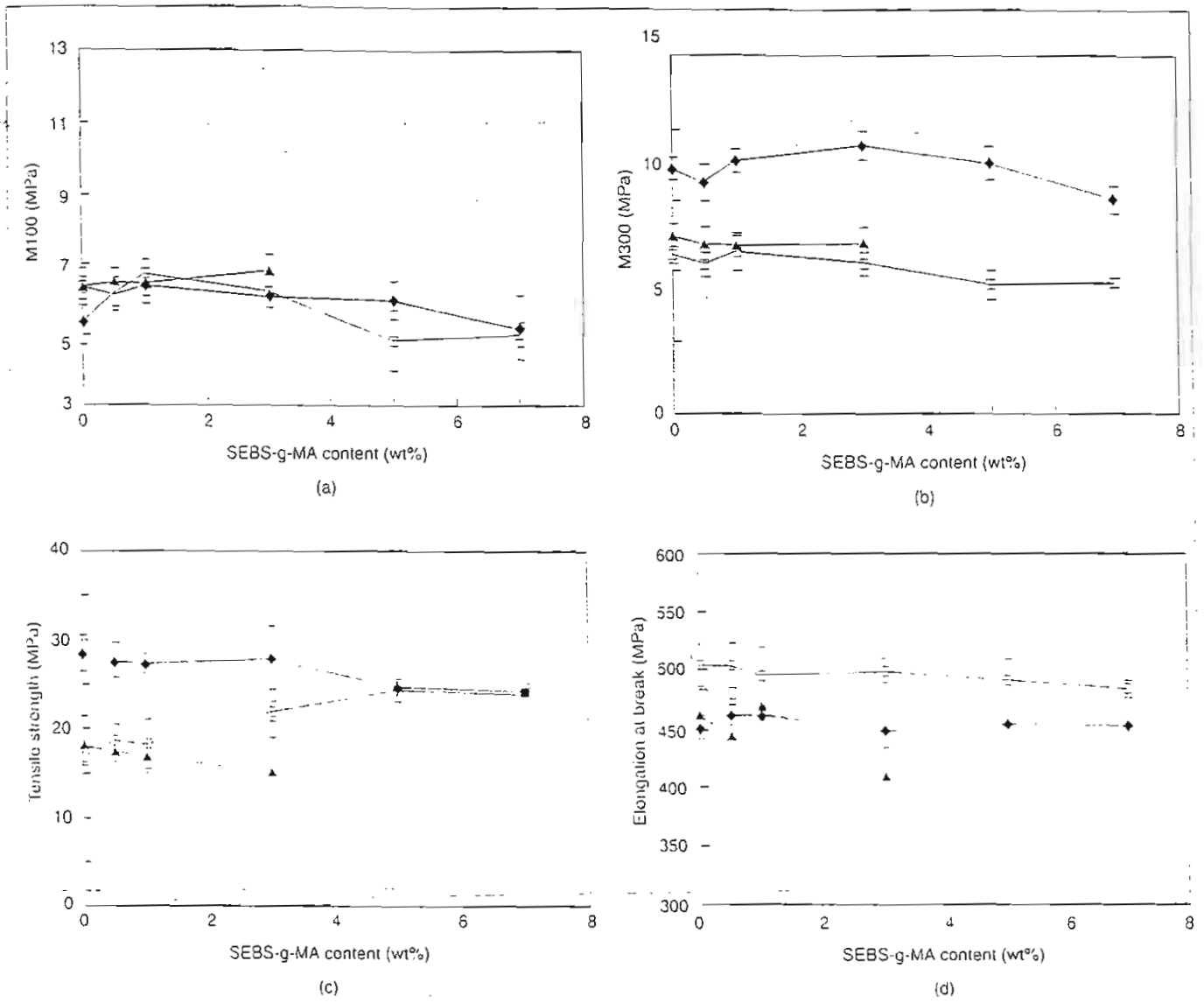

Fig. 3 Tensile properties of treated aramid fibre/SEBS composite with various compatibiliser contents (◆ : Kevlar, □ : Conex, ▲ : Technora) (a) Modulus at 100%, (b) Modulus at 300%, (c) Tensile strength, (d) Elongation at break.

is the evidence of the improvement of interfacial adhesion through the interaction of MA group and the reactive NH_2 end group of Conex. No improvement of tensile strength is found in the case of Kevlar pulp. It might be due to fibrillation of pulp during processing which peeled-off the treated surface. However, no improvement of tensile strength is observed in the case of Technora, though it is in the form of short fibre as Conex. This might be due to poor dispersion of Technora in SEBS matrix. This can be seen in the drop of elongation at break and large error bar (see Fig. 3d) at 3 wt% fibre loading. Poorer dispersion of Technora compared to Conex might be due to its larger fibre aspect ratio (length to diameter ratio) and hence fibres are curled and entangled to a greater extent.

Analysis of extracted fibres

FTIR spectra of Kevlar fibres extracted from the composites containing different concentration of compatibiliser, SEBS-g-MA, are shown in Fig. 4. The peaks at 2923 and 2853 cm^{-1} correspond to anti-symmetric and symmetric C-H stretching, respectively[18], of CH_2 group in the ethylene block of SEBS. Curve 4a is the infrared spectrum of extracted Kevlar pulp from the composite without compatibiliser, showing the typical peak at 3320 cm^{-1} which corresponds to N-H stretching in Kevlar. These spectra clearly demonstrate the increasing of bound SEBS on the fibre surface with increasing amount of compatibiliser, SEBS-g-MA. This clearly suggests the presence of the chemical bonding between the NH_2 group on aramid fibre and the maleic anhydride group on SEBS-g-MA. Similary, bound SEBS on extracted Conex and Technora fibres was also observed. The above finding suggests that chemical interaction between compatibiliser and fibre may or may not result in improvement of mechanical properties.

CONCLUSIONS

Reinforcement of SEBS thermoplastic elastomer with aramid fibres at low strain can be achieved without any

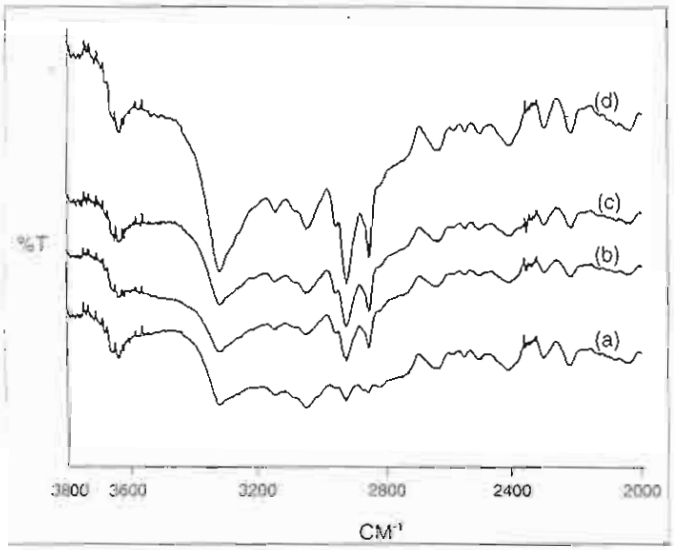

Fig. 4 DRIFT spectra of extracted Kevlar/SEBS composite containing various SEBS-g-MA (a) 0 wt% (b) 1 wt% (c) 3 wt% (d) 10 wt%.

compatibilisers. It appears that geometry of the fibre has greater effect on mechanical properties of the composites than the mechanical properties of the fibres. At the same fibre content, pulp was found to be more effective in reinforcing than short fibre.

Alkaline hydrolysis of fibre surface in conjuction with reactive compatibiliser was found to be effective on certain type of aramid fibre, i.e. Conex. No improvement was achieved for Kevlar and Technora composites despite surface modification had been achieved.

ACKNOWLEDGEMENTS

The financial support of The Thailand Research Fund is gratefully acknowledged.

The authors also would like to thank the Shell Chemical Co., Du Pont Co. and Tejin Ltd. for providing materials used in this work.

REFERENCES

1. Vaughan DJ. The Use of Coupling Agents to enhance the Performance of Aramid Reinforced Composites. *Polym Eng Sci* 1978; 18: 167-9.
2. Takayanagi M, Kajiyama T, Katayose T. Surface-Modified Kevlar Fiber-Reinforced Polyethylene and Ionomer. *J Appl Polym Sci* 1982; 27: 3903-17.
3. Takayanagi M, Katayose T. Surface Modified Kevlar Fibre Reinforced Ionomer, Dynamic Mechanical Properties and Their Interpretation. *Polym Eng Sci* 1984; 24: 1047-50.
4. Breznick M, Banbaji J, Guttmann H, Marom G. Surface Treatment Technique for Aramid Fibres. *Polym Commun* 1987; 28: 55-6.
5. Andreopoulos AG. A New Coupling Agent for Aramid Fibre. *J Appl Polym Sci* 1989; 38: 1053-64.
6. Wang Q, Kaliaguine S, Ait-Kadi A. Catalytic Grafting: A New Technique for Polymer-Fibre Composites: Analysis of the Fibre Surface. *J Appl Sci* 1993; 48: 121-36.
7. Yu Z, Ait-Kadi A, Brisson J. Nylon/Kevlar Composites. I: Mechanical Properties. *Polym Eng Sci* 1991; 31: 1222-7.
8. Ashida M, Noguchi T. Effect of Adsorbed Water on Dynamic Modulus for Short Fibre-CR Composites. *J Appl Polym Sci* 1984; 29, 4107-14.
9. Ashida M, Noguchi T, Mashimo S. Dynamic Moduli for Short Fibre-CR Composites. *J Appl Polym Sci* 1984; 29, 661-70.
10. Ashida M, Noguchi T, Mashimo S. Effect of Matrix's Type on The Dynamic Properties for Short Fibre-Elastomer Composite. *J Appl Polym Sci* 1985; 30: 1011-21.
11. Guo W, Ashida M. Mechanical Properties of PET Short Fibre-Polyester Thermoplastic Elastomer Composites. *J Appl Polym Sci* 1993; 49: 1081-91.
12. Bualek-Limcharoen S, Nakinpong T, Amornsakchai T, Meesin W. Kevlar Pulp-Thermoplastic Elastomer Composite: Morphology and Mechanical Properties. *J Sci Soc Thailand* 1997; 23: 101-14.
13. Amornsakchai T, Sinpatanapan B, Bualek-Limcharoen S and Meesin W. *Polymer* (in Press)
14. Modic J, Pottick LA. Modification and Compatibilisation of Nylon 6 With Functionalized Styrenic Block Copolymers. *Polym Eng Sci* 1993; 33: 819-26.
15. Technical information sheets from Du Pont Co (No.12/92) and Tejin Ltd. (CN02/95.9)
16. Nakinpong, T. Morphology and Mechanical Properties of Kevlar Pulp Styrene (Ethylene Butylene)Styrene Thermoplastic Elastomer Composite. *Thesis: Mahidol University* 1997
17. Chatzi EG, Tidrick SL, Koenig JL. Characterisation of the Surface Hydrolysis of Kevlar 49 Fibres by Diffuse Reflectance FTIR Spectroscopy. *J Polym Sci: Polym Phys Edn* 1988; 26: 1585-93.
18. Socrates G. Infrared Characteristic Group Frequencies: Tables and Charts, 2nd Edn John Wiley & Sons, Chichester, 1994.

Effect of Compatibilizers on Mechanical Properties and Morphology of In-Situ Composite Film of Thermotropic Liquid Crystalline Polymer/Polypropylene

SAUVAROP BUALEK-LIMCHAROEN*,[1], JAREERAT SAMRAN[1], TAWEECHAI AMORNSAKCHAI[1], *and* WIRIYA MEESIRI[2]

[1]*Department of Chemistry, Faculty of Science*
Mahidol University
Bangkok 10400, Thailand

[2]*Directorate of Armament*
Royal Thai Air Force
Donmuang, Bangkok 10210, Thailand

An *in-situ* composite film of a thermotropic liquid crystalline polymer (LC3000)/polypropylene (TLCP/PP) was produced using the extrusion cast film technique. The compatibilizing effect of thermoplastic elastomers, styrene-ethylene butylene-styrene (SEBS), maleic anhydride grafted SEBS (MA-SEBS), and maleic anhydride grafted polypropylene (MA-PP) on the mechanical properties and morphology of the TLCP/PP composite films was investigated. It was found that SEBS provided a higher value of tensile modulus than MA-SEBS, which in turn was higher than MA-PP, despite the expected stronger interaction between the MA chain and TLCP. The observation of the morphology under optical and scanning electron microscopes suggested that all three compatibilizers helped improve the dispersion of the TLCP fibers and increased the fiber aspect ratio to a different extent. The fractured surface of the specimens showed more fiber breakage than pull-out when a compatibilizer was added, which suggested the improvement of interfacial adhesion. The surface roughness of fibers with an added elastomeric compatibilizer may also provide mechanical interlocking at the interface. It is suggested that the increase in the viscosity ratio of TLCP/PP due to the added elastomeric compatibilizer, SEBS and MA-SEBS, compared with the thermoplastic compatibilizer, MA-PP, is more effective in improving the composite mechanical properties.

INTRODUCTION

The modification of polymers through the blending of a thermotropic liquid crystalline polymer (TLCP) with thermoplastics (TP) providing superior rheological and mechanical properties of the composite has drawn considerable attention (1–4). The processing of an incompatible TLCP/TP blend under an elongational flow condition is known to produce an oriented TLCP-fiber phase. Hence, the term "in-situ composite" was coined (5) for this type of polyblend, which means self-reinforcement due to the fibers formed during processing.

Blends of Hoechst Celanese Vectra A900 TLCP and SEBS (styrene-ethylene butylene-styrene) thermoplastic elastomer were intensively studied by De Boer *et al.* (6–8). They reported the formation of TLCP fibers in an almost pure shear flow condition, which contradicted previous works suggesting that the fibers only form in an elongational flow condition.

In-situ composites produced mostly by fiber spinning and injection molding have a higher modulus than sheet or film (9) because of a fibrillar structure that can be obtained more effectively by elongational force in the spinning process. *In-situ* composite film has only recently gained much interest for applications such as high-strength balloons (10). However, the main problem in the TLCP blend system in such an application has been due to the high degree of anisotropy of the mechanical properties, i.e., the properties along the machine direction (MD) are different from those along the transverse direction (TD). Chinsirikul *et al.* (11) attempted to reduce the anisotropy

*To whom correspondence should be addressed. E-mail: scsbl@mahidol.ac.th. Fax: (662) 247-7050.

using a counter-rotating die in film extrusion. Another approach to improve the properties was investigated by Datta *et al.* (12) through the addition of a compatibilizer. In their work, a blend of polypropylene (PP) and TLCP (Vectra A) with a maleic anhydride-grafted polypropylene (MA-PP) added as a compatibilizer was produced as an extruded strand and injection-molded sheet. An increase of about 25% in modulus was found in injected tensile bars containing about 30% TLCP. A similar investigation by O'Donnell (13) using MA-PP as a compatibilizer in a PP/Rodrun LC3000 (70/30 weight ratio) system also reported about a 30% increase in the modulus of the blend. It was concluded that the added compatibilizer helped produce more finely dispersed TLCP fibrils and consequently improved the tensile strength and modulus.

The objective of the present work is to improve the mechanical properties of *in-situ* composite film based on TLCP/PP using block and grafted copolymers as compatibilizers at various concentrations. Cast films were characterized in morphological and mechanical aspects.

EXPERIMENTAL

Materials

The thermoplastic polymer matrix used in this study was an injection grade polypropylene (PP6331) with a melt flow rate (MFR) of 12g/10 min (230°C, 2.16 kg load). A thermotropic liquid crystalline polymer was a copolyester comprising 60 mol% of p-hydroxybenzoic acid and 40 mol% of poly(ethylene terephthalate) (Rodrun LC3000) purchased from the Unitika Company. The crystal-nematic and nematic-isotropic transitions of LC3000 are 220°C and 280°C, respectively. A triblock thermoplastic elastomer of styrene ethylene butylene styrene (SEBS, styrene/rubber ratio 29/71, Kraton G-1652) and maleic anhydride-grafted SEBS (Kraton FG1901X, containing 1.8 wt% maleic anhydride) was provided by Shell Chemical Co. Maleic anhydride-grafted polypropylene (MA-PP), containing about 0.1 wt% maleic anhydride, was provided by the Mitsubishi Co.. The materials were vacuum dried at 60°C for 12 h before use.

Blending

Melt blending of PP and 10 wt% TLCP was performed using a co-rotating twin screw extruder (PRISM TSE-16TC) with a screw diameter of 16 mm, L/D = 25, intermeshing, at an extrusion rate of 150 rpm. The processing temperature profile was 180/220/220/225/225°C (14), representing temperatures at the hopper zone, the three barrel zones, and the heating zone in the die head, respectively. The strand exiting the extruder was immediately quenched in a water bath and subsequently was pelletized.

Extrusion Film Casting

TLCP/PP blend pellets were extruded using a 16-mm mini-extruder (Randcastle RCP-0625) equipped with a cast film line. The temperature profile was 190/220/230/240°C for the hopper zone, two barrel zones, and slit-die, respectively. The screw speed was 70 rpm. The gap of the die lip was adjusted at 0.65 mm and the width fixed at 152 mm. Extruded film was drawn downward as a molten blend exiting the die outlet and then quenched on a water-cooled roll. The draw ratio (slit width-to-film thickness ratio) was controlled by adjusting the take-off speed. The highest draw ratio used in this experiment was about 33. The film thickness was varied from 20 to 70 μm.

Mechanical Testing

Tensile testing was conducted using an Instron mechanical tester (Model 4301) with a grip length of 25 mm, a crosshead speed of 50 mm/min, and a full-scale load of 10N. Tensile properties of the dumbbell-shaped specimens (70 mm × 4 mm) were measured in the flow (machine) and transverse directions (ASTM D412). Data were taken and averaged from at least ten specimens for each blending system.

Impact testing was performed using a pneumatic driving impact tester Radmana ITR-2000 at a constant temperature and humidity (ASTM D3763). The test films were about 70 μm thick. The results are averaged values of at least ten measurements for each blending system.

Morphology

The distribution of TLCP fibrils in the PP matrix was directly observed under an optical microscope at a magnification of 100–400 times. In order to inspect the size and shape of the fibers more clearly, composite films were extracted in boiling xylene and the remaining fibers were dried before observation. The observation of the fractured surface of the composite films was performed using a scanning electron microscope (SEM, Hitachi S2500) operated at 15 kV. Fractured surfaces were prepared by fracturing the composite film in liquid nitrogen. Palladium film was coated on the specimens using a Hitachi E102 ion sputtering coater.

Order Parameter

The order parameter or orientation function (S) (15-17) defined as the degree of alignment of liquid crystal molecules with a preferred direction, was determined from the infrared dichroic ratio, $R = A_{\parallel}/A_{\perp}$, where $A_{\parallel}$ and $A_{\perp}$ are absorbance values for plane polarized light with the electric vector parallel and perpendicular to the preferred direction, respectively. For a band whose transition moment is parallel to the major molecular axis, $S = (R - 1)/(R + 2)$. The IR absorption spectra of composite films about 25 μm thick were recorded using a Perkin-Elmer FTIR (System 2000) with an aluminum wire-grid polarizer placed between the sample and the light source. The polarization directions of the polarizer were adjusted parallel and perpendicular to the machine direction of the film. Each spectrum was collected in a

transmission mode at a resolution of 4 cm^{-1} and 25 scans. An area under the peak at 1601.5 cm^{-1}, (C-C stretching vibration of para-substituted benzene ring of p-hydroxybenzoic acid) corresponding to the parallel transition moment was used to determine the order parameter of the TLCP.

RESULTS AND DISCUSSION

Mechanical Properties

Young's moduli of TLCP/PP/compatibilizer films with varied amounts of compatibilizer are shown in *Fig. 1*. Young's moduli of pure polypropylene film produced under the same processing conditions (not shown) were also determined and compared: 616 ± 66 MPa and 586 ± 44 MPa in machine direction (MD) and transverse direction (TD), respectively. The film evidently exhibited a slight anisotropy in its moduli. The addition of 10 wt% TLCP resulted in an increase in the modulus in MD by almost twice as much. The modulus in TD, however, increased slightly. It is evident that the composite film exhibited a high degree of anisotropy due to the preferred fiber orientation in the composite film. The effect of a compatibilizer on the film modulus, especially in MD, varies by different extents depending on the type and amount of compatibilizer. SEBS improved the film modulus in MD to the greatest extent with a peak value at 3 wt% SEBS. The improvement was about 46% over that without the compatibilizer (1,592 MPa vs. 1,091 MPa). The modulus decreases with an increasing SEBS content above 3 wt%. However, at 8 wt% SEBS the modulus is still slightly higher than without SEBS. Films with added MA-SEBS exhibited a similar effect as those with SEBS but to a lesser extent. A peak in modulus was found at 1.5 wt% MA-SEBS with a 21% improvement over that with no compatibilizer. On the other hand, MA-PP did not appear to have a significant effect on the film modulus.

The effect of a compatibilizer on the film modulus in TD is less pronounced than that found in MD. It appears that Young's modulus in TD was not significantly affected by the type and content of the compatibilizer, with an exception of an improvement of about 28% for film with 1.5 wt% SEBS.

The yield stress of composite films will now be discussed. *Figure 2* shows the yield stress of composite films containing various amounts of compatibilizer. For comparison, yield stress values of pure PP film were 20.2 ± 1.4 and 15.4 ± 1.5 in MD and TD, respectively (not shown in the *Figure*). The composite films were found to have a slightly higher yield stress than PP in both directions. A slight improvement of the yield stress in MD was found in the composite film with SEBS. In other cases, it was found that yield stress in both MD and TD decreases with an increasing amount of compatibilizer. In all cases, the yield stress in MD is higher than that in TD.

From the mechanical results presented above, it is rather surprising that such a soft elastomer such as SEBS improved the modulus of the composite films more than MA-SEBS, which in turn improved it more than MA-PP. This contradicts the expectation that the presence of a reactive MA group in the latter two compatibilizers could form a chemical or hydrogen bond with TLCP, which consequently, should improve the interfacial adhesion between the two phases. Such bonding between an MA group, and TLCP domains was probably formed during processing as previously

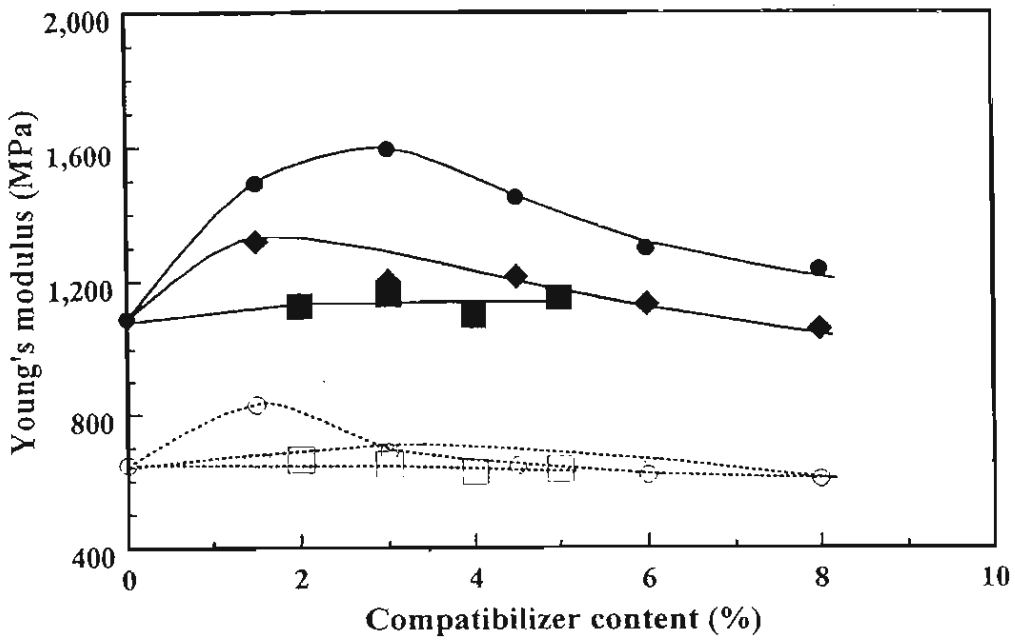

Fig. 1. Effect of compatibilizers on Young's Modulus of TLCP/PP composite films. (●, ○: SEBS; ◆, ❖: MA-SEBS and (■, □: MA-PP. MD: filled and TD: unfilled.)

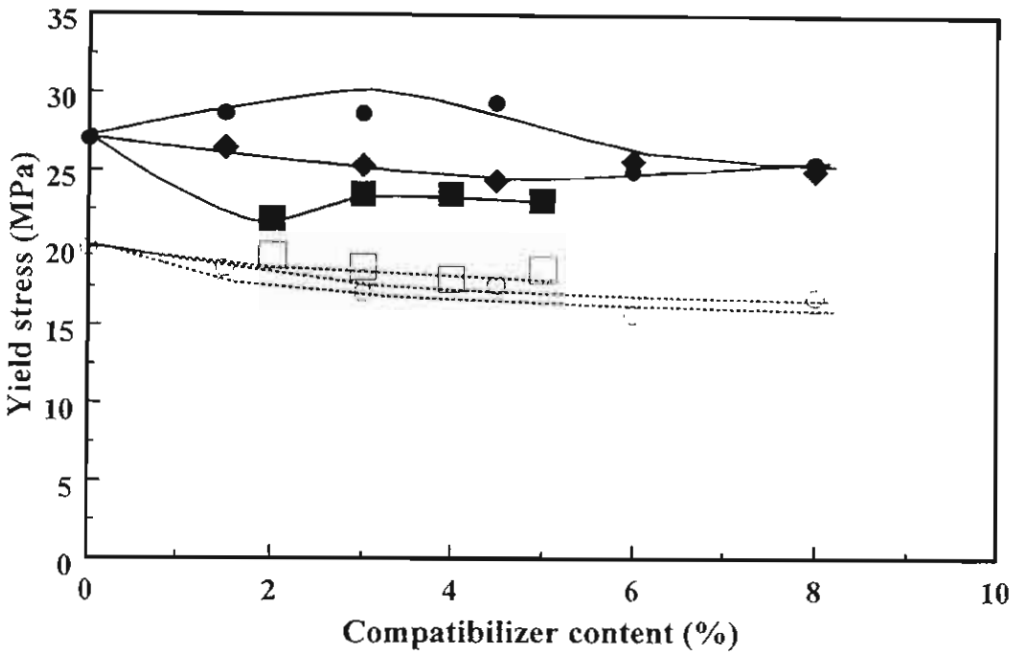

Fig. 2. Effect of compatibilizers on yield stress of TLCP/PP composite films. ●, ○: SEBS; ◆, ❖: MA-SEBS and ■, □: MA-PP. MD: filled and TD: unfilled.)

reported by O'Donnell (13) and Seo (18). However, this kind of bonding may retard the extension of the TLCP fibers by elongational flow. Hence, using MA-SEBS may give rise to thicker TLCP fibers (lower fiber aspect ratio) than those obtained in the case of SEBS. Since the modulus is measured at low strain, the difference in modulus would indicate a difference in the structure of the composite film, i.e., the size and aspect ratio of fiber formed in the film. The better properties of composite with the elastomeric compatibilizer may be due to the effect of a compatibilizer on the viscosity of the system. In order to support this assumption we measured the melt flow rate (MFR) (using 2.16 kg force at 230°C) of these blend systems. It was found that MFR reduces from 19.5g/10 min for the composite without a compatibilizer to 12.5, 13.2, and 17.6g/10 min for the blends containing 3 wt% SEBS, 1.5 wt% MA-SEBS, and 3 wt% MA-PP, respectively. A further addition of the compatibilizers showed no further significant change in MFR (see *Fig. 3*). The results reveal that SEBS and MA-SEBS increase the viscosity of the blend to a much greater extent than MA-PP, and hence, aid the formation of TLCP fibers. The effect of the viscosity ratio of LC3000/PP blends on their morphology was investigated by Heino *et al.*(14). They reported that the most fibrous structure was achieved when the viscosity ratio ranged from about 0.5 to 1. At the lower viscosity ratio the fiber structure was coarser, while at viscosity ratio above unity, the TLCP domains tended to be spherical. Similarly, in our work, the addition of SEBS to the TLCP/PP blend may affect the matrix viscosity to help form the fibrous structure of TLCP. The evidence from the morphology study will be discussed later.

A drop in the Young's modulus of the composite film at a high SEBS content will now be discussed. Since SEBS is a triblock copolymer with a styrene block at both ends and an ethylene/butylene block in the middle, it would be expected that the two ends containing aromatic rings would be compatible with the TLCP phase, while the rubbery EB block would be compatible with the PP matrix. Accordingly, SEBS should be present at the interface to promote interfacial adhesion and to help disperse the TLCP phase. At a high content, however, the amount of compatibilizer at the interface is likely to exceed the saturation limit (critical micelle concentration) and phase separation of the compatibilizer may take place (19, 20), resulting in an overall decrease in the properties of the blend. A further increase in the SEBS content lowers the Young's modulus of the composite due to the soft nature of the added rubber. However, even at 8 wt% SEBS, the composite film still shows a higher modulus than the film without a compatibilzer. This lowering effect at a high SEBS concentration was in agreement with the decrease in the shear modulus of PP on blending with SEBS (no reinforcing fibers), as reported by Gupta *et al.* (21).

The addition of MA-PP to the composite film shows only a slight increase in the modulus in MD. Although it is likely that the compatibilizer helps disperse the TLCP phase, it appears to be less effective than MA-SEBS. This may be due the lower concentration of the MA-group in MA-PP than in MA-SEBS and because MA-PP does not affect the viscosity of the blend (see *Fig. 3*).

Morphology

Figure 4 shows optical micrographs of composite films with: a) no compatibilizer, b) 3 wt% SEBS, c) 1.5 wt%

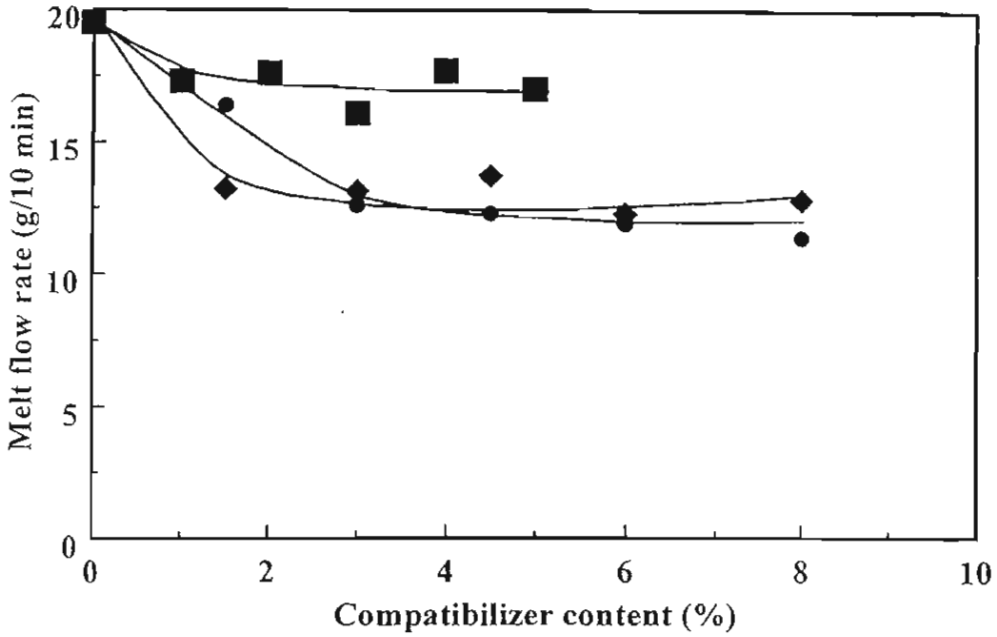

Fig. 3. Effect of compatibilizers on melt flow index of TLCP/PP blend. ●: SEBS; ◆: MA-SEBS and ■: MA-PP.

MA-SEBS, and d) 3 wt% MA-PP. At these concentrations of compatibilizer, a maximum value of tensile modulus is observed in each system. It is evident that the number of fibers per unit area as well as the aspect ratio of the TLCP fiber increase with the addition of a compatibilizer. The incorporation of a compatibilizer results in a more finely dispersed TLCP phase, and hence, more fibers are formed under shear and elongational forces. The addition of a compatibilizer, therefore, has a similar effect to increasing the fiber loading, giving rise to

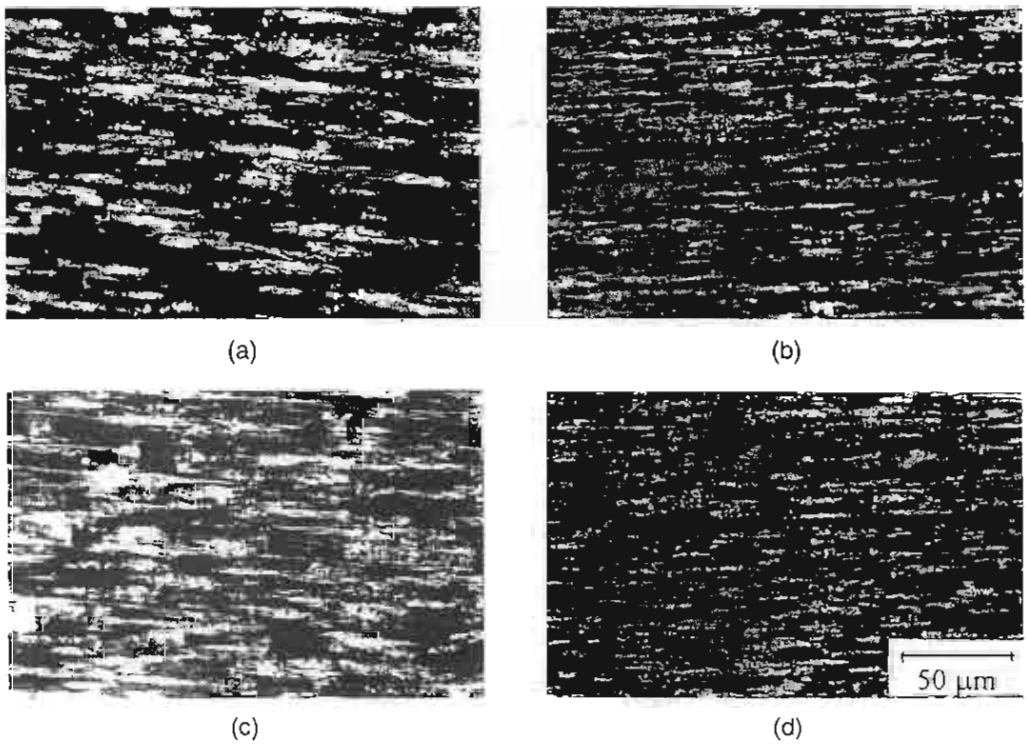

Fig. 4. Optical micrographs of in-situ composite films containing (a) no compatibilizer (b) 3 wt% SEBS (c) 1.5 wt% MA-SEBS and (d) 3 wt% MA-PP.

the enhancement of the modulus. This is in good agreement with the results reported by O'Donnell (13). In addition to the difference in shape of the dispersed TLCP fibers, the birefringence characterizing the frozen nematic phase of TLCP domains also differs. Without a compatibilizer, the TLCP phase exhibits a birefringence less homogeneous than that of the systems containing a compatibilizer, suggesting a better molecular orientation of the TLCP domains in the latter case. The result is supported by the increase in the order parameter of the TLCP phase, to be discussed later. To study the size and shape of fibers more clearly, composite films were extracted using boiling xylene, a good solvent for PP but a nonsolvent for TLCP. *Figure 5* shows photomicrographs of TLCP fibers extracted from films, taken at the same magnification. Fibers extracted from films containing compatibilizers (*Figs. 5b-d*) appear to be thinner and longer than those obtained from films with no compatibilizer (*Fig. 5a*). Among the three compatibilizers, SEBS yields the thinnest, and hence, the highest fiber aspect ratio, resulting in the highest Young's modulus discussed above.

Figure 6 shows SEM micrographs of the fractured surface of composite blends, broken along the direction normal to the flow direction. The film with no compatibilizer (*Fig. 6a*) shows a number of TLCP-fiber pull-outs with a smooth surface, suggesting a poor fiber-matrix interfacial adhesion. In the case of a composite with a SEBS compatibilizer (*Fig. 6b*), different features are observed: fiber breakage, fiber surface roughness, and fiber-tip bending. Similar features are also observed in the case of using an MA-SEBS compatibilizer (*Fig. 6c*). However, in the presence of MA-PP (*Fig. 6d*), the fiber surface is rather smooth with spike fiber tips and less fiber pull-out than in *Fig. 6a*, suggesting a better adhesion in the compatibilized composite. The appearance of fiber surface roughness in composites with an elastomeric compatibilizer may arise from an uneven extension of the TLCP phase caused by non-uniform friction due to the elastomer partly adhering at the interface. Such surface roughness was recently reported by Seo (22) for the ternary blend systems, nylon/TLCP/MA-EPDM, and PBT/TLCP/MA-EPDM. Though with higher viscosity of TLCP than the matrix, fibrillation of TLCP could be obtained at a low shear rate. Seo proposed the mechanism for the existing surface roughness: That it is a result of the relaxation of the elastomer surrounding the elongated TLCP phase.

Order Parameter

For thin film specimens, it is rather simple to determine the molecular orientation from the anisotropy of the absorption spectra (dichroism), especially in the infrared region. Since the selected peak used to measure the dichroic ratio belongs to the benzene ring in the TLCP molecule, the calculated order parameter,

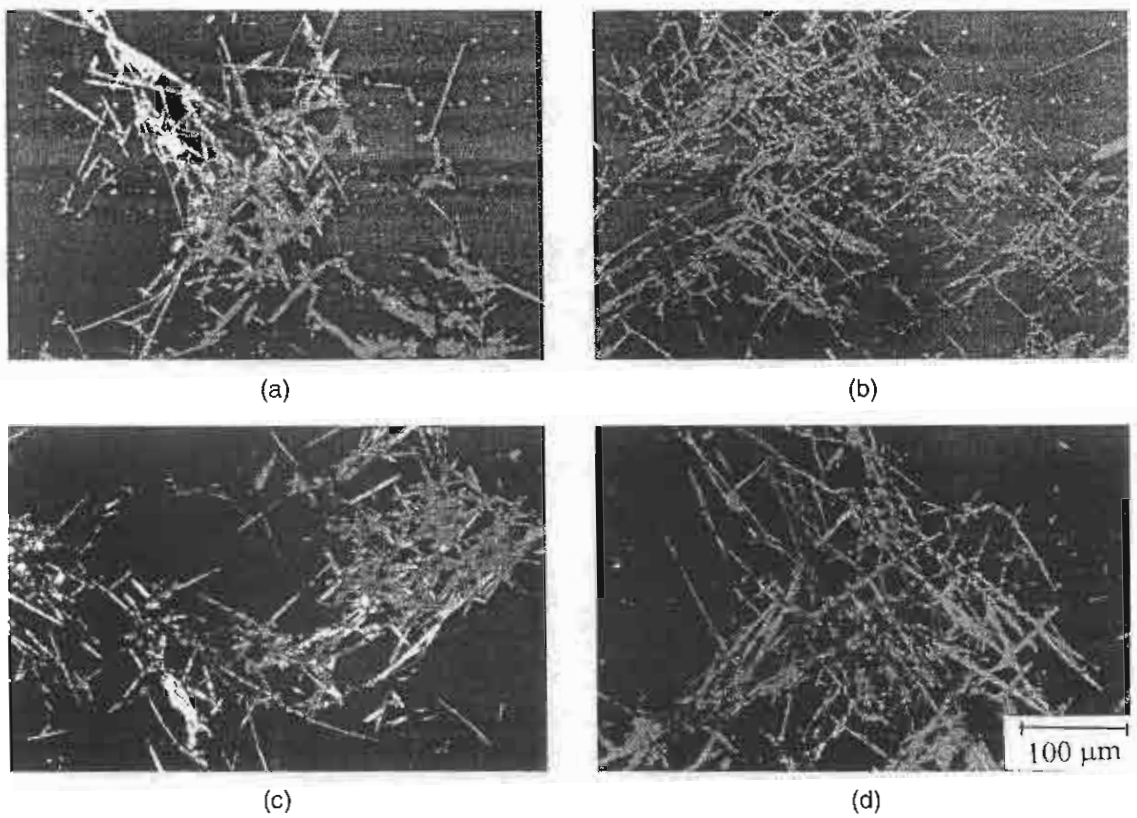

Fig. 5. Extracted TLCP fibers obtained from composite films containing (a) no compatibilizer (b) 3 wt% SEBS (c) 1.5 wt% MA-SEBS and (d) 3 wt% MA-PP.

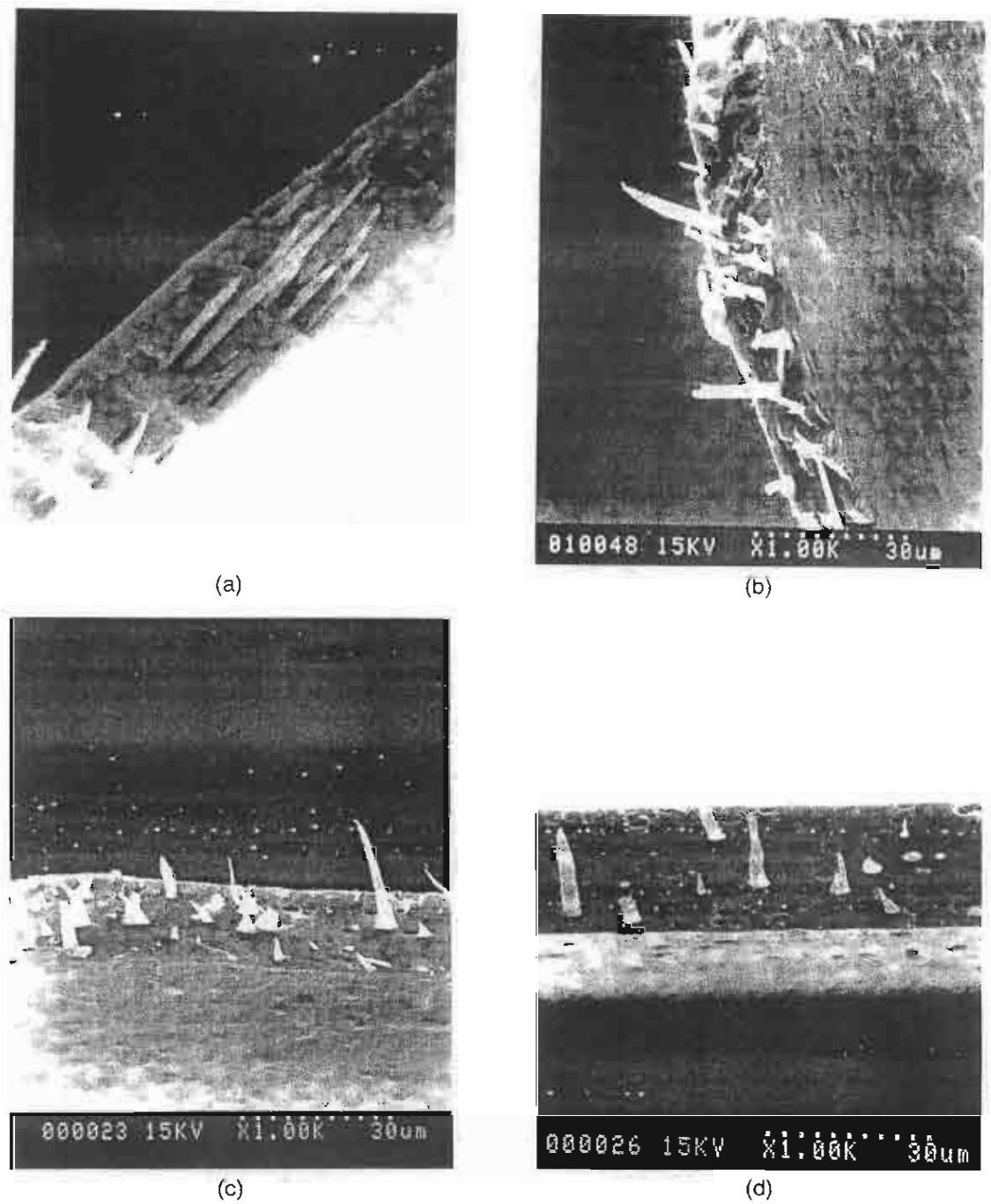

Fig. 6. SEM micrographs of fractured surface of composites film containing (a) no compatibilizer (b) 3 wt% SEBS (c) 1.5 wt% MA-SEBS and (d) 3 wt% MA-PP.

therefore, represents only the order in the TLCP phase. The order parameter of TLCP in the composite films containing compatibilizers is shown in *Fig. 7*. The films with about 1.5 wt% SEBS and with 1.5 wt% MA-SEBS have an increase of order parameter in the TLCP phase from about 0.5 to 0.6 and are roughly unchanged beyond this value. In the case of MA-PP, the less pronounced increase in order parameter is observed. This is in good agreement with the increase in modulus of the composite films at a low percentage of compatibilizer. Better molecular orientation in the TLCP phase translates to better mechanical properties of TLCP (16, 23), and hence, to a better composite.

Impact Strength

Results obtained from the impact testing of TLCP/PP composites without and with compatibilizers are illustrated in *Fig. 8*. Break energy in J/m is plotted

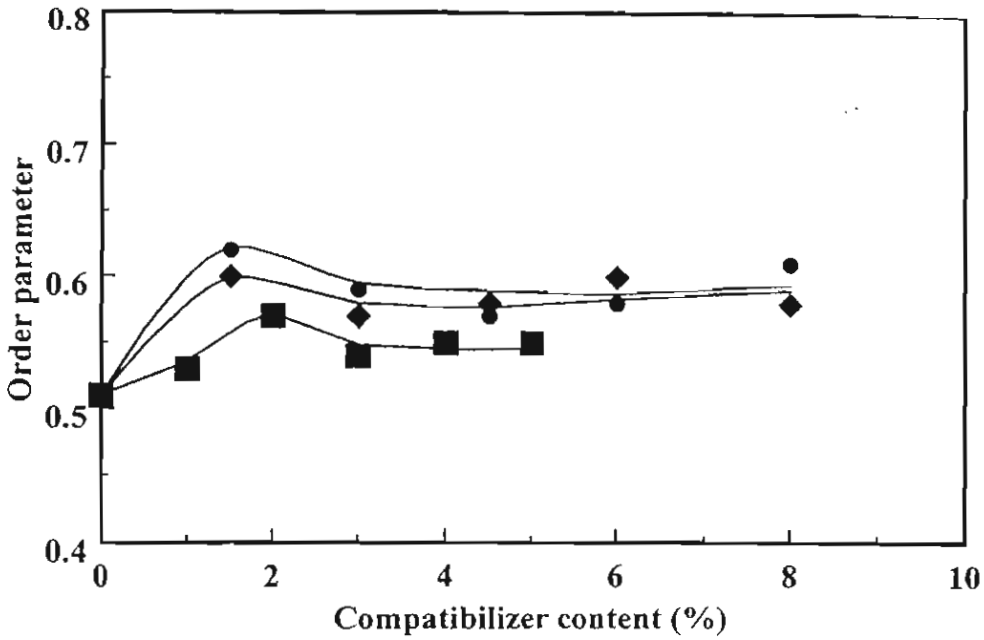

Fig. 7. Order parameter of TLCP phase in TLCP/PP composite films containing ●: SEBS; ◆: MA-SEBS and ■: MA-PP.

against the concentration of compatibilizer in percentage by weight. The composite without a compatibilizer has a very low impact strength (318 J/m) compared with that of pure PP (1,840 J/m). The results suggest poor interfacial adhesion between TLCP and the matrix, which is always a problem with *in-situ* composites. This results show an improvement of impact strength when an elastomeric compatibilizer was added. At a low level of compatibilizer concentration, e.g., up to about 5 wt% SEBS and MA-SEBS, the impact property improves slightly with an increasing amount of compatibilizer. With an 8 wt% compatibilizer, the impact strength increases steeply to about 1,300 J/m, approximately a four-fold increase. A sim-

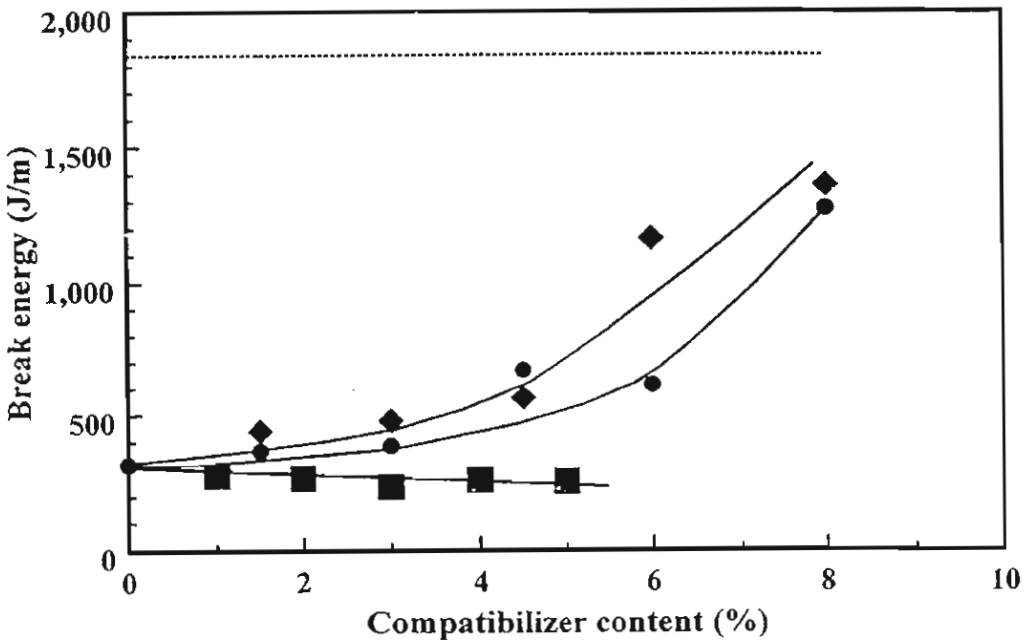

Fig. 8. Effect of compatibilizers of impact strength of TLCP/PP composite films ●: SEBS; ◆: MA-SEBS and ■: MA-PP; dotted line pure PP. Size of error bar is not bigger than twice the size of the symbol.

ilar result was observed by Gupta *et al.* (21, 24) and Setz *et al.* (25) for a PP/SEBS system with no fiber reinforcement. It is concluded that the addition of elastomeric compatibilizers not only improves the tensile modulus but also the impact strength of the composites. This large improvement of impact property at a high concentration of the elastomer may be due to its action as an impact modifier, the mechanism of which was explained in the established rubber-toughening theory (26). Evidently, MA-PP does not show any effect on the impact strength of the composite, since it is a thermoplastic in nature and is unable to absorb impact energy like the rubbery SEBS and MA-SEBS can.

CONCLUSIONS

All three compatibilizers used in this study, namely, SEBS, MA-SEBS, and MA-PP, were found to improve the dispersion and interfacial adhesion of the TLCP phase (Rodrun LC3000) and PP matrix, giving rise to the enhancement of the tensile modulus. In this study, thermoplastic elastomers, SEBS and MA-SEBS, were found to be more effective as compatibilizers than MA-PP. The addition of an elastomeric compatibilizer ehanced the viscosity of the system as evident in the decrease in its melt flow rate, which in turn affected the elongational flow of the dispersed phase to form thinner (and hence, higher aspect ratio) TLCP fibers. Surprisingly, SEBS was found to be a much more effective compatibilizer than MA-SEBS, despite the presence of an MA reactive group that could have improved the interfacial adhesion in the latter. An additional advantage of using an elastomeric compatibilizer is that it could also improve the impact strength of the *in-situ* composite due to its action as an impact modifier.

ACKNOWLEDGMENT

Support of this work by The Thailand Research Fund is gratefully acknowledged. The authors also would like to thank the Shell Chemical Co. for providing SEBS and MA-SEBS, and the Mitsubishi Company for providing MA-PP.

REFERENCES

1. D. Dutta, H. Fruitwala, A. Kohli, and R. A. Weiss, *Polym. Eng. Sci.*, **30**, 1005 (1990).
2. C. S. Brown, and P. T. Alder, in *Polymer Blends and Alloys*, M. J. Folkes and P. S. Hope, eds., Blackie Academic & Professional, Glasgow, Scotland (1993).
3. A. A. Handlos and D. G. B. Baird, *J. M. S. Rev. Macromol. Chem. Phys.*, **C35**, 183 (1995).
4. D. Acierno and A. A. Collyer, eds., *Rheology and Processing of Liquid Crystalline Polymers*, Chapman & Hall, London (1996).
5. G. Kiss, *Polym. Eng. Sci.*, **27**, 410 (1987).
6. H. Verhoogt, H. C. Langelaan, J. van Dam, and A. Postuma de Boer, *Polym. Eng. Sci.*, **33**, 754 (1993).
7. H. Verhoogt, C. R. J. Willems, J. van Dam, and A. Postuma de Boer, *Polym. Eng. Sci.*, **34**, 453 (1994)
8. A. G. C. Machiels, K. F. J. Denys, J. van Dam, and A. P. de Boer, *Polym. Eng. Sci.*, **36**, 2451 (1996).
9. G. Crevecoeur and G. Groeninckx, *Polym. Eng. Sci.*, **33**, 937 (1993).
10. T. C. Hsu, A. M. Lichkus, and I. R. Harrison, *Polym. Eng. Sci.*, **33**, 860 (1993).
11. W. Chinsirikul, T. C. Hsu, and I. R. Harrison, *Polym. Eng. Sci.*, **36**, 2708 (1996).
12. A. Datta and D. G. Baird, *Polymer*, **36**, 505 (1995).
13. H. J. O'Donnell and D. G. Baird, *Polymer*, **36**, 3133 (1995).
14. M. T. Heino, P. T. Hietaoja, T. P. Vainio, and J. V. Seppala, *J. Appl. Polym. Sci.*, **51**, 259 (1994).
15. A. Saupe and W. Z. Maier, *Naturforsch.*, **16a**, 816 (1961).
16. A. Kaito, K. Nakayama, and M. Kyotani, *J. Appl. Polym. Sci.*, **29**, 1321 (1991).
17. M. Kyotani, A. Kaito, and K. Nakayama, *J. Appl. Polym. Sci.*, **47**, 2053 (1993).
18. Y. Seo, S. M. Hong, and K. U. Kim, *Macromolecules*, **30**, 2978 (1997).
19. A. Y. Coran and R. Patel, *Rubber Chem. Tech.*, **56**, 1045 (1983).
20. R Asaletha and S. Thomas, *Rubber Chem. Tech.*, **68**, 671 (1995).
21. A. K. Gupta and S. N. Purwar, *J. Appl. Polym. Sci.*, **31**, 535 (1986).
22. Y. J. Seo, *J. Appl. Polym. Sci.*, **64**, 359 (1997).
23. A. T. Debenedetto, L. Nicolais, E. Amendola, C. Carfagna, and M. R. Nobile, *Polym. Eng. Sci.*, **29**, 153 (1989).
24. A. K. Gupta and S. N. Purwar, *J. Appl. Polym. Sci.*, **29**, 1079 (1984).
25. S. Setz, F.Stricker, J. Kressler, T. Duschek, and R. Muelhaupt, *J. Appl. Polym. Sci.*, **59**, 1117 (1996).
26. C. B. Bucknall, *Toughened Plastics*, Applied Science Publishers, London (1977).

ELSEVIER

Polymer 40 (1999) 2993–2999

polymer

Composite of aramid fibre (poly-*m*-phenylene isophthalamide)-thermoplastic elastomers (SEBS): enhancement of tensile properties by maleated-SEBS compatibiliser

Taweechai Amornsakchai[a], Budsaporn Sinpatanapan[a], Sauvarop Bualek-Limcharoen[a,*], Wiriya Meesiri[b]

[a]*Department of Chemistry, Faculty of Science, Mahidol University, Rama 6 Rd, Bangkok, 10400 Thailand*
[b]*Directorate of Armament, Thai Royal Air Force, Bangkok, Thailand*

Received 23 March 1998; revised 19 May 1998; accepted 24 June 1998

Abstract

Aramid fibre, poly-*m*-phenylene isophthalamide (Teijin-Conex), was used to reinforce thermoplastic elastomer, styrene (ethylene butylene) styrene (SEBS). It was found that the moduli at 100 and 300% elongation of the composite increased linearly with increasing fibre loading. On the other hand, tensile strength of the composites decreased as the fibre content was increased. Improvement of interfacial adhesion was carried out by, first, slightly hydrolysing the fibre with sodium hydroxide solution to increase the number of reactive amino end groups and then mixing with the matrix and compatibiliser, maleic anhydride grafted SEBS (MA-g-SEBS), at various concentrations. Tensile strength of the compatibilised composite was found to increase and then level-off at 5 wt% compatibiliser. Fractured surface of composite containing compatibiliser showed more fibre breakage than the uncompatibilised one. Examination of the extracted fibre revealed that some fraction of rubber was chemically bonded to the fibre surface. These results suggest good compatibilising performance of MA-g-SEBS for the system studied.

Keywords: Poly-*m*-phenylene isophthalamide; SEBS; Composites

1. Introduction

Short fibre reinforced rubber has now received much attention. The main advantage is that it allows greater speed and flexibility in processing as compared with continuous fibre [1]. A high degree of low strain reinforcement can also be achieved at relatively low content of fibre as compared with particulate fillers. Various systems of short fibre reinforced rubbers have been studied. The fibre studied includes Rayon, polyvinyl alcohol, Nylon, *p*-aramid (Kevlar), *m*-aramid (Nomex), polyester and glass fibres [2]. The nature of the fibre determines the interfacial interaction between fibre and matrix and also the strength of the composites. To achieve maximum reinforcement, strong fibre with good interaction with matrix rubber will be needed. As far as mechanical properties are concerned, aramid fibres (Kevlar for example) are good candidates. There is, however, a problem of poor interfacial adhesion between the fibre and a matrix. Various methods have been used to modify the surface of aramid fibre, Kevlar in particular. These include coupling agents [3], ionomer matrix, [4–5] chemical treatments [6–8] and plasma treatment [9–12]. One of the simple chemical treatment techniques reported in the literature is surface hydrolysis [10,13]. The technique allows simple and easy preparation of Kevlar with an increased number of active amino groups on its surface. These functional groups can then be employed in further reaction with other chemicals e.g. reactive or functionalised compatibilisers. The level of achievement depends to a great extent on the matrix studied.

In this paper, a system of poly-*m*-phenylene isophthalamide (Conex) short fibre reinforced styrene (ethylene butylene) styrene (SEBS) thermoplastic elastomer was studied. Thermoplastic elastomer was chosen as a matrix to ease composite preparation and avoid the need for curing used in a conventional rubber system. Conex fibre was first used as-received. In the second part, surface hydrolysis of the

* Corresponding author. Fax: +662-2477050; E-mail: scsbl@mahidol.ac.th

0032-3861/99/$ - see front matter
PII: S0032-3861(98)00524-2

fibre in conjunction with the use of reactive compatibiliser, MA-g-SEBS, was studied.

2. Experimental

2.1. Materials

The materials used in this study were styrene (ethylene butylene) styrene (SEBS, Kraton G 1652), which consisted of 29% styrene with $\bar{M}_w$ S-block = 7200, $\bar{M}_w$ EB-block = 37 500 and maleic anhydride grafted SEBS (MA-g-SEBS, Kraton FG 1901x), which consisted of 29% styrene and contained 1.84 wt% MA. These two thermoplastic elastomers were kindly provided by Shell.

Aramid short fibre, poly-*m*-phenylene isophthalamide (Teijin-Conex) with average length of 3 mm (aspect ratio, i.e. length to diameter ratio is about 200–250) was kindly provided by Teijin Ltd. These materials were dried at 50°C for at least 24 h in a vacuum oven to remove sorbed water before processing.

2.2. Treatment of aramid fibre

Aramid fibres used in this experiment are classified as untreated and treated fibres. As-received fibre was first washed with acetone and distilled water in order to remove the possible surface impurities, such as oil or lubricant, and dried in a vacuum oven. This is called untreated fibre. Then untreated fibre was dispersed in 10 wt% sodium hydroxide solution for 20 min at the ambient temperature. Following the hydrolysis, fibre was thoroughly washed with distilled water to remove excess sodium hydroxide, then washed with toluene, and dried at 50°C in vacuum oven. This will be called treated or hydrolysed fibre. Partial hydrolysis of the aramid fibre with alkaline solution was performed in order to create more chemical reactive $-NH_2$ end groups on the fibre surface, which should enhance the probability to react with the compatibiliser containing maleic anhydride group [14].

2.3. Preparation of composites

Sample weight 50 g of aramid fibre/SEBS at a specified weight ratio was mixed in an internal mixer (Haake Rheocord 90) at 175°C, rotor speed of 90 rpm, for 10 min. In order to obtain better dispersion, dried fibre was first pre-opened in a Moulinex blender for a few seconds then put in the internal mixer and the rotor was operated for half a minute. Thereafter, the compatibiliser was added and blended for half a minute, and finally SEBS was placed and blended further for 9 min. After that, the composite was discharged and passed through a two-roll mill once to obtain a flat sheet then kept in a desiccator at room temperature for 24 h in order to minimize moisture adsorption. The amount of added compatibiliser was 0, 1, 3, 5 and 7 wt% to the composite with the fixed amount of fibre at 3 wt%.

2.4. Characterisation

2.4.1. Mechanical properties

The aramid fibre/SEBS composite was compression moulded into 1-mm thick sheet at 185°C for 10 min and subsequently quenched with water. After being conditioned for at least 24 h, dumbbell-shape tensile specimens were cut with a cutting die of size 115 × 6 mm, parallel to the machine direction (direction passing through the two-roll mill). Testing was performed on an Instron testing machine model 4301 in accordance with ASTM D638 at a cross head speed of 500 mm/min with a full scale load cell at 100 kg. All the values were averages of at least five measurements.

2.4.2. Spectroscopic characterisation

An Infrared Fourier Transform Spectrometer attached with Diffuse Reflectance unit (DRIFT, Perkin Elmer PE 2000) was used to characterise the surface of the fibre before and after surface treatment. The infrared spectrum throughout the range of 4000–600 cm^{-1} was obtained by performing 200 scans at a resolution of 4 cm^{-1}.

2.5. Extraction of composite

The composite was extracted to remove SEBS in a soxhlet apparatus using toluene as a solvent for 72 h. The extracted fibre was collected, dried in a vacuum oven at 50°C and observed under SEM. The aspect ratio of the extracted fibre was measured with the optical microscope and was found to be in the range of 30–80.

2.6. Morphology

The morphology of the fibre surface and fractured surface of the composite was observed under a Scanning Electron Microscope (Hitachi S2500). A thin layer of palladium was coated with Hitachi E102 ion sputter on the specimen to prevent charging on the surface. SEM was operated at 15 kV. The fractured surface of the composites was prepared by freezing the composite in liquid nitrogen and then breaking rapidly above the surface of liquid nitrogen.

3. Results and discussion

3.1. Hydrolysis of aramid fibre surface

In this study, aramid fibre was partially hydrolysed on the surface in order to create more $-NH_2$ and $-COOH$ end

groups, as shown in the following reaction.

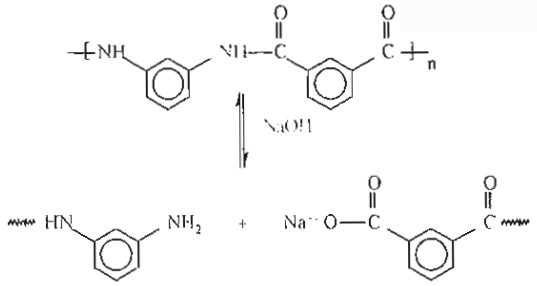

Fig. 1 shows infrared spectra of Conex fibres before and after hydrolysis using DRIFT technique. It can be seen that a new peak appears at 880 cm^{-1} (curve b) after hydrolysis. The peak is associated with the C–H out of plane bending of aromatic ring containing $COO^- Na^+$ substituent similar to that reported by Chatzi et al. [15] for Kevlar fibre. The surface hydrolysis was therefore considered successful.

3.2. Mechanical properties of composites

Stress–strain curves of untreated Conex fibre reinforced SEBS composites with various amounts of fibre content are illustrated in Fig. 2. Most of the curves exhibit similar stress–strain behaviour. For convenience in the discussion, the stress–strain curve will be divided roughly into three regions. In the first region, stress increases linearly with strain. Beyond a certain strain, depending on fibre content, the stress starts to level-off and then, in the third region, rises up sharply. The pronounced rising up of stress in the third region is known as self-reinforcing effect or strain-hardening effect [16–18]. This is a typical behaviour, and often an advantage, of a few elastomers such as natural rubber, styrene butadiene styrene (SBS) rubber and *cis*-polybutadiene.

Pure SEBS (curve a) shows stress–strain curves with all regions. The stress in the first and second regions is lowest among the others. On the other hand, stress in the third region reached a maximum value of almost 30 MPa. Addition of Conex fibre increases the stress in the first and second regions in all specimens. At Conex content up to 3%, the stress–strain behaviour does not significantly change, i.e., the curves still have three regions with strain-hardening effect. At the fibre content of 5 and 7% no more strain-hardening effect is observed. The composites broke at lower strain when higher content of fibre is added.

Fig. 3 shows the tensile properties of untreated Conex composite. It can be seen that tensile moduli at 100 and 300% extension increased with increasing fibre loading but the tensile strength decreased. Elongation at break of the composite was virtually unchanged up to 5 wt% of fibre loading then dropped sharply as the fibre content was further increased.

An enhancement in modulus at both 100 and 300% extension is as expected when fibre of very high modulus is incorporated into the elastomer matrix. At low strain (≤100%) a significant improvement can be clearly seen. Modulus at 100% strain increases almost four-fold when 7 wt% of Conex was incorporated. The level of improvement, however, decreases with increasing strain.

For untreated Conex/SEBS system, the adhesion between fibre and matrix is poor (as will be seen in the next section) and will de-bond at low strain. Therefore, the main mechanism of stress transfer is friction. Upon further straining, voiding at the ends of fibre will be created and crack initiation will start before strain-hardening takes place. Increasing fibre content will increase the number of voids and hence the probability of failure will be higher.

Modification of interfacial interaction was carried out by surface hydrolysis and use of a reactive compatibiliser. The effect of surface hydrolysis alone on mechanical properties of the composites was not found to be significant. Therefore, only surface hydrolysis in conjunction with the compatibiliser will be considered. Effects of MA-g-SEBS on tensile properties of the composite are illustrated in Fig. 4. There is no significant change of modulus at 300% extension as the

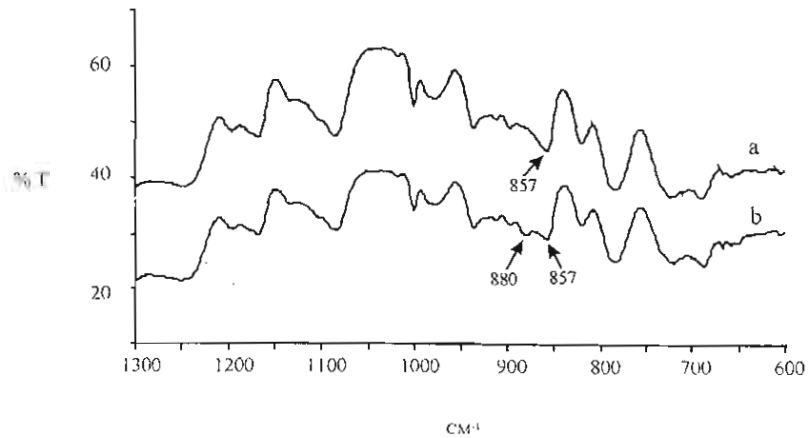

Fig. 1. Infrared spectra of Conex fibres before and after surface hydrolysis.

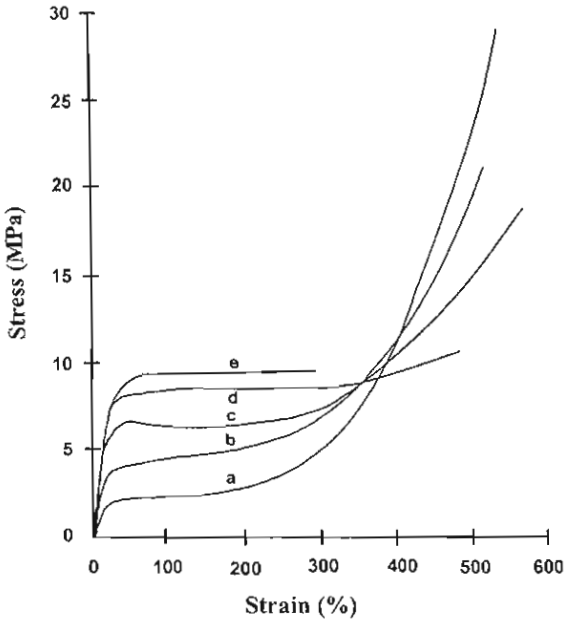

Fig. 2. Stress–strain curves of Conex/SEBS composites at different fibre loading (wt%): (a) 0, (b) 1, (c) 3, (d) 5 and (e) 7.

amount of MA-g-SEBS is increased, whereas the modulus at 100% elongation is slightly decreased when MA-g-SEBS is higher than 3%. No effect of compatibiliser on the elongation at break was observed. A significant improvement in tensile strength with the addition of MA-g-SEBS can be seen in Fig. 4(b). Tensile strength was found to level off at 5 wt% of MA-g-SEBS. The improvement is about 45% over that without MA-g-SEBS. This shows that MA-g-SEBS improves the interfacial adhesion between the fibre and the matrix. Further evidence regarding improved interfacial adhesion will be shown in the next section.

In order to understand the effect of added MA-g-SEBS, the stress–strain curve of the composites will be considered. Fig. 5 shows the stress–strain curves of composites (3 wt% Conex) without and with 3 wt% MA-g-SEBS. It can be seen that the addition of MA-g-SEBS reduced stress in the low strain region. As strain is increased, the tensile stress of the composite with MA-g-SEBS approached that of the composite without MA-g-SEBS. The composite without MA-g-SEBS failed at lower strain, and hence lower tensile strength. From these results, it is postulated that the softer MA-g-SEBS stays preferentially at the matrix–fibre interface (supporting evidence will be shown in the morphology section). Stress transfer through this softer layer will therefore be reduced. At high strain, however, the strain-hardening effect in this type of material comes into play and increases stress transfer. The fact that the composite with MA-g-SEBS failed at higher strain would suggest that interfacial bonding between the matrix and fibre is better. In other words, interfacial de-bonding in the composite with MA-g-SEBS started at higher strain than that in the composite without MA-g-SEBS. As a consequence, an

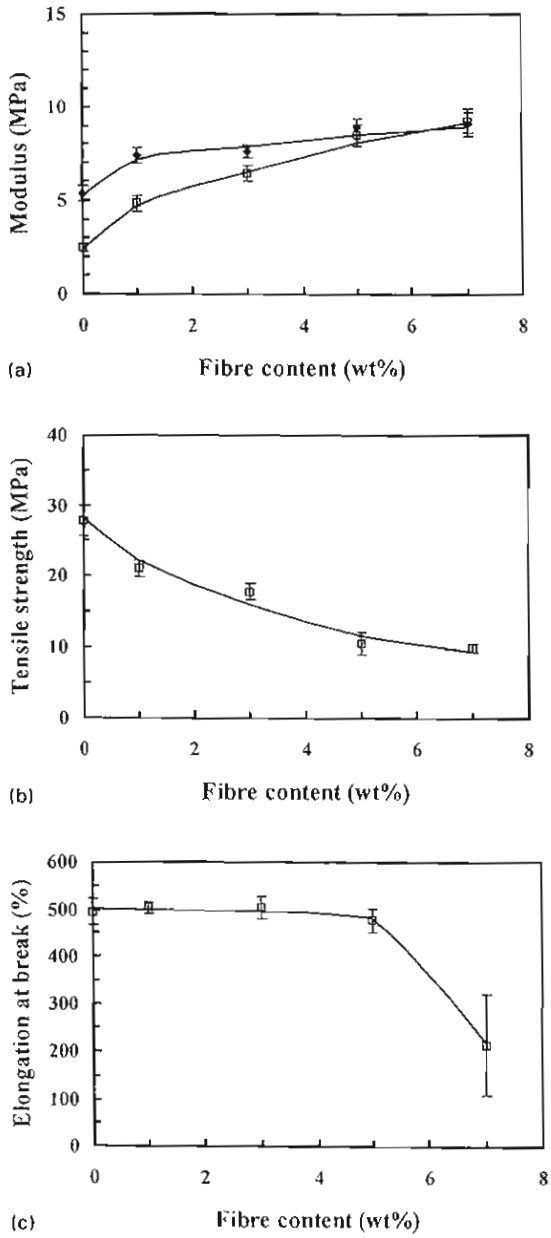

Fig. 3. Tensile properties of untreated aramid fibre/SEBS composite with various fibre loading. (a) Modulus at 100% (□) and 300% (◆) extensions, (b) tensile strength and (c) elongation at break.

improvement in tensile strength was observed in the composite with MA-g-SEBS.

3.3. Morphology

SEM micrographs (at × 2000 magnification) of fractured surface of 3 wt% Conex/SEBS composites without compatibiliser and with 3 wt% MA-g-SEBS are shown in Fig. 6(a) and (b), respectively. Without compatibiliser, fibre pull-out is observed, which indicates poor adhesion at the interface. However, fibre breakage is observed when MA-g-SEBS is added and adhesion of rubber at the base of

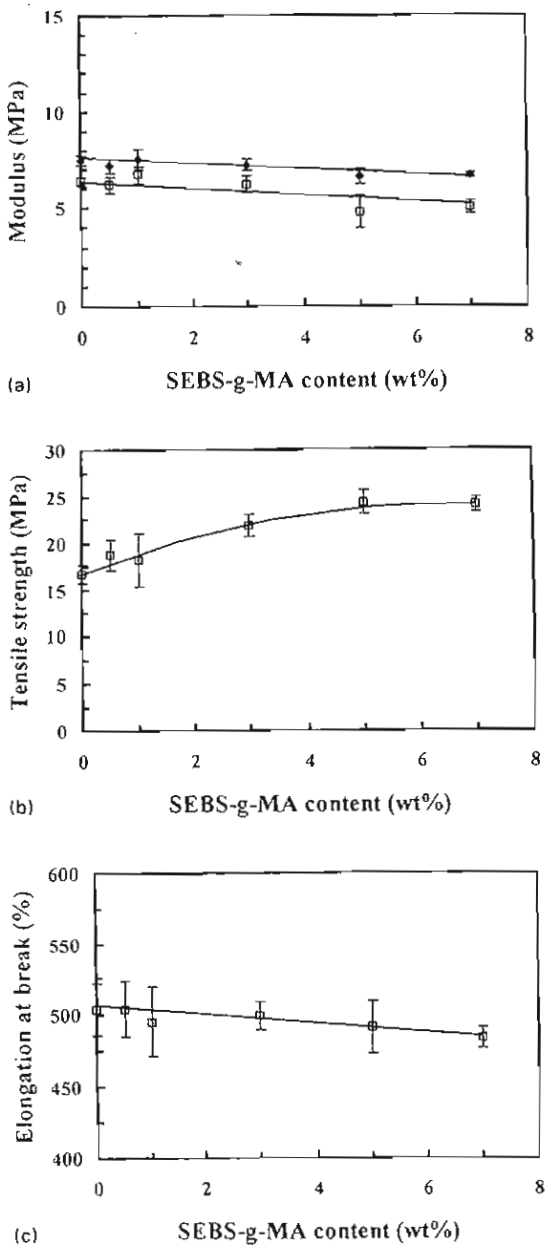

Fig. 4. Tensile properties of treated aramid fibre/SEBS composite with addition of compatibiliser. (a) Modulus at 100% (□) and 300% (♦) extensions, (b) tensile strength and (c) elongation at break.

fibres is observed which suggests the improvement of interfacial adhesion.

SEM micrographs (at ×500 magnification) of solvent extracted fibres from the composites without and with compatibiliser (3 wt% MA-g-SEBS) are presented in Fig. 6(c) and (d), respectively. In the case of the composite without MA-g-SEBS, very clean fibre was obtained after extraction. On the other hand, for the composite with MA-g-SEBS, the extracted fibre showed a rough and irregular surface and also lumps of unextractable rubber.

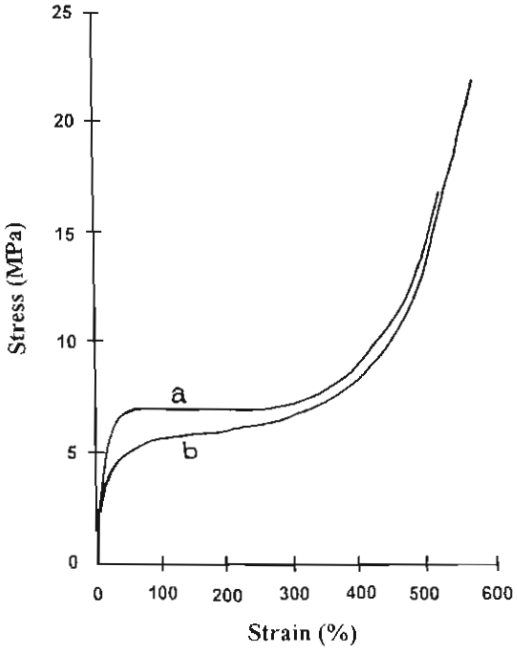

Fig. 5. Stress-strain curves of Conex/SEBS composites with 0 wt% (a), and 3 wt% (b) of MA-g-SEBS.

It is clear, from the above results, that in a system with MA-g-SEBS there are some fractions of rubber which can not be extracted. It is likely that this rubber is chemically bonded to the fibre surface and results in surface irregularity as seen above. This would suggest that MA-g-SEBS reacts with reactive end groups, i.e. $-NH_2$, on the surface of partially hydrolysed Conex fibre and hence the tensile strength of the compatibilised composite is improved.

4. Conclusion

Reinforcement of SEBS thermoplastic elastomer with Conex fibres at low strain can be achieved without any compatibiliser. Modulus of thermoplastic elastomer was enhanced to more than 100% at the fibre content as low as 3 wt%. The strain-hardening effect was found to decrease with increasing fibre loading.

Alkaline hydrolysis of fibre surface in conjunction with reactive compatibiliser, MA-g-SEBS, was found to be effective since this resulted in improvement of the tensile strength. SEM micrographs of the fractured surface revealed a high proportion of fibre breakage. The extracted fibres show patches of unextractable rubber on the surface which is taken as additional evidence for improvement of the bonding at the interface. The results observed in this work suggested good compatibilising effect of MA-g-SEBS for Conex short fibre/SEBS composite. Compared with our previous study on the properties of Kevlar pulp/SEBS system using a similar procedure [19], no improvement was

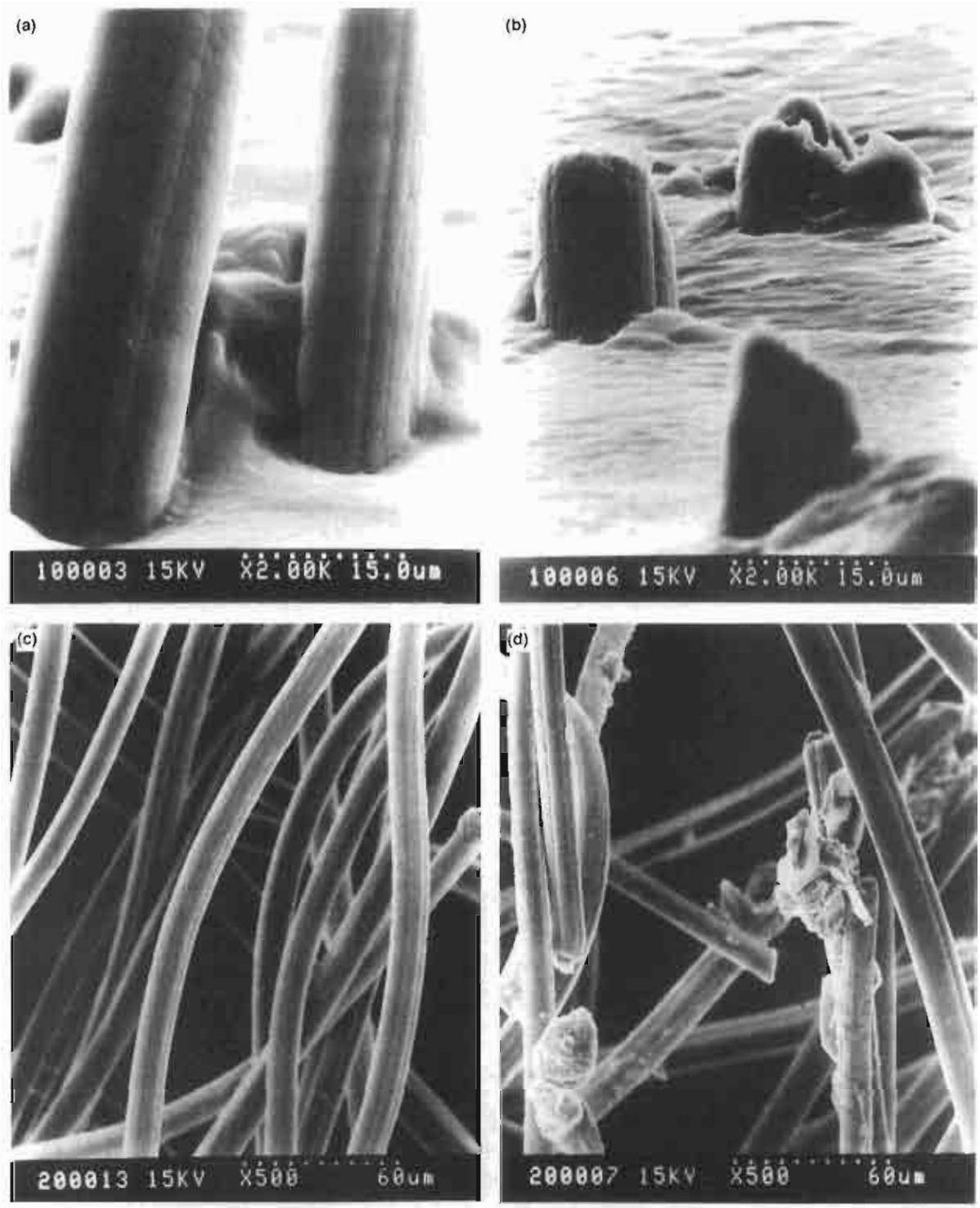

Fig. 6. SEM micrographs of the specimens: (a) fractured surface of the composite without compatibiliser; (b) fractured surface of the composite with 3 wt% MA-g-SEBS; (c) extracted fibres from specimen without compatibiliser; (d) extracted fibres from specimen with 3 wt% of MA-g-SEBS.

observed when MA-g-SEBS was added. In that case, it might be due to fibrillation of pulp during processing, causing the treated surface to peel-off, hence, no improvement of adhesion at the interface can be achieved.

Acknowledgements

Support of this work by The Thailand Research Fund is gratefully acknowledged. The authors also would like to

thank Shell Chemical Co. for providing SEBS and Teijin Ltd for providing Conex fibre.

References

[1] Foldi AP. In: Vigo TL, Kinzig BJ, editors. Composite applications. the role of matrix, fiber, and interface. New York: VCH Publishers, 1992.133–177.
[2] Foldi AP. Rubber Chem Tech 1976;49:379.
[3] Vaughan D. J Polym Eng Sci 1978;18:167.
[4] Takayanaki M, Kajiyama T, Katayose T. J Appl Polym Sci 1982;27:3903.
[5] Takayanaki M, Katayose T. Polym Eng Sci 1984;24:1047.
[6] Breznick M, Banhaji J, Guttmann H, Marom G. Polym Commun 1987;28:55.
[7] Andreopoulos AG. J Appl Polym Sci 1989;38:1053.
[8] Tarantili PA, Andreopoulos AG. J Appl Polym Sci 1997;65:267.
[9] Wang Q, Kaliaguine S, Ait-Kadi A. J Appl Polym Sci 1993;48:121.
[10] Yu Z, Ait-Kadi A, Brisson J. Polym Eng Sci 1991;31:1222.
[11] Sheu GS, Shyu SS. J Adhesion Sci Technol 1994;8:1027.
[12] Brown JR, Mathys Z. J Mater Sci 1997;32:2599.
[13] Garbassi F, Morra M, Occhiello E. Polymer surfaces: from physics to technology. Chichester: Wiley; 1994:251–254.
[14] Modic J, Pottick LA. Polym Eng Sci 1993;33:819.
[15] Chatzi EG, Tidrick SL, Koenig JL. J Polym Sci Part B: Polym Phys 1988;26:1585.
[16] Sperling LH. Introduction to physical polymer science, 2nd ed. Singapore: Wiley, 1993:521–522.
[17] Ward IM. Mechanical properties of solid polymers, 2nd ed. Chichester: Wiley, 1983:74.
[18] Edwards SF, Vilgis Th. Polymer 1986;27:483.
[19] Bualek-Limcharoen S, Nakinpong T, Amornsakchai T, Meesiri W. J Sci Soc Thailand 1997;23:101.

ELSEVIER

Polymer 40 (1999) 6437–6442

polymer

Kevlar reinforcement of polyolefin-based thermoplastic elastomer

Sunan Saikrasun[a], Taweechai Amornsakchai[a], Chakrit Sirisinha[a], Wiriya Meesiri[b], Sauvarop Bualek-Limcharoen[a,*]

[a]*Department of Chemistry, Faculty of Science, Mahidol University, Rama 6 Road, Bangkok 10400, Thailand*
[b]*Directorate of Armament, Royal Thai Air Force, Bangkok, Thailand*

Received 11 August 1998; accepted 24 November 1998

Abstract

Composite systems of Kevlar, poly(*p*-phenylene terephthalamide), and Santoprene, a polyolefin-based thermoplastic elastomer, were studied. Kevlar pulp was used as-received in one system, and modified in the other. The as-received Kevlar pulp was found to reinforce Santoprene to a certain degree. It was found that with increasing amount of Kevlar in the composite, low-strain modulus and tensile strength increased, while the elongation at break decreased sharply. To improve mechanical properties of the composite, hydrolysis of Kevlar pulp surface was employed in conjunction with maleic anhydride-grafted-polypropylene (MA-g-PP), a reactive compatibiliser. It was found that the treated Kevlar pulp greatly improved the low-strain modulus, tensile strength, and elongation at break of the composite. Dynamic mechanical analysis showed that the storage modulus of the Kevlar/MA-g-PP/Santoprene composite was significantly higher than the as-received Kevlar composite. A slight increase in transition temperatures of polypropylene matrix was also observed. As a result of the fact that low-strain modulus and tensile strength of the composite were improved when hydrolysed Kevlar pulp and MA-g-PP were used, it is suggested that such a combination might have increased the interfacial adhesion of the fibre and the matrix, and effective fibre volume fraction, resulting in a better distribution of stress along the reinforcing fibre.

Keywords: Kevlar composite; Santoprene; Polyolefin

1. Introduction

Fibre-reinforced rubber composites have widely been in use for some time, because of their good mechanical properties. Most systems employed continuous fibres because of the vastly improved properties of the composites [1]. Recently, interests have turned to short-fibre reinforced rubbers because of the greater speed and flexibility in processing inherent in these systems. In comparison with particulate-filler composites, a short-fibre reinforced system possesses a high degree of low-strain reinforcement even at relatively low-fibre content. Various studies on short-fibre systems include Rayon, poly(vinyl alcohol), Nylon, *p*-aramid (Kevlar), *m*-aramid (Nomex), polyester, and glass fibres [2]. The degree of reinforcement greatly depends on the nature of the system. The chemical structures of both the fibre and the matrix determine the extent of the interfacial adhesion, and thus the strength of the composites. In order to achieve maximum reinforcement, strong fibre with good compatibility with the matrix is required. As far as mechanical properties are concerned, aramid fibres (e.g. Kevlar) are good candidates as a reinforcement. Although these fibres are not very compatible with the matrix being used, attempts were made to tackle the problem of poor interfacial adhesion in their composites. Various methods include the incorporation of coupling agents [3], the use of ionomer matrix [4,5], chemical [6–8], and plasma treatments [9–12] of the fibre surface. Hydrolysis was reportedly one of chemical treatment techniques, allowing simple and easy modification of Kevlar surface [10,13]. Such treatment increased a number of active amine end groups on the surface, providing functional groups for further reaction with, e.g. a reactive or functionalized compatibiliser.

This article describes a composite system composed of Kevlar pulp, poly(*p*-phenylene terephthalamide), and Santoprene, a polyolefin-based thermoplastic elastomer. The thermoplastic elastomer is used as matrix because of its ease of preparation, with no need of curing, normally used in conventional rubber systems. A hydrolysis of Kevlar pulp, followed by reaction with a reactive compatibiliser are employed.

* Corresponding author. Fax: 00662 2477050.
E-mail address: scsbl@mahidol.ac.th (S. Bualek-Limcharoen)

0032-3861/99/$ - see front matter
PII: S0032-3861(98)00853-2

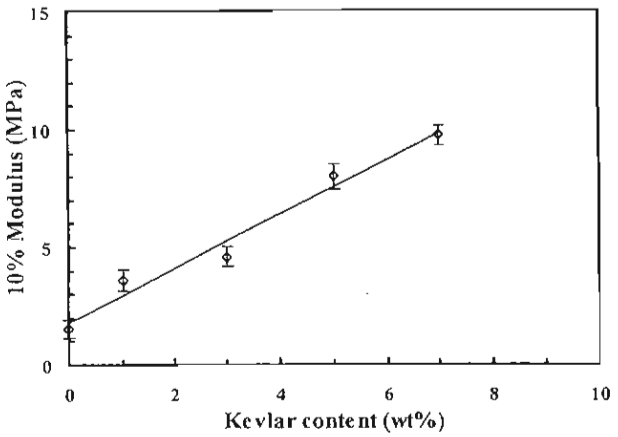

Fig. 1. Modulus at 10% strain of untreated Kevlar/Santoprene composites at various Kevlar content.

2. Experimental

2.1. Materials

The matrix is Santoprene thermoplastic elastomer grade 691-73W175 from Advance Elastomer Systems. The elastomer contains PP 18 wt.%, and EPDM 82 wt.%. Reinforced fibres were Kevlar-49 pulp and short fibre from DuPont. The compatibiliser, maleic anhydride-grafted-polypropylene (MA-g-PP, trade name POLYBOND 3150) was provided by Uniroyal Chemical Co. The compatibiliser contains 0.5 wt.% maleic anhydride and has a melt flow rate of 50 g/10 min.

2.2. Composites preparation

The composites were prepared by melt blending in a miniature internal mixer (Haake Rheocord 90) at a temperature of 165°C and a rotor speed of 90 rpm for 10 min. Kevlar pulp (or short fibre) was pre-opened using a Grinder

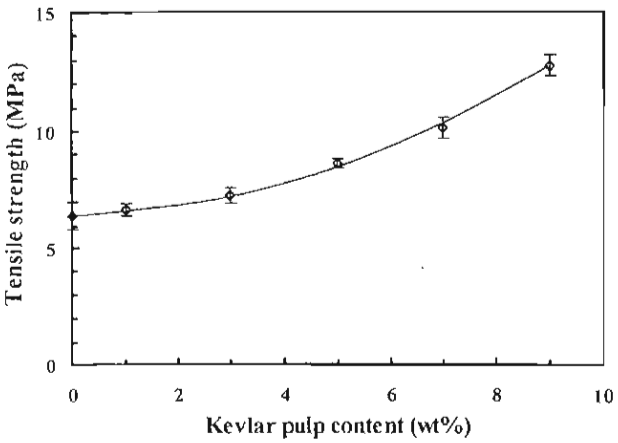

Fig. 2. Tensile strength of untreated Kevlar/Santoprene composites at various Kevlar content.

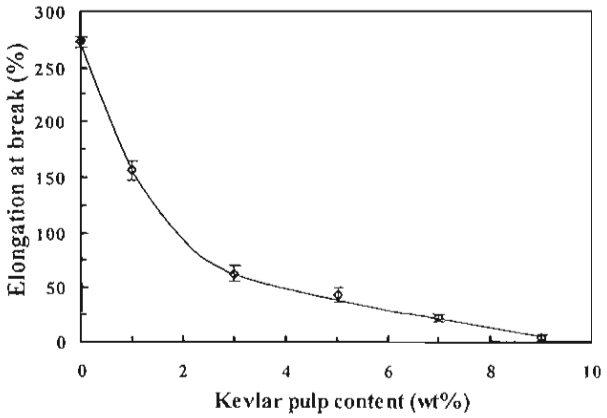

Fig. 3. Elongation at break of untreated Kevlar/Santoprene composites at various Kevlar content.

(Moulinex) with interior blades turning at a high rate of revolution for about 10 s before charging into the mixer. After that the mixture was passed through a two-roll mill once to obtain a flat sheet. The composite sheets were kept in a desiccator in order to minimize moisture adsorption.

2.3. Testing and characterizations

Composite sheets were compression moulded into sheets of 1 mm thickness. The moulding condition was 180°C under a pressure of 15 MPa for 10 min. Later, the mould was transferred to a water cooled press machine. The moulded sheets were kept in a desiccator for at least 24 h.

Dumb-bell-shaped samples were punched out (using Die C-ASTM D412-92) from the moulded sheets in the two-roll mill direction. Tensile properties were measured using an Instron 4301 tensile tester with a crosshead speed of 500 mm/min and a full scale load cell of 100 kg in accordance with ASTM D638. Dynamic properties were measured on Polymer Laboratories DMTA Mk II in bending mode at a frequency of 10 Hz. The sample length was 5 mm and peak to peak displacement was 64 μm. Measurements were carried out from −120°C to 120°C at a scan rate of 5°C/min.

Fracture surfaces of the composites were prepared by freezing the sample in liquid N_2 and breaking it rapidly. The samples were then coated with palladium (Hitachi E102 ion sputter) and observed under scanning electron microscope (SEM) (Hitachi S-2500) using an accelerating voltage of 15 kV.

3. Results and discussion

3.1. Untreated Kevlar pulp composites

Tensile properties of Kevlar/Santoprene composite with varying amount of Kevlar are shown in Figs. 1–3. As the composites with high Kevlar content failed at low elongation, the low-strain modulus was determined and reported

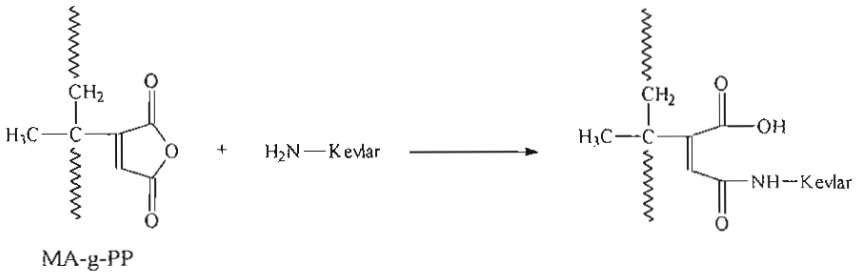

Fig. 4. Reaction between MA-g-PP and the amine group on the Kevlar surface.

here. Fig. 1 shows that stress at 10% extension (10% modulus) increases linearly with Kevlar content. The improvement is slightly above 1 MPa per 1 wt.% Kevlar added. The 10% modulus at 9 wt.% Kevlar could not be obtained as the composite failed before reaching the 10% extension.

Tensile strength as a function of Kevlar loading is shown in Fig. 2. The tensile strength of the composite increases slightly up to 3 wt.% Kevlar, and then more steeply approaches a value of 13 MPa at 9 wt.% Kevlar, an improvement of almost 100%. In this particular system, a minimum value of tensile strength at low-fibre content, or dilution effect [14], was not observed. Although the tensile strength improves significantly, the composite with high Kevlar content lost the extensibility property of the rubber matrix. Fig. 3 shows that elongation at break decreases sharply with increasing Kevlar content at low value, drops off more slowly at higher value, and reaches zero at about 9 wt.% Kevlar.

The aforementioned results suggest that the addition of Kevlar pulp significantly improved the properties of Santoprene, i.e. the modulus and tensile strength increased with increasing Kevlar content. However, the low extensibility at high Kevlar content may be a limiting factor that reduces the usability of the composite. These results, therefore, demonstrated that for a short-fibre reinforced composite, the mechanical properties are very much system dependent. Different results were reported in our previous study on Kevlar pulp/SEBS system in which tensile modulus increased, but tensile strength decreased with increasing Kevlar content [15]. Similar results were also reported in other systems [16–18].

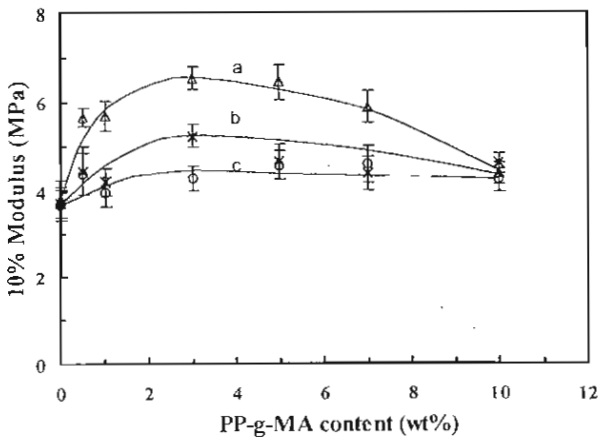

Fig. 5. Modulus at 10% strain of various Kevlar/Santoprene composites: (a) hydrolysed Kevlar/MA-g-PP/Santoprene (△), (b) hydrolysed Kevlar/PP/Santoprene (×), (c) untreated Kevlar/MA-g-PP/Santoprene (○).

3.2. Hydrolysed Kevlar pulp composites

To further our study, a composite system containing 3 wt.% Kevlar was chosen, because of the moderate improvement in modulus and tensile strength over the unreinforced matrix, and also because of the relatively high extensibility of the composite. In our system using Santoprene, a polypropylene-based matrix, MA-g-PP is used as a compatibiliser. The compatibiliser was incorporated in Kevlar pulp by first hydrolysing the fibre surface [10,13,15], introducing amine groups, which then react to form covalent bonds with MA groups of the compatibiliser added (Fig. 4), thus maximizing the compatibiliser efficiency. To compare the two systems, a third system containing hydrolysed Kevlar/polypropylene (PP)/Santoprene was investigated.

Fig. 5 shows curves of 10% modulus as a function of compatibiliser (MA-g-PP or PP) content. Curve a is the hydrolysed Kevlar/MA-g-PP/Santoprene composite with 3 wt.% Kevlar showing a maximum value at about 3 wt.% MA-g-PP, an improvement of about 50% over the untreated Kevlar/MA-g-PP/Santoprene system (curve c). The results of hydrolysed Kevlar/PP/Santoprene composite is shown in curve b, where modulus was only slightly improved.

Fig. 6 shows curves of tensile strength as a function of compatibiliser content. The hydrolysed Kevlar/MA-g-PP/Santoprene composite (curve a) shows the highest value of about 30% improvement at about 1 wt.% MA-g-PP, which levels off at higher MA-g-PP content. The addition of MA-g-PP and PP to the untreated and hydrolysed Kevlar composites, respectively, had no effect on tensile strength (curves b and c).

Fig. 7 shows curves of elongation at break (%EB) as a function of compatibiliser content. The hydrolysed Kevlar/MA-g-PP/Santoprene composite (curve a) shows an increase in %EB with increasing MA-g-PP content. At 3 wt.% MA-g-PP, where a maximum in 10% modulus was

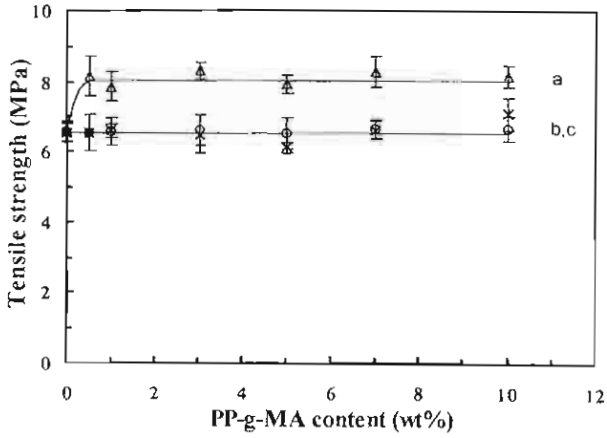

Fig. 6. Tensile strength of various Kevlar/Santoprene composites; (a) hydrolysed Kevlar/MA-g-PP/Santoprene (△), (b) hydrolysed Kevlar/PP/Santoprene (×), (c) untreated Kevlar/MA-g-PP/Santoprene (○).

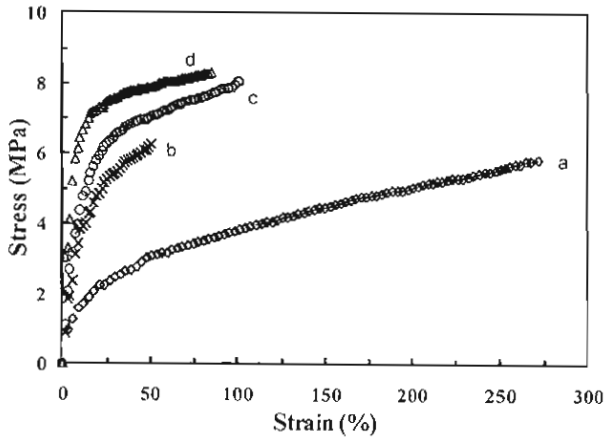

Fig. 8. Stress–strain curves of various Kevlar/Santoprene composites: (a) Santoprene, (b) 3 wt.% untreated Kevlar/Santoprene, (c) 3 wt.% hydrolysed Kevlar/3 wt.% PP/Santoprene, (d) 3 wt.% hydrolysed Kevlar/3 wt/% MA-g-PP/Santoprene.

obtained, an improvement in %EB is about 30% over that of the other two systems. The systems of untreated Kevlar/MA-g-PP/Santoprene and hydrolysed Kevlar/PP/Santoprene show no change in %EB.

From the results of these three composite systems shown in Figs. 5–7, it can be concluded that the presence of both the MA group on polypropylene chain and the amine groups on Kevlar surface are essential for the improvement of the mechanical properties.

Mechanical properties of Kevlar/Santoprene composite systems are summarized as stress–strain curves in Fig. 8. Santoprene with no reinforcement shows the highest strain at break as expected (curve a). The addition of 3 wt.% of Kevlar (untreated) to Santoprene caused a steep rise of stress and a break at a very low strain (about 50%) as shown in curve b. The 3 wt.% hydrolysed Kevlar/3 wt.% PP/Santoprene system shows an even steeper rise in stress and a break at higher strain (about 100%EB) shown in

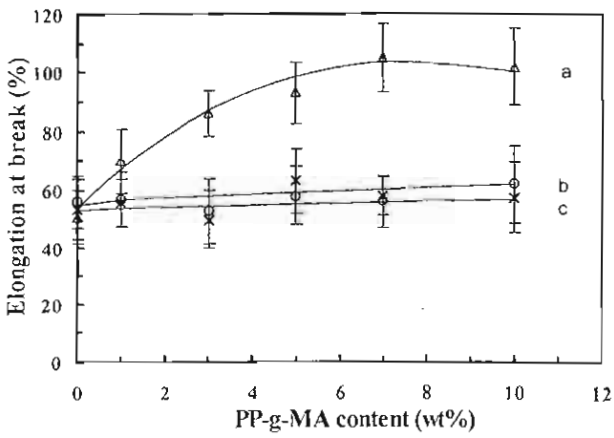

Fig. 7. Elongation at break of various Kevlar/Santoprene composites; (a) hydrolysed Kevlar/MA-g-PP/Santoprene (△), (b) hydrolysed Kevlar/PP/Santoprene (×), (c) untreated Kevlar/MA-g-PP/Santoprene (○).

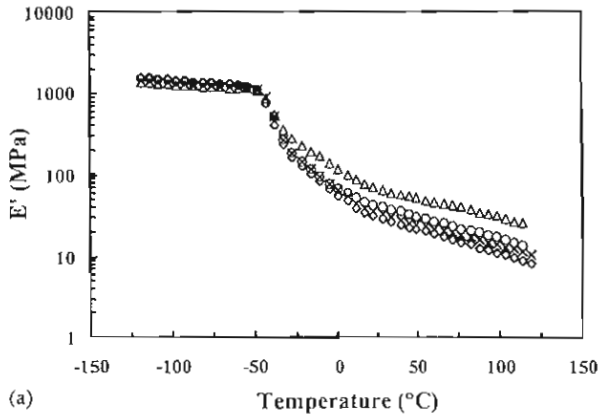

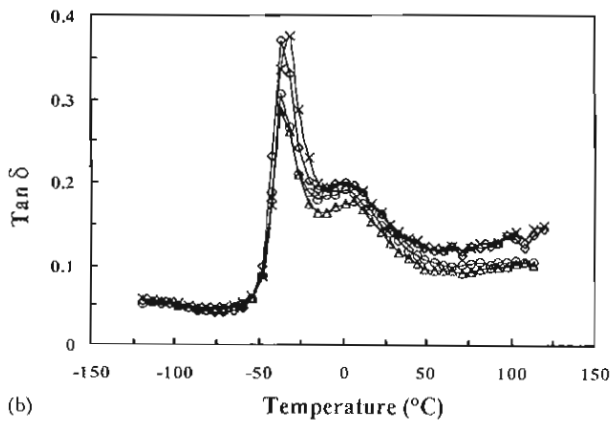

Fig. 9. (a) Storage modulus (E') and (b) tan δ of various Kevlar/Santoprene composites: 3 wt.% hydrolysed Kevlar/3 wt/% MA-g-PP/Santoprene (△), 3 wt.% untreated Kevlar/Santoprene (×), 3 wt.% hydrolysed Kevlar/3 wt.% PP/Santoprene (○), Santoprene (◇).

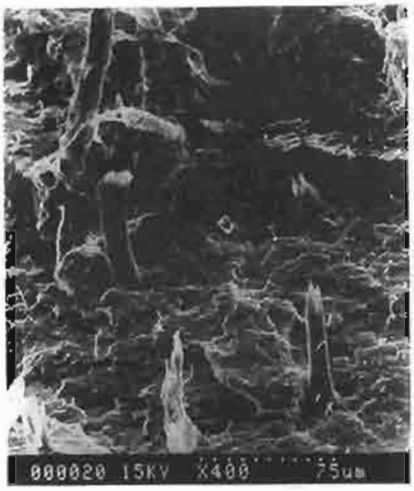

(a)

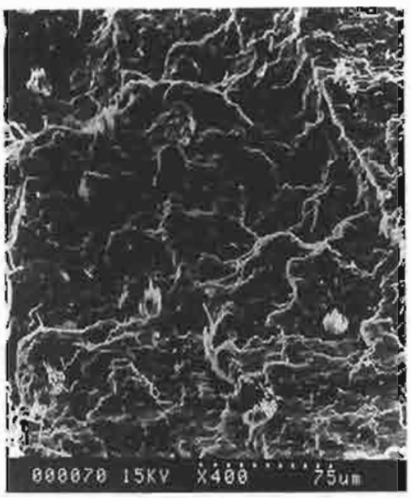

(b)

Fig. 10. SEM micrographs of fractured surfaces of (a) 3 wt.% untreated Kevlar/Santoprene composite and (b) 3 wt.% hydrolysed Kevlar/3 wt.% MA-g-PP/Santoprene composite.

curve c. The steepest rise and maximum value in stress (breaks at about 80% EB) found in the 3 wt.% hydrolysed Kevlar/3 wt.% Ma-g-PP/Santoprene system are shown in curve d. The results suggest that bonding through the reaction of MA groups grafted on PP with amine groups on Kevlar surface is the main factor improving the mechanical properties of Kevlar/Santoprene system.

In order to gain further information regarding the effect of MA-g-PP on interfacial adhesion of the composite, dynamic tests at various temperatures were conducted and summarized in Fig. 9. Storage modulus as a function of temperature is shown in Fig. 9(a). All materials have about the same values of storage modulus from −120°C to −50°C, but start to decay off at different rates from this point up to the end temperature of 120°C. It is shown that the hydrolysed Kevlar/MA-g-PP/Santoprene composite has the highest storage modulus over the whole temperature range, while the other two composite systems show relatively same values and Santoprene (control) shows the lowest value.

Fig. 9(b) shows curves of tan δ vs. temperature for Santoprene and all composites under study. The peaks at about −40°C are associated with the glass transitions of the EPDM part, and those at about 0°C with the PP part of Santoprene. It is shown that the PP peak shifts slightly to higher temperature and decreases to lower height in hydrolysed Kevlar/MA-g-PP/Santoprene system. The results suggest that PP chains are constrained by the compatibiliser as reported earlier [4]. Such a constraint is likely to occur at Kevlar/Santoprene interface, leading to better transfer of stress from the PP chains to the reinforcing Kevlar and resulting in the improvement of both the dynamic and tensile moduli. In other words, better stress transfer increases the effective fibre volume fraction and leads to composites with higher moduli.

Fig. 10 shows SEM micrographs of fractured surfaces of untreated Kevlar/Santoprene (Fig. 10(a)) and hydrolysed Kevlar/MA-g-PP/Santoprene (Fig. 10(b)). The untreated Kevlar composite shows a number of fibre pull-outs, while the hydrolysed Kevlar/MA-g-PP/Santoprene composite shows a rather smooth surface with no evidence of fibre pull-out. It appears that only the fractured fibres are seen. The results suggest an improved interfacial adhesion provided by the latter system.

Bonding of MA-g-PP and the amine group on Kevlar surface could not be directly investigated. An attempt was made to study what may remain on the Kevlar surface after solvent extraction of the elastomer matrix. However, a difficulty was encountered as the elastomer matrix did not dissolve in any available solvents because of the cross-linked EPDM part in Santoprene.

4. Conclusion

A system of Kevlar/Santoprene composite was studied. It was found that Kevlar pulp with no treatment can be used to reinforce Santoprene. However, the use of hydrolysed Kevlar and a small amount of MA-g-PP, a reactive compatibiliser, can significantly improve the modulus, tensile strength, and elongation at break of the composite. The results suggest the reaction between the MA groups on MA-g-PP, and the free amine groups on the hydrolysed surface of Kevlar, thus modifying the highly polar surface of Kevlar into a non-polar polypropylene surface. The non-polar modified fibre is expected to be miscible and be able to co-crystallize with polypropylene-containing Santoprene matrix, leading to a better stress transfer from the matrix to the reinforcing fibre.

4.6

Improvement of Interfacial Adhesion of Poly(*m*-phenylene isophthalamide) Short Fiber–Thermoplastic Elastomer (SEBS) Composites by N-Alkylation on Fiber Surface

ANONGNUCH CHANTARATCHAROEN[1], CHAKRIT SIRISINHA,[1] TAWEECHAI AMORNSAKCHAI,[1] SAUVAROP BUALEK-LIMCHAROEN,[1] WIRIYA MEESIRI[2]

[1] Department of Chemistry, Faculty of Science, Mahidol University, Rama 6 Road, Bangkok 10400, Thailand

[2] Directorate of Armament, Royal Thai Air Force, Bangkok 10210, Thailand

Received 23 November 1998; accepted 9 March 1999

ABSTRACT: A composite of short-fiber, poly(*m*-phenylene isophthalamide), and thermoplastic elastomer styrene (ethylene–butylene) styrene (SEBS), was investigated. The fiber surface was modified by N-alkylation (heptylation and dodecylation) to improve their compatibility with a less polar SEBS matrix. Observation of fiber-surface morphology by SEM revealed surface roughness after N-alkylation. Nearly complete coating of the polymer matrix on the fiber was observed on a fractured surface of the composite, which is evidence for the improvement of fiber–matrix adhesion. It was found that the modulus of the composites grew with increasing fiber loading to approximately the same extent for both unmodified and modified fiber composites. Tensile strength of the modified fiber composites was found to improve significantly over that of the unmodified fiber composite. This suggests that the presence of the alkyl group on the fiber surface is responsible for an improvement of interfacial adhesion. © 1999 John Wiley & Sons, Inc. J Appl Polym Sci 74: 000–000, 1999

Key words: short-fiber composite; aramid; poly(*m*-phenylene isophthalamide) thermoplastic elastomer; SEBS

INTRODUCTION

Aramid short fibers such as poly(*p*-phenylene terephthalamide) (under the trade name of Kevlar by Du Pont Co.) and poly(*m*-phenylene isophthalamide) (under the trade name of Nomex by Du Pont Co. or the trade name of Conex by Teijin Co. Ltd.) are important as reinforcing fibers for plastics and elastomers due to their high strength, good thermal stability, sufficient flexibility, and light weight. However, the problem of fiber dispersion in the matrix often arises due to inertness of the fiber surface and the agglomeration of fibers due to hydrogen bonding. In order to overcome this problem, chemical or physical bonding between the fiber and the matrix is usually introduced through the addition of a suitable coupling agent[1–2] or chemical modification of the fiber surface.[3–6] Plasma treatment has also been used to create a functional group on Kevlar and hence to provide bonding with the matrix.[7–10]

One chemical method used to modify the surface of aramid fiber is the metalation reaction of the fiber surface to form polyanions, which is then followed by reaction with some functional groups or the grafting of suitable polymer segments.[11–15]

Short-fiber reinforced thermoplastic elastomers have recently gained much attention due to their attractive properties.[16–17] The advantages of thermoplastic elastomers are ease and economy in processing, high strength, and rigid-

Correspondence to: S. Bualek-Limcharoen (scsbl@mahidol.ac.th).

Journal of Applied Polymer Science, Vol. 74, 000–000 (1999)
 CCC 0021-8995/99/000000-00

ity and recyclability, but some of their disadvantages are low thermal and low-dimensional stability at elevated temperatures. Incorporation of short fibers with high thermal stability and high strength, such as aramid fibers, in order to enhance dimensional stability is therefore interesting. We have investigated a system of poly(*m*-phenylene isophthalamide) (Conex) short-fiber reinforced styrene (ethylene–butylene) styrene (SEBS) thermoplastic elastomer composite. An improvement of interfacial adhesion of this composite system by partial hydrolysis on the fiber surface and the addition of a reactive compatibilizer, maleic anhydride–grafted SEBS, was reported.[18] In this study another method of surface treatment was carried out by N-alkylation to reduce the interaction through hydrogen bonding between fibers and to reduce the polarity of the highly polar surface. The alkyl groups on the fiber surface are expected to be compatible with the EB block in the SEBS matrix, which should facilitate the enhancement of interfacial adhesion and therefore will result in the improvement of tensile properties of the composite.

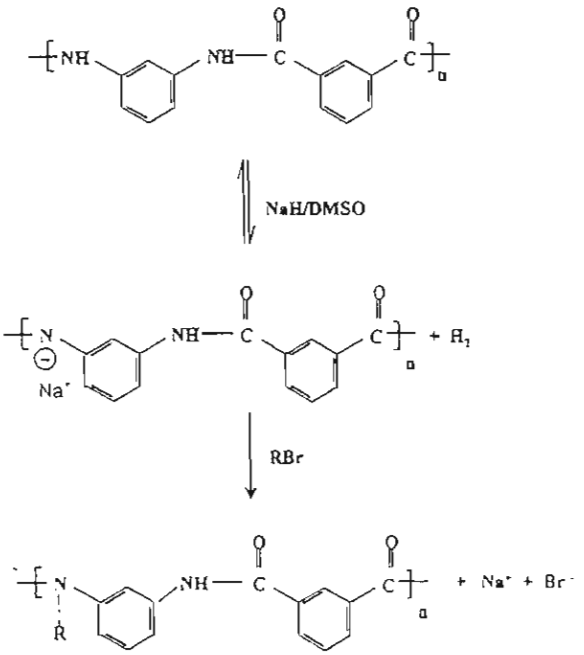

Figure 1 N-alkylation reaction on poly(*m*-phenylene isophthalamide) (Conex) short fiber.

EXPERIMENTAL

Materials

Materials used in this study were a styrene (ethylene–butylene) styrene block copolymer (SEBS, Kraton G1652), provided by Shell chemical Co. Ltd., with 29% styrene content as thermoplastic elastomer matrix, and poly(*m*-phenylene isophthalamide), Teijin-Conex, provided by Teijin Co. Ltd. in the form of short fibers with an approximate length of 3 mm and a diameter of 12–15 μm. The fibers were first washed with acetone, followed by distilled water to remove possible contamination, and they were then dried at 5°C to a constant weight in a vacuum oven. Anhydrous dimethyl sulfoxide (DMSO) and alkyl bromides were used as received. Sodium hydride (60% suspension in paraffin oil) was washed three times with dried hexane before use.

Surface Modification of Conex Fiber by N-alkylation

The technique used for N-alkylation of Conex fibers was similar to that reported earlier by Takayanagi et. al.[11] The reaction scheme is presented in Figure 1. Since only slight modification on the fiber surface is needed, a small amount of the reagents and short reaction times were employed. In the first step, i.e. a metalation reaction, about 1,000 mL of anhydrous DMSO and 0.05 mol of purified NaH were reacted for 40 min at 70°C in a nitrogen atmosphere. After cooling to 30°C, 30 g of fiber were added into the reactor and stirred mechanically for 10 min. At this stage, the skin color of the fiber changed from off-white to pale yellow. Then about 0.25 mol of heptyl bromide was added and stirred for a further 3 h. The reaction was stopped by transferring the fibers into a large quantity of distilled water. The products were washed with acetone and water several times and dried at 60°C to a constant weight in a vacuum oven. For dodecylation, only 0.025 mol of NaH was used; otherwise the resulting fibers became hard and stuck together, and hence were difficult to disperse in the matrix.

The alkyl group on the fiber surface was characterized by Fourier transform infrared (FTIR) spectroscopy recorded on a Perkin-Elmer PE2000 spectrometer using diffuse reflectance accessory (DRIFT). Two hundred scans at a resolution of 2 cm^{-1} were performed to obtain a good spectrum.

Preparation of Composites

The composites were prepared by a melt blending technique, using a laboratory-size internal mixer (Haake Rheomix 90) at the set temperature of 175°C at a rotor speed of 90 rpm. To obtain good

dispersion, the fiber was first preopened in a Moulinex blender for a few seconds, then put in the mixing chamber in which the rotor was operated for 30 sec before the SEBS was added. After mixing for 10 min, the composite was discharged from the mixer and immediately rolled into a single sheet using a small laboratory two-roll mill. The composite sheet was then compression molded into a sheet 2 mm thick under a pressure of 15 MPa at 180°C for 10 min. The molded sheets were kept in a desiccator for 24 h prior to tensile measurement.

Fiber loading was varied from 0 to 7% by weight. We studied low-fiber content composites so as to maintain an important property of elastomers—their high percentage of extension. Another reason for studying such composites is that at low-fiber concentration, there is less of a problem of fiber agglomeration, so we can evaluate the results by focusing only on the effect of adhesion at the interface.

Measurement of Tensile Properties

The composite sheets were cut into dumbbell-shaped specimens with a cutting die of size 115 × 6 mm, parallel to the direction passing through the two-roll mill. According to ASTM D638, tensile properties were measured using an Instron 4301 tensile tester with a cross-head speed of 500 mm min^{-1} and a full-scale load cell of 100 kg. All values presented were averages of at least five measurements.

Morphology Study

A scanning electron microscope (SEM, Hitachi S-2500) was utilized to characterize the surface morphology of Conex short fibers before and after modification, as well as the fractured surface of composites. The fractured surfaces of the composites were prepared by freezing the sample in liquid N_2 and breaking it rapidly. The samples were then coated with palladium (Hitachi E102 ion sputter) and observed using an accelerating voltage of 15 kV.

RESULTS AND DISCUSSION

N-Alkylation of Conex Fiber Surface

In this study, the aramid (Conex) fiber surface was modified by a deprotonation reaction with NaH in DMSO, followed by N-alkylation.

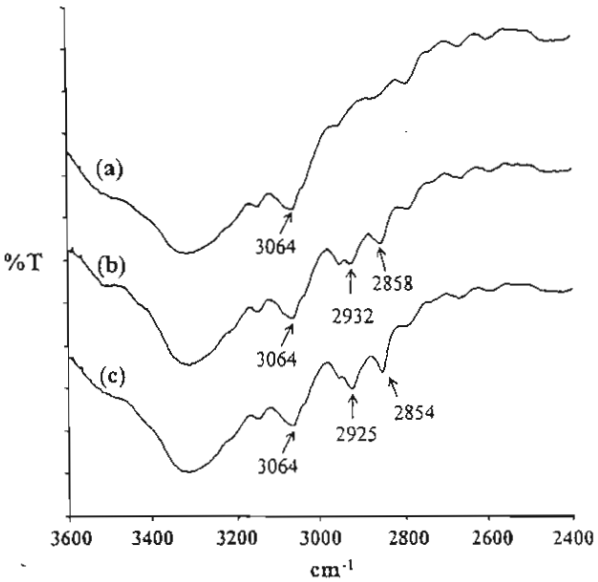

Figure 2 Infrared spectra (DRIFT) of (a) unmodified, (b) heptylated, and (c) dodecylated Conex fibers.

Infrared spectra of unmodified, heptylated, and dodecylated Conex fibers are presented in Figure 2 as curves a, b, and c, respectively. The C—H F2 stretching vibration peaks at 2,858 and 2,932 cm^{-1} are of the heptyl group, the peaks at 2,854 and 2,925 cm^{-1} are of the dodecyl group, and the N—H stretching peak appears in all spectra at 3,064 cm^{-1}. Therefore, the partial N-alkylation on the fiber surface is considered successful.

SEM micrographs demonstrating surface morphology of the fibers before and after modification are shown in Figure 3. The surface of controlled F3 fiber (unmodified) shown in Figure 3(a) is relatively smooth. Figure 3(b) shows the fiber taken from the reaction just after deprotonation for 10 min, that is, without alkyl groups on the surface, still shows a relatively smooth surface. It is seen that the ionization step does not affect the appearance of the fiber surface. In contrast, heptylated and dodecylated fibers exhibit high surface roughness, as shown in Figures 3(c,d), respectively. Takayanagi et al.[11] reported that deprotonated and N-heptylated Kevlar were soluble in DMSO. In our case, the Conex fiber surface was only partially deprotonated and then N-alkylated. During the alkylation reaction time of 3 h, some parts of modified fiber surface might be swollen in DMSO. When the reaction had been terminated with distilled water, the swollen parts might redeposit on the fiber surface and hence might cause the surface roughness as seen in Figure 3(c,d). Apart from the expected compatibility of the alkyl group and the EB block in the SEBS

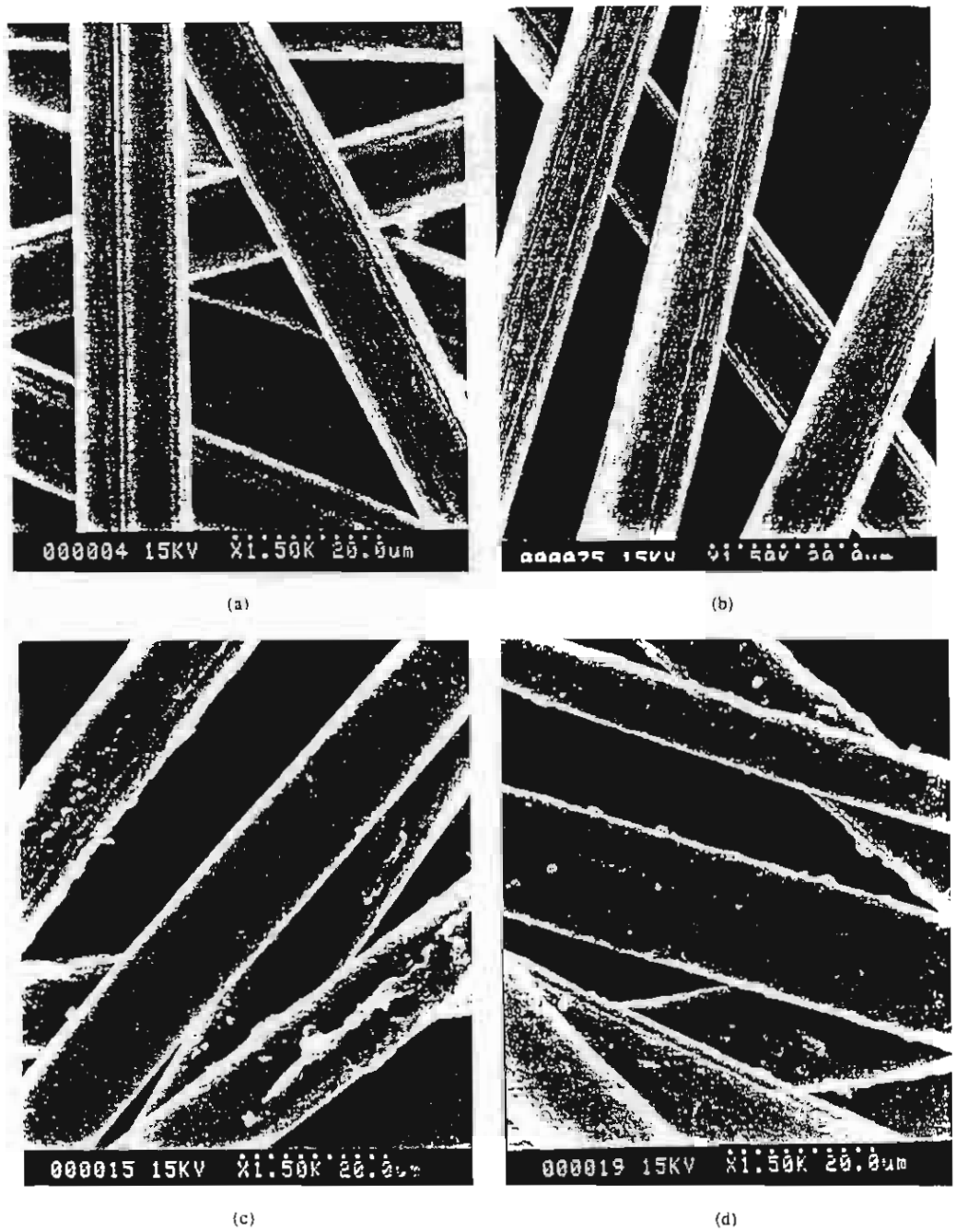

Figure 3 SEM micrographs of various Conex fibers (a) unmodified, (b) deprotonated, (c) heptylated, and (d) dodecylated Conex fiber.

matrix, this surface roughness of the alkylated Conex fibers will, in theory, also enhance the interfacial bonding between the fibers and polymer matrix via a physical interlocking or a friction mechanism.

Mechanical Properties of Composites

Plots of tensile properties of the composites containing unmodified and alkylated fibers—i.e., 100% modulus, 300% modulus, tensile strength, and elongation at break as a function of fiber loading—are shown in Figures 4–7, respectively. F7 The values of modulus at 100% and 300% extensions (Figs. 4 and 5, respectively) increase almost linearly with fiber loading at approximately the same extent for composites filled with unmodified and modified fibers. The increase in modulus of the composites with an increasing amount of fiber

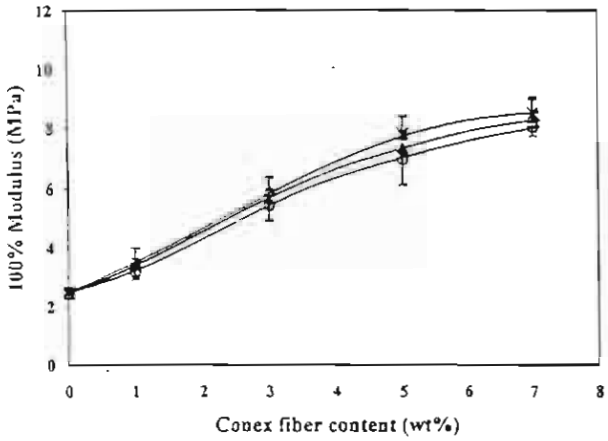

Figure 4 Tensile modulus at 100% strain versus fiber content of composites with (a) unmodified (Δ), (b) hetylated (X), and (c) dodecylated (O) Conex fibers.

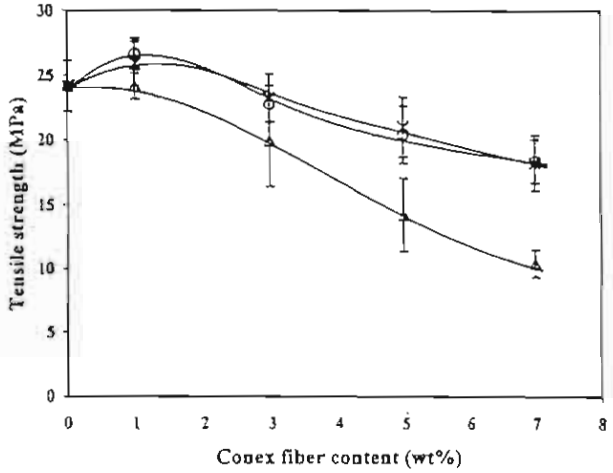

Figure 6 Tensile strength versus fiber content of composites containing (a) unmodified (Δ), (b) hetylated (X), and (c) dodecylated (O) Conex fibers.

is mainly a result of the modulus of Conex fibers, which is far greater than that of SEBS. The higher the fiber loading is, the larger the volume fraction of high-modulus phase and thus the greater will be the bulk modulus of the composites. It can be seen that the tensile modulus is not affected significantly by N-alkylation at low-fiber loading. A slight improvement in 300% modulus is observed at 7 wt % fiber loading. Tensile strength is decreased, however, with increasing fiber loading due to the dilution effect of the matrix (see Fig. 6). However, the tensile strength of N-alkylated Conex composites is significantly higher than that of the composite filled with the unmodified fiber, particularly at high-fiber loading. At 7 wt % fiber loading, tensile strength of N-alkylated fiber-filled composites (18 MPa) is about 80% higher than that of the composite with unmodified fiber (10 MPa). On the other hand, elongation at break, shown in Figure 7, is only slightly decreased with increasing fiber loading. A slight increase of elongation at break is observed for N-alkylated fiber-filled composites, particularly at higher fiber content. No effect of the length of the alkyl groups on tensile properties of the composites can be noticed. The remarkable enhancement in tensile strength might be due to an increase in interfacial adhesion between fiber and polymer matrix via improvement of the com-

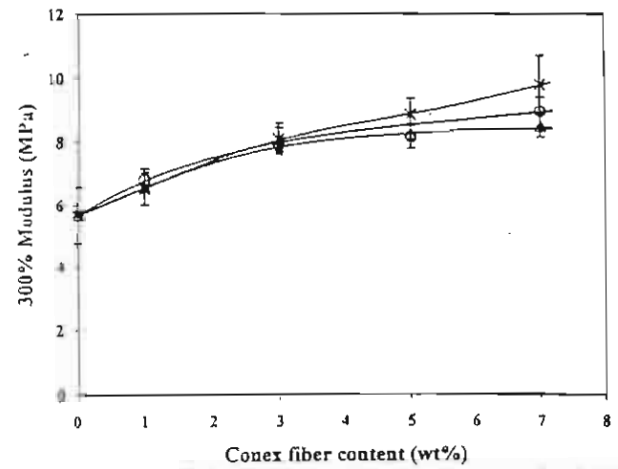

Figure 5 Tensile modulus at 300% strain versus fiber content of composites containing (a) unmodified (Δ), (b) hetylated (X), and (c) dodecylated (O) Conex fibers.

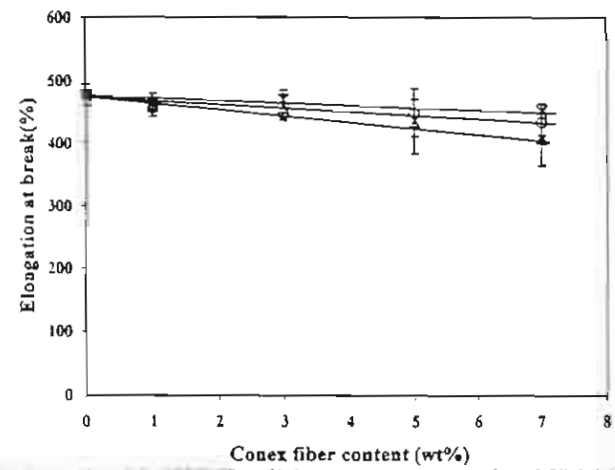

Figure 7 Elongation at break versus fiber content of composites containing (a) unmodified (Δ), (b) hetylated (X), and (c) dodecylated (O) Conex fibers.

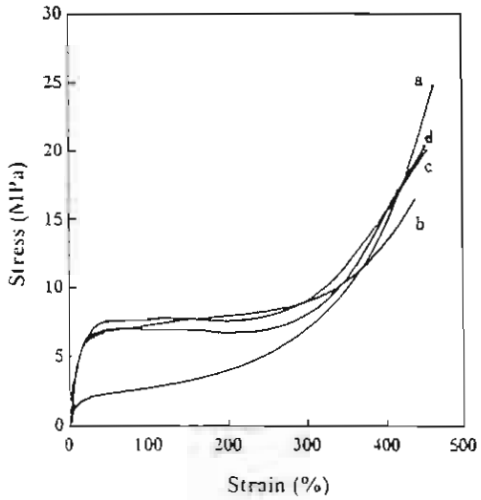

Figure 8 Stress–strain behavior of (a) neat SEBS, (b) 5 wt % unmodified Conex–SEBS, (c) 5 wt % heptylated Conex–SEBS and (d) 5 wt % dodecylated Conex–SEBS composites.

patibility between the alkyl group on the fiber surface and the EB block in SEBS matrix. In other words, the alkyl groups could assist the wetting of the fiber by the matrix. In addition, the bonded clumps on the surface could help enlarge the contact area between the fibers and the polymer matrix and hence enhance their interfacial bond strength. The evidence for improvement of adhesion at the interface can be clearly seen in SEM micrographs of fractured surfaces illustrated in the next section.

For comparison, the stress–strain behavior of unfilled SEBS and composites containing 5 wt % of unmodified and modified fibers is illustrated in Figure 8. It can be seen clearly that the unfilled SEBS (curve a) possesses the lowest tensile modulus at low strain and shows a strain-hardening effect (strain crystallization) at high strain. The thermoplastic elastomer SEBS exhibits similar behavior as a conventional strain crystallizing rubber due to the strong intermolecular interaction between the chains in the hard phase.[17] Obviously, the strain hardening of SEBS decreases, causing tensile strength to decrease, as 5 wt % of unmodified fiber is added (curve b). This is due to the dilution effect of the matrix, and the high-stress concentration at the fiber ends destroys adhesion at the interface. As heptylated and dodecylated fibers are incorporated (curves c and d), strain crystallization increases again, this is, tensile strength becomes higher than that of the composite with unmodified fiber. Since the stress–strain curves rise steeply near the break point, the elongation at break is therefore not much affected.

Morphology of Composites

To obtain more information on the effect of fiber surface, the composites were studied using SEM. The micrographs of fractured surfaces of compos-

(a)

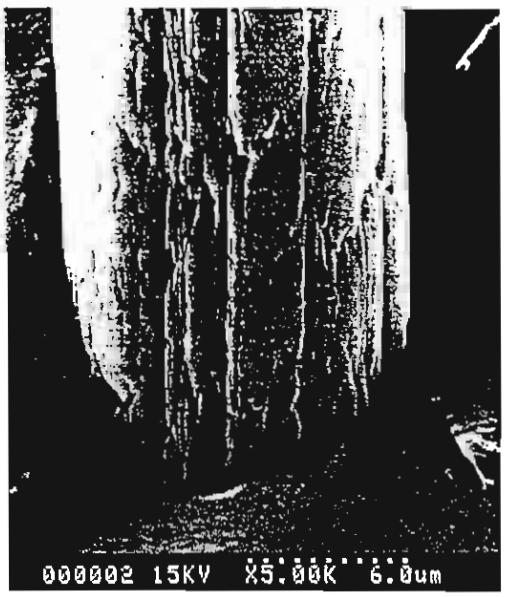

(b)

Figure 9 SEM micrographs of fractured surface of unmodified Conex composite at magifications of (a) ×200 and (b) ×5,000.

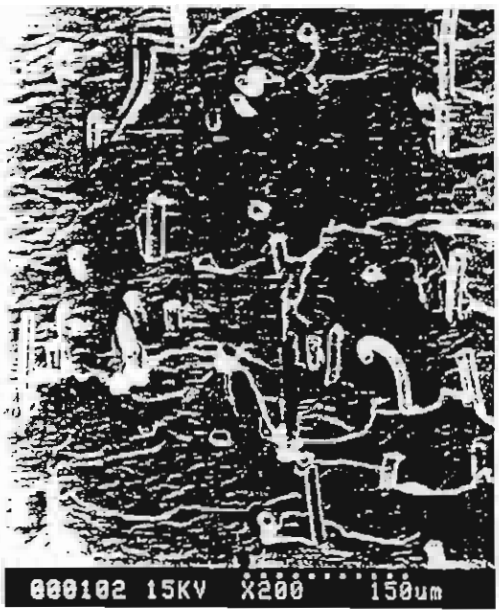

(a)

(b)

Figure 10 SEM micrographs of fractured surface of heptylated Conex composite at magifications of (a) ×200 and (b) ×5,000.

ites filled with unmodified and alkylated Conex fibers are shown in Figures 9(a)–11(a) at magnification ×200 and in Figures 9(b)–11(b) at magnification ×5,000. Evidently, long fiber pullout is seen on the fractured surface of unmodified Conex–SEBS composite [Fig. 9(a)], indicating poor interfacial adhesion between fiber surface and polymer matrix. Magnification of this specimen at ×5,000, shown in Figure 9(b), indicates a number of grooves and cracks on the fiber surface. By contrast, the composites filled with heptylated and dodecylated short fibers, presented in Figures 10(a) and 11(a), respectively, show fiber breakage rather than pullout phenomena, which are evi-

(a)

(b)

Figure 11 SEM micrographs of fractured surface of dodecylated Conex composite at magifications of (a) ×200 and (b) ×5,000.

dent in that the N-alkylation of the Conex fibers improves interfacial adhesion between Conex fiber and SEBS matrix. Clearer evidence of strong interfacial adhesion can be seen from micrographs at higher magnification power shown in Figures 10(b) and 11(b). In these figures, the surface of the fibers is coated by SEBS layer, thus no grooves and cracks can be observed. Also at the proximal end of the fiber that is buried in the matrix, there is good sticking between the matrix and the fiber. This evidence clearly supported the conclusion that the interaction force responsible for adhering the fiber to the matrix is the purely physical force acting through the alkyl groups since no chemical bonding between the fiber and the matrix is expected. The resulting improvement of interfacial adhesion is supported by a significant increase in tensile strength of the modified fiber-filled composites as discussed in the previous section.

Since the fibers were modified by using two successive steps—deprotonation followed by N-alkylation—we had to find out which step was more effective. To do this, deprotonated fibers were prepared by stopping the reaction in the first step with distilled water. The fibers obtained at this stage are shown in Figure 3(b). The other procedures used for preparation of the composites were the same as those described in the experimental sections. Tensile properties of deprotonated Conex–SEBS composites were measured (data not shown here). Modulus and elongation at break were found to be about the same as those of unmodified fiber. However, the tensile strength was found to be slightly higher than that of the unmodified Conex–SEBS system but lower than that of the alkylated Conex–SEBS system. These results ensured that the presence of the alkyl group was essential for the improvement of the composite properties.

Since the results from tensile measurements and the morphology shown in SEM micrographs are in good agreement, it can be concluded that the application of the N-alkylation process described to Conex fibers can significantly enhance the interfacial adhesion between the fibers and SEBS, and thus the mechanical properties of these Conex short-fiber-filled SEBS composites.

CONCLUSIONS

The partial N-alkylation onto short-fiber surface of poly(*m*-phenylene isophthalamide (Conex) was carried out by a metalation reaction with NaH in DMSO solution followed by the addition of alkyl bromide (heptyl and dodecyl). The presence of alkyl groups on the fiber surface was detected by FTIR DRIFT technique. Original and modified fibers were melt-blended with thermoplastic elastomer styrene (ethylene–butylene) styrene (SEBS). Tensile properties of compression-molded specimens were measured. The morphology of the modified fibers and the fractured surfaces of the composites were investigated using SEM. The results obtained were as follows:

1. N-Alkylated Conex fibers show characteristic C—H stretching of alkyl groups in the DRIFT spectra. The result reveals that the fiber surface is successfully modified.
2. By comparison with the unmodified Conex short fibers, the alkylated fibers enhance tensile strength of the composites, probably due to the improvement in interfacial adhesion between the fibers and the SEBS matrix. This result is evident by SEM micrographs of fractured surface, which show nearly complete coating of matrix on the fiber surface.
3. From the systems studied, no difference has been observed from the effect of the length of the alkyl groups, i.e. 7- and 12-carbon atoms on the fiber surface, on tensile properties of the composites.

Support of this work by the Thailand Research Fund is gratefully acknowledged. The authors also would like to thank the Shell Chemical Co. and Teijin Co. Ltd. for providing SEBS and Conex fibers, respectively.

REFERENCES

1. Vaughan, D. J. Polym Eng Sci 1978, 18, 168.
2. Andreopoulos, A. G.; J Appl Polym Sci 1989, 38, 1053.
3. Breznick, M.; Banbaji, J.; Guttmann, H.; Marom, G. Polym Comm 1987, 28, 55.
4. Wu Y.; Tesoro, G. C. J Appl Polym Sci 1986, 31, 1041.
5. Tarantili, P. A.; Andreopoulos, A. G. J Appl Polym Sci 1997, 65, 267.
6. Sheu, G. S.; Lin, T. K.; Shyu, S. S.; Lai, J. Y.; J Adhesion Sci Technol 1994, 8, 511.
7. Wang, Q.; Kaliaguine, S.; Ait-Kadi, A. J Appl Polym Sci 1993, 48, 121.
8. Mori, M.; Uyama, Y.; Ikeda, Y. Polymer 1994, 35, 5336.

9. Sheu, G. S.; Shyu, S. S. Comp Sci Technol 1994, 52, 489.
10. Brown, J. R.; Mathys, Z. J Mater Sci 1997, 32, 2599.
11. Takayanagi, M.; Katayose, T. J Polym Sci, Polym Chem Ed 1981, 19, 1133.
12. Takayanagi, M.; Ueta, S.; Lee, W. Y.; Koga, K. Polym J 1987, 19, 467.
13. Burch, R. R.; Sweeny, W.; Schmidt H.-W.; Kim, Y. H. Macromol 1990, 23, 1065.
14. Hsieh, Y.-L.; Barrall, G.; Xu, S. Polymer 1992, 33, 2143.
15. Hsieh, Y.-L. Polymer 1994, 35, 1218.
16. Kutty, S. K. N.; Nando, G. B. J Appl Polym Sci 1992, 46, 471.
17. Nando, G. B.; Gupta, B. R. In Short Fibre–Polymer Composites; De, S. K.; White, J. R., Eds.; Woodhead: Cambridge, 1996, pp 84–115.
18. Amornsakchai, T.; Sinpatanapan, B.; Bualek-Limcharoen, S.; Meesiri, W. Polymer 1999, 40, 2993.

RESEARCH ARTICLE ScienceAsia 25 (1999)

In-situ Composite Film of Thermotropic Liquid Crystalline Polymer/Polypropylene: Effect of Film Drawing on Molecular Orientation and Properties

Jareerat Samran[a], Wiriya Meesiri[b], Sauvarop Bualek-Limcharoen[c,*] and Taweechai Amornsakchai[c]

[a] Department of Science, Faculty of Science and Technology, Prince of Songkla University, Pattani 94000, Thailand.
[b] Directorate of Armament, Royal Thai Air Force, Donmuang, Bangkok 10210, Thailand.
[c] Department of Chemistry, Faculty of Science, Mahidol University, Rama 6 Road, Bangkok 10400, Thailand.
* Corresponding author.

Received 5 Feb 1999

ABSTRACT A Blend of thermoplastic, polypropylene, with a thermotropic liquid crystalline polymer (TLCP), copolyester comprising 60 mol% of p-hydroxybenzoic acid and 40 mol% ethylene terephthalate was prepared, using a twin screw extruder. Polymer blend pellets were extruded through a microtruder as thin films, using different draw ratios. Effect of film drawing on molecular orientation and properties was investigated. The order parameter of liquid crystalline domain evaluated from polarized infrared spectra was found to increase with increasing film draw ratio. Morphology of the film observed under an optical microscope revealed increasing TLCP fibre aspect-ratio. Young's modulus of the film measured in the machine direction was found to increase significantly with increasing TLCP fibre aspect-ratio and molecular ordering. Young's modulus of TLCP fibres embedded in PP matrix was estimated using the Halpin-Tsai equation and found to correlate linearly with the fibre aspect-ratio and the order parameter.

KEYWORDS: *In-situ* composite, thermotropic liquid crystalline polymer, film drawing, molecular orientation.

INTRODUCTION

Main chain thermotropic liquid crystalline polymers (TLCPs) are known to possess good thermal and mechanical properties and high dimensional stability.[1] Blends of TLCPs with various kinds of thermoplastics to improve processability and properties of the latter have been intensively investigated.[2-6] These are incompatible blend systems comprising a dispersed phase, ie droplets of TLCP, which deform into fibres by elongational force during melt processing. Following melt solidification, the TLCP fibres are frozen in the matrix and hence reinforced the product in a similar manner as the short-fibre reinforced composites. Therefore the name "*in situ* composite" was coined for such a self-reinforced system.[7]

TLCP was found to improve the mechanical properties of the matrix to various degrees depending on processing procedures and conditions which affect morphology and molecular orientation of the blends.[8,9] For a thick product like an injected bar, the skin-core effect was found to occur.[10] The skin of the moulded part exhibited longitudinally oriented TLCP fibrils, whereas droplets were formed in the core region. Morphology of the product developed in the mould depends very much on mould thickness, processing temperature and speed of injection. This in turn results in composites with different mechanical properties. Other forms of composites such as filaments[11,12] and films[13,14] have also been investigated. For these thin-wall specimens the skin-core effect is minimized. However, in the case of blown or extruded films, there is a major problem of anisotropy in physical properties, ie the properties measured in the direction along the flow path (machine direction, MD) are different from that in the transverse direction (TD). This problem has been solved to some extent by using a counter-rotating die for thin film extrusion.[15]

Correlation of the processing conditions to molecular orientation and mechanical properties of pure TLCP produced as extruded rod and fibres has been investigated.[16-18] The increase in drawn-down ratio was found to increase birefringence, ie the difference of refractive indices measured in directions parallel and perpendicular to the fibre axis, which indicated the improvement of molecular orientation.[19] For the *in situ* composite, the elongational flow field was not sufficient to increase the orientation function of TLCP.[20] Greater TLCP fibril elongation could be achieved at the exit of the die during spinning of the blend.

In this work, a blend system of polypropylene and TLCP (Rodrun LC3000, a copolyester comprising 60 mol% of p-hydroxybenzoic acid and 40 mol% ethylene terephthalate) was investigated. It is of interest to improve the properties of a commodity polymer like polypropylene. Rodrun LC3000 is chosen to reinforce PP because of their overlapping windows of processing temperature. The specimen was prepared as an extruded film. Thin film has advantages over an injection-moulded specimen, due to the absence of skin-core effect and weld line. For thin film, it is quite simple to evaluate the molecular orientation from the measurement of transmission spectra in the infrared region. Particular attention has focused on the effect of film drawing on the molecular orientation in TLCP fibres and their aspect ratio, and consequently, tensile modulus of the composite.

Experimental

Materials

A thermoplastic polymer matrix used in this study was injection grade polypropylene (PP6331 HMC, Thailand), density = 0.903 g cm^{-3}, measured melt flow rate (MFR) 17 g/10 min at 230°C, 2.16 kg loading). Thermotropic liquid crystalline polymer (TLCP) was a copolyester comprising 60 mol% p-hydroxybenzoic acid and 40 mol% ethylene terephthalate (Rodrun LC3000), density 1.4 g cm^{-3}, mesophase range from 220 to 280°C, purchased from Unitika Company. TLCP pellets were vacuum dried at 60°C for 12 h before use.

Blending

Melt blending of polypropylene (PP) and 10 wt% TLCP was performed using a co-rotating twin screw extruder (PRISM TSE-16TC) with a screw diameter of 16 mm, L/D 25, intermeshing, at a fixed screw speed of 150 rpm. The processing temperature profile was 180/220/220/225/225°C, representing temperatures at hopper zone, three barrel zones, and heating zone in die head, respectively. Strand exiting the extruder was immediately quenched in a water bath and subsequently pelletized.

Film Extrusion

TLCP/PP blend pellets were extruded using a 16-mm mini-extruder (Randcastle RCP-0625) equipped with a cast film line. The temperature profile was 190/220/230/240°C for the hopper zone, two barrel zones, and slit-die, respectively. Screw speed was 70 rpm. The gap of the die lip was adjusted at 0.65 mm and the width fixed at 152 mm. Extruded film was drawn as molten blend exiting the die outlet, then quenched on a water-cooled roll and collected by a film assembly with adjustable take-off speed. The film was drawn at the draw ratio (slit width-to-film thickness ratio) of 9, 19 and 33 by adjusting the take-off speeds at 1.6, 3.8 and 6.4 m/min respectively. Film thickness was varied from approximately 20 to 70 μm.

Morphology

Morphology of the thin composite films was directly observed under a polarized optical microscope (Olympus) at the magnification range of 100 to 200 times. Fibre distribution as well as the texture of TLCP phase was also observed. However, for the film thicker than 25 μm, it was quite difficult to see the real domain size, because of the overlapping of fibres in different layers, and hence some areas were out of focus. In order to observe the fibres more clearly, a small piece of each film specimen was extracted with boiling xylene and the TLCP fibres were filtered through a sieve of 200 mesh. The extracted fibres were observed under an optical microscope and the distribution of the fibre aspect-ratio (length-to-diameter ratio) was determined from at least one hundred fibres.

Order Parameter

The order parameter or orientation function (S) of the nematic liquid crystalline phase is defined as the following equation,[21]

$$S = 0.5 \langle 3\cos^2\theta - 1 \rangle \qquad (1)$$

where θ is the angle between the axis of mesogenic unit and the preferred direction of the nematic phase. S = 1 for a phase comprising perfectly aligned molecules and S = 0 for the case of random alignment. Infrared dichroism is one of the simple techniques often used to determine the order parameter of liquid crystalline phase.[17-18,22-24] Absorbance values were measured: $A_{\parallel}$ and $A_{\perp}$ for plane polarized light with the electric vector parallel and perpendicular to the preferred direction (the machine direction), respectively. The dichroic ratio R, defined as $R = A_{\parallel}/A_{\perp}$, for a particular absorption band is used to calculate the order parameter from the following equations:

$$S = \frac{(R - 1)}{(R + 2)} \frac{t}{0.5\,(3\cos^2\alpha - 1)} \qquad (2)$$

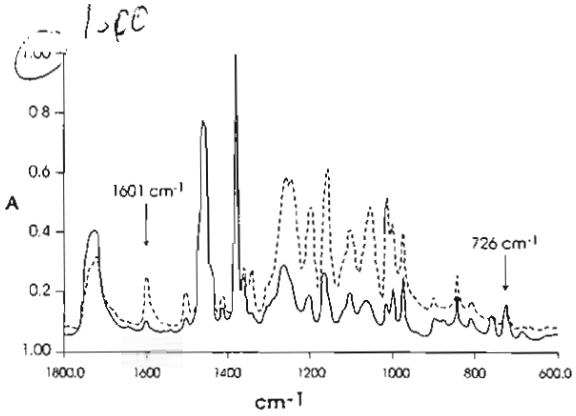

Fig 1. Polarized IR absorption spectra of TLCP/PP recorded at the positions of polarizer parallel (------) and perpendicular (——) to machine direction of the film.

where α is the angle between the transition moment and the major molecular axis. This equation is reduced to

$$S = (R - 1)/(R + 2) \text{ where } R > 1 \qquad (3)$$

for a band whose transition moment is parallel to the major molecular axis (parallel transition moment) and

$$S = 2(1 - R)/(R + 2) \text{ where } R < 1 \qquad (4)$$

for a band whose transition moment is perpendicular to the major molecular axis (perpendicular transition moment).

The order parameter of the TLCP phase in TLCP/PP blend was evaluated from the IR absorption spectra measured using Perkin-Elmer FTIR (system 2000) with an aluminium wire-grid polarizer placed in the sample compartment, next to the film specimen. FTIR spectra were recorded at the polarization directions of the polarizer parallel and perpendicular to the machine direction of the film (see Fig 1). Areas under two peaks, the parallel band at 1601 cm^{-1} and perpendicular band at 726 cm^{-1} (corresponding to C-C stretching vibration and C-H out-of-plane bending of para-substituted benzene ring), were used to determine order parameters of TLCP utilizing equations (3) and (4), respectively.

Tensile Testing

Tensile testing was conducted using an Instron mechanical tester (Model 4301), with a grip length of 25 mm, crosshead speed of 50 mm/min, and a full-scale load of 10N. Tensile properties of the dumbbell-shaped specimens (70 mm x 4 mm) were measured in the machine (MD) and transverse (TD) directions, according to ASTM D412. Each data point was an averaged value obtained from at least ten specimens.

Results and Discussion

Morphology

The optical micrographs shown in Figs 2 - 3 are obtained from the TLCP/PP films produced at the draw ratios of 9, 19 and 33. Figs 2a - 2c are photographs of the films, while Figs 3a - 3c are those of TLCP fibres extracted from the films, using hot xylene. The optical micrograph shown in Fig. 2a was taken from the film prepared at the lowest draw ratio. This film is quite thick (ca. 70 μm) and therefore shows some regions that are out of focus. It can be clearly seen that the apparent aspect ratio of TLCP fibres in this figure is the shortest compared to Figs. 2b and 2c. In addition, it shows a typical schlieren texture of nematic phase which reveals the inhomogeneity of molecular orientation. On the other hand, the texture of TLCP fibres (bright lines) in Fig 2c, which produced at the highest draw ratio, is the most homogenous. This suggests the highest degree of molecular orientation of TLCP domains in the film. In order to see the size and shape of TLCP fibres more clearly, the composite films were extracted with boiling xylene. Photographs of extracted fibres are shown in Figs 3a - 3c. From several photographs, the fibre length (l) and width (d) were measured, and the fibre aspect-ratio (l/d) were calculated. Distribution curves of TLCP fibre aspect-ratio, measured from about one hundred fibres for each specimen of different draw ratios, are presented in Fig 4. From the film of draw ratio 9, the mean fibre aspect-ratio obtained is about 10, with rather narrow range of distribution. Fibres with very small aspect ratio may be filtered out through the sieve. TLCP Fibres extracted from the film of draw ratio 19 and 33 show broader range of distribution and the mean aspect ratio of about 40 and 80, respectively. However, short fibres are also found in the last two cases, which may arise from breakage of long fibres. In general, it can be clearly seen that as the film draw ratio increases, TLCP fibres are more elongated, ie the fibre aspect-ratio increases. These results agree with the increase of tensile modulus of the films, discussed in the next section.

Order Parameter

The molecular orientation in polymer specimen is known to determine its strength and stiffness. Hence the order parameter is related to the modulus

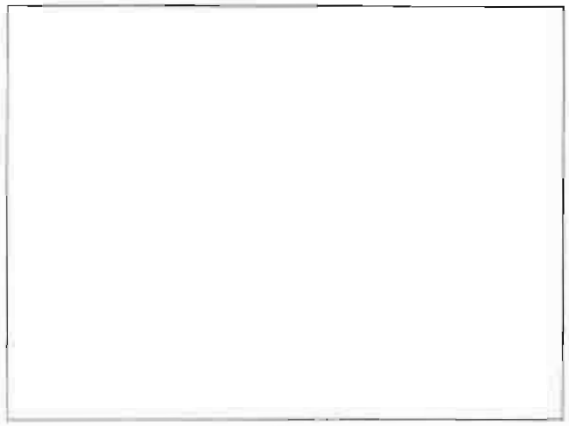

(a)

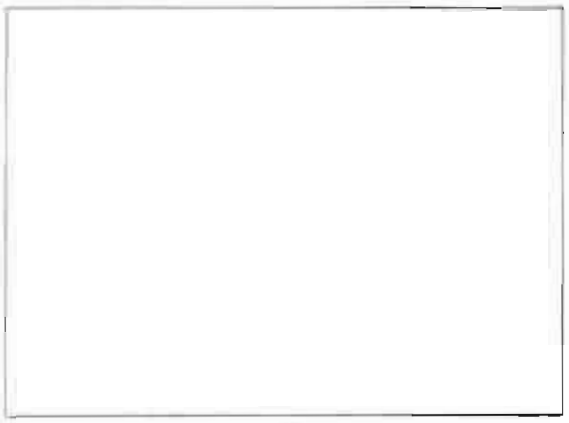

(b)

(c)

Fig 2. Optical micrographs of TLCP/ PP films produced at different draw ratios.
(a) 9 (b) 19 (c) 33.

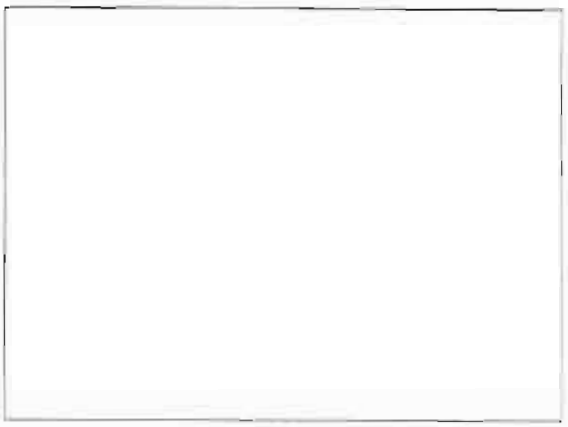

(a)

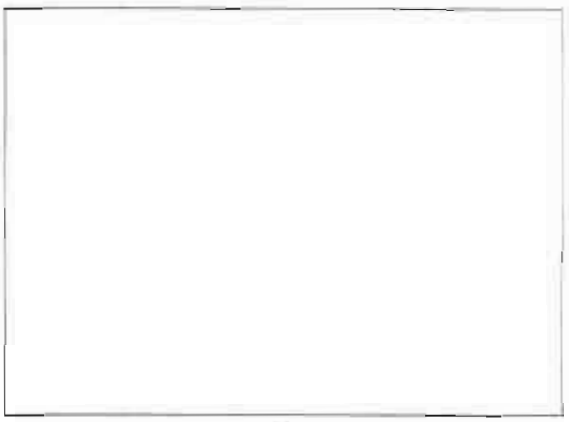

(b)

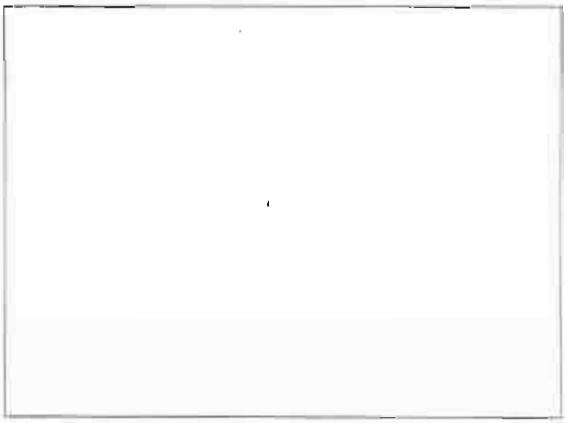

(c)

Fig 3. TLCP fibres extracted from films produced at different draw ratios.
(a) 9 (b) 19 (c) 33.

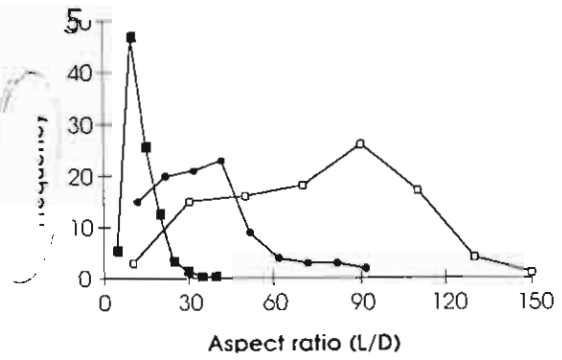

Fig 4. Distribution of aspect-ratio of TLCP fibres obtained from film produced at draw ratios: ■ 9, ● 19 and □ 33.

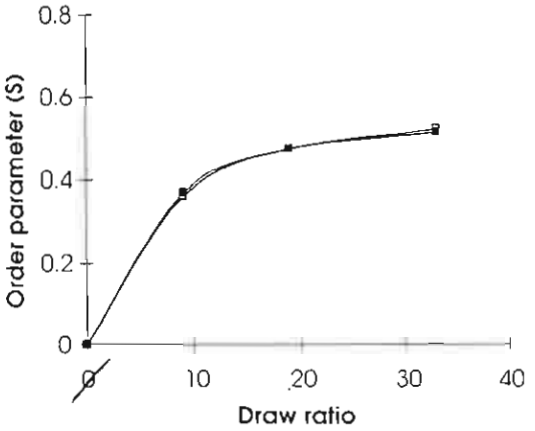

Fig 5. Effect of draw ratio on order parameter of TLCP fibres calculated from the peaks at 1601 cm^{-1} (-□-) and 726 cm^{-1} (-■-)

of the polymer. The molecular ordering in TLCP phase embedded in PP matrix ought to be one of the parameters determining the strength the fibres which contributes to the composite properties. For thin film specimens, it is rather simple to determine molecular orientation from the anisotropy of absorption spectra (dichroism), especially in the infrared region. Since the selected absorption bands used to measure the dichroic ratio belong to the benzene ring in TLCP molecule, the calculated order parameters, therefore, represent only the molecular orientation of the TLCP phase. The order parameters of TLCP in the composite film plotted as a function of draw ratio are illustrated in Fig 5. The order parameter of TLCP phase is found to increase from 0.37 to 0.52 as the draw ratio increases from 9 to 33. Assuming that without drawing, S = 0, ie TLCP appears as spherical droplets, the curves start from the origin. The order parameters calculated from two peaks, at 1601 and 726 cm^{-1}, yield the same results.

Tensile properties

Young's moduli of pure PP and TLCP/PP films prepared at different draw ratios are shown in Fig. 6. The reported results are obtained by measuring in the machine direction (MD) and transverse direction (TD).

Pure polypropylene film, produced using the same processing condition as TLCP/PP composite, exhibits nearly isotropic modulus, i.e., the moduli in both MD and TD are nearly equal. Increasing of draw ratio has no significant influence on the modulus of PP. This might be due to the high flexibility of PP polymer chain and rapid relaxation of these molecules.

The MD modulus of the composite TLCP/PP film markedly improves with increasing draw ratio. The MD modulus of the composite produced at the draw ratio 33 increases by about 30% from that of the composite film produced at the draw ratio 9 and by about 77% from that of pure PP prapared at draw ratio 33. The results are apparently due to the reinforcement of TLCP fibres and the higher fibre aspect ratio formed at higher degree of film drawing.

For short fibre-filled composites, the longitudinal moduli of the composite (E_c) is related to the fibre modulus (E_f) and matrix modulus (E_m) and fibre aspect-ratio by the well-known equation of Halpin-Tsai[25].

$$\frac{E_c}{E_m} = \frac{1 + ABX}{1 - BX} \qquad (5)$$

where X is the fibre volume fraction and

$$B = \left|\frac{E_f}{E_m} - 1\right| / \left[\frac{E_f}{E_m} + A\right| \qquad (6)$$

The quantity A is equal to 2(l/d), where l/d is the length to diameter ratio (aspect ratio) of the fibres. We predict the modulus of TLCP fibres embedded in PP matrix by rearranging the Halpin-Tsai equation as,

$$E_f = \frac{E_c(A + X) + AE_m(X - 1)}{\frac{E_c}{E_m}(X - 1) + (XA + 1)} \qquad (7)$$

From our results, using the measured values of E_c, E_m, and l/d and $X = 0.07$, the calculated E_f at the film draw ratio of 9, 19 and 33, are 2.99, 6.64 and 7.86 GPa, respectively. The highest value of the modulus is close to the value of flexural modulus of pure TLCP

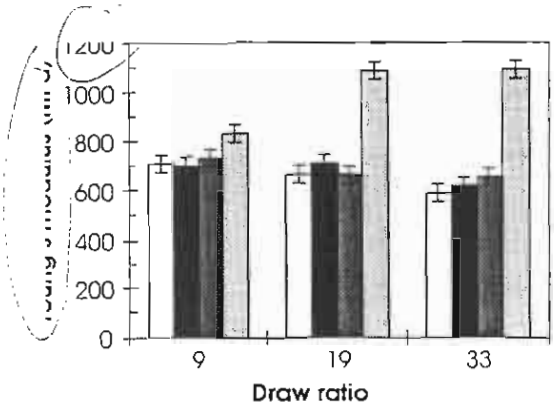

Fig 6. Young's moduli of PP and TLCP/PP films prepared at different draw ratios, measured in machine direction (MD) and transverse direction (TD).
□ PP(TD) ■ PP(MD) ▩ PP/TLCP(TD) □ PP/TLCP(MD)

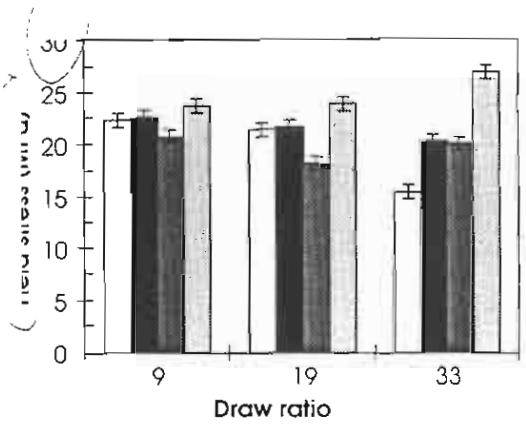

Fig 7. Yield stresses of PP and TLCP/PP films prepared at different draw ratio, measured in machine direction (MD) and transverse direction (TD).
□ PP(TD) ■ PP(MD) ▩ PP/TLCP(TD) □ PP/TLCP(MD)

reported by the manufacturer, ie 9.3 GPa. However, it is much lower than elastic modulus of pure TLCP as spun fibre, prepared at a every high draw ratio of 100, which was reported by Dibenedetto[16] at about 35 GPa. The reason for this large difference could be due to the broad distribution of fibre aspect ratio in our sample. The calculated values of E_f are found to correlate linearly with fibre aspect-ratio and also with the order parameter of TLCP phase.

On the other hand, the TD moduli of pure PP and TLCP/PP composite are not significantly affected by increasing film draw ratio. In accordance with the composite theory,[2,25] the TD modulus of the composite can be estimated by the inverse rule of mixture :

$$\frac{1}{E_c} = \frac{X}{E_f} + \frac{(1 - X)}{E_m} \qquad (8)$$

For small X, the TD modulus of the composite is dominated by that of the matrix and independent of fibre aspect ratio.

Yield stresses of PP and TLCP/PP films, produced at different draw ratios, measured in both directions are shown in Fig 7. Yield stresses in MD direction of the composite are slightly higher than that of pure PP at draw ratio 9 and 19, but are about 34% improved in the composite at draw ratio of 33. The difference in MD and TD yield stresses of the composite film is larger than that of PP film because of the different morphology of the two systems. When the composite is being stressed perpendicularly to the fibre axis of the dispersed phase, the ends of TLCP fibres with small radius of curvature could act as stress concentrators.[25] Consequently, anisotropy of yield stress of composite films is expected to be higher than that of PP.

It can be concluded that increase of film draw ratio provided an increase in order parameter of TLCP phase and fibre aspect ratio, which match the mechanical results, ie the enhancement of MD Young's modulus. This summarized that better molecular orientation in TLCP phase translates to the better mechanical properties of TLCP,[17,24] and hence better composite properties.

Conclusion

In situ composite films of 10 wt% TLCP/PP were prepared at different draw ratios by extrusion cast film technique. Order parameter of TLCP phase was determined from infrared dichrosim. Film morphology was observed under optical microscope and their tensile properties were measured. It was found that as the film draw ratio increased, the fibre aspect ratio increased and so did the order parameter. These results are in good agreement with the enhancement of the film modulus. The modulus of TLCP fibres embedded in PP matrix estimated from the Halpin-Tsai equation was found to correlate well with the order parameter and the aspect ratio of TLCP phase.

Acknowledgment

The financial support of The Thailand Research Fund is gratefully acknowledged.

REFERENCES

1. Luise, RR (1997) in *Applications of High Temperature Polymers*, (Edited by Luise, RR) pp 25-40. Plenum Press, New York.
2. Dutta D, Fruitwala H, Kohli A and Weiss RA (1990) Polymer blends containing liquid crystals: a review. *Polym Eng Sci* 30, 1005.
3. Brown CS and Alder PT (1993) in *Polymer Blends and Alloys*, (Edited by Folkes, MJ and Hope, PS), pp 195-227. Blackie Academic & Professional, Glasgow.
4. Handlos AA and Baird DG (1995) Processing and associated properties of *in situ* composites based on thermotropic liquid crystalline polymers and thermoplastics. *JMS Rev Macromol Chem Phys* C35, 183-238.
5. Machiels AGC, Denys KFJ, van Dam J Nd and de Boer AP (1996) Formation, stability and properties of *in situ* composites based on blends of a thermotropic liquid crystalline polymer and a thermoplastic elastomer. *Polym Eng Sci* 36, 2451-66
6. Jin X and Li W (1995) Correlation of mechanical properties with morphology, and processing parameters for thermotropic liquid crystalline polymer-containing blends. *JMS Rev Macromol Chem Phys* C35(1), 1-13
7. Kiss G (1987) *In situ* composites: blends of isotropic polymers and thermotropic liquid crystalline polymers. *Polym Eng Sci* 27, 410
8. Heino MT, Hietaoja PT Vainio TP and Seppala JV (1994) Effect of viscosity ratio and processing conditions on the morphology of blends of liquid crystalline polymer and polypropylene. *J Appl Polym Sci* 51, 259-70
9. Hull JB and Jones AR (1996) in *Rheology and Processing of Liquid Crystalline Polymers*, (Edited by Arcierno D and Collyer, AA), pp 218-50. Chapman & Hall, London
10. Baird DG and Wilkes GL (1983) Sandwich injection molding of thermotropic copolyesters and filled polyester. *Polym Eng Sci* 23, 632-6
11. Qin Y (1994) On the *in situ* generation of reinforcing fibers. *J Appl Polym Sci* 54, 735-42
12. Qin Y (1994) Drawing behavior of Polyblend fibers from polypropylene and liquid crystal polymers. *J Appl Polym Sci* 54, 873-80
13. Crevecoeur G and Groeninckx G (1993) Sheet extrusion of *in-situ* composites : influene of processing parameters. *Polym.Eng.Sci.*, 33, 937-943
14. Hsu TC, Lichkus AM and Harrison IR (1993) Liquid crystal polymer/polyethylene blends for thin film applications. *Polym Eng Sci* 33, 860-62
15. Chinsirikul W, Hsu TC and Harrison IR (1996) Liquid crystalline polymer (LCP) reinforced polyethylene blend blown film: effect of counter-rotating die on fiber orientation and film properties. *Polym Eng Sci* 36, 2708-17
16. Debenedetto AT, Nicolais L, Amendola E, Carfagna C and Nobile MR (1989) The effect of hot drawing on the properties of thermotropic polymer fibers. *Polym Eng Sci* 29, 153-62
17. Kaito A, Nakayama K and Kyotani M (1991) Surface orientation of a liquid-crystalline polymer studied by polarized reflection spectroscopy. *J Appl Polym Sci* 29, 1321-8
18. Kaito A, Kyotani M and Nakayama K (1995) Effects of shear rate on the molecular orientation in extruded rods of a thermotropic liquid crystalline polymer *J Appl Polym Sci* 55, 1489-93
19. Pan L and Liang B (1998) A comparative study of in situ composite reinforced with different rigid liquid crystalline polymer. *J Appl Polym Sci* 70, 1035-45
20. Carfagna C, Amendola E, Nicolais L, Acierno D, Francescangeli O, Yang B and Rustichelli F (1991) Blends of a polyetherimide and a liquid crystalline polymer: fiber orientation and mechanical properties. *J Appl Polym Sci* 23, 839-44
21. Saupe A and Maier W (1961) Methoden zur Bestimmung des Ordnungsgrades nematischer kristallinfluessiger Schichten. *Z Naturforsch*, 16a, 816-24
22. Kelker H, Hatz R and Wirzing G (1973) Untersuchung des Infrarot-dichroismus in Fluessig-Kristallinen Schichten ohne Verwendung von Polarisiertem Licht. *Z Anal Chem* 267, 161-6
23. Chingduang P, Bualek S, Phaovibul O and Schrader B (1986) Study of orientation and order of non-mesogenic solutes in liquid crystalline matrix by infrared spectroscopy. *Mol Cryst Liq Cryst* 132, 131-41
24. Kyotani M, Kaito A and Nakayama K (1993) Structural, mechanical and thermal properties of extruded sheets of a liquid-crystalline copolymer. *J Appl Polym Sci* 47, 2023-63
25. Nielsen LE (1974) *Mechanical Properties of Polymer and Composites* Vol 2 pp 294-6, 453-510. Marcel Dekker, New York.

Rheol. Acta (revised)

Effect of Melt Viscosity of Polypropylene on Fibrillation of Thermotropic Liquid Crystalline Polymer in *In-situ* Composite Film

Banchob Wanno[a], Jareerat Samran[b] and Sauvarop Bualek-Limcharoen[a*]

[a]Department of Chemistry, Faculty of Science, Mahidol University, Rama 6 Road, Bangkok 10400, Thailand.

[b]Department of Science, Faculty of Science and Technology, Prince of Songkla University, Pattani 94000, Thailand

*Corresponding author, FAX (662)2477050, e-mail: scsbl@mahidol.ac.th

Keywords : Liquid crystalline polymers, *In-situ* composite, Melt viscosity, Polypropylene, TLCP Fibrillation, polymer blend

Abstract

Various grades of polypropylene were melt blended with a thermotropic liquid crystalline polymer, a block copolymer of p-hydroxy benzoic acid and ethylene terephthalate (60/40 mole ratio). The blends were extruded as cast films at different values of draw ratio (slit width/film thickness). Fibrillation of TLCP dispersed phase with high fiber aspect ratio (length/width) was obtained with the matrix of low melt flow rate, i.e., high viscosity and with increasing film drawing. Melt viscosities of pure components and blends measured by using capillary rheometer were found to decrease with increasing shear rate and temperature. Viscosity ratio (dispersed phase to matrix phase) of the systems being investigated at 255°C at the shear rate ranged from 10^2 to 10^4 s^{-1}, was found to lie between 0.04 and 0.15. Addition of a few percent of elastomeric compatibilizers, a tri-block copolymer SEBS, EPDM rubber and

maleated-EPDM, was found to affect the melt viscosity of the blend and hence their morphology. Among these three compatibilizers, SEBS was found to provide the best fibrillation.

1. Introduction

An immiscible blend of a thermotropic liquid crystalline polymer (TLCP) with a thermoplastic resulted in fiber-reinforced thermoplastic called *in-situ* composite, the term coined by Kiss (1987). Such composite arose due to the formation of fibrillar TLCP phase during extensional melt flow. They are interesting because of their several outstanding features. In addition to the improvement on physical and dimensional stability of the matrix, the incorporation of TLCP also enhances the ease of processing, resulted form reduced overall melt viscosity of the system. Processing conditions including temperature, shear and elongational forces strongly affect the molecular orientation of TLCP phase as well as the fiber aspect ratio which determine the final physical properties of the composite. Research works on this subject are reviewed by Dutta *et al.* (1990), Hanlos and Baird (1995), and Arcierno & Collyer (1996). There are several important factors affecting the morphology, i.e., size, shape and distribution of TLCP domains in the finished product. These are, for examples, blend composition, viscosities of the blend components, interfacial adhesion and processing conditions such as temperature, shear or elongational forces which depends on mixing procedure and specimen preparation. The effect of viscosity ratio (dispersed phase-to-matrix phase) on morphology of *in-situ* composites has been investigated by several researchers. Good fibrillation was found to achieve when viscosity of TLCP phase is lower than that of the matrix. Heino *et al.* (1994, 1996) investigated polypropylene of various grades blended with two types of TLCP: a copolymer of p-hydroxy benzoic acid and ethylene

terephthalate (60/40 mole ratio HBA/PET), and Vectra A950 (a copolymer of 4-hydroxy benzoic acid and 6-hydroxy-2-naphthonic acid). They found that extruded strand with most fibrous structure was achieved when the viscosity ratio ranged from about 0.5 to 1. The HBA/PET-PP blend system was also investigated by Rivera-Gastelum and Wagner (1996), showing that the rheological properties depended, in a complex manner, on composition and applied shear. Both positive and negative deviations from the log additivity rule were observed at low shear rate, and the state of dispersion of TLCP influenced the viscosity reduction of the system. He et al. (1995) reported that a blend of 10% TLCP (a copolyester of 4-hydroxy benzoic acid and 2-chloro-4-hydroxy benzoic acid) and polyethersulfone or polysulfone with the viscosity ratio as low as 0.01 was sufficient for fiber formation. They concluded that in a blend system with low viscosity ratio and low TLCP content, the TLCP phase is easier to deform and has less chance to coalesce, and hence, good fibrillation could be achieved.

Addition of compatibilizer was found to improve the dispersion of TLCP phase and in some cases enhance the final mechanical properties of the blend systems. Better dispersion of TLCP in the matrix through incorporation of a compatibilizer was expected to be due to the reduction of interfacial tension. Dutta and Baird (1995) and O'Donnell and Baird (1995) used maleic anhydride grafted polypropylene, as a compatibilizer for polypropylene-based composites and found an improvement in the modulus up to about 30%. Seo (1997) found that maleic anhydride grafted ethylene propylene diene terpolymer (EPDM) could improve both modulus and toughness of *in-situ* composites of Nylon 6 and polybutylene terephthalate. Using tri-block copolymer of styrene (ethylene-butylene) styrene (SEBS), a thermoplastic elastomer as compatibilizer, Bualek-Limcharoen et al. (1999) observed a significant improvement of Young's modulus and impact strength of *in-situ* composite comprising TLCP (60/40 mol% HBA/PET) and polypropylene. The enhancement of impact strength was due to

the action of SEBS as an impact modifier. Better dispersion of the TLCP phase was caused by the improved interfacial adhesion due to SEBS. In addition, SEBS was found to be a more effective compatibilizer than maleic anhydride grafted PP. This might be due to the influence of the elastomer on rheological properties of the blend system.

In the present study, we investigated the effect of melt viscosity of various PP matrices on fibrillation of TLCP in the composite films, and the effect of elastomeric compatibilizer on melt viscosity and morphology of the blends. Melt flow rate measurements obtained using a conventional method will be compared with the viscosity measurements performed on a capillary rheometer. We prepared the specimens in the form of thin films so as to minimize the skin-core morphology and maximize the homogeneity of the sample, i.e., no weld-lines are formed as in the case of injection-molded specimens (Engberg et al. (1990)). The fibrillation of TLCP phase in the thin films can also be observed directly under a polarized optical microscope. Scanning electron microscope was used to investigate the composite fracture surface.

2 Materials and Methods

2.1 Materials

Four grades of polypropylene obtained from HMC Polymer Co., namely, PRO-FAX 6531, PW583, 6331 and 6231 with the measured melt flow rate (MFR) of 5, 9, 14 and 28, respectively, and the melting point of 165°C, were used in this study. For simplicity, these PPs are denoted as PP5, PP9, PP14 and PP28. The dispersed phase was a liquid crystalline polymer, Rodrun LC3000, which is a copolyester of p-hydroxy benzoic acid and ethylene terephthalate (60/40 mol% HBA/PET), purchased from Unitika Co. Three compatibilizers used were elastomers: 1) tri-block copolymer of styrene (ethylene-butylene) styrene (SEBS,

KratonG 1652) kindly provided by Shell Chemical Co.; 2) ethylene propylene diene monomer (EPDM, Royalene 501); and 3) maleic anhydride grafted EPDM (MA-g-EPDM, Royaltuf 490, with 1% MA content) kindly provided by Uniroyal Co. All materials were dried in a vacuum oven at 70°C for 12 h before use.

2.2 Blending and film extrusion

Blend composition of 10 wt% TLCP and 3 wt% compatibilizer in PP matrix was used throughout this study. All components were melt blended in a co-rotating twin screw extruder (PRISM TSC-16-TC) with a screw diameter of 16 mm, length-to-diameter ratio (L/D) of 25, the die diameter of 2 mm; and the screw speed of 150 rpm. The temperature profile was 180/220/220/225/225°C, representing the temperatures at the hopper zone, three barrel zones, and the die, respectively. The extruded strand was immediately quenched in a water bath and subsequently pelletized. At the output rate of 1.2 - 2.1 kg h^{-1}, the apparent shear rate in the die was estimated to be 400 - 1,000 s^{-1}. In the second step, the dried blend pellets were extruded using a mini-extruder with a screw diameter of 16 mm, length to diameter ratio of 24, equipped with a cast film line (Rancastle-RCP-0625). The gap of the die lip and the die width were fixed at 0.65 mm and 152 mm, respectively. The screw speed was fixed at 70 rpm. Two different temperature profiles were used, i.e., 190/220/220/240°C and 220/240/255/255°C, representing the temperatures at the hopper zone, two barrel zones, and the die, respectively. After exiting the die outlet the film was immediately quenched on a water-chilled roll and uniaxially drawn at take-off speeds, ranged 1 – 6 m min^{-1} (output rate approximately 0.6 – 1.2 kg h^{-1}. At this step the apparent shear rate in die is estimated to be in the range 20 to 45 s^{-1}. The extruded films of draw ratio (slit-width to film thickness) ranged approximately 8 - 30, were obtained. The film thickness was in the range 70 – 20 μm.

2.3 Viscosity measurement

Melt flow rate of various grades of pure PP and all blends were measured on a melt flow index tester (Kayeness 7053) at 230°C with an applied load of 2.16 kg (ASTM D1238).

Melt viscosities of all pure components and blends were measured using a Rosand RH710 capillary rheometer at 240 and 255°C, equaling the die temperatures used for film preparation. A capillary of diameter 1 mm and length of 16 mm (L/D = 16) was used for the viscosity measurement. The shear rate was varied from 60 to 10^4 s^{-1}. The end effects (Bagley corrections) and the Rabinowitsch corrections were performed in all cases using two dies (a zero die and a 16-mm die) with flat ends, as specified for the Rosand system.

2.4 Morphology

TLCP fibrils dispersed in the thin film of PP matrix could be directly observed under a polarized optical microscope (Olympus SC-35) at 200X magnification. The degree of fiber density per unit viewing area of different systems can be compared. To see the actual size and shape of TLCP fibers more clearly, PP was dissolved away by dropping xylene on a small piece of film placed on the heating stage at about 150°C.

Morphology of the film fracture surface was investigated using a scanning electron microscope (Hitachi S2500) operated at 15 kV. The film fracture surface was prepared by freezing a strip of the blend film sandwiched between two polystyrene sheets in liquid nitrogen for about 30 min and snapping in half. A thin layer of palladium was coated (Hitachi E102 ion sputter) on the specimen to prevent charging on the surface.

3 Results and discussion

3.1 Rheology

Presented in Fig. 1 are the values of MFR of pure PP, PP/TLCP blends, and blends containing a compatibilizer (SEBS, EPDM or MA-g-EPDM). Maximum errors were about ± 1 unit for the samples with high MFR and less for the samples with low MFR. When very low viscosity TLCP was added to PP, the blend MFR increased (and hence viscosity decreased). After addition of 3 wt% compatibilizer, the MFR of all blends decreased, implying that the apparent viscosity of the blend increased. This leads us to expect that some of elastomeric compatibilizer, in particular SEBS, is located at the interface between the fiber and the matrix having the two styrene end blocks embedded in the TLCP phase and the middle EB block in the PP matrix. This would enhance molecular entanglement at the interface so that at the low shear rate the dispersed phase might have a certain level of resistance to flow.

Melt flow curves of TLCP and PP of different grades measured at 240 and 250°C are shown in Fig. 2a and b, respectively. It is seen that the true viscosity of TLCP is very much lower than those of the neat PPs. The true viscosity of PP with low MFR is higher than that of PP with higher MFR values as expected. All pure components exhibit shear thinning behavior due to the shear-induced chain orientation and hence the reduction of entanglement density at higher shear stress levels (Dealy and Wissbrun (1990)). PP with lower MFR shows stronger shear thinning behavior. The polymer with higher molecular weight (and hence high degree of entanglement) therefore exhibits a more pronounced shear thinning when a high stress is applied. At all shear rates, the viscosity of TLCP at 255°C is evidently lower than that measured at 240°C, demonstrating the improvement of flow behavior of TLCP melt with increasing temperature in this range. Our results are in good agreement with Tormes et al. (1998) who investigated the temperature dependence of the viscosity of LC3000 (the same TLCP used in our work) at a shear rate of 1 s^{-1}. Their results showed that the viscosity of TLCP decreased rapidly as the temperature increase in the range 200 - 260°C, but was almost

temperature independent in the range 260 - 300°C. The lesser temperature dependence of the viscosity of TLCP in the high temperature range was probably caused by an opposing effect, that the increase in viscosity with temperature is due to the decrease in the degree of molecular ordering as the mesophase approaches the transition point to the isotropic melt. The shear thinning behavior of TLCP is observed at both temperatures with a value of the exponent n = 0.6 in the power law equation, $\eta = k\,\gamma^{(n-1)}$. On the other hand, the viscosity of each grade of PP does not significantly vary at these two temperatures. As a consequence, the viscosity ratio (defined as the ratio of the viscosity of TLCP to that of PP), $\rho = \eta_{TLCP}/\eta_{PP}$, at 240°C is higher than that at 255°C as shown in Fig.3a and b, respectively. The viscosity ratio at 240°C lies in the range 0.07 - 0.23, whereas that at 255°C in the range 0.04 - 0.15. It is seen that the viscosity ratio increases with increasing shear rate, due to the faster drop of the viscosity of PP than that of TLCP at high shear rate.

Melt viscosity plots of the blends of 10wt% TLCP and PP with MFR 5, 9, and 14 are shown in Fig. 4a, b and c, respectively. Viscosity plots of the blends containing 3wt% compatibilizer (SEBS, EPDM or MA-g-EPDM) are also presented. It is seen that for PP5 system (Fig. 4a), the viscosity of all blends (without and with compatibilizer) are approximately the same. Compared with systems PP9 (Fig. 3b) and PP14 (Fig. 3c), the addition of compatibilizer, especially SEBS, reduced the viscosity of the blends, which the effect is more pronounced in the shear rate region 60 – 500 s^{-1}. This result contradicts with the observation obtained by measuring the melt flow rate. The discrepancy of the results obtained from these two methods might be due to different ranges of shear rate involved, and the much different lengths of the two dies resulting in different entrance pressure drops. It should be noted that Bagley correction was not applied for the data obtained from MFR tester as in the case of capillary rheometer. Furthermore, the effect of wall slip in the longer die used in the capillary rheometer may be greater than that in the MFR tester, and hence

resulting in a greater reduction of the viscosity (Sirisinha and Freakley (1997)). Gupta and Purwar (1984) investigated the melt viscosity of PP/SEBS blends using a capillary rheometer and observed a minimum viscosity at the blend containing 5% SEBS. They suggested this to be due to the high deformability of the small domains of SEBS dispersed phase, i.e. the plasticizing effect. Similar to our PP/TLCP/SEBS blends, some excess SEBS might be distributed as small droplets in PP matrix, acting as a plasticizer for the system. As a result, the melt viscosity of PP/TLCP/SEBS system appeared to decrease at the high shear rate used in the capillary rheometer.

3.2 Morphology

3.2.1 Effect of melt viscosity of PP matrix

Morphology of *in-situ* composite films observed under an optical microscope are illustrated in Fig. 5. The films were prepared using the die temperature at 255°C, with a draw ratio of 30, and using PP matrices of different MFR: (a) PP5, (b) PP9, (c) PP14 and (d) PP28. The effect of melt viscosity of PP on fibrillation of TLCP is clearly demonstrated here. PP5 matrix gives the thinnest TLCP fibers and also the highest number of fibers per unit viewing area, whereas PP28 gives the thickest and shortest fibers, and also the lowest number of fibers per unit area. As seen in the previous section, the molten PP5 is the most viscous fluid among all PPs used in this study, and thus could exert the highest shear force to break up the TLCP phase into fine droplets and deform them into thin elongated fibrils. SEM micrographs of the fracture surface of the films (the same series as shown in Fig. 5) are presented in Fig. 6. The film specimens were fractured perpendicular to the machine direction. The pull out feature of TLCP fibers are seen in every sample, suggesting poor interfacial adhesion between the fibers and the matrix. The effect of melt viscosity of PP matrix on fibrillation of TLCP is evident from the size of the fibers. The approximate widths

of the fiber (measured at the point adjacent to the matrix) are about 6, 5, 4 and 3 μm for the films prepared from PP matrices with MFR 28, 14, 9 and 5, respectively. That means the PP matrix with lower MFR (higher viscosity) generates thinner TLCP fibers. The highest number of fibers per unit cross-sectional area is also evident in PP5/TLCP composite film. This suggests that the fiber dispersion is improved with increasing melt viscosity of the matrix.

3.2.2 Effect of film drawing

The effect of additional drawing of the film on the length of TLCP fibers is shown in Fig. 7. These are optical micrographs of TLCP fibers extracted from the films produced at the draw ratio 8 (column I) and draw ratio 30 (column II). The samples in both columns are prepared from matrices: (a) PP5, (b) PP9, (c) PP14 and (d) PP28. Hot xylene was used to extract the fibers and spread them out in order to minimize overlapping. Comparison of the micrographs in two columns reveals that TLCP fibers in films produced at the draw ratio 8 are shorter than those prepared at the draw ratio 30. For the film with PP28 matrix, produced at draw ratio 8, the TLCP dispersed phase appeared as droplets. The dispersed phase becomes more elongated as the MFR of PP decreases. Films produced at the draw ratio of 30 exhibit elongated TLCP fibers. It is evident that the additional drawing of the films just after exiting the die greatly increase the fiber aspect ratio. Our observation agrees with that of Qin (1994) who studied polyblend fibers of PP/TLCP (Vectra A900 and B950) and concluded that the drawing at high temperature preserved the long length of TLCP fibrils due to the high degree of mobility of TLCP. Although the viscosity ratio of each blend system in this study is quite low (i.e., in the range 0.04 to 0.15), compared to that reported by Heino et al. (1994). We have demonstrated that it is possible to obtain good fibrillation in the last step of specimen preparation, i.e., film extrusion at high draw ratio.

3.2.3 Effect of compatibilizers

The effect of compatibilizer on fibrillation of TLCP dispersed phase are shown in Fig. 8. These are optical micrographs of TLCP fibers extracted from various composite films prepared from PP5 without and with 3 wt% of a compatibilizer: (a) no compatibilizer, (b) SEBS, (c) EPDM and (d) MA-g-EPDM. SEM micrographs of the fracture surface of the same series of specimens are illustrated in Fig. 9. It is clearly seen that TLCP fibrils in the composites containing compatibilizer are thinner than that in the uncompatibilized specimen. Finer and shorter fiber pull-out is observed in the film containing SEBS, indicating the improvement on the dispersion of TLCP phase. SEBS thus seems to be more effective compatibilizer than the other two. This is due to the tri-block structure of the thermoplastic elastomer, SEBS, which the middle EB block is compatible with PP and the styrenic blocks at the two ends are compatible with the aromatic groups of TLCP. Hence, SEBS should be present at the interface, with each block diffused into corresponding phases of similar chemical structure. This will help reduce the interfacial tension between PP and TLCP phases and therefore improve the dispersion of TLCP. As reported in our previous work (Bualek-Limcharoen et al.(1999)), significant improvement of tensile modulus and impact strength were observed in the SEBS compatibilized blend of PP (MFR = 12) with TLCP.

4 Conclusion

TLCP (Rodrun LC3000) was melt blended with different grades of polypropylene (MFR 5, 9, 14 and 28). The specimens were prepared in the form of extruded film at various draw ratios. Melt viscosities of these blends were measured using a capillary rheometer. The effect of melt viscosity of PP matrix, as well as the effect of elastomeric compatibilizers on fibrillation of TLCP were investigated. We have demonstrated that, although the viscosity ratio of

PP/TLCP in this study is quite low (ranged from 0.04 to 0.15 at 255°C), long TLCP fibrils can be formed in the last step by drawing the extruded films at high draw ratio. Addition of an elastomeric compatibilizer caused a reduction in the blend melt viscosity as measured by a capillary rheometer. However, the MFR values showed an increase in viscosity with the addition of an elastomeric compatibilizer. The discrepancy might be due to the higher molecular entanglement at the interface caused by the added elastomer and this effect resists the shear flow especially at low shear rate used in MFR measurement.

The morphology of the blends suggests that all compatibilizers help improve dispersion of TLCP phase. SEBS is found to be more effective compatibilizer than EPDM and MA-g-EPDM, as longer TLCP fibers are observed in the former.

5. Acknowledgement

Financial support by the Thailand Research Fund is gratefully acknowledged.

References

Arcierno D and Collyer AA (Eds.) (1996) Rheology and Processing of Liquid Crystalline Polymers. Chapman & Hall, London

Bualek-Limcharoen S, Samran J, Amornsakchai T and Meesiri W (1999) Effect of Compatibilizers on Mechanical Properties and Morphology of In-Situ Composite Film of Thermotropic Liquid Crystalline Polymer/Polypropylene. Polym Eng Sci 39: 312-320

Dealy JM and Wissbrun KF (1990) Melt Rheology and Its Role in Plastics Processing. VNR, New York.

Dutta D, Fruitwala H, Kohli A and Weiss RA (1990) Polymer Blends Containing Liquid Crystals and Thermoplastics. Polym Eng Sci 30: 1005-1018

Datta A and Baird DG (1995) Compatibilization of Thermoplastic Composites Based on Blends of Polypropylene with Two Liquid Crystalline Polymers. Polymer 36: 505-514

Engberg K, Knuttson A and Werner P-E *et al.* (1990) Knit Line Features in Injection Molded Liquid Crystalline Polymer Polym Eng Sci 30: 1620-9

Gupta AK and Purwar SN (1984) Melt Rheological Properties of Polypropylene/SEBS (Styrene-Ethylene Butylene-Styrene Block Copolymer) Blends. J Appl Polym Sci 29: 1079-1093

Handlos AA and Baird DGB (1995) Processing and Associated Properties of *in-situ* Composites Based on Thermotropic Liquid Crystalline Polymers. J. M. S. Rev. Macromol. Chem. Phys C35: 183-238

He J, Bu W and Zhang H. (1995) Factors Influencing Microstructure Formation on Polyblend Containing Liquid Crystalline Polymers. Polym Eng Sci 35: 1695-1704

Heino MT, Hietaoja PT, Vainio TP and Seppala JV (1994) Effect of Viscosity Ratio and Processing Conditions on the Morphology of Blends of Liquid Crystalline Polymer and Polypropylene. J Appl Polym Sci 51: 259-270

Heino MT and Vainio TP (1996) Effect of Viscosity Ratio and Processing Conditions on the Morphology of Blends of Liquid Crystalline Polymer and Polypropylene. in Handbook of Applied Poymer Processing Technology. Cheremisinoff WA and Cheremisinoff PN(eds), Marcel Dekker, New York, pp233-263

Kiss G (1987) *In-situ* Composite: Blends of Isotropic Polymers and Thermotropic Liquid Crystalline Polymers. Polym Eng Sci 27: 410-423

O'Donnell HJ and Baird DG (1995) In-Situ Reinforcment of Polyproplene with Liquid Crystalline Polymers: Effect of Maleic Anhydride-Grafted Polypropylene. Polymer 36: 3113-3126

Qin Y (1994) Drawing Behavior of Polyblend Fibers from Polypropylene and Liquid Crystal Polymers J Appl Polym Sci 54: 783 - 880

Rivera-Castelum MJ and Wagner NJ (1996) A Rheological and Morphological Study of a Copolyester Liquid Crystal/Polypropylene Blend System. J Polym Sci B34, 2433-2445

Seo YJ (1997) Interfacial Adhesion and Deformation of Thermotropic Liquid Crystal Polymers in Engineering Thermoplastics: Blends of a Poly(ester amide) with Nylon 6 and a Polyester with PBT J Appl Polym Sci 64: 359

Sirisinha C and Freakley PK (1997) Influence of Some Lubrication Agents on Extrudate Swell of Carbon Black Filled Styrene/Butadiene Rubber Compound Plast Rubb Comp Process Appl 26: 113-117

Tormes M, Munoz MR, Pena JJ and Santamaria A (1998) Rheology of Rodrun Liquid-Crystalline Polymers. J Polym Sci B36: 253-253

Figure captions

Fig. 1 Melt flow rate (MFR) of pure PPs (PP5, PP9 and PP14), PP/TLCP blends and blends containing compatibilizers (SEBS, EPDM and MA-g-EPDM)

Fig. 2 Melt viscosity versus corrected shear rate for PPs and TLCP measured at (a) 240°C and (b) 255°C

Fig. 3 Viscosity ratio versus corrected shear rate at (a) 240°C and (b) 255°C

Fig. 4 Melt viscosity versus corrected shear rate for pure PPs, TLCP and PP/TLCP blends without and with compatibilizer (SEBS, EPDM and MA-g-EPDM) measured at 255°C, for different PP grades: (a) PP5 (b) PP9 and (c) PP14

Fig. 5 Optical micrographs of PP/TLCP films prepared from (a) PP5, (b) PP9, (c) PP14 and (d) PP28

Fig. 6 SEM micrographs of fractured surfaces of PP/TLCP films prepared from (a) PP5, (b) PP9, (c) PP14 and (d) PP28

Fig. 7 Optical micrographs of TLCP fibers extracted from PP/TLCP films prepared from (a) PP5, (b) PP9, (c) PP14 and (d) PP28 : films were prepared at draw ratio 8 (column I) and 30 (column II)

Fig. 8 Optical micrographs of TLCP fibers extracted from PP5/TLCP films containing (a) no compatibilizer, (b) SEBS, (c) EPDM and (d) MA-g-EPDM

Fig. 9 SEM micrographs of the fractured surfaces of PP5/TLCP films containing (a) no compatibilizer, (b) SEBS, (c) EPDM and (d) MA-g-EPDM

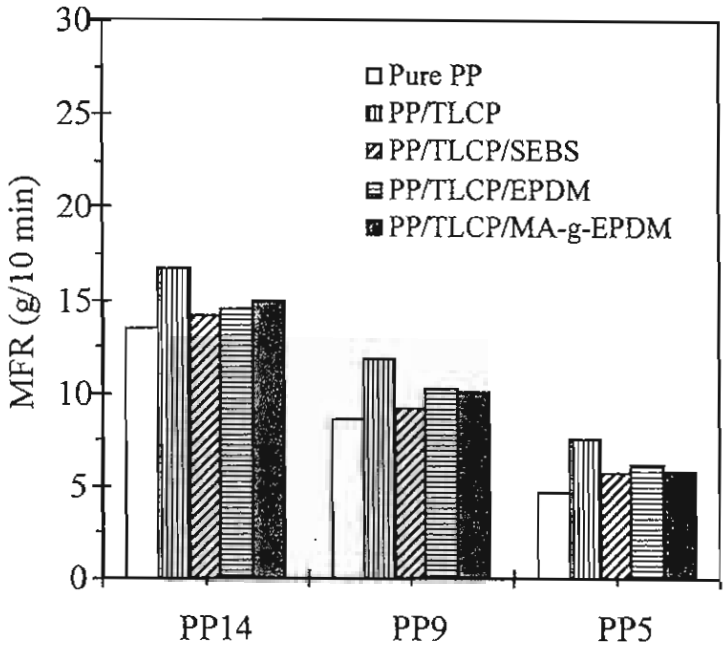

Fig. 1 Melt flow rate (MFR) of pure PPs (PP5, PP9 and PP14), PP/TLCP blends and blends containing compatibilizers (SEBS, EPDM and MA-g-EPDM)

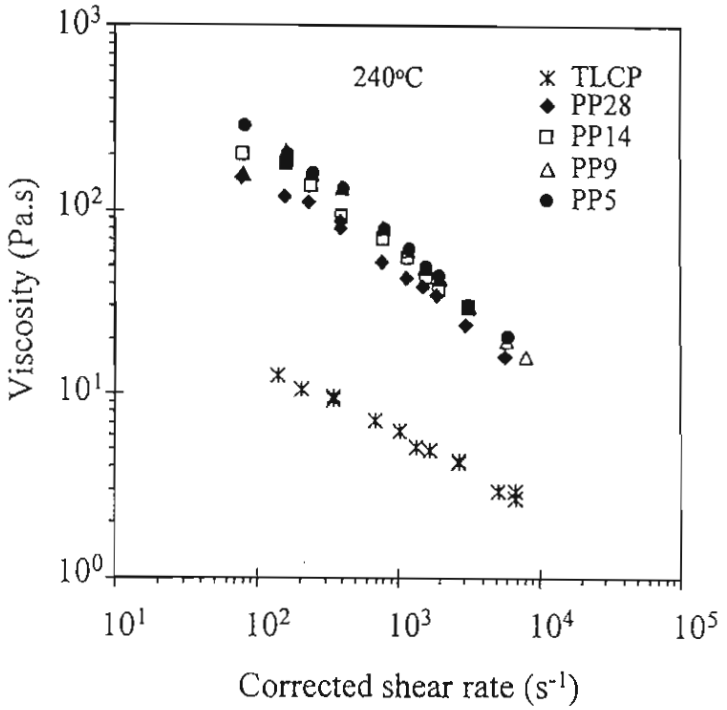

(a)

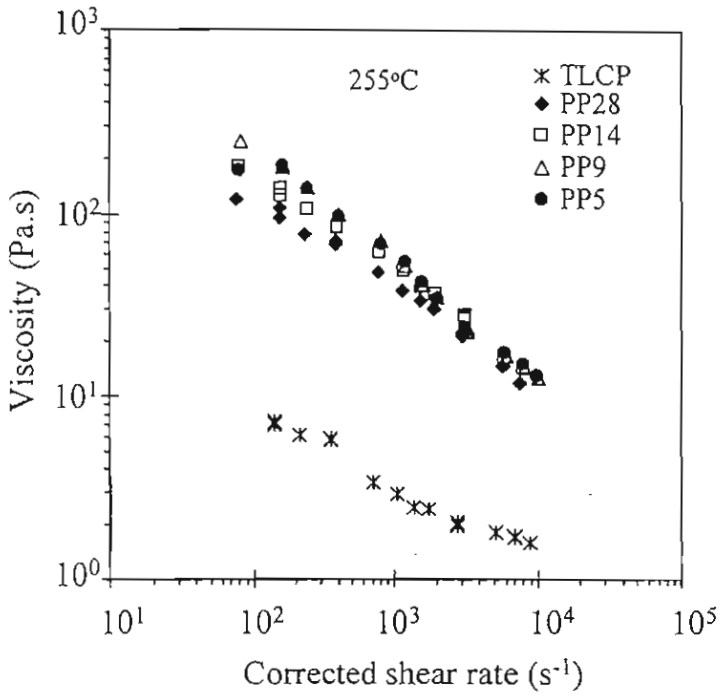

(b)

Figure 2 Melt viscosities versus corrected shear rate for PPs and TLCP measured at (a) 240°C and (b) 255°C.

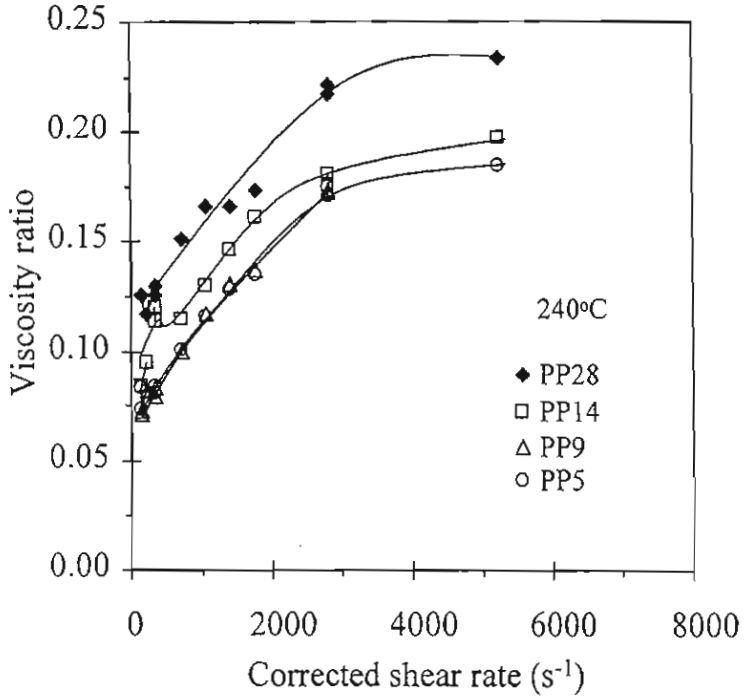

(a)

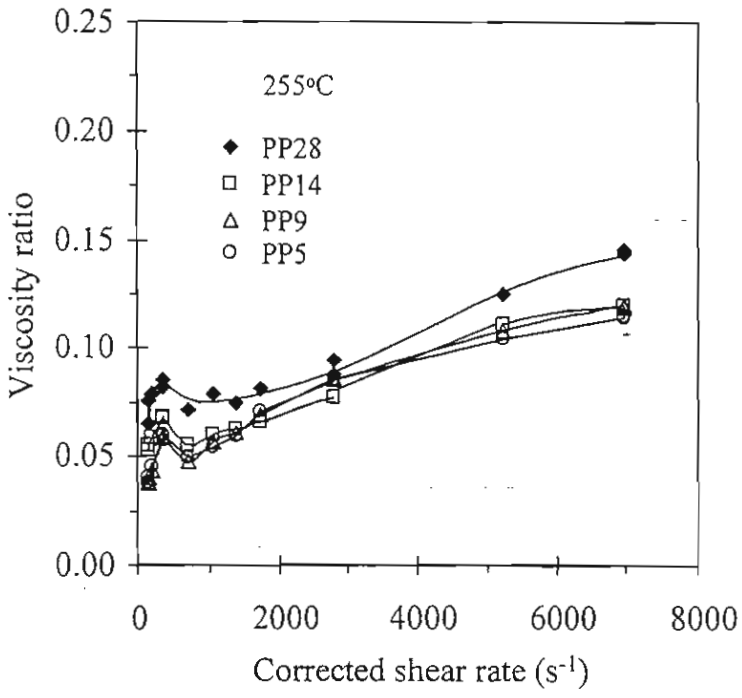

(b)

Figure 3 Viscosity ratio, η_{TLCP}/η_{PP}, versus corrected shear rate at (a) 240°C and (b) 255°C.

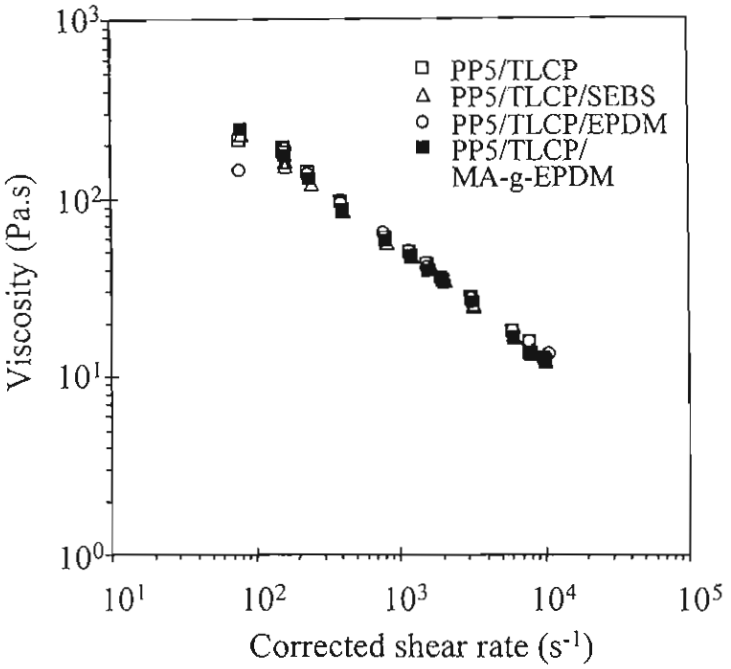

(a)

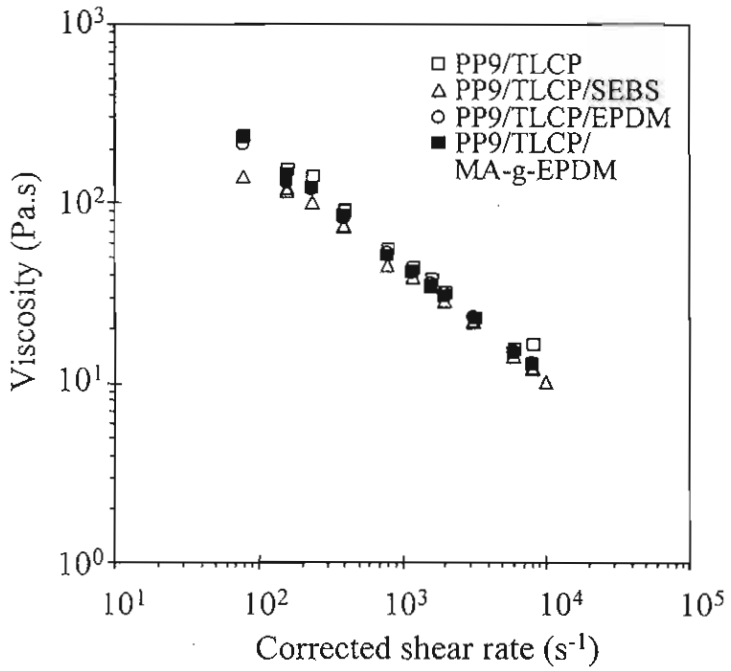

(b)

Fig. 4 (continued)

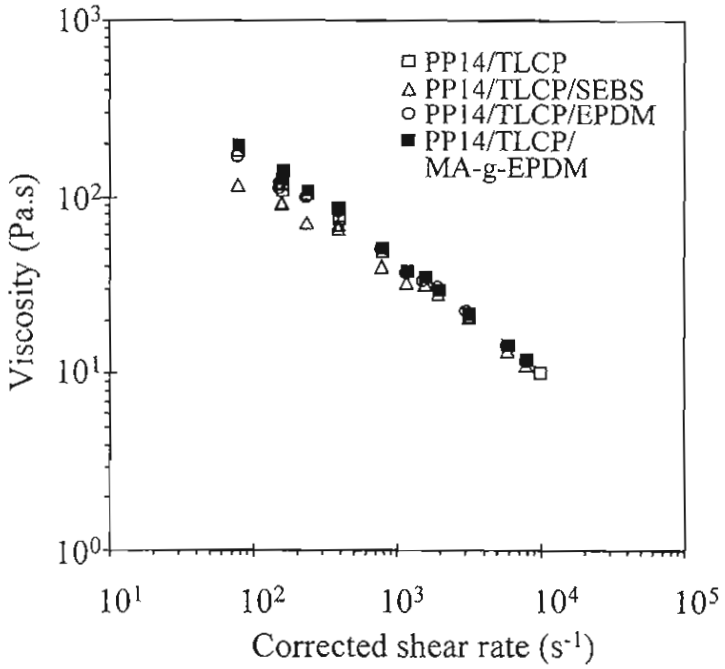

(c)

Fig. 4 Melt viscosity versus corrected shear rate for pure PPs, TLCP and PP/TLCP blends without and with compatibilizer (SEBS, EPDM and MA-g-EPDM) measured at 255°C, for different PP grades: (a) PP5 (b) PP9 and (c) PP14

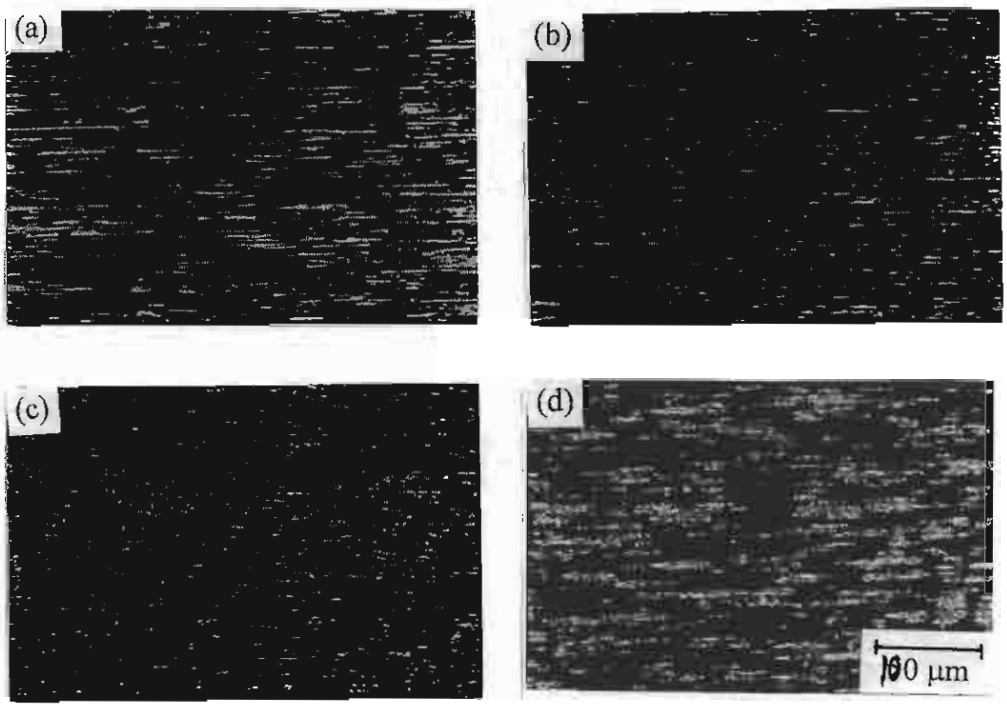

Fig. 5 Optical micrographs of PP/TLCP films prepared from (a) PP5, (b) PP9, (c) PP14 and (d) PP28

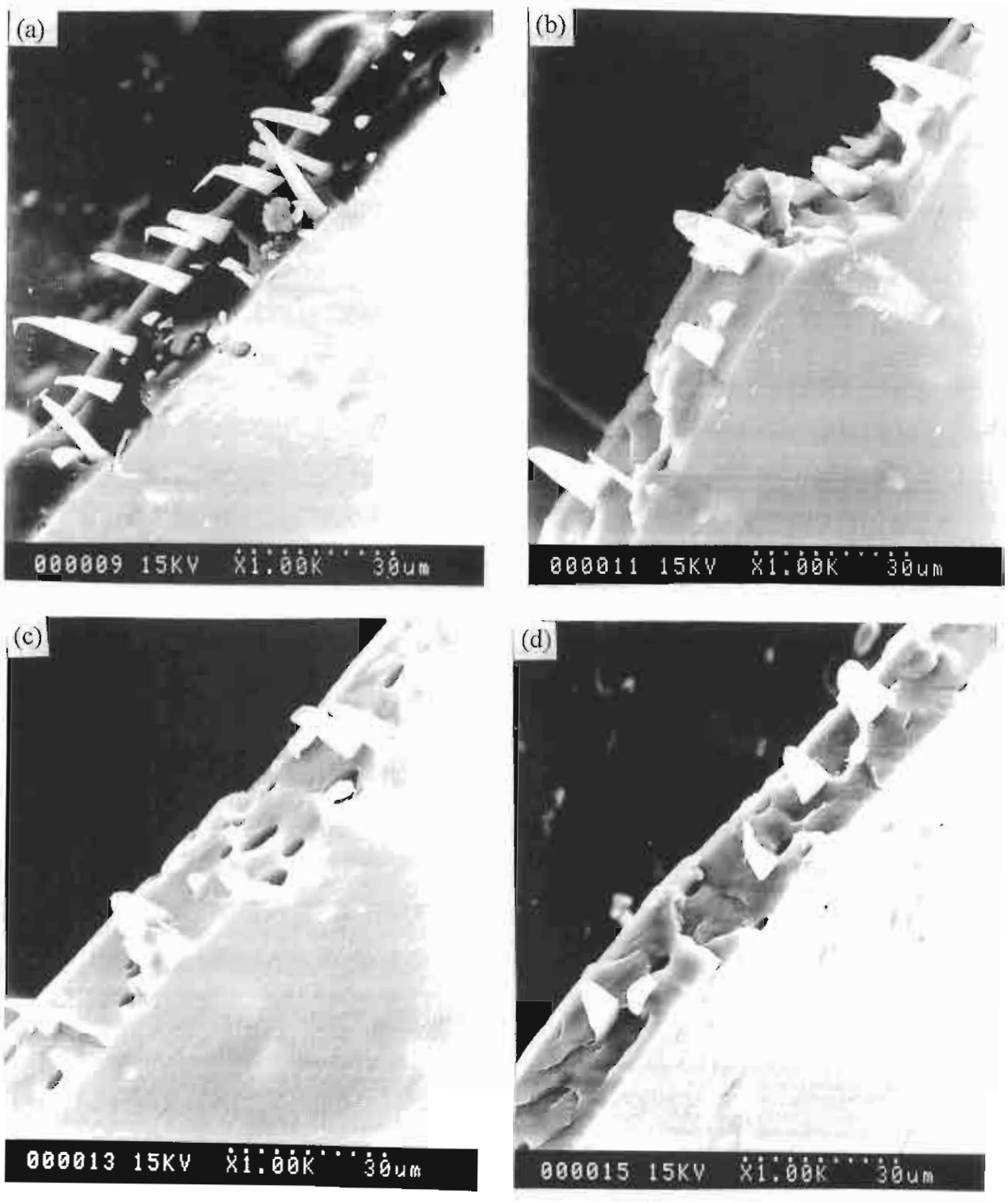

Fig. 6 SEM micrographs of fractured surfaces of PP/TLCP films prepared from (a) PP5, (b) PP9, (c) PP14 and (d) PP28

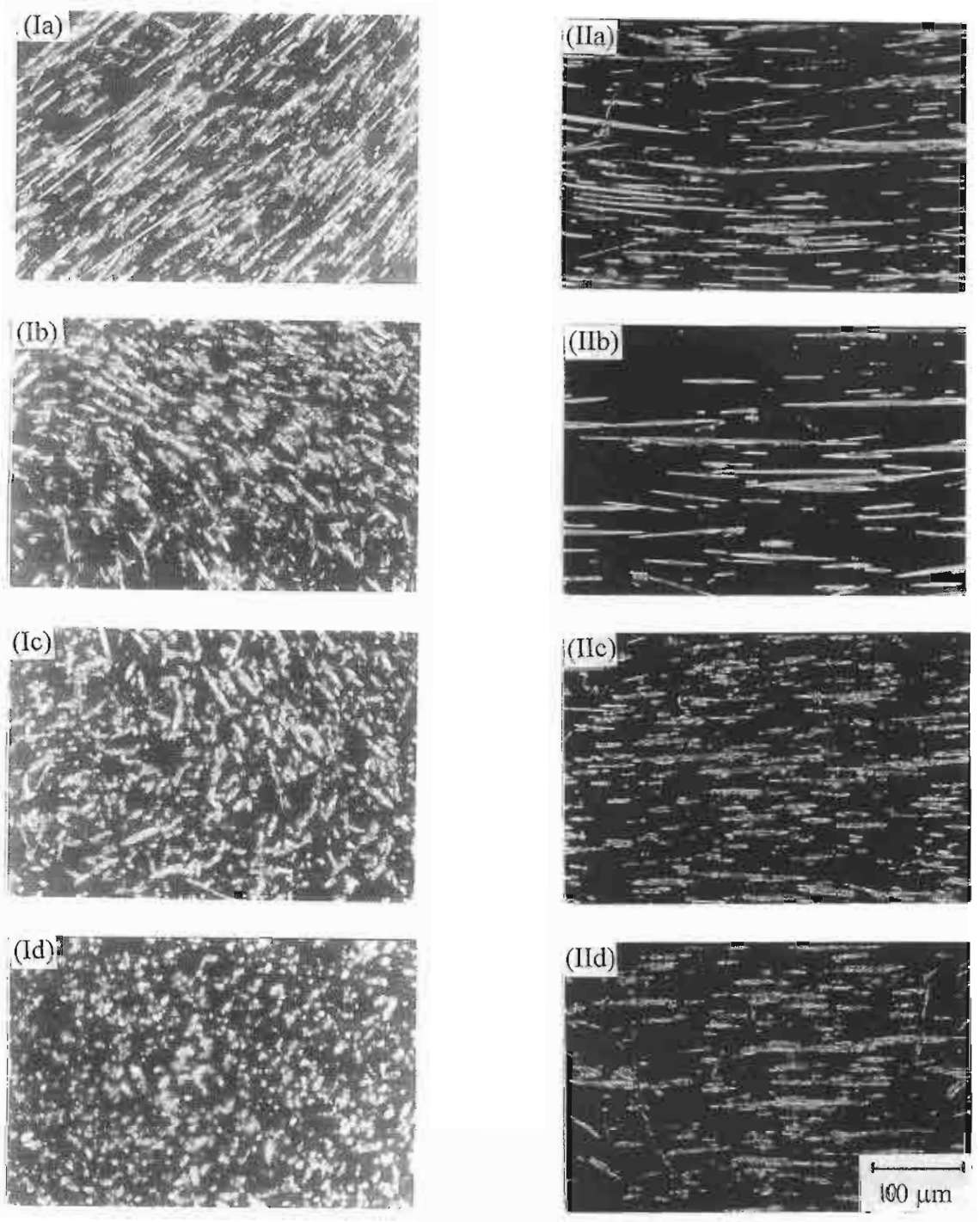

Column I Column II

Figure 7 Optical micrographs of TLCP fibers extracted from TLCP/PP films prepared from (a) PP5, (b) PP9, (c) PP14 and (d) PP28 . Films were prepared at draw ratio 8 (column I) and 30 (column II)

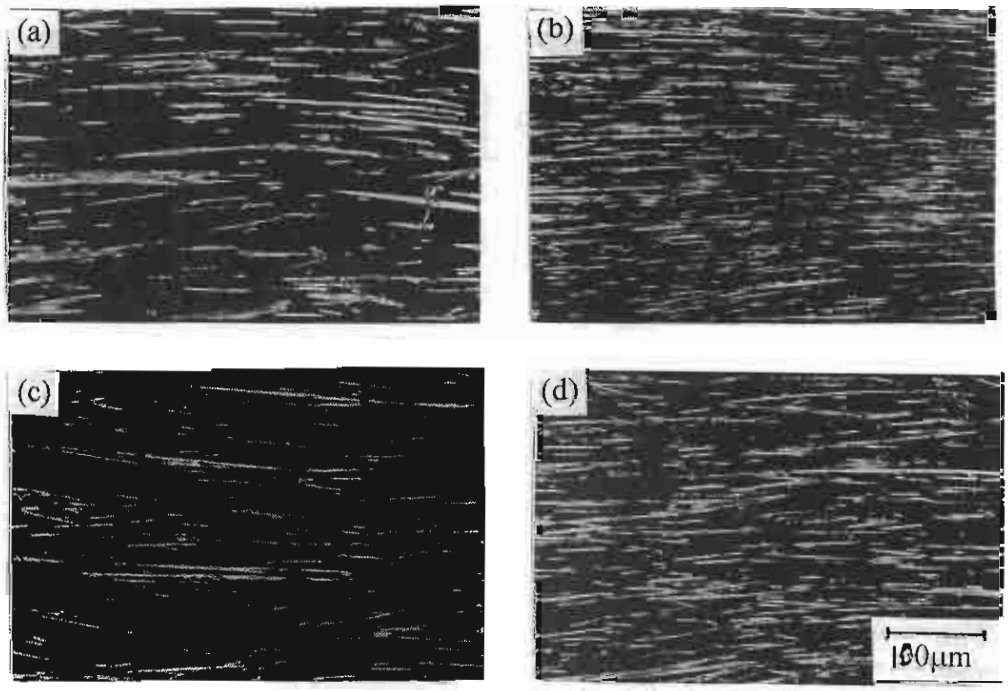

Fig. 8 Optical micrographs of TLCP fibers extracted from PP5/TLCP films containing (a) no compatibilizer, (b) SEBS, (c) EPDM and (d) MA-g-EPDM

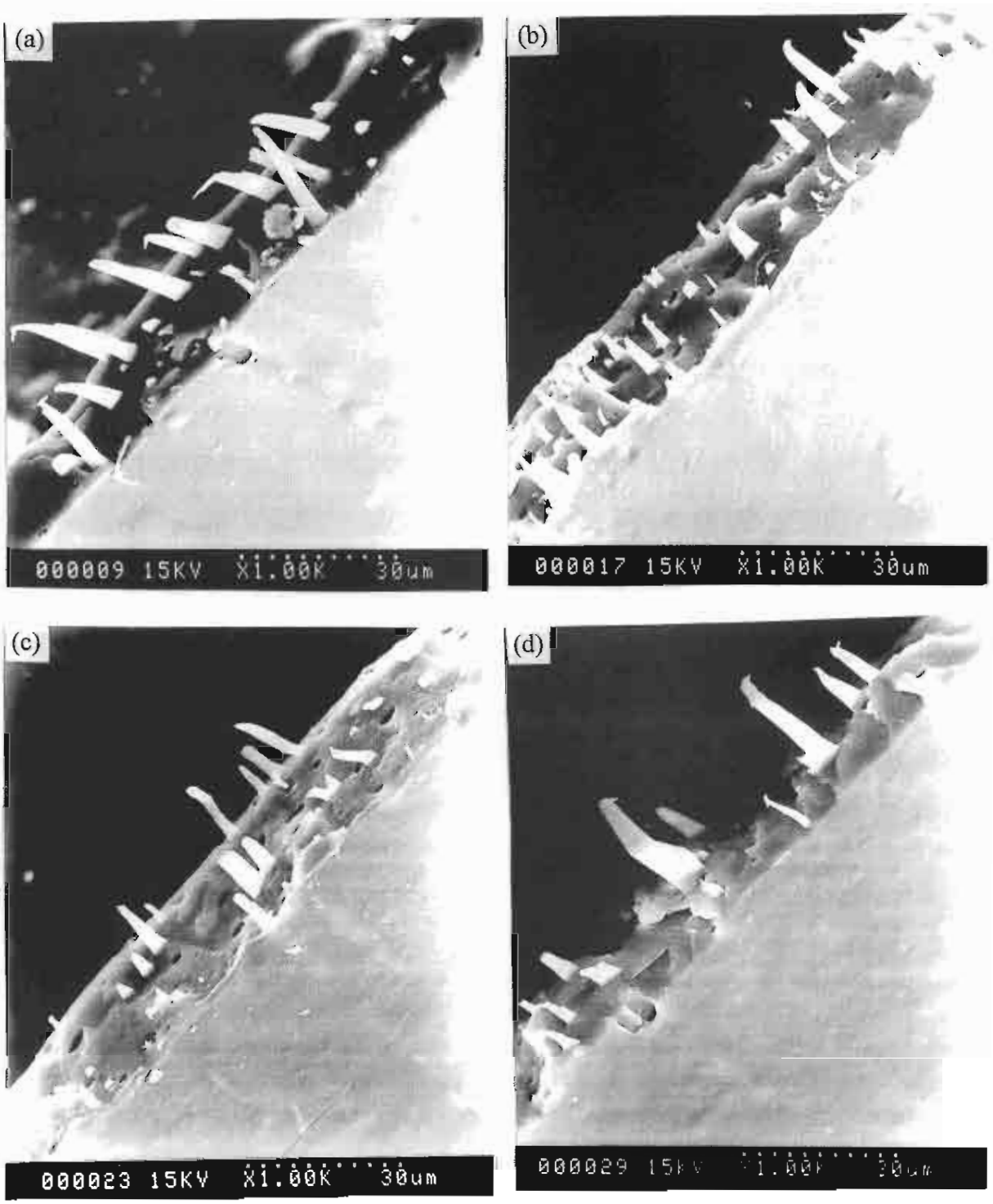

Fig. 9 SEM micrographs of the fracture surface of PP5/TLCP films containing (a) no compatibilizer, (b) SEBS, (c) EPDM and (d) MA-g-EPDM

INTERNATIONAL CONFERENCE ON MATERIALS TECHNOLOGY:
RECENT DEVELOPMENTS AND FUTURE POTENTIAL
9-10 January 1997 Chiang Mai, Thailand

Effect of Surface Treatment on Mechanical Properties of Aramid Pulp-Thermoplastic Elastomer Composites

Teeravut Nakinpong,[1] Taweechai Amornsakchai,[1] Wiriya Meesiri[2] and Sauvarop Bualek[1*]

[1]Department of Chemistry, Faculty of Science, Mahidol University, Rama 6 Road, Bangkok 10400
[2]Directorate of Armament, Royal Thai Air Force, Donmuang, Bangkok 10210

ABSTRACT

Reinforcement of Styrene (Ethylene Butylene) Styrene thermoplastic elastomer (SEBS) with aramid pulp was investigated. As the loading of aramid pulp increased, tensile modulus increased but tensile strength and elongation at break decreased. The observation of fracture surface under Scanning Electron Microscope (SEM) revealed that both fibre fracture and pull-out occured. Surface treatment of the fibre was carried out by alkali hydrolysis and maleic anhydride grafted SEBS was added as a compatibiliser. The blend was prepared by using one step process in an internal mixer. Quantitative analysis of the solvent extracted fibre surface by diffuse reflectance infrared technique showed that in the presence of compatibiliser, higher percentage of rubber was adsorped at the surface. However, the tensile properties of the blends was not improved.

INTRODUCTION

The excellent thermal and mechanical properties of poly (*p*-phenylene terephthalamide) (aramid) fibre make it a good candidate as reinforcement fibre in polymer composites. However, the main problem is the adhesion of the fibres to the polymer matrix. In order to improve adhesion, it is necessary to modify the surface to obtain higher reactivity. Vaughan[1] applied various commercial coupling agents and obtained some improvement on adhesion. Fibre modification by dispersion in an ionomer matrix seemed to be very effective[2,3]. Marom et al.[4] proposed a surface treatment technique using bromine water which led to surface roughening resulting in improvement of interlaminar shear strength. Andreopoulos[5] used various compounds to promote adhesion of aramid fibre and pulp with unsaturated polyester. Treatment of fibre with methacryloyl chloride gave considerably high tensile strength compared to that of untreated fibre. Wang et al.[6] prepared plasma treated aramid fibre - polyethylene composites. The reactive groups such as -COOH, -OH, $-NH_2$ were generated on the aramid fibre surface by oxygen plasma. These groups were used to chemically anchor

* To whom correspondence should be addressed

Preparation of SEBS/Kevlar 49 pulp composites

Samples weight 50 grams of various Kevla pulp/SEBS composites were blended in Haake Rheocord 90 mixer at 165°C rotor speed of 90 rpm for 10 minutes and passed through a two-rol mill twice. The composites were collected promptly and kept in a desiccator in order to mininize moisture adsorption.

Loading of Kevlar pulp was varied from 0, 1, 3, 5, 7 and 10% by weight. The effect of compatibiliser was studied in a composite of 3% of Kevlar in SEBS. The amount of SEBS-g-MA varied from 0, 0.5, 1, 3, 5, 7 and 10% by weight was added to the composites using the same mixing condition.

Extraction of the Composites

A known weight of the composite was extracted in Soxhlet apparatus using toluene as a solvent for 72 hours. The sample was then dried in a vacuum oven at 50 °C. The amount of the bound rubber can be calculated by gravimetric method. The extracted pulp was also characterised by DRIFT.

Mechanical Properties of the Composites

Kevlar 49 pulp/SEBS composites were compression moulded at 180°C for 10 minutes and quenched with cold water. After conditioned for at least 24 hours, tensile specimens were cut with die of size 11.5 cm. x 2.5 cm. x 1 mm.Testing was carried out on an Instron testing machine model 4301 in accordance with ASTM D.638 at a cross head speed of 500 mm/min.

Scanning Electron Microscopy (SEM)

Observation of fibre surface and fracture surfaces of the composite were performed on Hitachi S2500 A thin layer of palladium was coated using Hitachi E102 ion sputter on the specimen to prevent charging on the surface. SEM was operated at 15 kV.

Fracture surface of the composites was prepared by freezing the composite in liquid nitrogen for 5 minutes and then broken rapidly above the surface of liquid nitrogen.

RESULTS AND DISCUSSION

Hydrolysis of Kevlar surface

It is generally known that Kevlar aramid is poly(p-phenylene terephthalamide) or PPTA. The chemical structure of Kevlar is shown below. Pulp product is very short and highly fibrillated fiber having high surface area.

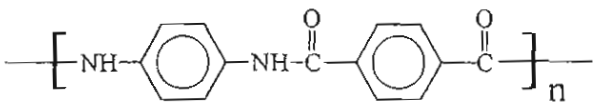

Chemical structure of Kevlar

In this study, Kevlar pulp was partially hydrolised on the surface by using 10% NaOH for 20 minutes to create more -NH_2 and -COOH end groups as indicated in the following reaction.

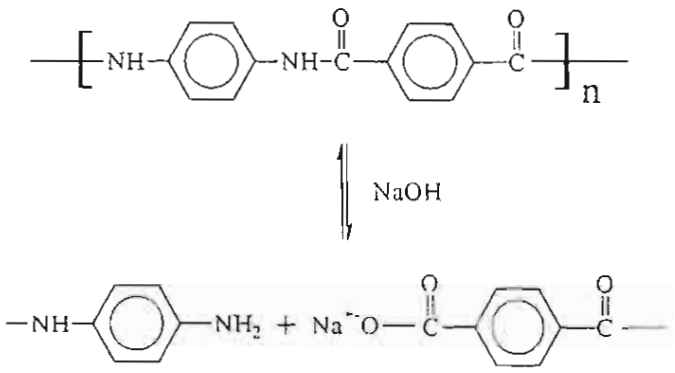

Figure 1 shows infrared spectrum of Kevlar pulp before and after hydrolysis using DRIFT technique. It can be seen that there is a new peak appears at 883 cm^{-1}. The peak is associated with the C-H out of plane bending of aromatic ring next to -COO^-Na^+ substituent as reported by Chatzi.[12] The pulp was thoroughly washed with distilled water, followed by toluene and dried to constant weight at 50°C under vacuum. The resulting pulp had a pale yellow colour. At this stage the 883 cm^{-1} peak disappeared. This can be explained by the fact that washing the pulp with distilled water would change -COO^-Na^+ to -COOH. It was found that the washing step was very important. If care was not taken the resulting pulp would turn dark yellow to brown after storage for a few days. Blending of this dark colour pulp with SEBS elastomer gave rise to a composite with very poor tensile properties.

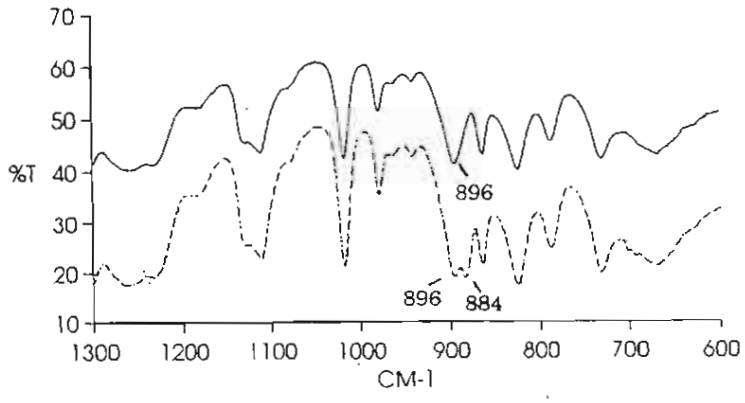

Figure 1. Infrared spectra of Kevlar surface (a) before and (b) after hydrolysis (without washing with water)

Mechanical properties

Tensile properties of Kevlar reinforced SEBS are shown in Figure 2. It can be seen that as the Kevlar loading is increased the tensile strength of the composite decreases. Modulus at 100 and 300% are, on the other hand, increase with increasing Kevlar loading. Elongation at break of the composite was found to drop slightly when Kevlar loading was increased. Beyond 10% Kevlar loading the elongation at break drop sharply. This was found to coincide with the observation of poorly dispersed Kevlar in SEBS.

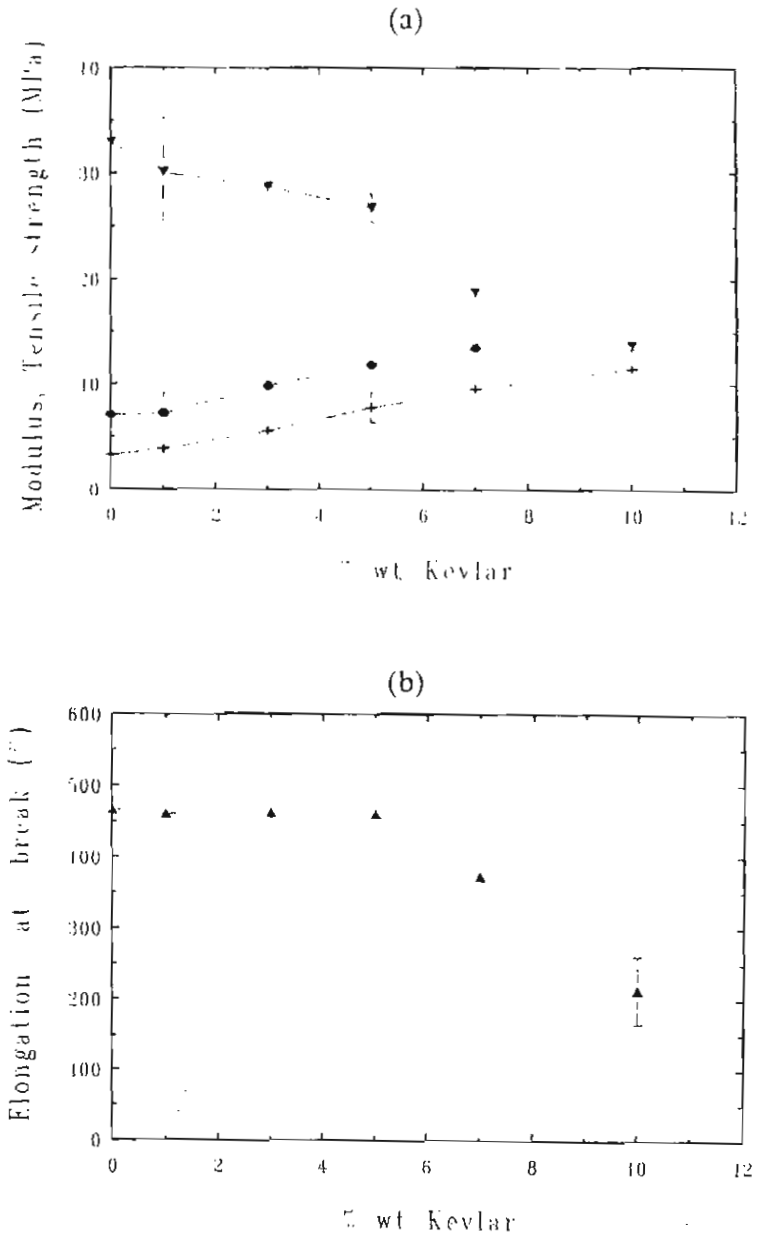

Figure 2 Shows a) Modulus at 100 % (▲), 300% (●) and Tensile strength (▼) and b) Elongation at break of SEBS/Untreated Kevlar composite

An increase in modulus at both 100 and 300% was as expected when pulp of very high modulus Kevlar was incorporated into SEBS elastomer matrix. A monotonic decrease in tensile strength with pulp loading was due to the fact that SEBS could be strain hardened at very high strain. Incorporation of Kevlar pulp could reduce such effect and/or impart weak points, which, at relatively low strain may induce cracks.

Hydrolysis of Kevlar surface was found to have negligible effect on mechanical properties of the composites.

Effect of compatibiliser, SEBS-g-MA, on a composite containing 3% wt. Kevlar can be seen from Figure 3. Two sets of Kevlar were studied, i.e. as received Kevlar and surface hydrolysed Kevlar. It was found that surface hydrolysed Kevlar resulted in a composite with approximately the same mechanical properties to that of untreated Kevlar.

In order to determine how SEBS was adsorbed on Kevlar surface the blends were subjected to extraction with toluene. Since SEBS can be dissolved in toluene at room temperature, it should be completely leached out after extraction for 72 hours at boiling temperature of toluene. Solvent extraction of the composite shows that the amount of bound (unextractable) rubber increases as SEBS-g-MA was added. Without SEBS-g-MA the extracted pulp was found to contain about 2 %wt SEBS whereas the specimen with more than 3 wt% SEBS-g-MA yielded extracted Kevlar containing about 20 %wt of SEBS. This suggests that SEBS-g-MA reacted with active group on the surface of Kevlar. The amount of bound rubber is, however, less than the amount of added SEBS-g-MA. The rest of SEBS-g-MA (unreacted) is likely to disperse in SEBS matrix and could weaken the composite if phase-separation occurs.

Figure 4a shows Infrared spectrum (DRIFT) of SEBS in the range 2500-3500 cm^{-1}. Peaks at 2923 and 2853 cm^{-1} correspond to asymmetric and symmetric stretchings, respectively, of the $-CH_2-$ groups from ethylene block of SEBS. Figure 4b displays Infrared spectrum of as-received Kevlar pulp in the same region. It can be seen that there is a peak at 3320 cm^{-1} which corresponds to intermolecular hydrogen bonding in Kevlar. The Infrared spectra of the extracted pulp from specimen containing 3% wt. Kevlar without and with 3% wt. SEBS-g-MA, are shown in Figures 4c and 4d, respectively, displaying both typical peaks of SEBS and Kevlar. The ratio of the peak at two positions clearly show the higher percentage of SEBS on the Kevlar surface as SEBS-g-MA was added.

Solvent extraction and spectroscopic evidences clearly suggest that the compatibiliser, SEBS-g-MA, reacted with Kevlar. The mechanical properties of the blends are, however, not improved. Ishihara et al.[14] reported that, for poly (ethylene terephthalate) - hydrogenated styrene-isoprene triblock copolymer (PET-SEPS) composite, treatment of PET fibre improved tensile strength in the fibre direction significantly. Tensile strength in the transverse direction was, however, not affected. It seems that in our composite Kevlar pulp distributes randomly hence no significant improvement on mechanical properties. Additional measurements of mechanical properties of the composites in the direction parallel and transverse to machine direction (two-roll mill) were found to be the same.

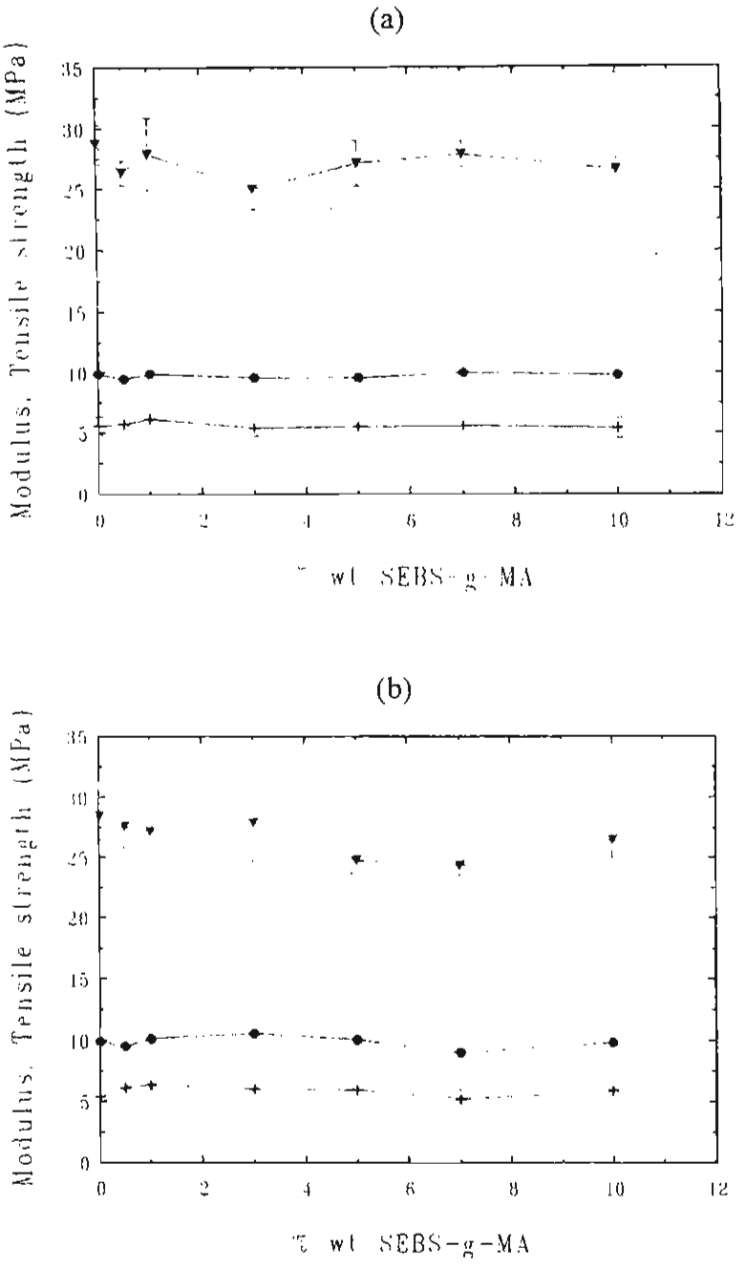

Figure 3 Shows effect of SEBS-g-MA on modulus at 100% (✚), 300% (●) and Tensile strength (▼)of (a) SEBS/Untreated Kevlar composite and (b) SEBS/Treated Kevlar composite

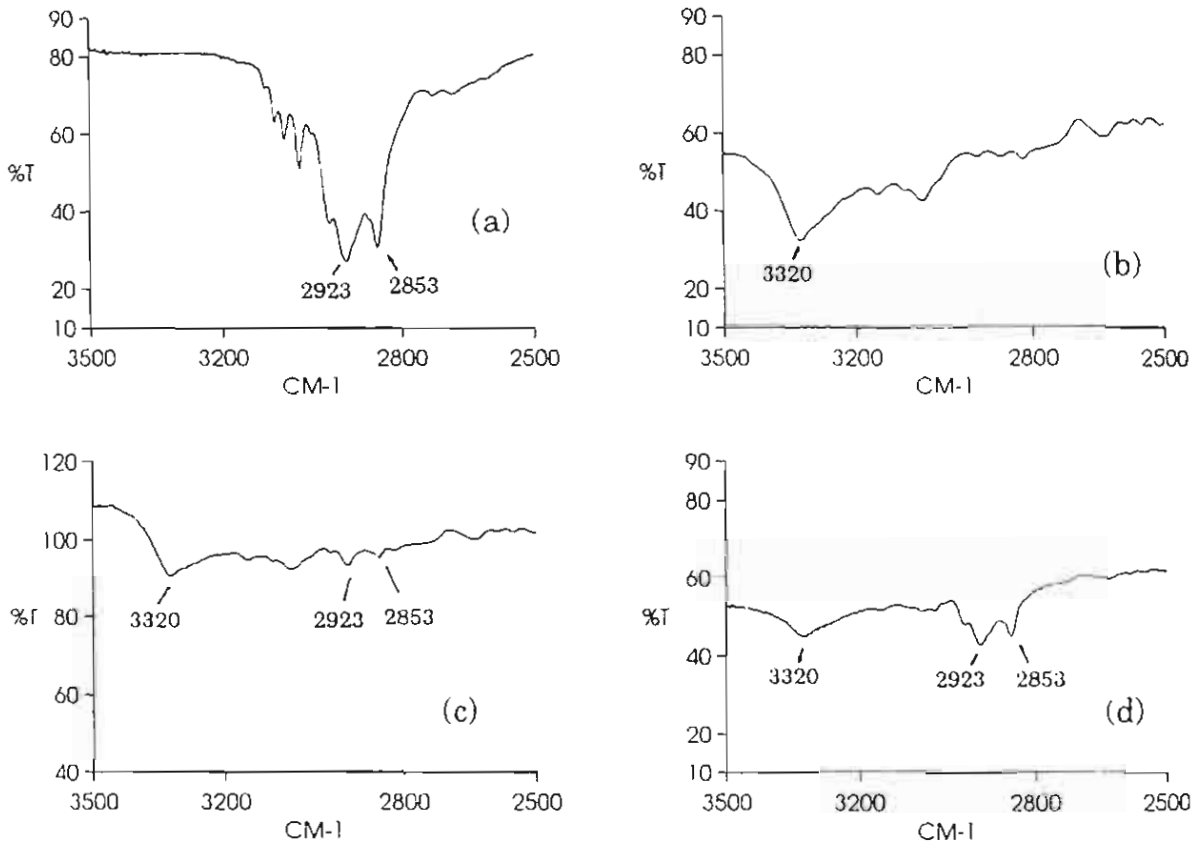

Figure 4 Shows spectra of extracted samples of (a) SEBS pure, (b) Kevlar, (c) SEBS/Kevlar and (d) SEBS/SEBS-g-MA/Kevlar

Morphology

Fracture surfaces of composites with and without compatibiliser are shown in Figure 5. Detail investigation of the photographs reveal very much different fracture charactersitics of the two systems. Composite with compatibiliser exhibits mostly fibre breakage whereas composite without compatibiliser exhibits both fibre pull out and breakage. Fibre pull-out in the latter case seems to be dominate. This evidence confirms that the compatibiliser, SEBS-g-MA, improves the adhesion between fibre and matrix.

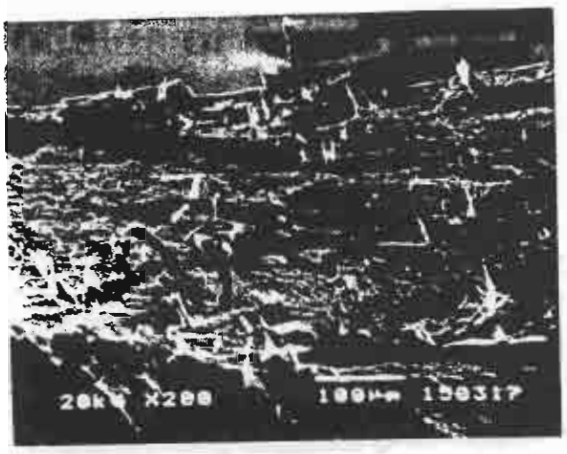

(a)

(b)

Figure 5 SEM micrographs of
a) SEBS/Kevlar (97/3)
b) SEBS/SEBS-g-MA/Kevlar (94/3/3)

CONCLUSIONS

The above results can lead to the following conclusions:

1. No significant difference in tensile properties could be observed from composites of treated and untreated Kevlar pulp.
2. Moduli at 100 and 300% of the composites increase as the loading of Kevlar increase. However, beyond 10%wt of Kevlar loading the dispersion is poor and as a result the elongation at break drops sharply.
3. From gravimetric measurement and DRIFT, it was found that higher amount of SEBS adhered at the surface of Kevlar pulp as SEBS-g-MA was added. However, the mechanical properties of the composites containing SEBS-g-MA is not affected. This is attributed to random orientation of Kevlar pulp.
4. SEM micrographs of fracture surface of the composite showing both pull-out and breakage of the long fibre.

ACKNOWLEDGEMENT

Support of this work by The Thailand Research Fund is greatfully acknowledged. The authors also would like to thank the Shell Chemical Co. and the E.I. Du Pont Co. for supplying SEBS and Kevlar pulp respectively.

REFERENCES

1. D.J. Vaughan, Polym. Eng. Sci., **18**, 167-169 (1978)
2. M. Takayanaki, T. Kajiyama and T. Katayose, J. Appl. Polym. Sci., **27**, 3903-3917 (1982)
3. M. Takayanaki and T. Katayose, Polym. Eng. Sci., **24**, 1047-1050 (1984)
4. M. Breznick, J. Banhaji, H. Guttmann and G. Marom, Polym. Commun., **28**, 55-56 (1987)
5. A.G. Andreopoulos, J. Appl. Polym. Sci., **38**, 1053-1064 (1989)
6. Q. Wang, S. Kaliaguine and A. Ait-Kadi, J. Appl. Sci., **48**, 121-136 (1993)
7. Z. Yu, A. Ait-Kadi and J. Brisson, Polym. Eng. Sci., **31**, 1222-1227 (1991)
8. W. Guo and M. Ashida, J. Appl. Polym. Sci., 49, 1081-1091 (1993)
9. M. Ashida and T. Noguchi, J. Appl. Polym. Sci., **29**, 4107-4114 (1984)
10. M. Ashida and T. Noguchi, J. Appl. Polym. Sci., **29**, 661-670 (1984)
11. M. Ashida, T. Noguchi and S. Mashimo, J. Appl. Polym. Sci., **30**, 1011-1021 (1985)
12. J. Modic and I.A. Pottick, Polym. Eng. Sci., **33**, 819-826 (1993)
13. E.G. Chatzi, S.L. Tidrick and J.L. Koenig, J. Polym. Sci. **B26**, 1585-1593 (1988)
14. M. Ishihara, A. Nagatani, M. Mori, J. Okumura and K. Yamaguchi, Proceeding of International Rubber Conference, IRC 95, Kobe, 319-322 (1995)
15. M. Panar, P. Avakian, R.C. Blume, K.H. Gardner, T.D. Gierke and H.H. Yang, J. Polym. Sci. Polym. Phys. Edn., **21**, 1955-1969 (1983)

Thermoplastics-Liquid Crystalline Polymer Blends: Processing, Characterisation and Properties of *in situ* Composite Films

Sauvarop Bualek-Limcharoen,[1*] Jareerat Samran,[1] Wiriya Mecsiri[2]
and Taweechai Amornsakchai[1]

[1]Department of Chemistry, Faculty of Science, Mahidol University, Rama 6 Road, Bangkok 10400, Thailand
[2]Directorate of Armament, Royal Thai Air Force, Donmuang, Bangkok 10210 Thailand

ABSTRACT

Blends of thermoplastics, polypropylene with liquid crystalline polymer (Rodrun LC3000), were prepared using twin screw extruder. Pellets of polymer blend were extruded through a microtruder as cast films. Processing parameters were varied in order to obtain the best tensile properties. Styrene ethylene butylene styrene (SEBS) was used as a compatibiliser. It was observed that this compatibiliser enhanced the modulus of the films in both machine and transverse directions. The order parameter of liquid crystalline domain, evaluated from infrared dichroism, was found to increase in the presence of compatibiliser indicating better molecular orientation. Morphology of the film was investigated under optical microscope.

INTRODUCTION

Blends of thermotropic liquid crystalline polymer (LCP) and thermoplastics (TP) have drawn high attention from several research groups due to its superior rheological and mechanical properties. Recent review articles on this subject are given by Dutta,[1] Brown[2] and Handlos.[3] Processing of incompatible TP/LCP blend under elongational flow is known to create the oriented fibres of LCP phase. The word '*in situ* composite' has been coined[4] for this kind of blend which means self-reinforcement due to the fibres formed during processing. Mostly, the *in situ* composites produced by fibre spinning give higher modulus than in the form of sheet or

---

* To whom correspondence should be addressed

film,[5] because the elongational force is more effective for producing fibrillar structure. However, *in situ* composite film is recently becoming interesting for application such as film for high strength balloon.[6] The main problem of LCP blend system is the high degree of anisotropy of its mechanical properties, i.e. the properties measured in the machine direction (MD) and transverse direction (TD) are different. Chinsirikul et al.[7] tried to reduce such anisotropic properties using counter-rotating die technique for film extrusion.

Blend of polypropylene and LCP produced by means of extruded strand and injection molding using maleic anhydride grafted polypropylene (PP-g-MA) as compatibiliser has been investigated by Baird *et al.*[8-9] An enhancement of modulus of about 25 % was found for specimens in the form of injected tensile bar containing LCP (Vectra A) 20%, while there was no statistical change in the modulus of PP/LC3000 (70/30) with addition of PP-g-MA. In the first case, addition of compatibiliser causes more finely dispersed fibrillar structure of LCP than that in specimen without compatibiliser and therefore tensile strength and modulus are improved.

The objective of this work is to improve the mechanical properties of *in situ* composite produced in the form of film of polypropylene/LCP using thermoplastic elastomer as a compatibiliser. A fixed amount of 10wt% Rodrun LC3000 in polypropylene was used for production of film by extrusion casting. Concentration of compatibiliser was varied. Cast films were characterized in terms of morphology and mechanical properties. The order parameter of LCP phase was determined from polarized infrared spectra of the films.

EXPERIMENTAL

Materials

Thermoplastic polymer matrix used in this study was polypropylene (PP) injection grade 6331 from HMC Co., Ltd. Thermotropic liquid crystalline polymer was a copolyester composed of 60 mol% of p-hydroxybenzoic acid and 40 mol% of poly(ethylene terephthalate) (Rodrun LC3000) purchased from Unitika Company. A triblock copolymer thermoplastic elastomer of styrene ethylene butylene styrene (SEBS, styrene/rubber ratio 29/71, Kraton G-1652) was provided by Shell Chemical Co.. The materials were vacuum dried at 60°C for 12 h before mixing.

Blending

Melt blending of PP and 10%wt LCP was performed using co-rotating twin screw extruder (PRISM TSE-16TC) with a screw diameter of 16 mm, L/D = 25, intermeshing, and extrusion rate of 150 rpm. The temperature profile was 180/220/220/225/225°C, representing temperatures at hopper zone, three barrel zones and heating zone in die head, respectively. Strand exiting the extruder was immediately quenched in a water bath and subsequently pelletized.

Extrusion Film Casting

PP/LCP blend pellets were extruded using a 16 mm mini-extruder (Randcastle RCP-0625) equipped with a cast film line. Temperatures at hopper zone, two barrel zones and at slit-die were 190/220/230/240°C, respectively. Screw speed was 70 rpm. The gap of the die lip was adjusted at 0.65 mm and the width fixed at 152 mm. Extruded film was drawn down in the molten state upon exiting die outlet, and quenched on water-cooled roll. The film draw ratio, defined as the ratio of die separation to the thickness of the extruded film, was controlled by varying take-off speed at 1.6, 3.8 and 6.4 m min^{-1} which gave rise to the draw ratios of 9.3, 18.6 and 32.5, respectively. Film thickness obtained was in the range 20 - 70 μm.

Tensile testing

Tensile testing was conducted using an Instron mechanical tester (model 4301), with grip length of 25 mm, crosshead speed of 50 mm min^{-1} and a full scale load of 10N. Tensile properties of the dumbbell-shape specimens (70 mm long, 4 mm wide and 20 -70 μm thick) were measured in the flow (machine) and transverse directions (ASTM D412). For each specimen, the averaged value and the standard deviation of the tensile properties were calculated using at least ten samples.

Morphology

Morphology of the thin composite films could be directly observed under a polarized optical microscope (Nikon 70562) at the magnification range of 100 to 400 times. The fibre aspect ratio (length to diameter ratio) was determined by averaging the values measured from several photomicrographs.

Measurement of order parameter

Order parameter (S) is defined as the degree of alignment of liquid crystal molecules with the preferred direction,[10]

$$S = 0.5 \langle 3\cos^2\theta - 1 \rangle \qquad (1)$$

where θ is the angle between the axis of mesogenic unit and the prefered direction of nematic phase. Infrared dichroism is one of the techniques used to determine the order parameter.[11-13] Absorbance values were measured: $A_{\parallel}$ and $A_{\perp}$ for plane polarized light with the electric vector parallel and perpendicular to the preferred direction, respectively. The dichroic ratio R, defined as $R = A_{\parallel}/A_{\perp}$, for a particular absorption band is used to calculate the order parameter from the following equation:

$$S = \frac{(R-1)}{(R+2)} \frac{1}{0.5(3\cos^2\alpha - 1)} \qquad (2)$$

where α is the angle between the transition moment and the molecular axis. This is reduced to

$$S = (R-1)/(R+2) \qquad \text{where } R > 1 \qquad (3)$$

for a band whose transition moment is parallel to the major molecular axis (parallel transition moment) and

$$S = 2(1-R)/(R+2) \qquad \text{where } R < 1 \qquad (4)$$

for a band whose transition moment is perpendicular to the long molecular axis (perpendicular transition moment).

Order parameter of the LCP phase in PP/LCP blend was evaluated from the IR absorption spectra measured using Perkin-Elmer FTIR (system 2000) with an aluminium wire-grid polarizer placed between sample and the light source. The FTIR spectra were recorded at the polarization directions of the polarizer parallel and perpendicular to the machine direction of the film (see Fig. 1). Area under the peak at 1601.5 cm^{-1}, (C-C stretching vibration of para-substituted benzene ring of p-hydroxybenzoic acid) corresponding to the parallel transiton moment, was used to evaluate the order parameter of LCP in equation (3).

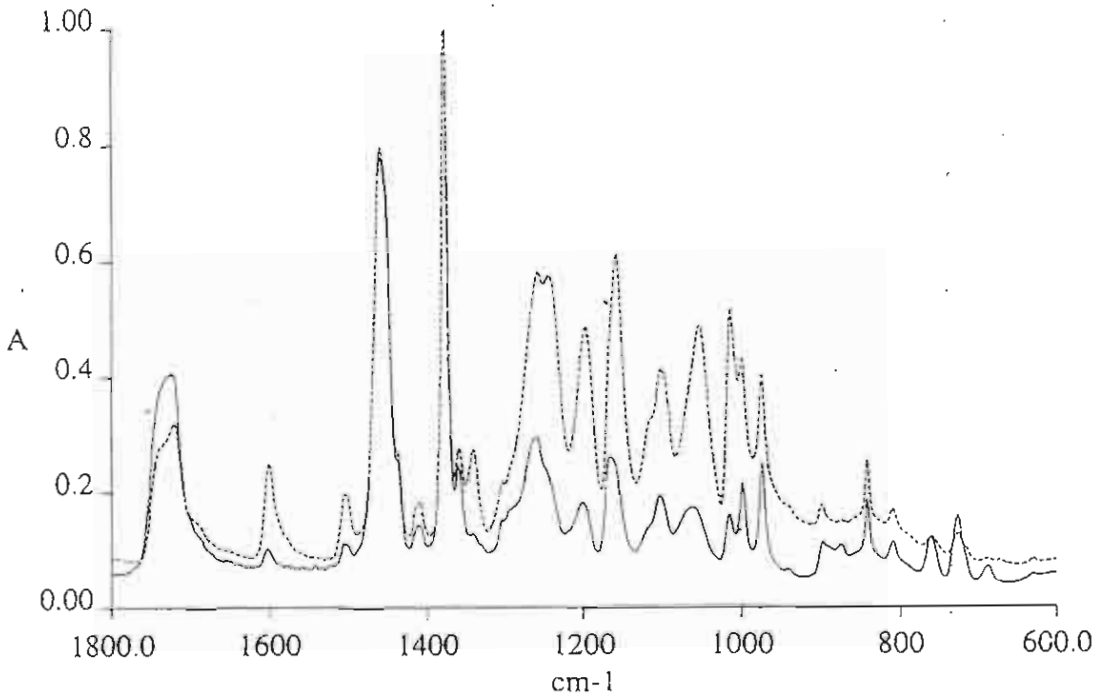

Fig. 1 Polarized IR absorption spectra of PP/LCP recorded at the positions of polarizer parallel (------) and perpendicular (——) to machine direction of the film.

RESULTS AND DISCUSSION

All composites in this study are composed of 10 wt% LCP in polypropylene matrix. In order to obtain the best processing condition, screw speed and take-off speed for film production were varied. Tensile properties of composite specimens were measured and used as criteria in this optimization. The optimum processing parameters for film extrusion were 70-rpm screw speed, and 6.4 m min^{-1} take-off speed which gave rise to the film draw ratio of 32.5. The amount of compatibiliser was varied from 0 to 8 wt%. Tensile properties, morphology and order parameter of the composite films are presented below.

Tensile properties

Tensile properties of films of pure PP, PP/LCP, and PP/LCP/SEBS with varied amount of SEBS are listed in Table 1. The reported properties include Young's modulus, yield stress, ultimate tensile strength, and elongation at break, in machine direction (MD) and transverse direction (TD).

Table 1. Tensile properties PP, PP/LCP and compatibilized composite films with varying concentration (wt%) of SEBS, measured in machine direction (MD) and transverse direction (TD). Standard deviations are given in parentheses.

Film	Young's Modulus (MPa)		Yield Stress (MPa)		Strength (MPa)		Elongation at Break (%)	
	MD	TD	MD	TD	MD	TD	MD	TD
PP pure	616	586	20.2	15.4	34.4	21.6	678	546
	(66)	(44)	(1.4)	(1.5)	(3.2)	(1.6)	(60)	(85)
PP/LCP	1091	649	27.0	20.0	31.7	25.0	557	556
	(50)	(31)	(0.6)	(1.1)	(2.3)	(1.5)	(77)	(67)
PP/LCP/1.5% SEBS	1491	828	28.7	18.7	24.1	16.7	466	606
	(35)	(44)	(0.8)	(0.8)	(3.7)	(3.1)	(54)	(69)
PP/LCP/3.0% SEBS	1592	687	28.7	17.1	29.1	22.3	533	657
	(45)	(20)	(1.1)	(0.6)	(2.6)	(2.2)	(59)	(65)
PP/LCP/4.5% SEBS	1450	645	29.4	17.6	26.8	22.1	504	618
	(57)	(50)	(1.3)	(0.7)	(3.1)	(2.2)	(68)	(68)
PP/LCP/6.0% SEBS	1299	617	25.0	15.7	28.0	18.0	489	566
	(52)	(34)	(1.5)	(0.7)	(2.9)	(1.9)	(75)	(59)
PP/LCP/8.0% SEBS	1236	605	25.6	16.9	25.1	20.5	471	586
	(67)	(38)	(1.2)	(0.6)	(3.8)	(2.8)	(47)	(81)

Pure polypropylene film produced using the same processing condition as PP/LCP composite, exhibits isotropic modulus, i.e., the modulus in both machine and transverse directions are nearly equal. The modulus of the composite PP/LCP film in the machine direction is about 100% higher than that of the pure PP, but remains about the same in the transverse direction. Yield stresses measured in both directions are somewhat higher for the composites than the pure PP. The difference in yield stress of the composite measured in MD and TD directions are larger than that of PP film, suggesting the different morphology of the composite possesses. Observation through a microscope revealed ends of LCP fibre with small radius of curvature which could act as stress raiser when the composite is being

stressed perpendicularly to the major axis of the dispersed phase. The anisotropy of yield stress of composite films will therefore be higher than that of polypropylene. Ultimate tensile strength of PP presented in Table 1 is the highest compared to the composite films due to the weaker attractive forces at the interface of different phases in the latter. Addition of SEBS results in similar trends of the value of ultimate tensile strength as the yield stress. The value of elongation at break is, on the other hand, not much affected by the presence of compatibiliser.

The addition of SEBS enhanced MD modulus of the composite in all cases. The maximum value of MD modulus is found at 3 wt% of SEBS, exhibiting an enhancement of 46% over the composite without compatibiliser (1,091 MPa vs. 1,592 MPa). However, TD modulus is maximized at 1.5 wt% SEBS, and where the lowest degree of anisotropy in modulus is observed. The results are quite surprising in that such a soft elastomer like SEBS can improve the modulus of the composite films. Since SEBS is a triblock copolymer with two styrene blocks at the ends and ethylene/butylene block in the middle, it is expected that the two ends containing aromatic rings be compatible with LCP phase, while the rubbery EB block be compatible with the PP matrix. Accordingly, SEBS should be present at the interface to promote interfacial adhesion and to help disperse the LCP phase. However, increasing of SEBS to higher than 3wt% cause a reduction in modulus. As often found in the other compatibilising systems,[14-15] if the amount of compatibiliser on the interface exceeds the saturation limit (critical micelle concentration), phase separation of compatibiliser can take place, forming separate micelles and resulting in overall decrease in properties of polymer blend.

Morphology

Effect of the film draw ratio

The optical micrographs shown in Figure 2a and 2b are obtained from the films produced at the draw ratios of 9.3 and 32.5, respectively. It can be clearly seen that as the draw ratio increases LCP fibres become more elongated, i.e. the fibre aspect ratio is increased. In addition, the frozen schlieren texture of nematic phase within LCP fibres of the film taken at the lowest draw ratio (Fig. 2a) shows inhomogeniety of orientation of LCP domains, whereas the textures of LCP fibre in Fig. 2b is more homogenous than that in Fig.2a, indicating better orientation of LCP molecules.

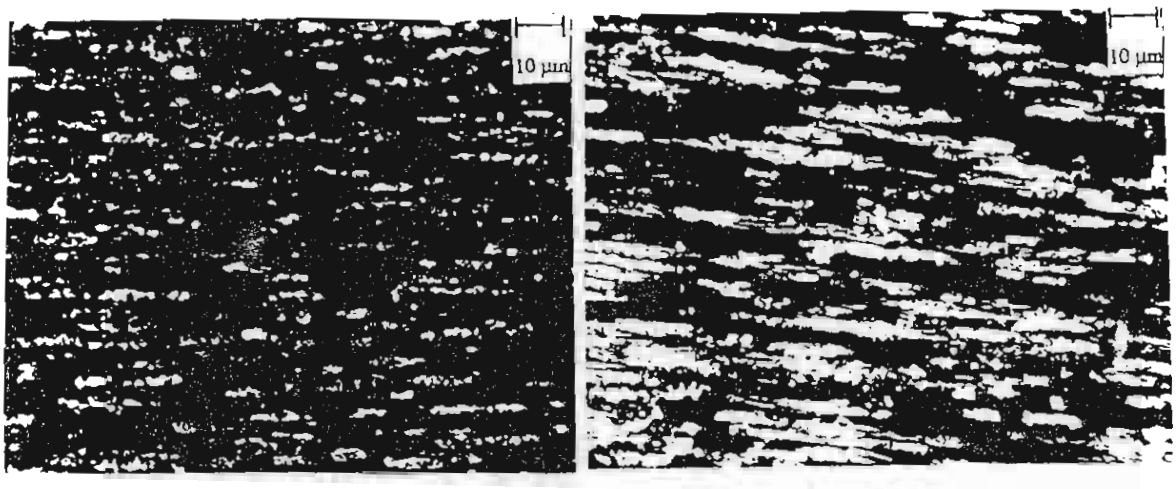

(a) (b)

Fig. 2 Optical micrographs of PP/LCP films produced at the draw ratio of
(a) 9.3 (b) 32.5

Effect of compatibiliser

The micrographs shown in Fig. 3a and 3b are taken from the films with the draw ratio of 32.5. These are obtained from the composite films without and with 3% SEBS compatibiliser, respectively. It is clear that number density as well as aspect ratio of LCP fibres increase with addition of SEBS. The addition of compatibiliser results in more finely dispersed fibrillar structure of LCP phase and hence higher number of fibre formed. The result of addition of SEBS is therefore similar to the effect of increasing fibre loading giving rise to enhancement of modulus as shown in Table 1. In addition to the shape of the dispersed LCP fibre, the texture with characteristic birefringence of frozen nematic phase in LCP domains was also different. Without compatibiliser, LCP phase exhibits birefringence with more inhomogeneous texture than that in the case with compatibiliser, indicating better molecular orientations of the LCP domains in the latter case.

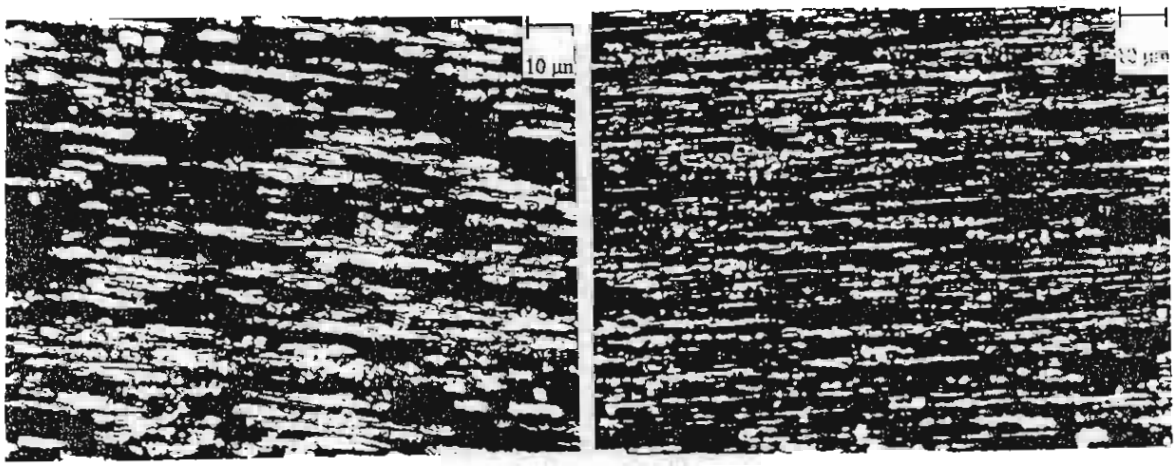

(a) (b)

Fig. 3 Morphology of *in situ* composite films of PP/LCP by polarizing microscope (cross polarizers) produced at the draw ratio of 32.5.
(a) composite without compatibiliser (b) composite containing 3wt% SEBS

Order Parameter

As it is well known for the *in-situ* composite, that LCP phase can be elongated to give a reinforced material with improved mechanical properties. Degree of molecular alignment within the LCP domains is the intrinsic properties of the fibres which determine its stiffness. Order parameter of LCP phase ought to be one of the parameter determining the nature of LCP fibres. Order parameters calculated from the dichroism of the films produced at the draw ratio 32.5, containing various concentrations of SEBS are listed in Table 2. It is evident that the order parameter somewhat increases with addition of compatibiliser (from 0.52 to 0.62). However, increasing of the amount of SEBS shows no more remarkable effect. This result agrees well with the observation through optical microscope showing more homogeneous texture of LCP phase in the presence of compatibiliser. The range of aspect ratio of LCP fibres formed is also given in Table 2. Although the value of fibre aspect ratio reduced from 75-150 for the film without compatibiliser to 69-113 for the film with 3% SEBS, modulus of the film with compatibiliser do increase (see Table 1). The effect of lowering of aspect ratio is not pronounced in this case because the value of aspect

ratio in the range 69-113 is sufficiently large for reinforcement. Another effect which should be more pronounced is the larger number of fibres formed in the presence of compatibiliser. This effect is similar to the effect of increasing fibre loading giving rise to enhancement of modulus.

Table 2 Order parameters and aspect ratios of composite PP/LCP films produced at the draw ratio of 32.5, containing various amounts of SEBS

SEBS content (wt%)	Aspect ratio	Order parameter (S)
0	75-150	0.52
1.5	69-108	0.62
3.0	69-113	0.59
4.5	50-80	0.57
6.0	56-89	0.58
8.0	50-90	0.61

CONCLUSION

Thermoplastic elastomer, SEBS, used as a compatibiliser for PP/LCP film, an *in-situ* composite, gave rise to enhancement of modulus. Tensile properties of the composite are governed by the morphology, i.e., the aspect ratio of the LCP dispersed phase as well as the degree of dispersion of fibres which can be improved by addition of an elastomeric compatibiliser. Such effect was also observed recently by Seo[16] for Nylon 6/LCP blend using maleic anhydride grafted ethylene propylene diene rubber (EPDM). The order parameter of the LCP domains which can be simply determined by FTIR spectroscopic technique is one of the parameters indicating the degree of orientation of LCP fibres which affect tensile properties of the composites.

ACKNOWLEDGEMENT

Support of this work by The Thailand Research Fund is gratefully acknowledged. The authors also would like to thank the Shell Chemical Co. for providing a free sample of SEBS.

REFERENCES

1. Dutta, D., Fruitwala, H., Kohli, A. and Weiss, R. A. Polym.Eng. Sci.,1990, 30, 1005
2 Brown, C. S. and Alder, P. T. in Polymer Blends and Alloys, Folkes, M. J. and Hope. P.S. Eds., Blackie Academic & Professional, Glasgow 1993
3 Handlos, A. A. and Baird, D. G. J. M. S. Rev. Macromol. Chem.Phys., 1995 C35,183
4 Kiss, G. Polym. Eng, Sci., 1987, 27, 410
5 Crevecoeur, G. and Groeninckx, G. Polym. Eng. Sci., 1993, 33, 937
6 Hsu, T. C., Lichkus, A. M. and Harrison, I. R. Polym. Eng. Sci. 1993, 33, 860
7 Chinsirikul, W., Hsu, T. C., and Harrison, I. R. Polym. Eng. Sci. 1996, 36, 2708
8 Datta, A. and Baird, D. G. Polymer, 1995, 36, 505
9 O'Donnell, H. J. and Baird, D. G. Polymer, 1995, 36, 3133
10 Saupe, A. and Maier, W. Z. Naturforsch.,1961, 16a, 816
11 Kelker, H. Hatz, R. and Wirzing, G. Z. Anal. Chem., 1973, 267,161
12 Chingduang, P., Bualek, S., Phaovibul, O. and Schrader, B. Mol. Cryst. Liq. Cryst., 1986, 132, 131
13 Kaito, A., Kyotani, M. and Nakayama, K. Macromolecules 1991, 24, 3244
14 Coran, A. Y. and Patel, R. Rubber Chem. Tech. 1983. 56, 1045
15 Asaletha, R. and Thomas, S. Rubber Chem. Tech. 1995, 68, 671
16 Seo, Y., J. Appl. Polym. Sci. 1997, 64, 359

Aramid Fibres-Thermoplastic Elastomer Composites: I. Properties of Composites Using Maleic Anhydride Grafted Compatibiliser

TAWEECHAI AMORNSAKCHAI[1], WIRIYA MEESIRI[2], TEERAVUT NAKINPONG[1], BUDSAPORN SINPATANAPAN[1] AND SAUVAROP BUALEK-LIMCHAROEN[1]
[1]Department of Chemistry, Faculty of Science, Mahidol University, Rama 6 Rd, Bangkok 10400 THAILAND.
[2]Directorate of Armament, Thai Royal Airforce, Bangkok, THAILAND.

Composites of SEBS containing short aramid fibres were studied. Three types of fibres which include Kevlar, Conex and Technora, were used. Firstly, the fibres were used as-received. It was found that for all types of fibres, the modulus at 100% strain increased with increasing fibre content and there was no different between the type of loaded fibres. For modulus at 300% strain, similar trend was still seen with Kevlar-SEBS exhibits approximately 50% higher moduli than those of Conex and Technora-SEBS composites. Tensile strength of Kevlar-SEBS composites increased slightly with increasing fibre content and drop off above 5%. Tensile strengths of Conex and Technora-SEBS composites, however, decreased with increasing fibre content and lower than that of Kevlar-SEBS composites at all compositions. Secondly, attempt was made to improve the interfacial adhesion between fibres and matrix by modifying the fibre surface using alkali hydrolysis to increase the number of active end groups on fibre surface. These active end groups could then be able to react with maleic anhydride grafted SEBS (SEBS-g-MA) which was used as a compatibiliser. It was found that surface hydrolysis and compatibiliser has little effect on moduli at 100 and 300% strain of the composites. Tensile strength of compatibilised Kevlar and Technora-SEBS decreased slightly with increasing the content of SEBS-g-MA. However, significant improvement of tensile strength was observed for compatibilised Conex-SEBS composites. The tensile strength of compatibilised Conex-SEBS composites reached that of compatibilised Kevlar-composites at SEBS-g-MA content above 5%.

INTRODUCTION

Polymer composites using aramid fibre (e.g. Kevlar, Conex, Technora) as reinforcement exhibit excellent thermal and mechanical properties. However, problems due to poor adhesion between the fibre and polymer matrix still remain to be solved. Researchers have carried out different techniques to obtain desired properties. Vaughan[1] applied various commercial coupling agents to composite mixtures and obtained improved adhesion. Other techniques involving modification of fibre reinforcement by dispersion in an ionomer matrix seemed to be very effective[2,3]. Marom *et al.*[4] proposed a technique using bromine water to roughen fibre surface which resulted in improved interlaminar shear strength. Andreopoulos[5] used methacryloyl chloride, an adhesion-promoting compound, to treat Kevlar fibre in an unsaturated polyester matrix and obtained higher tensile strength than the composite without such compound. In another surface modification technique, Wang *et al.*[6] prepared plasma-treated aramid fibre/polyethylene composites. Oxygen plasma was used to generate reactive groups such as -COOH, -OH, $-NH_2$ on the fibre surface. The reactive groups were used to chemically anchor Ziegler-Natta catalyst and followed ethylene polymerization on the surface.. Yu *et al.*[7] reported works on nylon/Kevlar composites using various fibre surface treatment methods including hydrolysis, and hydrolysis followed by acid chloride grafting. The composites exhibited better mechanical properties compared to composites with unmodified fibre.

Short-fibre reinforced elastomer has only recently attracted several researching groups[8-12]. Reinforcement used in these works involved conventional fibres like poly(ethylene terephthalate) (PET), and nylon. It is, therefore, quite logical to includes such high-performance fibre like aramid in this type of composite.

In the present work, Styrene (Ethylene Butylene) Styrene (SEBS) represented a model thermoplastic elastomer to be reinforced by organic aramid fibres including Conex, Technora, and Kevlar. On a molecular level these two components are quite incompatible. The incompatibility arises from the relatively non-polar olefinic and styrenic blocks in SEBS and the highly polar hydrogen-bonded amide groups in aramid fibres. To improve compatibility, partial hydrolysis of amide group, followed by the addition of maleic anhydride grafted SEBS (SEBS-g-MA), used as a compatibiliser, were carried out. The treatment should introduce imide groups due to the reaction of maleic anhydride and amine groups on the fibre surface similar to other report[13]. The resulted composites were expected to exhibit improved adhesion between the components and thus provide better mechanical properties.

EXPERIMENTAL

Materials

The materials used in this study are summerized in Table 1. Mechanical properties of the fibres are shown in Table 2.

Hydrolysis of Aramid Fibre

The as-received aramid fibre was washed with distilled water, followed by acetone, and dried in a vacuum oven at 50°C for 24 h. Hydrolysis was carried out by dispersing about 10 grams of fibre in 400 ml of 10% sodium hydroxide aqueous solution at ambient temperature for 20 min. After hydrolysis, the fibre was thoroughly washed with distilled water, followed by toluene, and dried in a vacuum oven at 50°C for 48 h. The dried fibre was stored in a desiccator prior to use.

FTIR Characterisation

An FTIR spectrometer with a DRIFT attachment (Diffuse Reflectance Infrared Fourier Transform spectrometer, Perkin Elmer PE 2000) was used to probe the surface of fibre before and after hydrolysis. Each spectrum was obtained from 200 scans at 4 cm^{-1} resolution.

TABLE 1. MATERIALS USED FOR THIS STUDY.

Materials (Commercial designation)	Specification	Manufacturer
Styrene (Ethylene Butylene) Styrene (SEBS, Kraton G 1652)	29% styrene Mw S-block = 7200 Mw EB-block = 37500	Shell Chemical Co.
SEBS grafted with maleic anhydride (SEBS-g-MA, Kraton FG 1901x)	29% styrene 1.84 wt% MA	Shell Chemical Co.
Poly-*p*-phenylene terephthalamide (Kevlar) pulp	length = 2 mm.	Du Pont Co.
Poly-*m*-phenylene isophthalamide (Conex) short fibre	length = 3 mm.	Teijin Ltd.
Poly-*p*-phenylene-3,4′-oxydiphenylene terephthalamide (Technora) short fibre	length = 3 mm.	Teijin Ltd.

TABLE 2. TENSILE PROPERTIES OF ARAMID LONG FIBRES[14]

Properties	Kevlar	Conex	Technora
Modulus (GPa)	24-25	8-10	20-21
Tensile strength (GPa)	1.8-2.1	0.5-0.6	3.0-3.2
Elongation at break (%)	3-4	35-45	5-7

Preparation of Composites

Various compositions of aramid fibre/SEBS composite were prepared. The dried fibre was first pre-opened in a blender for a few seconds, followed by blending for 0.5 min in an internal mixer with a rotor speed of 90 rpm at 175°C. The compatibiliser was then added and blended for another 0.5 min, and finally, SEBS was blended in for 9 min. The 50-gram batch composite was passed through a two-roll mill twice to attain fibre orientation. The composite sheet was kept in a desiccator at room temperature for 24 h.

Extraction of Composites

Extraction of composite specimen was carried out using a Soxhlet apparatus and toluene as a solvent. After extraction for 72 h, the sample was dried in a vacuum oven at 50°C for 24 h. The amount of bound rubbery matrix was determined gravimetrically.

Mechanical Properties of Composites

The composite sheet was compression moulded at 185°C for 10 min under a pressure of 15 MPa, into a 1-mm thick sheet, followed by conditioning at room temperature for at least 24 h. Tensile specimen was die cut at the size of 11.5x2.5x0.1 cm^3 with the long dimension parallel to the machine direction of the two-roll mill. Test were performed using an Instron testing machine model 4301, in accordance with ASTM D638, and with a cross head speed 500 mm/min and a 100 kg load cell.

RESULTS AND DISCUSSION

Hydrolysis of Aramid Fibre Surface

Aramid fibres were partially hydrolysed to create $-NH_2$ and -COOH end groups on the surface. It was found that, for 10% aqueous solution of NaOH, hydrolysis time of 20 min was required to create more active end groups detectable by DRIFT technique as shown in Figure 1. The peak at 880-884 cm^{-1} is due to C-H out-of-plane bending of the aromatic ring adjacent to $-COO^-Na^+$ as reported by Chatzi[15]. After washing with distilled water, followed by toluene, and dried, the peak disappeared, apparently due to the change from $-COO^-Na^+$ to -COOH. Without this washing step, sodium hydroxide would further hydrolyse to amide bonds on the fibre surface, resulting in a dark brown colour and reduced tensile properties of the composite.

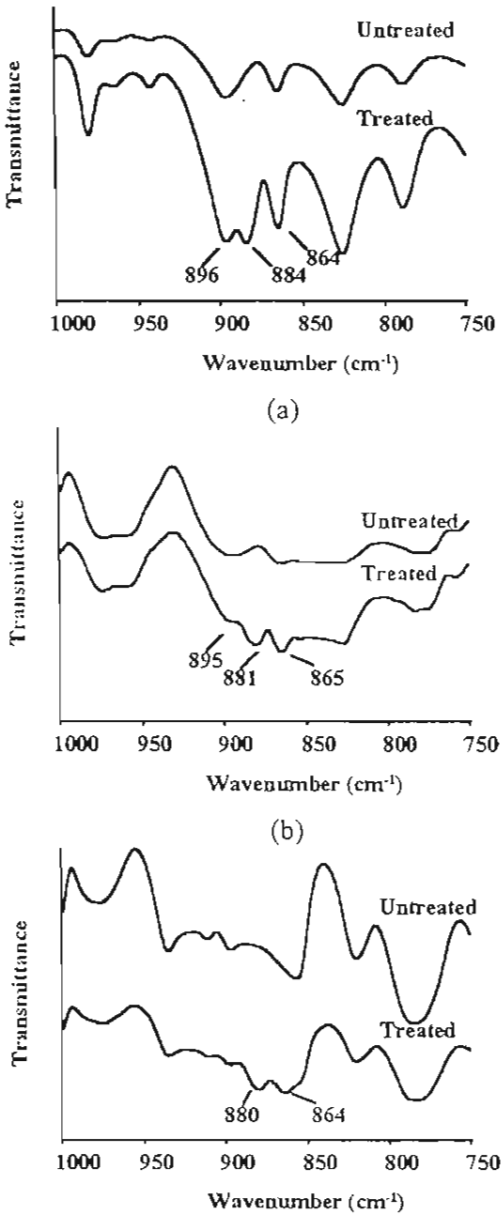

Figure 1 Infrared spectra of untreated (as-received) and treated (surface hydrolysed) aramid fibres (a) Kevlar (b) Technora (c) Conex

Mechanical Properties of Composites

1. As-received fibres

Tensile properties of the aramid fibre/SEBS composites are shown in Figure 2. It is evident that for all composites modulus at 100% (M100) increases linearly with increasing the amount of fibre loading and there is virtually no effect of fibre types on M100. An increase in M100 with fibre loading is due to incorporation of high modulus fibre in soft matrix. The fact that all type of fibres resulted in the same M100 would suggest that there is a saturation in M100 of the composites, regardless the mechanical properties and geometry of the reinforcing fibre. Similar effect of fibre loading are seen for Modulus at 300% (M300). In this case, however, Kevlar composites exhibit significantly higher M300 than Conex and Technora composites. Again, no different was found between M300 of Conex and Technora composites. It appears that at this high strain (300%) stress transfer to Kevlar is greater than that to Conex and Technora. This would suggest that reinforcing element in pulp geometry is better than short cylindrical fibre.

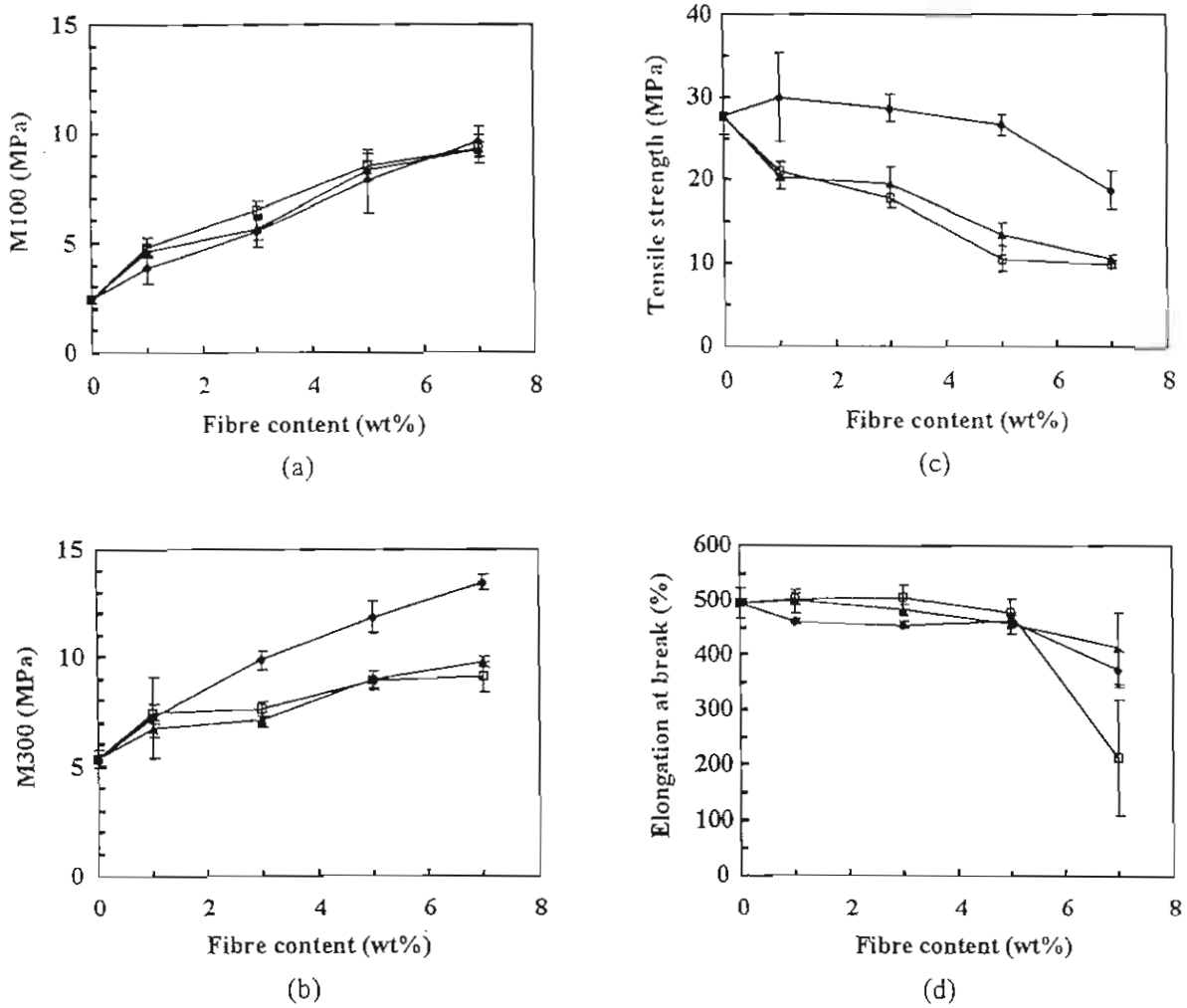

Figure 2 Tensile properties of untreated aramid fibre/SEBS composite with various fibre loading (◆ : Kevlar, □ : Conex, ▲ : Technora) (a) Modulus at 100%, (b) Modulus at 300%, (c) Tensile strength, and (d) Elongation at break

Tensile strength of the composites are shown in Figure 2 (c). It can be seen that, for Kevlar composites, addition of fibre upto 5% slightly affects tensile strength of the composites. At higher fibre loading tensile strength dropped. For Conex and Technora composites, it can be seen that tensile strength decreased with increasing fibre content. This can be understood as a debonding of fibre-matrix interface at very high strain which was seen as sample whitening. The samples will therefore be weaken.

Elongation at break of all types of composites is slightly affected by fibre content upto 5%. Above 5% fibre content, elongation at break dropped sharply. This is due to severe weakening of interface debonding and poor dispersion of fibre at high fibre content.

2. Surface-hydrolysed fibres

Surface hydrolysis of aramid fibre was carried out to increase the number of reactive end groups. These end groups could then react with SEBS-g-MA compatibiliser and modify surface properties of the fibres closer toward that of SEBS matrix. Figure 3 displays the amount of bound (unextractable) SEBS formed in Kevlar-SEBS composites at various SEBS-g-MA contents. It can be seen that the amount of bound SEBS increased with increasing SEBS-g-MA content. This indicates that modification of fibre surface was achieved as expected. For Technora and Conex composites, no bound rubber was found.

Although spectroscopic evidents proved an increase in number of active end groups, only Kevlar composites contain bound rubber. This suggests that chemical reactions between compatibiliser and active groups on fibre surface is material dependent. Surface roughness of the highly fibrillated pulp might also play an important role in adhesion of rubber particles.

Tensile properties of the composites containing 3% of treated fibres and compatibiliser are shown in Figure 4. It can be seen that compatibiliser content slightly affects the properties of Kevlar and Technora composites. For Conex composites, it is clearly seen that compatibiliser only affect the tensile strength of the composite. Tensile strength was found to increase with increasing compatibiliser content and approaching that of Kevlar composites at 5%.

The above finding would suggest that chemical reaction between compatibiliser and fibre may not result in composite with improved mechanical properties. Furthermore, improvement could be achieved by using compatibiliser without chemical bonding.

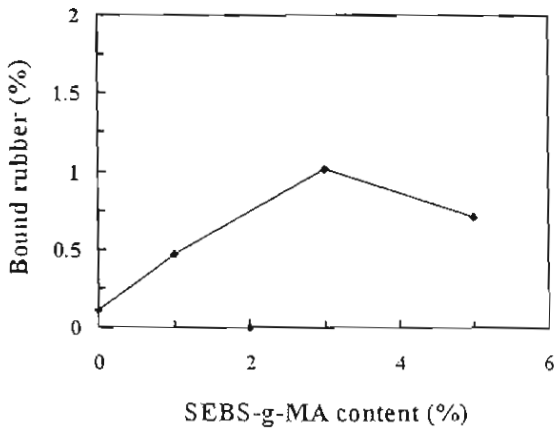

Figure 3 Bound (unextractable) rubber of Kevlar-composites containing various SEBS-g-MA contents.

CONCLUSIONS

Reinforcement of SEBS thermoplastic elastomer with aramid fibres at low strain can be achieved without any compatibilisers. It appears that geometry of the fibre has greater effect on mechanical properties of the composites than the mechanical properties of the fibres. At the same fibre content, pulp was found to be more effective in reinforcing than short fibre.

Alkaline hydrolysis of fibre surface in conjuction with reactive compatibiliser was found to be effective on certain type of aramid fibre, i.e. Conex. No improvement was achieved for Kevlar and Technora composites despite surface modification had been achieved.

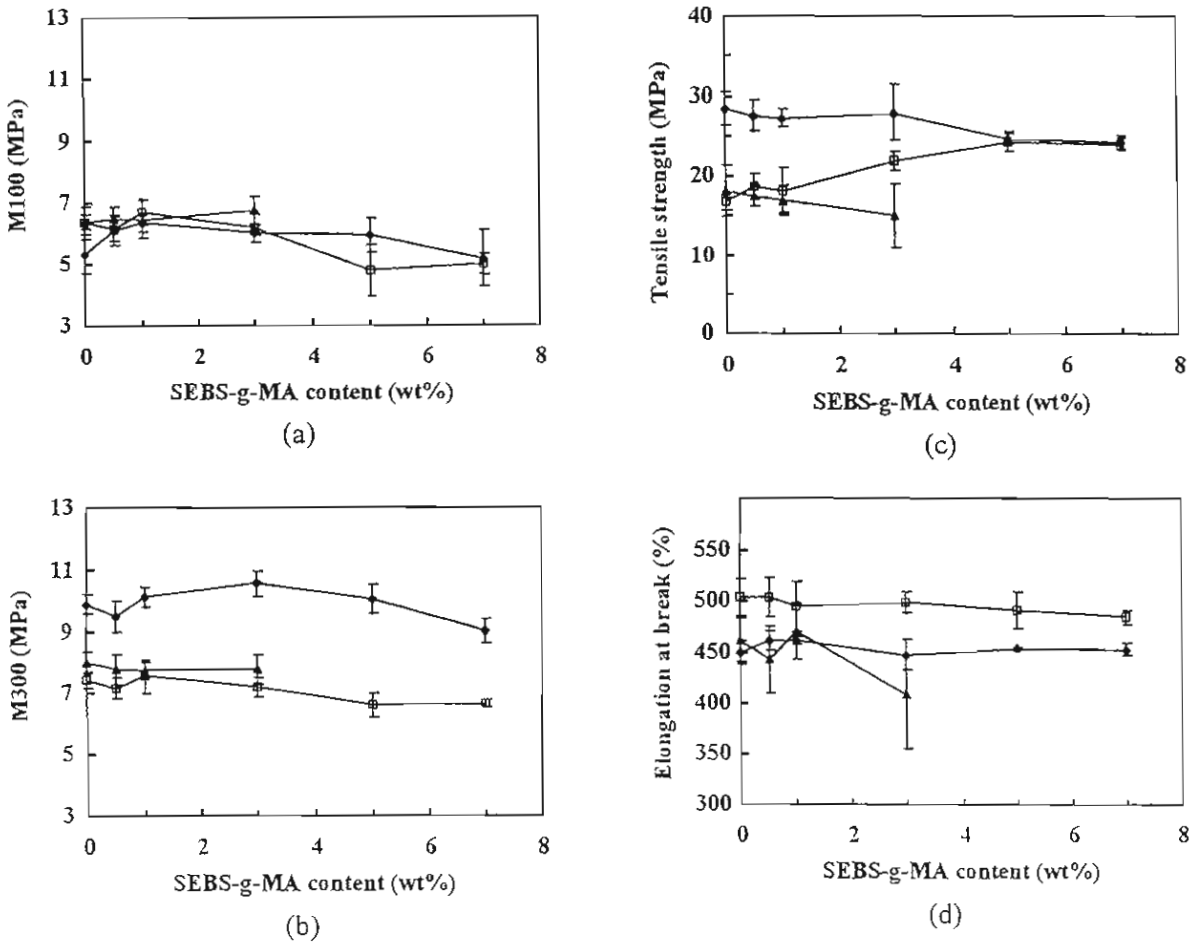

Figure 4 Tensile properties of treated aramid fibre/SEBS composite with various compatibiliser contents (◆ : Kevlar, □ : Conex, ▲ : Technora) (a) Modulus at 100%, (b) Modulus at 300%, (c) Tensile strength, (d) Elongation at break.

ACKNOWLEDGEMENTS

The authors would like to thank The Thailand Research Fund for funding and Shell Chemical Co., Du Pont Co. and Tejin Ltd. for providing materials used in this research.

REFERENCES

1. VAUGHAN, D.J. (1978) *Polym. Eng. Sci.* **18**, 167.
2. TAKAYANAKI, M., KAJIYAMA, T. and KATAYOSE, T. (1982) *J. Appl. Polym. Sci.* **27**, 3903.
3. TAKAYANAKI, M. and KATAYOSE, T. (1984) *Polym. Eng. Sci.* **24**, 1047.
4. BREZNICK, M., BANBAJI, J., GUTTMANN, H. and MAROM, G. (1987) *Polym. Commun.* **28**, 55.
5. ANDREOPOULOS, A.G. (1989) *J. Appl. Polym. Sci.* **38**, 1053.
6. WANG, Q., KALIAGUINE, S. and ABDELLATIF, AIT-KADI. (1993) *J. Appl. Polym. Sci.* **48**, 121.
7. YU, Z., ABDELLATIF, AIT-KADI., A. and BRISSON, J. (1991) *Polym. Eng. Sci.* **31**, 1222.
8. ASHIDA, M. and NOGUCHI, T. (1984) *J. Appl. Polym. Sci.* **29**, 4107.
9. ASHIDA, M. and NOGUCHI, T. (1984) *J. Appl. Polym. Sci.* **29**, 661.

10. ASHIDA, M., NOGUCHI, A. and MASHIMO, S. (1985) *J. Appl. Polym. Sci.* **30**, 1011.
11. GUO, W. and ASHIDA, M. (1993) *J. Appl. Polym. Sci.* **49**, 1081.
12. FOLGI, A.P. in *Composite Applications: The Role of Matrix, Fiber and Interfaces*, Vigo, T.L. and Kinzig, B.J. (Eds.) Verlag Chemie, Weinheim, 1992
13. MODIC, M.J. and POTTICK, L.A. (1993) *Polym. Eng. Sci.*, **33**, 819.
14. Technical information sheets from Du Pont Co. (No.12/92) and Teijin Ltd. (CN02/95.9)
15. CHATZI, E.G., TIDRICK, S.L. and KOENIG, J.L. (1988) *J. Polym. Sci : Polym. Phys.* **26**, 1585.

IUPAC

International Union of Pure and Applied Chemistry
Macromolecular Division

PREPRINTS

WORLD POLYMER CONGRESS

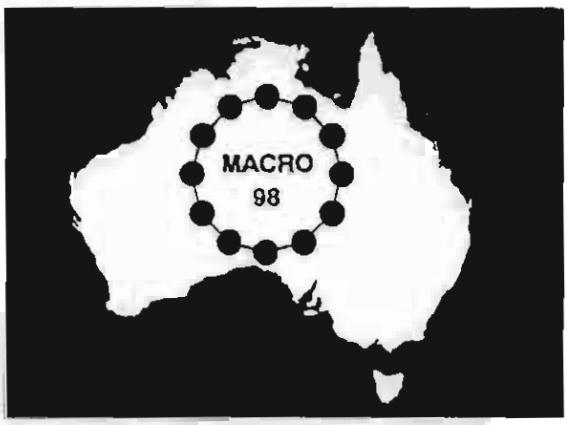

37th International Symposium on Macromolecules

Gold Coast. Australia
12 - 17 July 1998

Organised by :

Polymer Division
Royal Australian Chemical Institute

Sponsored by : International Union of Pure and Applied Chemistry

In-Situ Composite PP/LCP Films : Enhancement of Modulus and Impact Strength by Compatibilisers

Sauvarop Bualek-Limcharoen,* Taweechai Amornsakchai and Jareerat Samran

Department of Chemistry, Faculty of Science, Mahidol University, Rama 6 Road, Bangkok 10400, Thailand

ABSTRACT

In-situ composite liquid crystalline polymer (p-hydroxy benzoic acid/ethylene terephthalate, 60/40)/polypropylene(PP) film was produced using extrusion cast film technique. Compatibilising effect of thermoplastic elastomers, styrene ethylene butylene styrene (SEBS), maleic anhydride grafted SEBS (MA-g-SEBS) and maleic anhydride grafted polypropylene (MA-g-PP) on mechanical properties and morphology of the composite films was investigated. It was found that a few weight percent of SEBS provided higher value of tensile modulus than MA-g-SEBS which was in turn higher than MA-g-PP (see Fig.1). Impact strength of composite films was found to improve four folds by elastomeric compatibilisers SEBS and MA-g-SEBS due to their action as impact modifier. Observation of the films under optical microscope revealed that all three compatibilisers improve the dispersion of LCP fibre and enhance the LCP fibre aspect ratio. SEM micrographs of fractured surface of the specimens showed more fibre breakage than fibre pull-out when compatibiliser was added which was the evidence for improvement of interfacial adhesion. In addition to fibre breakage, surface roughness of fibres was also observed when thermoplastic elastomers were used as compatibilisers. Mechanical interlocking at the fibre/matrix interface should certainly be the reason why elastomeric compatibilisers provided higher tensile properties than thermoplastic compatibiliser.

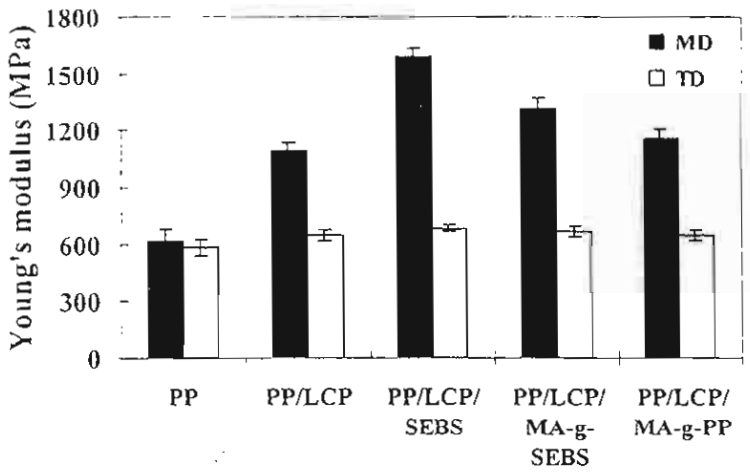

Fig.1 Young's Modulus of PP, PP/LCP, PP/LCP/SEBS, PP/LCP/MA-g-SEBS, PP/LCP/MA-g-PP (MD = machine direction, TD = transverse direction)

The 7th INTERNATIONAL Seminar on [redacted]

16–17 December 1998

Organized by

National Metal and Materials Technology Center (MTEC)
National Science and Technology Development Agency (NSTDA)
Ministry of Science, Technology and Environment (MOSTE)
Thailand

Composites of Aramid Fiber-Thermoplastic Elastomer: Improvement of Interfacial Adhesion by Chemical Modification of Fiber Surface

Sauvarop Bualek-Limcharoen

Department Chemistry, Faculty of Science, Mahidol University, Bangkok 10400, Thailand

ABSTRACT

Composites of aramid fibers and thermoplastic elastomers were investigated.
Aramid fibers used were poly-p-phenylene terephthalamide (Kevlar pulp) and poly-m-phenylene isophthalamide (Teijin-Conex short fiber) and thermoplastic elastomers were styrene (ethylene butylene) styrene block copolymer (SEBS) and crosslinked-EPDM/PP (Santoprene). Two chemical treatments were carried out to modify the fiber surface in order to promote fiber-matrix interfacial adhesion. The first method was partial hydrolysis of fiber surface to increase the number of reactive end groups and addition of a reactive compatibilizer to form chemical bonds at the interface. The second method was partial N-alkylation on fiber surface to enhance the compatibility between the polar fiber and the non-polar matrix. Tensile properties of compression-molded composites with unmodified and modified fibers were measured. The morphology of the modified fiber as well as the fractured surface of composites were characterized by FT-IR (DRIFT) and SEM techniques. It was found that interfacial adhesion was improved in the systems of Conex/SEBS using both methods of chemical treatments and hence enhancement of their tensile properties. For Conex/Santoprene system, the properties were improved merely with addition of MA-g-PP, the hydrolysis step was not necessary. For Kevlar/SEBS system, on the other hand, no improvement of physical properties could be obtained by such treatments. However, for Kevlar/Santoprene composite, partial hydrolysis of fibers, followed by addition of maleic anhydride grafted polypropylene (MA-g-PP), could greatly enhance fiber-matrix interfacial adhesion and hence their tensile properties.

REFERENCES

1. A. P. Foldi, in *Composite Applications: The Role of Matrix, Fibre and Interface*, T. L. Vigo and B. J. Kinzig, editors, VCH Piblisher, New York, 1992, pp133-177.
2. G. B. Nando and B. R. Gupta in *Short Fibre-Polymer Composites*, S. K. De and J. R. White, editors, Woodhead Publisher, Cambridge, 1996, pp89-115
3. S. Bualek-Limcharoen, T. Nakinpong, T. Amornsakchai and W. Meesiri, *J.Sci. Soc. Thailand*, **23**, 101 (1997)
4. T. Amornsakchai, B. Sinpatanapan, S. Bualek-Limcharoen and W. Meesiri, *Polymer* (in press).
5. S. Saikrasun, T. Amornsakchai, C. Sirisinha, W. Meesiri and S. B. Limcharoen, *Polymer* (in press)

This work has been supported by The Thailand Research Fund

RESULTS AND DISCUSSION

Morphology

The figures below are SEM micrographs of fibers and fractured surfaces. Modified fibers reveal surface roughness. Fractured surfaces of modified-fiber composites show more fiber breakage than fiber pull-out, compared with the unmodified fiber composites. This is the evidence for improvement of fiber-matrix interfacial adhesion.

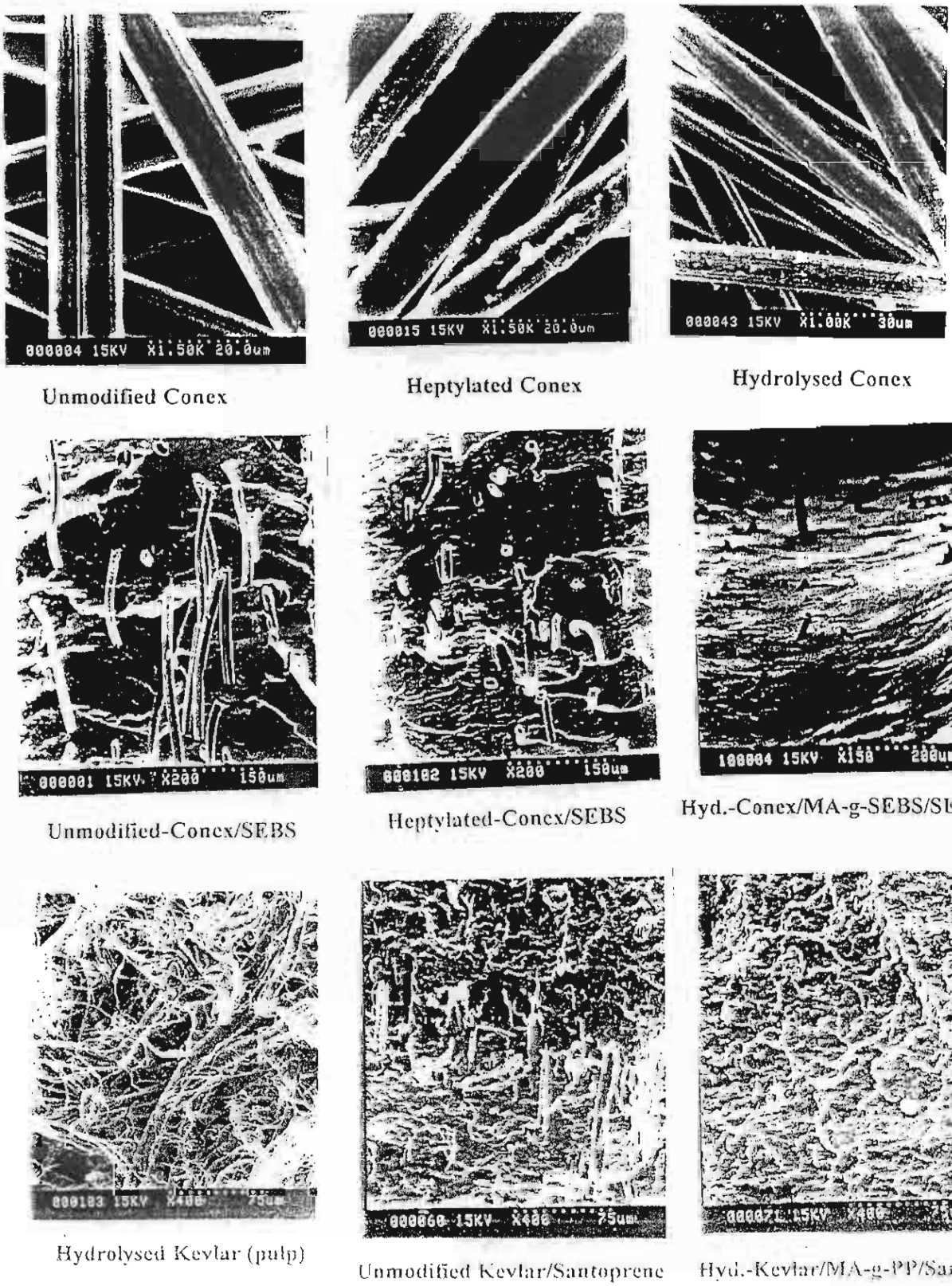

Unmodified Conex | Heptylated Conex | Hydrolysed Conex

Unmodified-Conex/SEBS | Heptylated-Conex/SEBS | Hyd.-Conex/MA-g-SEBS/SEBS

Hydrolysed Kevlar (pulp) | Unmodified Kevlar/Santoprene | Hyd.-Kevlar/MA-g-PP/Santoprene

Fig. 1. morphology of short fibers before and after modification, as well as the fractured surface of composites.

Mechanical Properties

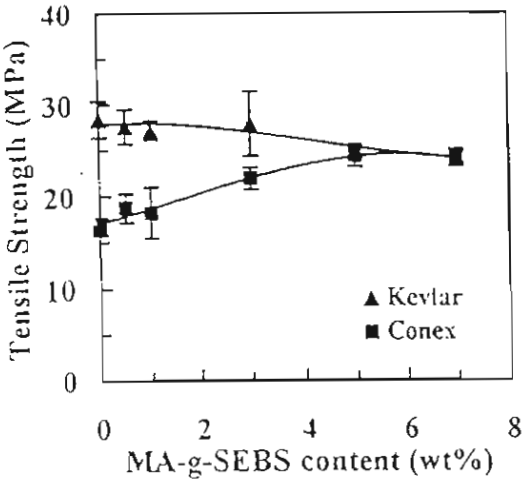

(2a)

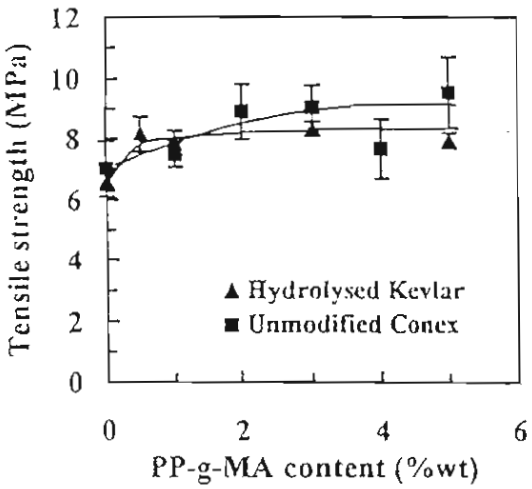

(2b)

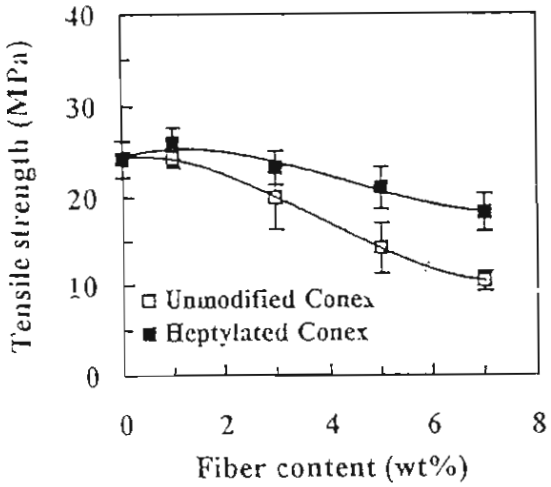

(2c)

Tensile moduli of all composites increase with increasing fiber loading, as expected, due to the action of the high strength fiber phase. In most cases, however, tensile strength decreases when low content of fiber is added, because of the dilution effect. Chemical treatments used in this study could improve tensile strength of some systems, such as Conex/SEBS/MA-g-SEBS, alkylated-Conex/SEBS, Conex/Santoprene/MA-g-PP and hydroylsed Kevlar/Santoprene/MA-g-PP as shown in Figs. 2a - c.

Fig. 2a Tensile strength of 3wt% Conex/SEBS composite as a function of added MA-g-SEBS

2b Tensile strength of 3wt% unmodified Conex/Santoprene and hydrolysed Kevlar/Santoprene composites as a function of added MA-g-PP

2c Tensile strength of unmodified and heptylated Conex/SEBS composites as a function of fiber loading

europhysics
conference
abstracts

Europhysics Conference on Macromolecular physics
EURORHEO 99-1

Rheology, Rheo-Physics and Flow-Induced Structures of Liquid Crystalline Polymers, Surfactants and Block Copolymers

Sophia-Antipolis (France), May 3-7 1999

Volume Editors: M. Haw, P. Navard, E. Peuvrel-Disdier

Published by: European Physical Society
Series Editor: Prof. R.M. Pick, Paris
Managing Editor: C. Bastian, Mulhouse

VOLUME
23 A

L-25

Effect of Melt Viscosity of Polypropylene on Fibrillation of Thermotropic Liquid Crystalline Polymer in *In-situ* Composite Film

Banchob Wanno[a], Jareerat Samran[b] and Sauvarop Bualek-Limcharoen[a]

[a]Faculty of Science, Mahidol University, Rama 6 Road, Bangkok 10400, Thailand.
[b]Faculty of Science and Technology, Songkla University, Pattani 94000, Thailand

Polypropylene (PP) of different melt flow indices (MFI) was melt blended with thermotropic liquid crystalline polymer (TLCP), block copolymer of 60 mol% p-hydroxy benzoic acid and 40 mol% ethylene terephthalate), in a twin screw extruder. Films of these polymer blends were prepared by extrusion cast film technique to obtain the so-called *in-situ* composite.

This terminology was coined because the dispersed TLCP droplets were elongated under the extensional force after which they were solidified and acting as reinforcing fibers[1]. Viscosity ratio of the blend components was found important for the formation of TLCP fibers in this blend system[2]. Tensile strength and morphology of the films produced at different processing condition were investigated. It was found that as the melt viscosity of the matrix increased, the fiber aspect ratio (length to width ratio) of TLCP phase increased and hence resulted in an improvement of the film modulus (see Fig. 1). Addition of a few percent of elastomeric compatibilizers, such as EPDM[3] and SEBS[4], which enhanced the over all viscosity of the blend, also improved the final properties of the films. We observed that these elastomers enhanced film modulus only for the systems prepared from PP with higher MFI. Viscosities of these blend systems at different temperatures and shear rates were measured using capillary rheometer. Correlation between the melt viscosity of the blend and the formation of TLCP fibers will be discussed.

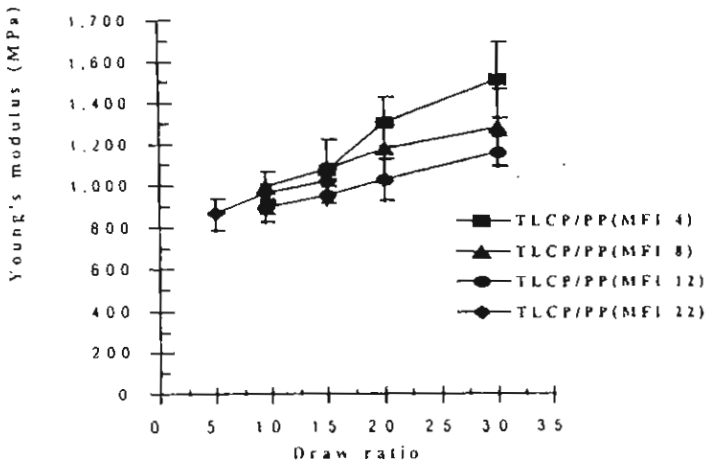

Fig. 1 Young's modulus versus draw ratio of TLCP/PP films prepared from PP with MFI 4, 8, 12 and 22.

References

1 G. Kiss, Polym. Eng. Sci., **27**, 410 (1987).
2 M. T. Heino, P.T. Hietaoja, T. P. Vainio, and J. V. Seppala, J. Appl. Polym. Sci., **51**, 259, (1994).
3 Y. J. Seo, J. Appl. Polym. Sci., **64**, 359, (1997).
4 S. Bualek-Limcharoen, J. Samran, T. Amornsakchai, and W. Meesiri, Polym. Eng. Sci. (in Press).

This work as been supported by the Thailand Research Fund.

5.7

Proceedings 2

The 5th Asian Textile Conference

Diversity in Harmony
Asian Textile in the 21st Century

Kyoto Research Park,Kyoto, Japan
September 30-October 2, 1999

Organized by
The Society of Fiber Science and Technology, Japan
The Textile Machinery Society of Japan
The Japan Research Association for Textile End-Uses

In cooperation with
Fukui University
Kyoto City
Kyoto Institute of Technology
Tokyo University of Agriculture and Technology

Chemical Treatments of Aramid Fibers to Improve Adhesion with Non-polar Polymer Matrices

Sauvarop Bualek-Limcharoen[1], Sunan Saikrasun[2] and Anongnuch Chantaratcharoen[1]

[1]Department of Chemistry, Faculty of Science, Mahidol University, Bangkok 10400, Thailand
[2]Department of Chemistry, Faculty of Science, Mahasarakham University, Mahasarakham 44000, Thailand

ABSTRACT

Aramid fibers, poly-p-phenylene terephthalamide (Kevlar) and poly-m-phenylene isophthalamide (Teijin-Conex) were chemically treated to modify the fiber surface in order to promote interfacial adhesion between the fiber and the non-polar polymer matrices. The polymer matrices used in this work were thermoplastic elastomers, styrene (ethylene butylene) styrene block copolymer (SEBS) and polyolefin-based thermoplatic elastomer (Santoprene). Two chemical treatments were used to modify aramid short fibers. The first method was partial hydrolysis on fiber surface using an alkaline solution. After that, the treated short fibers and a polymer matrix were melt blended in an internal mixer, with addition of a reactive compatibilizer to promote chemical bonding at the interface. The second method was partial N-alkylation on fiber surface to make it non-polar and hence compatible with the matrix. The new functional groups on the treated fibers were characterized by FT-IR (DRIFT).. Tensile properties of the composites were measured. Observation of the morphology under scanning electron microscope suggested the improvement of interfacial adhesion in the systems of Conex/SEBS by both methods of chemical treatment. These results were in good agreement with the enhancement of the tensile properties. For Conex/Santoprene system, the properties were improved merely with addition of maleic anhydride grafted polypropylene, (MA-g-PP) and the hydrolysis step is not necessary. For Kevlar/SEBS system, on the other hand, no improvement of physical properties can be obtained by both treatments. However, for Kevlar/Santoprene composite, partial hydrolysis of fibers followed by addition of MA-g-PP could greatly enhance its interfacial adhesion and hence the tensile properties.

INTRODUCTION

Polymer composite, a combination of plastic or rubber with filler, is widely used in several areas of application to replace conventional materials such as wood, metals, glasses and ceramics, due to their high specific strength, ease of fabrication and relatively low cost. A fiber-reinforced composite usually shows an increase in rigidity provided by the fiber phase, which is stiffer and stronger than the matrix phase. For rubber matrix, reinforcing fiber greatly enhance its dimensional and thermal stability. Short fiber reinforced polymer has gained much more attention than continuous fibers due to their ease of fabrication, though it offers lower strength. Reviews of short-fiber reinforced rubber have been reported elsewhere[1]. Composites of short fiber-thermoplastic elastomer have been very recently studied by a few groups of researcher[2-3]. Thermoplastic elastomer combining advantages properties of two classes of polymers, i.e. recyclability, ease and economy in processing like thermoplastic, and possesses the important elasticity of rubber. However, some disadvantages of thermoplastic elastomer are low thermal and low dimensional stability at elevated temperature. Incorporation of reinforcing fiber into thermoplastic elastomer is therefore fruitful in enhancing the strength and overall stability of the product.

In this work, we present the combination of aramid fibers and thermoplastic elastomers. Two types of thermoplastic elastomers used were SEBS[4-5] and Santoprene[6]. The reinforcing fibers were Kevlar pulp and Teijin-Conex short fiber. Since the polarity of the fibers and polymer matrices are greatly different, two chemical treatments were used to modify the fiber surface to make it less polar. The first method is by addition of a reactive compatibilizer, i.e., MA-g-SEBS and MA-g-PP in the cases of SEBS and Santoprene matrices, respectively. Maleic anhydride group should react with the free amine end group of aramid, allowing the rest of the molecule, i.e., SEBS or PP part which is now attached on the fiber, to be compatible with the matrix. In order to increase the number of amine end group, the fiber was first partially hydrolysed in alkaline solution. The second method was the slight modification of the fiber surface by N-alkylation. The alkyl groups attached on the surface make the fiber less polar and hence should be compatible with the non-polar matrix.

EXPERIMENTAL

Materials

Aramid fibers used are Kevlar pulp (poly-p-phenylene terephthalamide) length ~ 2 mm from Du Pont Co. and Teijin conex fiber (poly-m-phenylene isophthalamide) length ~3 mm fromTeijin Co.Ltd. Polymer matrices are triblock copolymer of styrene (ethylene butyrene) styrene, SEBS (KRATON G1652) with S/EB = 29/71, kindly provided by Shell Chemical Co. and polyolefin-based thermoplastic elastomer, Santoprene, (crosslinked ethylene propylene diene rubber (EPDM) and polypropylene) with EPDM/PP = 24/76 (determined by DSC) from Uniroyal Chemical Co. Inc. Compatibilizers are MA-g-SEBS (KRATON FG1901X, MA content = 1.84% from Shell Chemical Co. and MA-g-PP (Polybond 3150), MA content = 0.5% from Uniroyal Chemical Co. Inc.

Methods

Chemical Modifications

1) Hydrolysis : Fiber was hydrolysed in 10 wt% aqueous NaOH solution at ambient temperature for 20 min. after which it was thoroughly washed with distilled water and toluene and dried in vacuum oven at 50 °C to a constant weight.

2) N-Alkylation : Preparation of N-alkylation on aramid fiber surface was similar to that described by Takayanaki[7]. The fiber was first deprotonated by dispersing in DMSO and NaH mixture and then alkyl bromide was added. Since only slight modification was required, the smaller amount of NaH and the shorter reaction time for alkylation step was applied[6].

Characterizations

Diffuse Reflectance Infrared Fourier Transform (DRIFT) spectrometer (Perkin Elmer FTIR 2000) was used to characterize the surface of Aramid fiber. Two hundred scans at a resolution 4 cm^{-1} were usually required to obtain a good spectrum.

Morphology of fiber surface and fractured surface of the composites were observed by SEM (Hitachi S2500). A thin layer of palladium was coated by Hitachi E102 ion sputter on the specimen. The microscope was operated at 15 kV. Fractured surface of the composites was prepared by freezing the specimen in liquid nitrogen and then broken rapidly.

Preparation of composites

The composite was prepared in the internal mixer, Haake Rheocord 90, at the set temperature of 175°C for SEBS matrix and 165°C for Santroprene matrix, rotor speed of 90 rpm, for 10 minutes. Then it was collected and sheeted by passing through a two-roll mill. Loading of Aramid fiber was varied up to 7% by weight. The effect of compatibilizer was studied in a composite containing 3wt% of fiber.

Measurement of tensile properties

The specimens were compression molded at 180°C for 10 minutes and quenched with cold water. After being conditioned for at least 24 hours, tensile specimens were cut with a die of size 115 mm. x 6 mm. x 1 mm parallel to the machine direction . Testing was carried out on an Instron testing machine model 4301 in accordance with ASTM D638 at a cross head speed of 500 mm min^{-1} with a 100 kg load cell.

RESULTS AND DISCUSSION

Morphology

SEM micrographs of the fractured surfaces of the SEBS and Santoprene composites containing untreated and treated aramid fibers are shown in Fig. 1. It is evident that the untreated fiber gives the fractured surface with long fiber pull-out whereas those of the composites with treated fibers show more fiber breakage. These are good evidences for the improvement of interfacial adhesion.

Mechanical properties

Improvement of the tensile strength of the composite systems can be considered as a criterion for improvement of the interfacial adhesion. The tensile strengths of aramid/SEBS composites as a function of added MA-g-SEBS are shown in Fig.2a. It can be seen that without addition of compatibilizer the tensile strength of Conex/SEBS system is lower than that of Kevlar/SEBS system. But when the amount of added compatibilizer increased the tensile strength of Conex/SEBS enhanced and then level-off at about 5% of added MA-g-SEBS, which is at this point equal to that of Kevlar/SEBS system which declined slightly as the amount of compatibilizer is increased. In these composite systems the moduli and elongation at break are not affected by addition of MA-g-SEBS. Fig. 2b illustrates the results of aramid fiber/Santoprene composites. Tensile strengths of both Kevlar and Conex fibers reinforced Santroprene are slightly improved by incorporation of MA-g-PP. In the case of Kevlar/Santoprene, hydrolysis step could help to get better results whereas in the case of Conex/Santoprene, the hydrolysis step is not essential. Addition of MA-g-PP also enhances the modulus of both composite systems. The elongation at break, on the other hand, increases for Kevlar but sharply decreases for Conex composite system as MA-g-PP is added (the results are not shown here). Fig. 2c shows the effect of N-alkylation of Conex fiber on tensile strength of Conex/SEBS composite. The results revealed that the N-alkylated fiber give a composite with higher tensile strength than that of the unmodified fiber, especially at higher fiber content. Modulus and elongation at break of these systems are not affected by the alkyl groups.

Conclusion

The surface treatment of the highly polar fiber, like aramids, to a less polar surface by attachment of the alkyl groups or attachment of non-polar moiety through interaction with reactive compatibilizers could help improve the physical interaction at the interface. This is evident by observation of the fractured surface by SEM technique, and as a consequence the improvement of the tensile properties of the systems is obtained.

Acknowledgement

Financial support by the Thailand Research Fund is gratefully acknowledged.

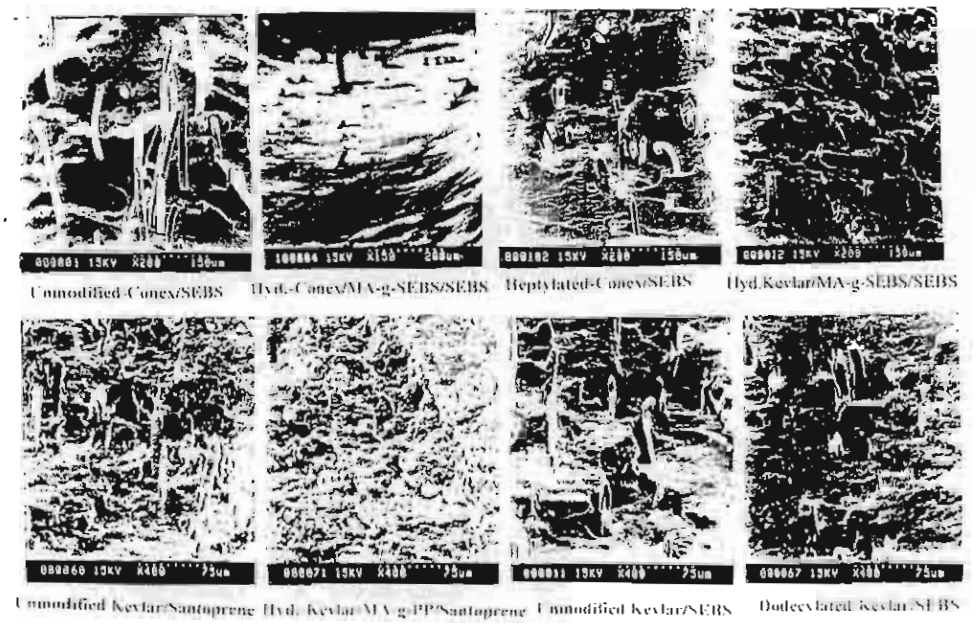

Fig. 1 SEM micrographs of fractured surfaces of untreated and treated aramid fiber reinforced SEBS and Santoprene

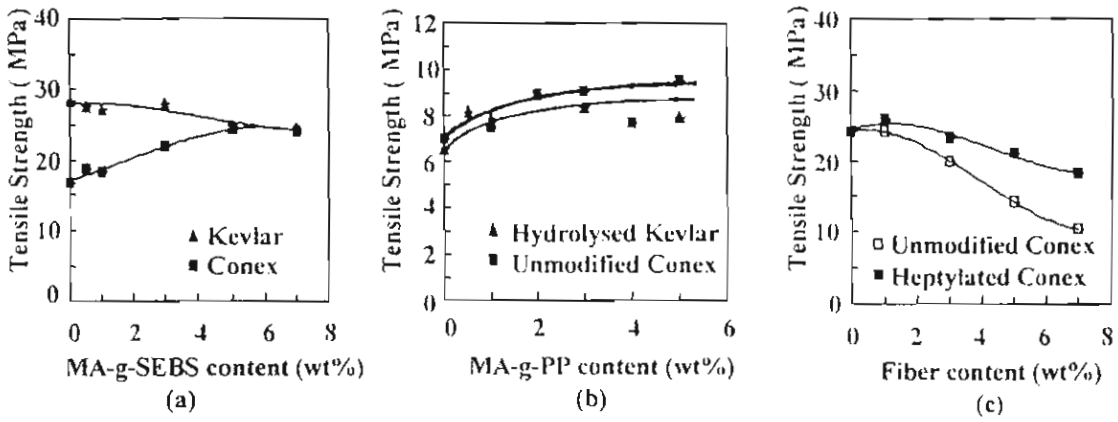

Fig. 2 Tensile strength of (a) 3wt% aramid/SEBS composites as a function of MA-g-SEBS (b) 3wt% aramid/Santoprene composites as a function of MA-g-PP (c) unmodified and heptylated Conex/SEBS composites as a function of fiber loading.

References:

1 G. B. Nando and B. R. Gupta in *Short Fiber-Polymer Composites*, S. K. De and J. R. White, editors, Woodhead Publisher, Cambridge, 1996, pp 84-115

2 S. K. N. Kutty and G. B. Nando, *J. Appl. Polym Sci.*, **46**, 471 (1992).

3 S. Bualek-Limcharoen, T. Nakinpong, T. Amornsakchai and W. Meesiri, *J.Sci. Soc. Thailand*, **23**, 101 (1997)

4 T. Amornsakchai, B. Sinpatanapan, S.. Bualek-Limcharoen and W. Meesiri, *Polymer*, **40** 2993 (1999)

5 S. Saikrasun, T. Amornsakchai, C. Sirisinha, W. Meesiri and S. Bualek-Limcharoen, *Polymer* (in press)

6 A. Chantaratcharoen, C. Sirisinha, T. Amornsakchai, S. Bualek-Limcharoen and W. Meesiri, *J. Appl. Polym. Sci.* (in press)

7 M. Takayanagi and T. Katayose, *J. Polym. Sci.. Polym. Chem. Ed.* **19**, 1133 (1981).